DESIGN AND SYNTHESIS OF CONFORMATIONALLY AND TOPOGRAPHICALLY CONSTRAINED AMINO ACIDS AS PEPTIDOMIMETICS

by

Wei Qiu

A Dissertation Submitted to the Faculty of the

DEPARTMENT OF CHEMISTRY

In Partial Fulfillment of the Requirements
For the Degree of

DOCTOR OF PHILOSOPHY

In the Graduate College

THE UNIVERSITY OF ARIZONA

2001

UMI Number: 3010257

UMI®

Bell & Howell Information and Learning Company
300 North Zeeb Road
P.O. Box 1346
Ann Arbor, MI 48106-1346

THE UNIVERSITY OF ARIZONA ®
GRADUATE COLLEGE

As members of the Final Examination Committee, we certify that we have read the dissertation prepared by Wei Qiu

entitled DESIGN AND SYNTHESIS OF CONFORMATIONALLY AND TOPOGRAPHICALLY CONSTRAINED AMINO ACIDS AS PEPTIDOMIMETICS

and recommend that it be accepted as fulfilling the dissertation requirement for the Degree of Doctor of Philosophy

Victor J. Hruby — Date 1/24/01

Robert B. Bates — Date 1-16-01

Richard S. Glass — Date 1/16/01

Robert D. Feltham — Date 1/24/01

Zhiping Zheng — Date 1/23/01

Final approval and acceptance of this dissertation is contingent upon the candidate's submission of the final copy of the dissertation to the Graduate College.

I hereby certify that I have read this dissertation prepared under my direction and recommend that it be accepted as fulfilling the dissertation requirement.

Dissertation Director Victor J. Hruby — Date 1/25/01

STATEMENT BY AUTHOR

This dissertation has been submitted in partial fulfillment of requirements for an advanced degree at The University of Arizona and is deposited in the University Library to be made available to borrowers under rules of the Library.

Brief quotations from this thesis are allowable without special permission, provided that accurate acknowledgment of source is made. Requests for permission for extended quotation from or reproduction of this manuscript in whole or in part may be granted by the head of the major department or the Dean of Graduate College when in his judgment the proposed use of the material is in the interests of scholarship. In all other instances, however, permission must be obtained from the author.

SIGNED: Wei C—

ACKNOWLEDGMENTS

I would like to thank my research advisor, Dr. Victor J. Hruby, for his valuable guidance and encouragement throughout the period of my work. I would also like to thank the other members of my committee, Drs. Robert B. Bates, Richard S. Glass, Robert D. Feltham and Zhiping Zheng for their time and stimulating discussion about my research.

I would like to thank Dr. Vadym A. Soloshonok for his help, criticism and friendship.

I would like to thank the following colleagues for their help and friendship: Drs. Scott Cowell, Preeti M. Balse, Kati E. Kövér, Chaozhong Cai, Andrew Burritt, Wei Yuan, Guoxia Han, Jung-Mo Ahn, Subo Liao, Yinglin Han, Jun Lin, Steve Waller, Yeon Sun Lee, and my fellow graduate students Xuyuan Gu, Jinfa Ying, Chiyi Xiong, Xuejun Tang, Haiyong Gan and Huiwei Wu.

I am also very grateful to Margie Colie and Cheryl McKinley.

Finally, I would like to thank my dear wife, Wei Jia, my parents Jinhong Qiu and Qingfang Guo, my parents-in-law Yuqing Jia and Hong Zhao for their affection during this study.

TABLE OF CONTENTS

LIST OF ILLUSTRATIONS

LIST OF ILLUSTRATIONS -continued page

LIST OF TABLES

ABSTRACT

A major goal of peptide research has been to elucidate or understand the relationships between a peptide's three-dimensional structure and its biological activity. *De Novo* design of peptide mimetics requires assembling all components necessary for molecular recognition and transduction, which needs the proper choice of a template that can place the key side chain residues in 3D space. Two widely used methods are novel β-substituted amino acids and conformationally constrained secondary structure mimetics. In this thesis, we report our efforts to fulfill the aforementioned criteria in synthesizing β-isopropyl aromatic amino acids and constrained reverse turn dipeptide mimetics.

Through asymmetric Michael addition reaction, highly topographically constrained β-isopropyl aromatic amino acids have been synthesized. In order to develop a general approach to synthesize these novel amino acids, we re-examined the reaction conditions for Evans' diastereoselective 1,4-addition, and found conditions which gave excellent diastereoselectivities and good chemical yields.

A concise and straightforward five-step synthesis of [5.5]-bicyclic reverse turn dipeptide mimetic scaffolds with side chain functionality at the i+1 and i+2 positions has been developed. In the bicyclic structure, two dihedral angles (ψ_2 and ϕ_3) are greatly restricted. Further development of this synthesis will enable us to prepare various types of reverse turns with different backbone geometry and side chain topography.

Enantiomerically pure (*S*)-*trans*-cinnamylglycine and (*S*)-α-*trans*-cinnamyl-α-alanine have been prepared via reaction of chiral Ni (II)-complexes of glycine and alanine respectively, with cinnamyl halides. Inexpensive and readily available reagents and solvents are used, including a recyclable chiral ligand. The simplicity of the

experimental procedures and high stereochemical outcome make this method synthetically attractive for preparing the target amino acids on multi-gram scales.

Further studies by incorporating these mimetics into potent peptide analogues will greatly help us to understand the bioactive conformation of the parent peptides.

Chapter 1

INTRODUCTION

Almost a century ago, in 1902, Emil Fischer and Frank Hofmeister revealed that proteins are made up of amino acids, linked *via* "peptide bonds".[1] Though progress was initially slow due to difficulties in polypeptide structure determination and synthesis, three major breakthroughs in the 1950s served to revolutionize the field. First, du Vigneaud's isolation, structure determination and total synthesis of oxytoxin; second, Sanger's elucidation of the structure of insulin; and third, the discovery of the double helix of DNA suggesting that there is a connection between nucleic acid and polypeptide sequences.[2,3] Today, peptides as neurotransmitters, neuromodulators, hormones, antibiotics, growth factors, cytokines, antigens, etc. are known to influence essentially all vital physiological processes *via* inter- and intracellular communication, and signal transduction mediated through various classes of receptors.[4,5] During the last two decades, the central role of peptides in the maintenance of human health, in behavior and in many diseases has been unequivocally proven, and the human genome project will add hundreds or thousands of new polypeptide ligands and targets. Thus a major goal of peptide research has been to elucidate or understand the relationships between a peptide's three-dimensional (3D) structure and its biological activity so as to develop suitable therapeutic agents in the control or intervention of human health, disease and dysfunction.

The combination of twenty natural amino acids provides numerous peptides and proteins. The major feature of the amide bond is the delocalization and coplanar arrangement of the three $2p_z$ orbitals in O, C, and N atoms that make the amide bond have partial double bond character. The *trans*-geometry is generally favored energetically. Only in the case of proline or N-alkylated amino acids as C-terminal partners does the *cis*- geometry become likely. In solution, natural peptides exist in multiple conformations with only a few kcals/mole energy separations. Thus they often possess multiple biological properties and lack bio-specificity.

The initial event that is essential for eliciting (or blocking) a biological response is molecular recognition. In the case of the ligand, the portion of the 3D surface involved in the interaction often is referred to as the *pharmacophore*, and may involve either a continuous sequence of amino acids (*sychnologic* organization) or amino acid residues separated from each other throughout the primary structure (*rhegnylogic* organization)[6] but brought together on a surface by the 3D structure of the polypeptide.[4,7] In either case, the peptide backbone serves as a scaffold for the key side chain groups involved in the interaction, and in some cases, also serves as a hydrogen bond donor and/or acceptor in molecular recognition (binding). In all cases, the side chain moieties involved directly in the binding are critical for the interaction, and their 3D architecture (topography) and stereoelectronic properties provide the critical complementary shape and chemical properties that favor efficient molecular recognition.

Although native biologically active peptides have a great potential for medical applications, they often need to be modified to overcome certain problems inherent in current drug-delivery strategies. The desired properties include: high receptor/acceptor selectivity; high potency; high stability against proteolytic breakdown; and appropriate biodistribution and bioavailability. These issues often have been addressed by the design of peptide mimetics and non-peptide ligands.

More success has been obtained with the development of "peptide mimetic" antagonists. But since these antagonists generally come from natural products or company collections, it is not clear that they are truly peptide mimetics. So what is a peptide mimetic? Since this question has developed into an "Alice-in-Wonderland" quality with almost as many definitions as investigators, Hruby and Slate gave a precise but simple definition.[8] A peptide mimetic is "a designed compound whose pharmacophore and stereostructural elements mimic a peptide in 3D space, and which mimic the binding, biological activities, selectivities, and structure-activity relationships (SAR) of a natural endogenous peptide ligand or peptide analogue with equivalent or superior bioactivities." Agonists and antagonists would follow the same definition. For compounds that are developed from screening synthetic or natural product libraries and that only mimic some aspects of the peptide ligands, Veber has suggested[9] the term "peptide limetic" (a limetic is short for ligand mimetic). This is an excellent suggestion, to which we fully subscribe.

Structure–based rational design of peptide and non-peptide ligands has dramatically advanced over the last two decades.[10-27] Ultimate goals have been set for this research including high potency, high receptor selectivity, high stability both *in vitro* and *in vivo*, and high efficacy *in vitro* and *in vivo* for agonists. A systematic stepwise strategy has been developed to accomplish these goals. Once the natural peptide's structure is known, the first phase in this approach involves the identification of the key amino acid side chain residues necessary for receptor recognition by single amino acid modifications in the peptide ligand and, in the case of agonist activity, those required for information transduction. Simultaneously, local constraints are built into the ligand to constrain the local backbone conformation (ϕ, ψ and ω angles, Fig. 1.1) to the most appropriate local minima in a way that is compatible with molecular recognition. Two widely used methods are novel β-substituted amino acids and/or amide bond replacements. Alternatively, more global constraints are incorporated *via* cyclization to make an appropriate template for all the structural elements that make up the pharmacophore. Compounds with rigid or semi-rigid conformations are thus produced, and the most active structures are selected for studying conformation-activity relationships.

In addition to the determination of the preferred backbone conformation, which can serve as a template for the bioactive conformation (α-helix, reverse-turn, β-sheet, etc.), it is also very important to examine and determine the preferred side chain topography in χ space (χ^1, χ^2, etc.), in order to provide insight into the topographical requirements for ligand-receptor interactions. The methodology developed includes specific covalent and non-covalent constraints which can place the constrained side chains at highly preferred conformations (*gauche*(-), or *gauche*(+), or *trans* for χ^1), and careful analysis of the 3D arrangement of critical side chain groups that are critical for bioactivity. These biophysical studies include state-of-the-art NMR spectroscopy, X-ray crystallography if possible, circular dichroism measurements, and computational methods (molecular mechanics and molecular dynamics calculations) utilizing the biophysical structural parameters as key constraints.

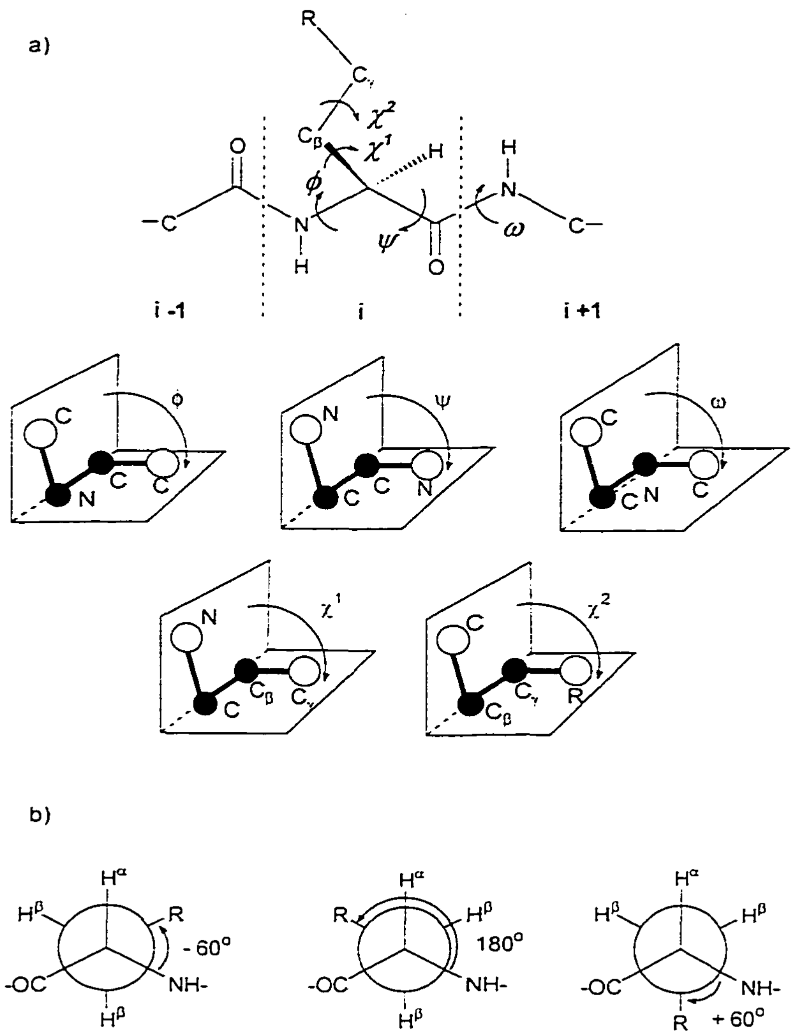

Fig. 1.1. (a) Definition of the ϕ, ψ, ω, χ^1 and χ^2 torsional angles; (b) Newman projections of the three staggered rotamers in an L-amino acid.

Usually, at this point, one can obtain a quite precise 3D-conformation of the pharmacophore. In many cases such studies can lead to highly potent, selective and efficacious drug candidates, and provide the starting point for the non-peptide ligands with high stability to biodegradation and good bioavailability including the ability to cross membrane barriers. Now the major effort is to find other organic moieties that can replace the peptide scaffold and position the crucial recognition elements correctly in 3D space and with appropriate dynamic properties. This approach provides a systematic framework for the *de novo* design of peptide mimetic and non-peptide ligands as outlined in Fig. **1.2**. For G-protein coupled receptors (GPCRs), it is often desirable to develop both agonists and antagonists, and in the case of enzymes, inhibitors are usually desired. Studies over the past 20 years have demonstrated that agonists and antagonists have different structure-activity relationships. There still is no universal approach to develop antagonists from agonists for peptide hormones and neurotransmitters, but once a lead has been obtained, there are general approaches that can be used to further develop antagonists.[28] It is worth mentioning here that peptide mimetic design is a highly multidisciplinary area that often relies on: 1) new asymmetric syntheses and methodologies for the preparation of novel molecules; 2) high-throughput screening of ligands and libraries of ligands using multiple *in vitro* and *in vivo* biological assays; 3) computational methods; and 4) state-of-the-art biophysical methods for determining the structural, conformational, topographical and dynamic properties of designed ligands.

In order to develop peptide mimetic ligands, efforts are in progress to develop templates and aspects of conformational design that permit assembling of all components necessary for molecular recognition and transduction. Here the proper choice of template that can place the key side chain residue in 3D space is still difficult, and thus only partial success has been achieved in terms of potent and selective ligands.

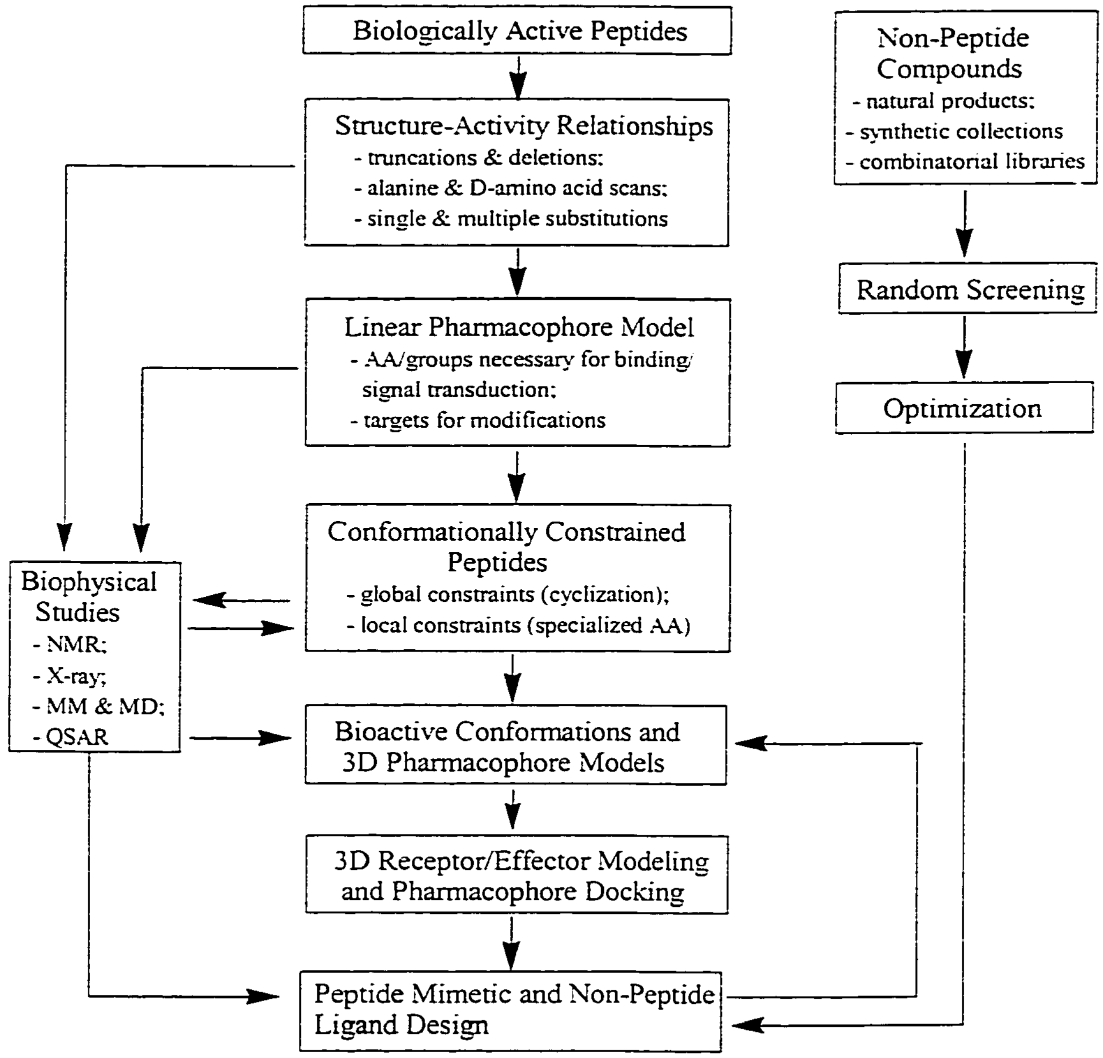

Fig. 1.2. A *de novo* approach for peptide and non-peptide ligand design.

De novo design of peptide mimetics to mimic all of the chemical and biological features of a bioactive peptide is still a considerable challenge, especially if the goal is to obtain an agonist. Though considerable success has been obtained in designing peptide mimetics that incorporate some aspects of the overall structural and topographical features of a peptide, efforts to design other important features, such as the proper topographical relationships of 3 or 4 critical side chain groups in 3D space, and of certain H-bond donating and accepting properties, has been difficult. As a result of these "missing" structural, stereoelectronic or dynamic properties that the native peptide ligand possess, not surprisingly these peptide mimetics often lack some of the critical biological properties that the native ligand possesses. Since overall it has been much easier to design potent and selective peptide mimetic antagonists for peptide agonist receptors, once one has a lead structure, perhaps these results are telling us something regarding the requirements for information transduction resulting from peptide ligand-receptor interactions. For example, since agonists require that the ligand-receptor interaction lead to structural changes compatible with information transduction, it might suggest that receptors for relatively small peptide ligands (up to 10 residues) may require the design of peptide mimetics that still retain some key features of the peptide structure such as H-bond accepting or donating properties, dynamic behavior of the peptide backbone for appropriate structural changes, and appropriate side chain group conformations and topographies.

Whatever the structural or dynamic features that need to be incorporated into peptide mimetics, it is hoped that with more effort we will learn how to incorporate these features. Given the importance of the goal, it is certain that synthetic chemists will continue to develop this field.

Strategies in the Design of Peptide Mimetics

1. Modification of amino acid side chains

In peptides and proteins, the major secondary structures such as α-helix, β-sheet, reverse turns, extended conformations, etc. are determined by the ϕ and ψ angles of the peptide chain (Fig. 1.1). The ω angle, also important, is generally *trans* (180 ± 20°), except for proline, where it can be both *trans* and *cis* (0 ± 20°). The favored low energy conformations of ϕ and ψ angles were first examined by Ramachandran and coworkers[29] in the 1960s. Subsequent studies by Scheraga *et al.*[30,31] and many others showed that only certain regions of the ϕ–ψ space (often referred to as Ramachandran space) are energetically preferred by most L-amino acids. The ability to design templates with specific secondary structural features is critical to the *de novo* design of peptides and peptide mimetics.

An equally critical feature is the 3D structure (topography) of the amino acid side chain moieties, often referred to as chi (χ) space.[19] As illustrated in Fig. 1.1, each side chain χ^1 torsional angle (and some of the subsequent torsional angles in longer side chains, χ^2, χ^3, etc.) can assume three low energy staggered conformations (rotamers): -60° [*gauche*(-), *g*(-)]; +60° [*gauche*(+); *g*(+)]; and ± 180° [*trans*, *t*]. In the case of a *g*(-) conformation of an L-amino acid, the side chain will "point" toward the *N*-terminus of the peptide chain; for the *g*(+) conformation , the side chain group will be located over the peptide backbone; and for the *trans* conformation, the side chain group will be directed toward the *C*-terminus of the peptide chain. Thus, in a chain of four or five residues, different dispositions of side chain groups in terms of χ^1 space will give rise to a remarkable diversity of 3D surfaces even with a single peptide backbone template. Design in chi space then is to build side chain structural features either covalent, steric or steroelectronic that will force or bias the various torsional angles to specific values that might be favorable for molecular recognition.

The side chain conformation can be controlled in several ways, for example, by introducing an alkyl group at the β-position or on the ring of an aromatic amino acid residue to constrain χ^1 and χ^2, respectively. These kinds of modifications generally do not perturb the backbone conformation drastically, and still allow the peptide backbone structures and side chain torsional angles some degree of flexibility. The orientation of the aromatic ring of an aromatic amino acid residue also can be restricted by these modifications. Introduction of extra alkyl groups also enhances the lipophilicity of the peptide analogue, and can thus help in overcoming blood-brain barrier and other membrane barrier problems frequently associated with native peptides.

β-Substitution generates a second asymmetric center and thus four stereoisomers (*S,S; S,R; R,S; R,R*). Since each stereoisomer has three low energy side chain conformations, twelve different 3D arrangements are available in principle for the β-alkyl α-amino acids. The populations of χ^1 conformers can be determined by modern NMR techniques measuring homonuclear and heteronuclear coupling constants.[32,33] Another useful side chain topographical constraint is to insert a covalent bond between the aromatic ring and the backbone of an α-amino acid residue. For example, 1,2,3,4-tetrahydroisoquinoline carboxylic acid (Tic) is a cyclic constrained analogue of phenylalanine in which a methylene bridge is placed between the nitrogen and the 2′-carbon of the aromatic ring (Fig. 1.3).

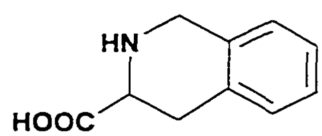

Fig. 1.3. 1,2,3,4-Tetrahydroisoquinoline carboxylic acid (Tic)

Using extensive computational, NMR and X-ray methods, Hruby and coworkers showed that Tic could be a part of a β–turn or an α-helix and that the preferred conformations were $g(-)$ or $g(+)$.[34] Successful applications of some topographically constrained amino acids in peptidomimetic design have been achieved.

2. Modification of the Peptide Backbone

Backbone modifications generally refer to the isosteric or isoelectronic exchange of NHCO units in the peptide chain and/or introduction of additional groups (CH_2, O, etc.). Some of these peptide bond surrogates are listed in Fig. 1.4 and have been reviewed by Spatola.[35] A detailed discussion of these modifications is beyond the scope of this brief review, but a few features will be highlighted here. Amide bond isosteres resemble the peptide bond to varying degrees. However, they are more resistant to proteolytic cleavage. Such modifications can serve to introduce local backbone constraints, e.g. *N*-alkylation greatly restricts the ϕ torsional angle but eliminates the hydrogen bonding donating capability of the amide bond. *N*-Methylated amino acids have been incorporated into bioactive analogues of opioid peptides,[36] bradykinin,[37] thyrotropin releasing hormone (TRH),[38] angiotension II,[39] and cholecystokinin (CCK).[40-42] α-Alkyl amino acids show restricted rotation around the $N\text{-}C\alpha(\phi)$ and $C\alpha\text{-}C(O)(\psi)$ bonds. Aib (α-aminoisobutyric acid), a naturally occurring α-alkyl amino acid observed in channel-forming peptides has been extensively investigated. Aib residues favor the formation of α- and 3^{10} helices.[43,44] This residue has been incorporated into numerous bioactive peptides including enkephalin,[45] angiotensin,[46] and bradykinin.[47] Other backbone-type modifications include retro-inverso,[48] reduced amide,[49] thiomethylene,[50] oxomethylene,[51]

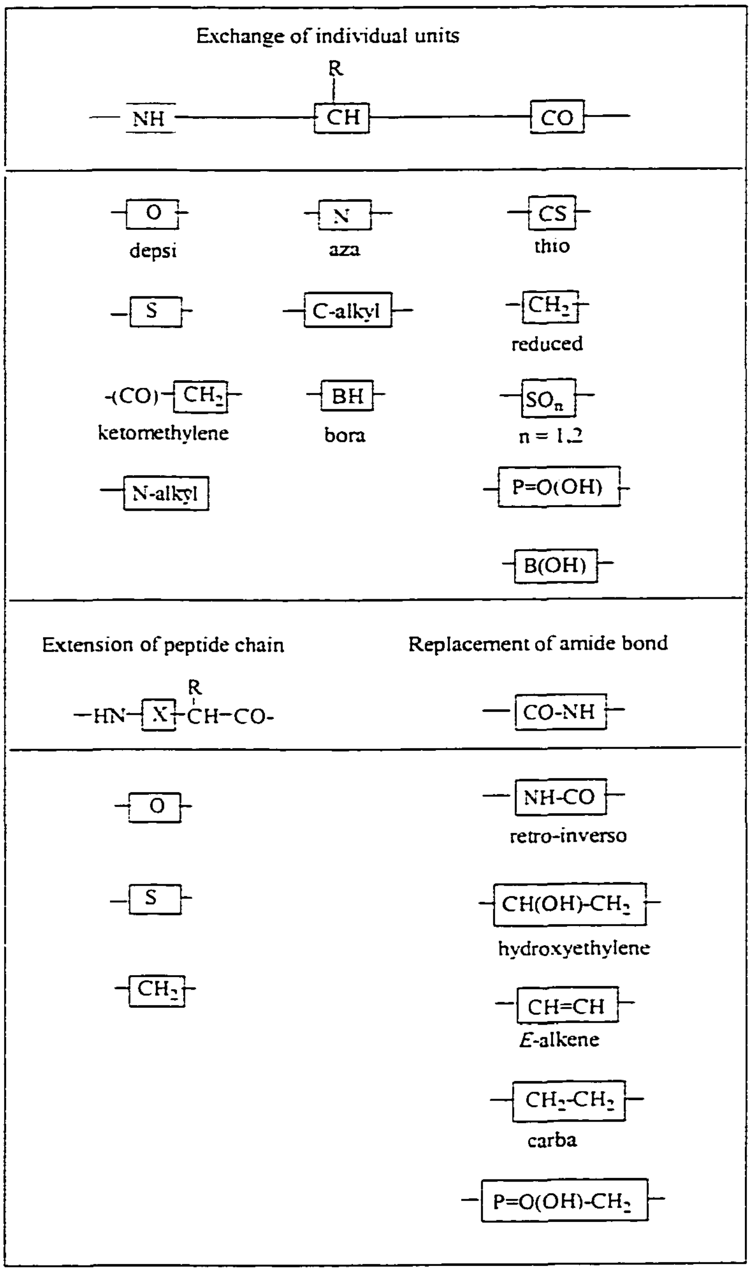

Fig. 1.4. The most frequent modifications to the peptide backbone.

ethylene,[52,53] thioamide,[54] olefinic[55,56] and ketomethylene[57] analogues and many others. Each modification has its own unique stereoelectronic and stereostructural features that need to be considered before replacement of the peptide bond as a "peptide mimetic." For example, retro-inverso analogues modify the secondary structure and "invert" the topographical features of the peptide. Olefinic analogues show a high degree of conformational rigidity, at the expense of greatly decreased hydrogen bonding capabilities and increased lipophilicities.

3. Global Restrictions of Conformation in Peptides and Peptidomimetics

Global restrictions in the conformation of a peptide are possible by limiting the flexibility of the peptide through cyclization when examining peptide structure-activity relationships. For this purpose, the amino acid side chain groups and backbone moieties that are not directly involved in molecular recognition are covalently connected together or to the peptide backbone.[10,12] A selection of cyclic side chain to side chain constraints is illustrated in Fig. 1.5. It should be recognized that other kinds of cyclic constraint are possible including side chain to *C*- or *N*-terminal, side chain to backbone nitrogen (Fig. 1.6) rather than $C\chi$ to $C\chi$ as in Fig. 1.5. Depending on the size of the side chain and the ring size, ϕ, ψ, ω, and χ angles either will be fixed or will have biased or limited flexibility. Short range cyclization (residue i to i-1 or $i+1$) can significantly reduce the conformational space accessible to the peptide segment in which they are incorporated. A $C\alpha_i$-to-N_i-type cyclization is achieved *via* alkylation or acylation of the backbone nitrogen atom or *via* trans guanidation. These types of cyclizations significantly restrict the ϕ torsion angle.[58] $C\alpha_i$-to-N_{i-1} type cyclizations are achieved either through alkyl, thioether or acyl linkages.[44]

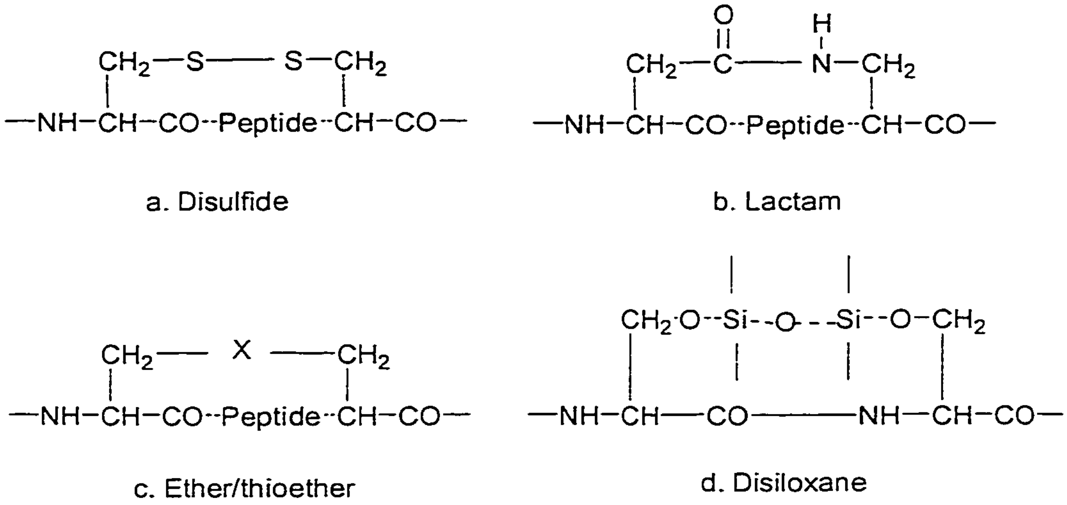

Fig. 1.5. Covalent side-chain to side-chain cyclizations.

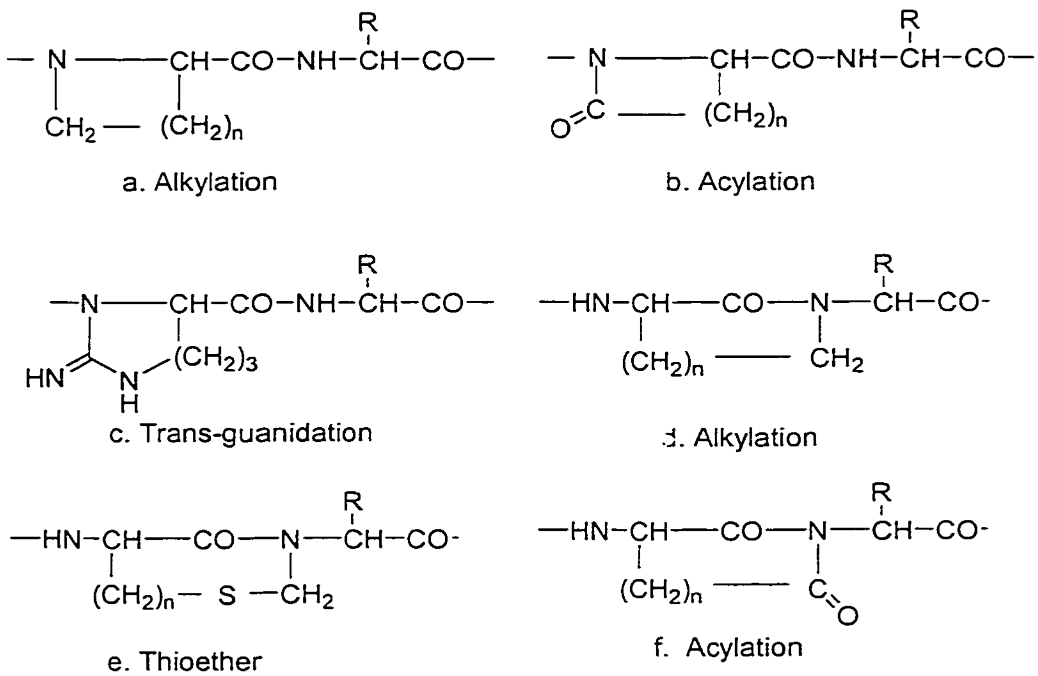

Fig. 1.6. Cyclic constraints: $C\alpha_i$-N_i-type (**a**, **b**, **c**) and $C\alpha_i$-N_{i+1}-type (**d**, **e**, **f**).

Side chains that have reactive functional groups offer the possibility of covalent attachment to each other to form cyclic peptides. Thus disulfides, lactams, lactones, thioethers, ethers, substitututed aromatics, ureas, ketones, etc. can be formed by reaction of various side chain groups to form cyclic, constrained peptides (some examples are shown in Fig. 1.5.)

Disulfide bond formation between two cysteine side chains is used by nature to form cyclic peptides and proteins, and also is a popular means of designed cyclization in peptide analogues. If the size of the ring is small, ϕ, ψ, and χ angles may become restricted with such a cyclization, and/or secondary structures (α-helix, β-turns, β-sheets) may be further stabilized. If β-carbons are substituted with alkyl groups (e.g. penicillamine), additional constraints on the disulfide conformation and chirality can be obtained *via* transannular effects. Lactam formation between a side chain that has an amino group (Lys, Orn, etc.) and one that has a carboxylic group (e.g., Asp, Glu) greatly restricts the backbone conformation and ϕ, ψ, ω and χ angles in the two side chain groups. For example, disulfide containing cyclic enkephalins, melanotropins, etc., and potent cyclic **MSH** and CCK lactam analogues have been made.[52,59-66] Disiloxane linkages (-Si-O-Si-) have been constructed between two serine residues that are close to each other. Conformational studies indicate that this latter type of constraint leads to a conformational twist in the peptide that is analogous to a type I β-turn. Many of the other types of constraints have been used to stabilize β-turns or α-helices or β-sheets in peptides and miniproteins.[10-12,67-69] This approach is now widely used as a method to design bioactive peptides and peptidomimetics with high potency, receptor/acceptor selectivity for stability against proteolytic degradation, bioavailability and membrane permeability.

A. Reverse Turns (β-Turns and γ-Turns)

The surface localization of turns in proteins and the predominance of turns in peptides containing potentially critical pharmacophore information, have led to the hypothesis that turns play critical roles in a myriad of recognition events. Reverse turns are classified into γ-turns, consisting of three residues (sometimes referred to as a C7 conformation), and β-turns (C10 conformation), formed by a tetrapeptide (Fig. 1.7).[67] β-Turns are classified further according to the backbone dihedral angles of the second and third residues.[31]

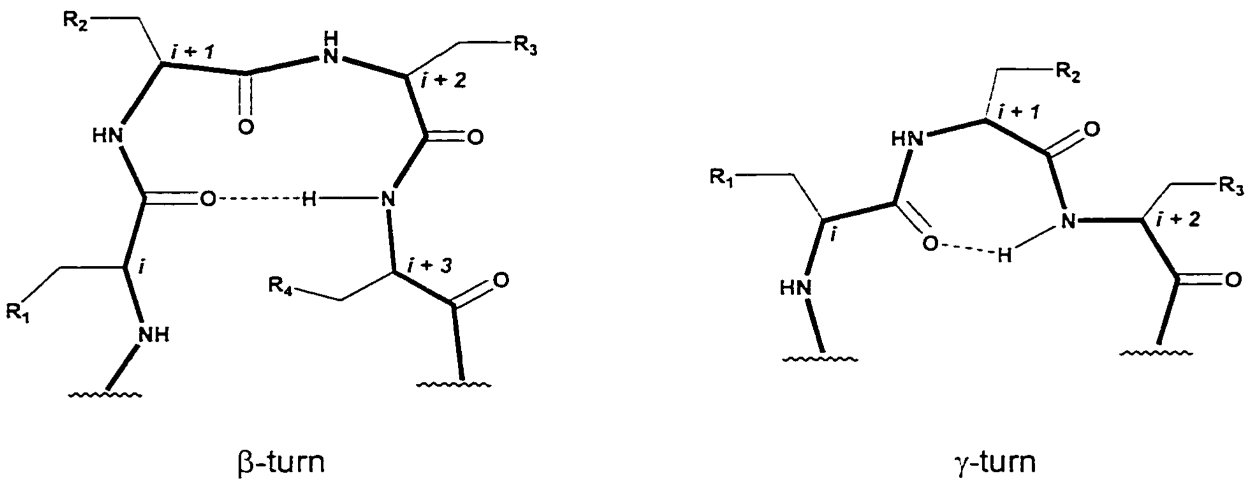

Fig. 1.7. Structures of reverse turns

The stabilization of turn structures in biologically active polypeptides discussed above has been very successful in designing a wide variety of peptides and peptidomimetics with novel structures and unique biological profiles.[10-12,18,67,68] This success has been widely applicable to both agonists and antagonists in large part because not only backbone but also side chain groups can be placed in three dimensional space with topographies similar to, or identical with, natural peptides and proteins.

More recently great effort has been made to design β- and γ-turn mimicking non-peptide or pseudopeptide scaffolds. In general these have met with more limited success with bioactive peptide ligands where the β-turn itself contains most of the pharmacophore elements. This approach has been reviewed.[15,17] A selection of β- and γ-turn mimicking scaffolds is shown in Fig. 1.8.

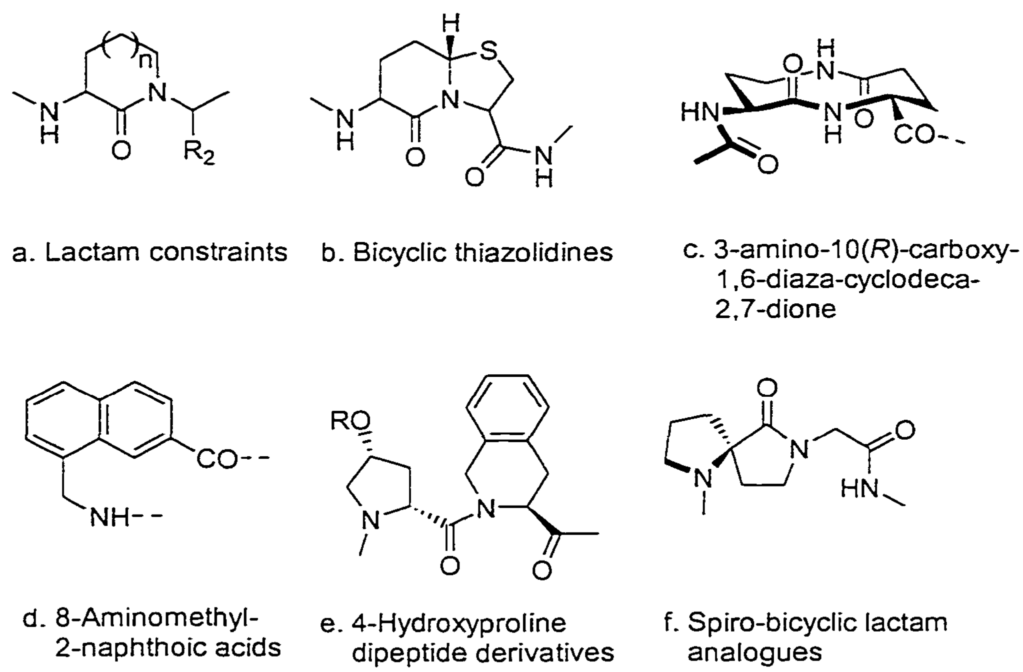

Fig. 1.8. β- and γ-Turn mimetics of various types.

Lactam constraints (Fig. 1.8a) cause a turn in the basic peptide backbone, but it is difficult to place R groups stereospecifically to match peptide side chain moieties. The bicyclic thiazolidines (Fig. 1.8b) and the 10-membered cyclodecadiones (Fig. 1.8c) are type II β-turn mimetics with more promise since they can be derived from a chiral pool of amino acids. The fused bicyclic ring (naphthalene, Fig. 1.8d) used to constrain a portion of the peptide, corresponds to the central dipeptide part of a β-turn. Dipeptides such as the one formed between 4-hydroxyproline derivatives and tetrahydroisoquinoline carboxylic acid (Tic, Fig. 1.8e) are known to induce constraints similar to type II′ β–turns. The spiro-bicyclic systems (Fig. 1.8f) are also representative of β-turns. A vast number of examples of reverse turn mimics are available in the literature.[15,17,67,70-73]

B. Oligopyrrolinones: β-Strand/β-Pleated Sheet Mimetics

The binding interactions of the backbones of many proteases and their substrates or inhibitors are known to proceed *via* hydrogen bonding leading to the formation of β-pleated sheets, either parallel or antiparallel. In either case, the side chains are oriented orthogonal to the sheet surface with an antiperiplanar disposition of adjacent side chains of the same strand. Thus the conformational requirements of a β-strand mimic are appropriate side chain trajectories as well as hydrogen bonding capabilities (Fig. 1.9). This strategy has been exploited in the design of inhibitors of the aspartyl protease renin[74] and of HIV-1 protease.[75,76]

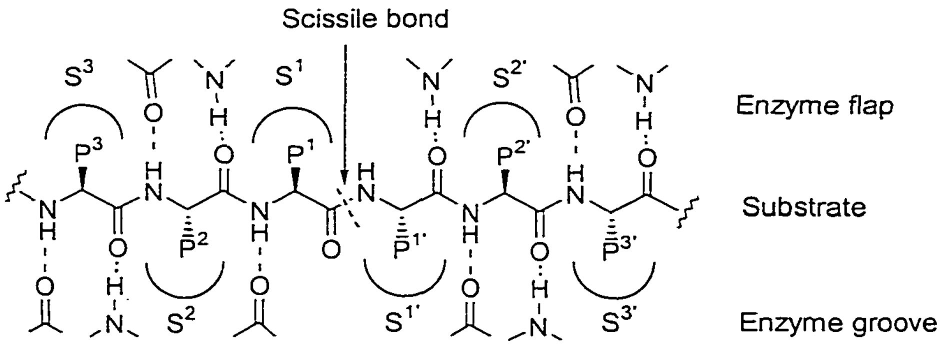

Fig. 1.9. Typical aspartic acid protease active site.

To address the bioavailability and proteolytic stability problems associated with traditional peptidyl peptidomimetics, Smith *et al.* designed a pyrrolinone-based non-peptide scaffold for β-strand mimics.[77,78] The design was derived from the native peptide in the extended conformation (Fig. 1.10). Displacement of the amide nitrogens from the backbone allowed for incorporation of the olefins (enaminones), and cyclization of the nitrogens onto the backbone then generated pyrrolinone rings. This scaffold compares with the peptide bond in terms of basic nitrogens and the hydrogen bonding ability of the carbonyls. Furthermore the olefin linkage and cyclization of the nitrogens provide an element of rigidity which might confer a degree of conformational stability.

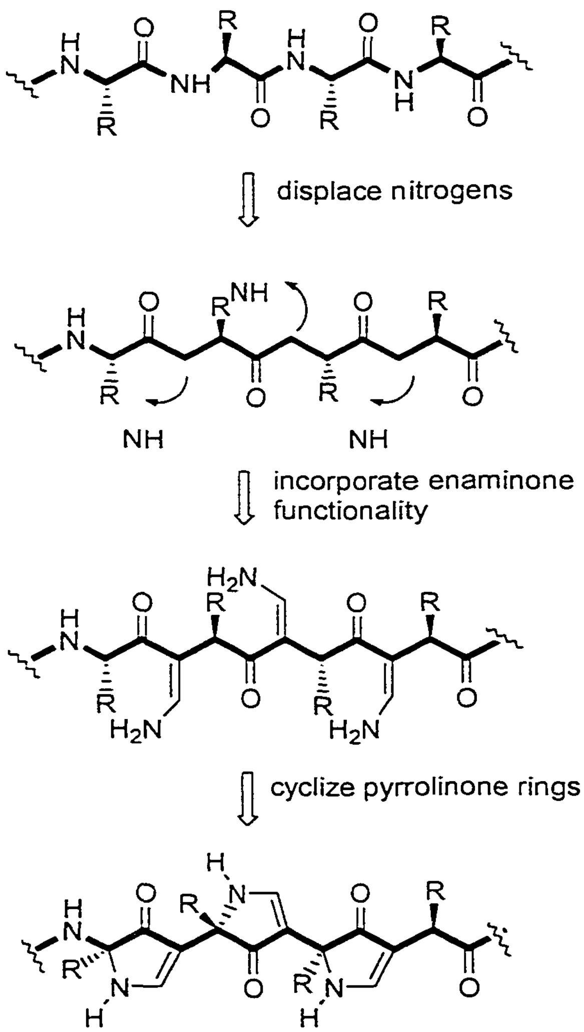

Fig. 1.10. Conceptual derivation of pyrrolinone-based β-sheet mimetics.

To determine whether a series of 3,5-linked pyrrolinone rings could adopt an energetically favorable conformation mimicking a peptide β-strand, a variety of molecular mechanics calculations with the MM2 force field were performed. Comparison of dipeptide **1.1** and bispyrrolinone **1.2** indicated that significantly fewer degrees of freedom are available to **1.2** (Fig. 1.11a). The ψ and ω angles of bispyrrolinone **1.2** are locked at 120 and 180° respectively; only ϕ can rotate through 360°. Calculation of the energy of rotation about the ϕ bond in **1.2** revealed an overall minimum at 310° (*vide infra*) and a local minimum at 205°, the latter mimicking the desired β-strand ϕ angle. Examination of the lowest energy linear conformations of pairs of adjacent pyrrolinones revealed a six-membered-ring hydrogen bond between a carbonyl oxygen and the NH of the neighboring ring (Fig. 1.11b).

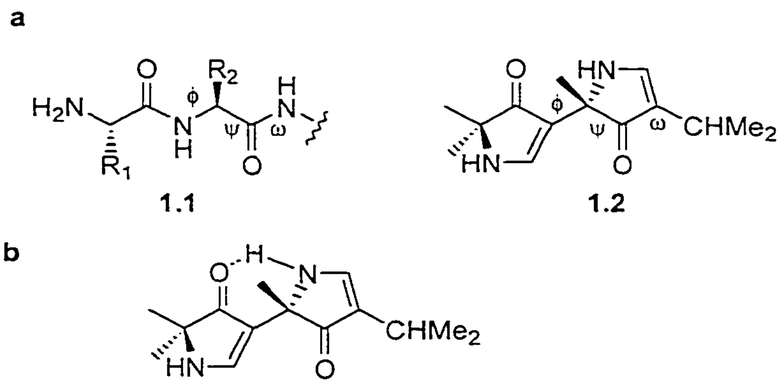

Fig. 1.11. a) Rotational degrees of freedom for dipeptide **1.1** and bis(pyrrolinone) **1.2**; b) Six-membered-ring hydrogen bond linking adjacent pyrrolinones in the lowest energy conformation of **1.2**.

Using the structure of the Merck compound L-682,679, a potent inhibitor of the HIV-1 protease (IC_{50} = 0.4 nM, CIC_{95} = 6 μM) as a model, a pyrrolinone-based motif was generated in which the $P_{1'}$-$P_{3'}$ tripeptide sequence in L-682,679 was replaced by a bis(pyrrolinone) bearing the three requisite side chains, and the P_1 Phe, the hydroxyethyl transition-state mimic, and the *N*- and *C*-terminal endcaps were also adopted (Fig. 1.12). The resulting bis(pyrrolinones) were then compared by cellular antiviral assays with L-682,679 (Table 1.1). The $P_{3'}$ tert-butyl amide and methyl ester endcaps gave somewhat diminished potency in enzyme inhibition (IC_{50}) compared with their original primary amides. In both the Boc and 3-hydroxy THF series, the methyl ester analogues were slightly more active than the *tert*-butyl amides.

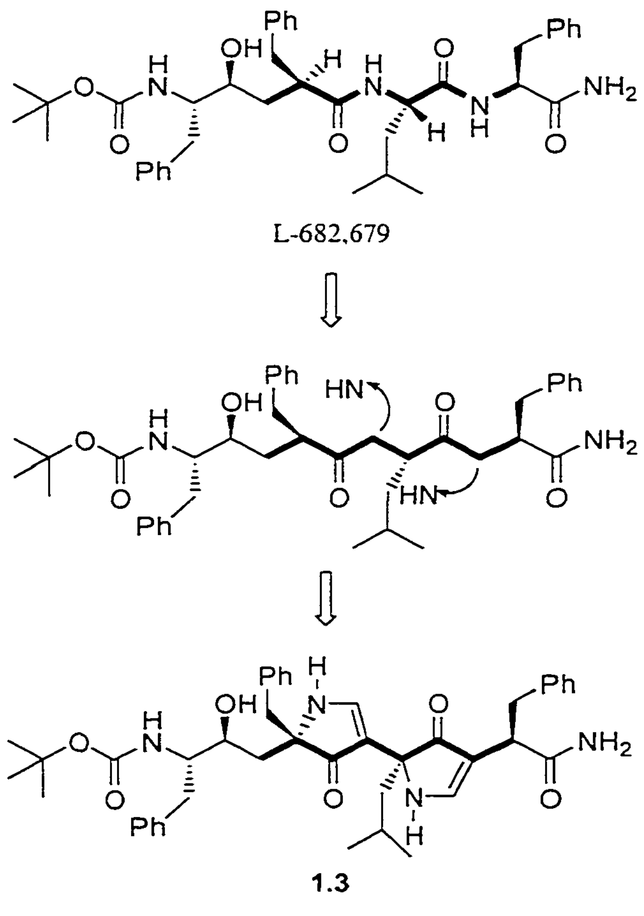

Fig. 1.12. Merck inhibitor L-682,679 as the model for a prototypical pyrrolinone-based inhibitor **1.3**. Pyrrolinone motif is generated by NH displacement from peptide backbone.

Table 1.1. Bioassay aata: inhibition of HIV-1 protease (IC_{50}), cellular antiviral activity (CIC_{95}) and C/I ratios.

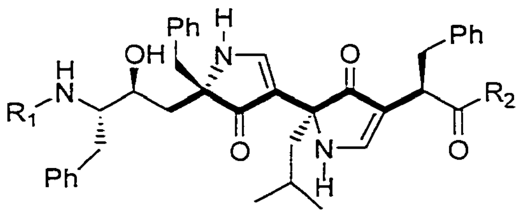

Inhibitor	N-terminus	C-terminus	IC_{50} (nM)	CIC_{95} (nM)	C/I
L-682,679	Boc	NH_2	0.6	6000	10000
1.3	Boc	NH_2	10	1500	150
1.4	Boc	OMe	37		
1.5	Boc	NH-*t*-Bu	48		
1.6	Furanyl Carbamate	NH_2	1.3	800	615
1.7	Furanyl Carbamate	OMe	2	400	200
1.8	Furanyl Carbamate	NH-*t*-Bu	3.3	800	242

In the furanyl carbamate series, the *C*-terminal *tert*-butyl amide **1.8** was as active as the corresponding primary amide **1.6** in the cellular assay (CIC_{95}), while the methyl ester **1.7** gave the lowest value observed to date. The superior C/I ratios for these two compounds compared with the primary amide **1.6** indicate better transport properties, which could be attributed to decreased solvation of the mimetics.

Chapter 2

DESIGN AND SYNTHESIS OF TOPOGRAPHICALLY CONSTRAINED AROMATIC AMINO ACIDS

2.1 INTRODUCTION

In order to understand the nature of peptides, it is necessary to understand the characteristics of the amino acid subunits. Amino acids contain an amino group, a carboxyl group, a hydrogen atom, and a side chain group all connected to an α carbon atom. Amino acids in solution generally exist as zwitterions, that is their amino and carboxyl groups are both charged at pH values between 3 and 9.

As amino and carboxyl groups are common to all amino acids, it is the side chain group that defines amino acids and determines their individual characteristics. The chemical and structural natures of the side chain groups determine the structure and function of the amino acid within the context of a protein or peptide. A variety of functional groups are available as side chains, including acidic, basic, hydrophobic, hydrophilic, redox-active, bulky, and compact chemical moieties. This range of functional groups provides the chemical basis of the vast array of biochemical properties displayed by peptides and proteins.

There is overwhelming evidence that the stereochemical properties of the side chain groups of amino acid residues in bioactive peptides are extremely important in peptide-receptor/acceptor recognition and bioactivity.[10,13] A topographical approach has been developed in our lab to explore the side chain stereochemical requirements for the binding of peptides to their receptors and for signal transduction.[13] This approach involves incorporation of conformationally constrained amino acids into polypeptide or non-peptide templates, and requires novel amino acids. What are the principles we need to follow in the design of such topographically constrained novel amino acids? How do we know what kind of side chain orientation may have the most promising opportunity for maximizing molecular recognition and biological transduction? Although these fundamental issues cannot be fully answered until a variety of these novel amino acids are incorporated into biologically active peptides, a reasonable hypothesis is that the conformation has to be consistent with nature's preferences to produce biological functions. Thus, the biased conformations of the side chain groups must have preferred orientations consistent with those accessible to the natural amino acids and not difficult to obtain energetically in ligand-receptor interactions. In principle, this can be done by introducing conformational constraints into the natural amino acids that "choose" specific conformations out of the multiple low energy conformations available to the natural amino acids.

In order to put in side-chain constraints without disturbing the backbone conformation too much, we chose to manipulate the β-carbon of the natural amino acids. Substitution of the diastereotopic β-protons with various alkyl or aryl groups not only restricts the χ^1 and χ^2 torsional angles, but also produces a new stereogenic center. A series of β-branched aromatic amino acids including β-methylphenylalanine, β-methyltyrosine, β-methyltryptophan, 2′,6′-dimethyl-β-methyltyrosine, and 2′,6′-dimethyl-β-methylphenylalanine have been designed and synthesized in our lab (Fig. 2.1).

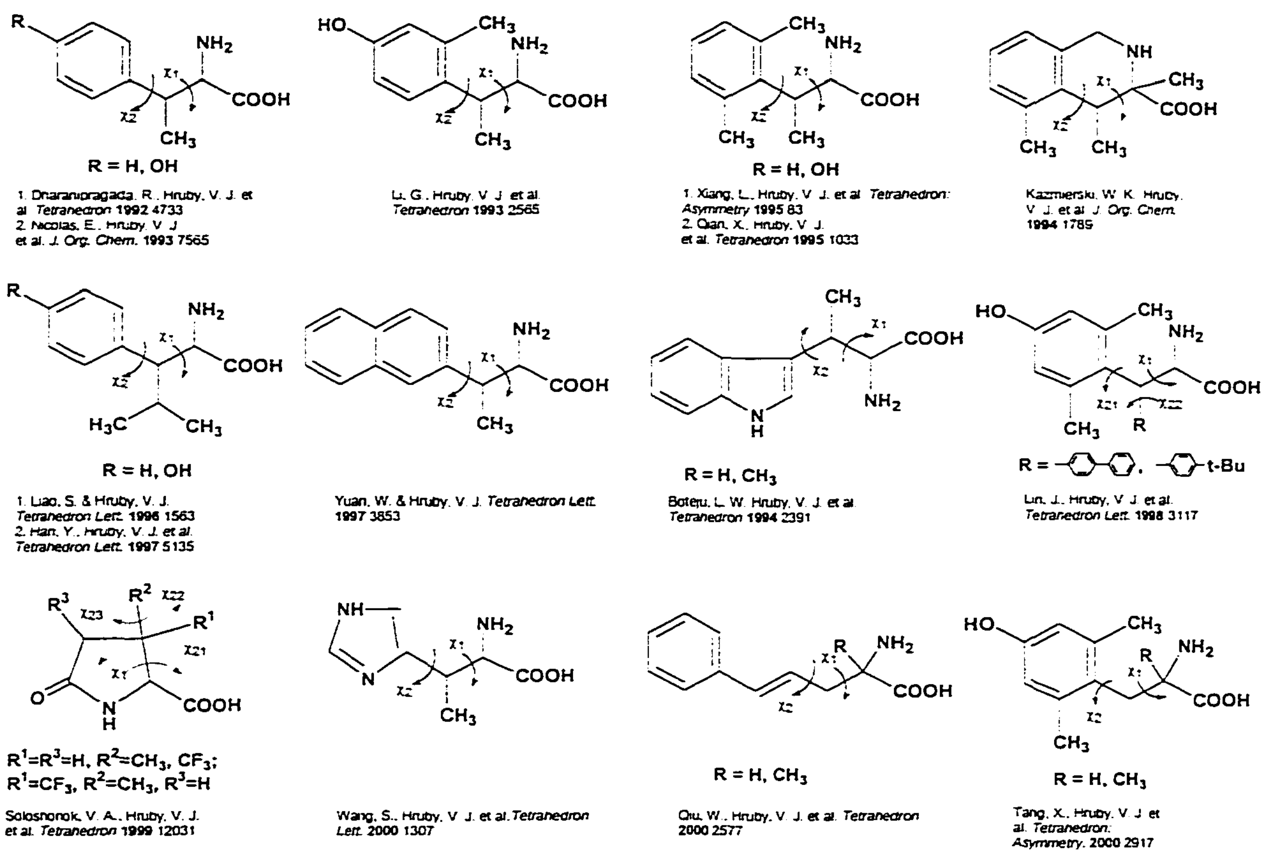

Fig. 2.1. Topographically constrained aromatic amino acids.

Incorporation of these unusual amino acids into bioactive peptide hormones has produced highly selective and potent peptide hormone analogues, and provided new insights into the stereochemical requirements in peptide-receptor interactions.[79-82] These studies also have shown that the development of new topographically constrained amino acids with more restriction on side chain mobility could be crucial to the study of conformation-activity relationship of peptide ligands. Thus, highly conformationally constrained novel amino acids have been desired to meet the needs in the design of topographically constrained bioactive peptides.

For example, in an effort to develop ligands based on the endogenous opioid peptide enkephalin (H-Tyr-Gly-Gly-Phe-Leu-OH or H-Tyr-Gly-Gly-Phe-Met-OH) that would be highly potent and selective for the δ opioid receptor (rather than the μ or κ opioid receptor), the cyclic analogue of enkephalin c[DPen^2, DPen^5]enkephalin (Fig. 2.2) was designed in the Hruby group. In this analogue the Gly^2 and Met^5 (or Leu^5) residues were replaced by D-penicillamine (D-Pen, β,β-dimethylcysteine) and formed a 14-membered disulfide ring.[61] The compound was found to be highly potent and selective for the δ opioid receptor[61] and to be completely stable to proteolytic

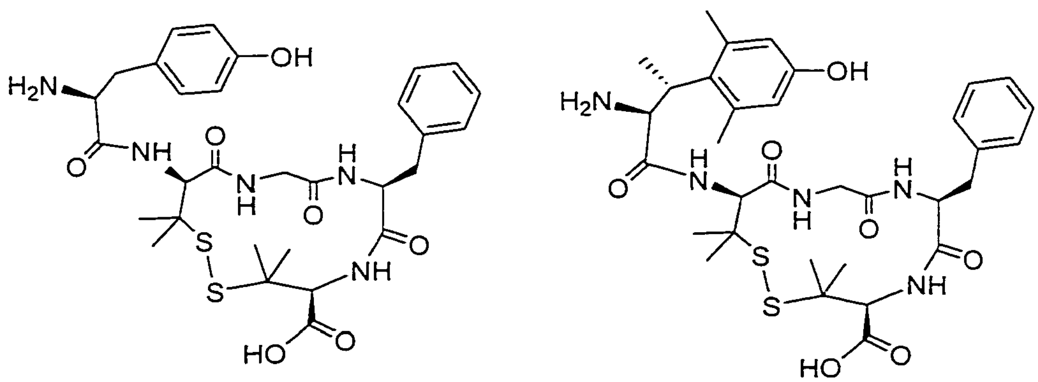

DPDPE [(2*S*,3*R*)TMT^1]**DPDPE**

Fig. 2.2. Structures of DPDPE and [(2*S*,3*R*)-TMT^1]-DPDPE.

breakdown *in vitro* and *in vivo*.[83-85] Extensive biophysical studies on DPDPE and some of its critical analogues using NMR,[86-88] molecular dynamics[89] and X-ray crystallography[90,91] clearly established the preferred conformation of the 14-membered ring template of the cyclic analogue, but left unanswered the unambiguous topographical preferences of the side chain groups of the critical Tyr^1 and Phe^4 residues. Though we had established a highly consistent three dimensional conformation for the 14-membered disulfide-containing ring system from the above mentioned studies, it was also necessary to determine the preferred side chain conformations of the Tyr^1 and Phe^4 residues, two key pharmacophore elements for the δ opioid receptor. The preferred side chain conformation for Phe^4 was obtained by the use of β-methylphenylalanine (all four stereoisomers)[92] and β,β-dimethylphenylalanine. The only potent and highly δ opioid receptor ligand was the *(2S,3S)*-β-$MePhe^4$-containing analogue of DPDPE[81] and subsequent NMR and computational studies[82] demonstrated that the *gauche*(-) χ^1 angle was the critical topographical requirement for δ opioid receptor selectivity. Extensive NMR studies further showed that the backbone conformation was very similar to that in DPDPE. The determination of the preferred side chain conformation for the Tyr^1 residue turned out to be a little more difficult. When all four isomers of β-methyltyrosine were incorporated into DPDPE,[84] though [*(2S,3R)*-β-MeTyr]-DPDPE turned out to be the most potent and selective ligand, it was significantly less potent and selective than DPDPE, and also was somewhat conformationally flexible.[82]

These problems were overcomed by the design and asymmetric synthesis of the four stereoisomers of β-methyl-2',6'-dimethyltyrosine.[93] Computational calculations showed that each of the four isomers (*2S,3S; 2S,3R; 2R,3S; 2R,3R*) had its own unique χ^1 side chain conformation and significant restriction of the χ^2 torsional angle also was obtained.[94] By dynamic NMR measurement, the energy barrier for rotation about the χ^2 angle,[94] correlated very well with the results obtained from computational studies,[19] was determined.

When each of the four stereoisomers was placed in DPDPE analogues, very interesting biological activities were obtained (Table **2.1**).[79,80] As can be seen only the analogue [*(2S,3R)*TMT^1]DPDPE has a high potency and δ opioid receptor selectivity. As would be predicted from the topographical differences, all three other stereoisomers were

100 to >10,000 less potent in binding to the δ opioid receptor. Interestingly, however, the [(*2S,3S*)-TMT[1]]DPDPE analogue bound quite well to the μ opioid receptor, suggesting that the μ opioid receptor had a different topographical side chain requirement for the Tyr[1] residue than the δ receptor. This will be further evaluated using μ opioid ligands. Even more interesting was the observation that in functional assays involving information transduction, the (*2S,3R*)TMT[1]-analogue was completely specific as an agonist at the opioid receptor with an EC_{50} of 1.8 nM in the MVD (δ receptor) assay (Table **2.2**) and showed no agonist activity up to 60,000 nM in the guinea pig ileum (μ receptor) assay.

Table 2.1. Binding affinities and selectivities of the four [TMT[1]]DPDPE analogues in competition with [^{3}H]CTOP (μ) and [^{3}H][*p*-ClPhe^4]DPDPE (δ) in rat brains.[79]

Peptide	IC_{50}, nM [^{3}H]CTOP	IC_{50}, nM [^{3}H][*p*-ClPhe^4]DPDPE	Selectivity (μ/δ)
DPDPE	609	1.6	380
[(2*S*,3*S*)-TMT[1]] DPDPE	722	211	3
[(2*S*,3*R*)-TMT[1]] DPDPE	4270	5.0	850
[(2*R*,3*R*)-TMT[1]] DPDPE	77100	3500	22
[(2*R*,3*S*)-TMT[1]] DPDPE	0% at 10 μM[a]	9% at 10 μM[a]	N/A

[a]Percent of maximum effect achieved with this concentration of peptide.

Table 2.2. Potency and selectivity of [TMT[1]]DPDPE analogues in MVD and GPI bioassays.[79]

Peptide	EC_{50}, nM GPI (μ)	EC_{50}, nM MVD (δ)	Selectivity (μ/δ)
DPDPE	7300	4.1	1780
[(2*S*,3*S*)-TMT[1]]DPDPE	290	170	2
[(2*S*,3*R*)-TMT[1]]DPDPE	0% at 60 μM[a] (antag.,IC_{50}=5μM)	1.8	>33000
[(2*R*,3*R*)-TMT[1]]DPDPE	49900	2200	23
[(2*R*,3*S*)-TMT[1]]DPDPE	75% at 82 μM[a]	28% at 10 μM[a]	N/A

[a]Percent of maximum effect achieved with this concentration of peptide.

Indeed, the analogue was a weak antagonist at the μ opioid receptor, suggesting even more strongly that the μ opioid receptor requires a different side chain conformation for Tyr[1] for forming an agonist ligand-receptor complex. NMR studies and computational studies both determine that a trans χ^1 conformation is therefore the topographical pharmacophore requirement for the Tyr[1] residue for the δ opioid receptor.

2.2 DESIGN AND RETROSYNTHETIC ANALYSIS

Design. A β-methyl substituent can provide constraint to the side chain topography of the natural amino acids, but it is still not enough to trap a specific conformer. A bigger side chain substituent, such as an isopropyl group, could induce much higher energy barriers that restrict both χ^1 and χ^2 torsional rotations so that each diastereomer would favor only a few low-energy conformations. In addition, the newly derived amino acids can be considered as either derivatives of aromatic amino acids or of leucine or isoleucine (Fig. 2.3).

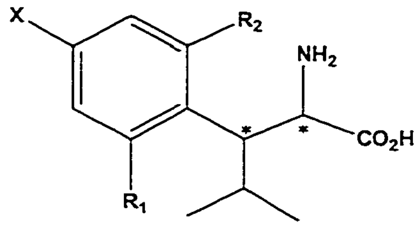

X = H, OH, R_1 = R_2 = H, CH_3

Fig. 2.3. β-Isopropyl aromatic amino acids

The combination of phenyl and isopropyl groups could provide significantly increased hydrophobicity. Thus, peptide ligands containing these novel amino acids will possess unique physical-chemical properties and provide useful information about the stereochemical requirements for the peptide ligand-receptor interaction.

Retrosynthetic Analysis. The target novel amino acids have two chiral centers, which generate four stereoisomers. The synthetically efficient way to prepare these four stereoisomers is divergent synthesis as late in the synthetic route as possible. Since all the target molecules have a common α-aminoisohexanoic acid moiety, the common starting point could be isohexanoic acid. The functionalization and chirality at the α-carbon could be generated and controlled by the chemistry developed in Evans' group and our laboratory if intermediate **2.2** is synthetically feasible[95] (Scheme 2.1).

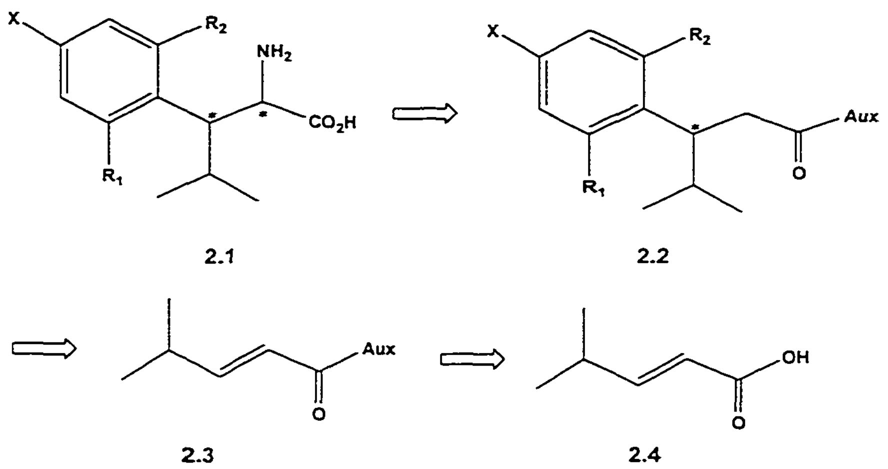

Scheme 2.1. Retrosynthetic analysis.

The precursor for asymmetric Michael addition could be synthesized from (2*E*-isohexenoic acid (**2.4**) coupled with a chiral auxiliary. Therefore, the key step in this synthesis is the asymmetric Michael addition.

2.3 SYNTHESIS AND DISCUSSION

Asymmetric Michael Addition. The stereoselective Michael addition of organometallic nucleophiles to α,β–unsaturated acyl derivatives which contain a chiral auxiliary is one of the most reliable methods to synthesize optically pure β-branched carbonyl derivatives.[96-100] Although various products have been prepared with high diastereoselectivity via asymmetric Michael addition with the use of chiral oxazoline,[98] ester,[99] and amide[100] derivatives, to our knowledge there have not been any examples of syntheses of highly sterically hindered β-isopropyl carboxylic acid derivatives by this method. As part of our effort to design and synthesize novel β-branched aromatic amino acids,[12,13] we have developed an efficient procedure to prepare these important intermediates (*i.e.* enantiomerically pure β-methyl carboxylic acid derivatives) via asymmetric Michael addition by using optically pure 4-phenyloxazolidinone as auxiliary.[93,101-104]

Using this methodology, asymmetric Michael addition of various Grignard reagents in the presence of CuBr·SMe_2 and dimethyl sulfide as co-solvent was carried out with high stereoselectivity and in reasonably good yields (Scheme 2.2). However, in our initial attempt to synthesize much more sterically hindered β–isopropyl aromatic amino acids, the Michael addition of isopropyl magnesium chloride to the Michael acceptor (4*R*,2*E*)-3-[3′-(4-methoxyphenyl)propenyl]-4-phenyl-2-oxazolidinone did not work well using the previously developed reaction conditions. Therefore, we re-examined this asymmetric Michael addition reaction in order to develop a general approach. A new Michael acceptor, (4*S*,2*E*)-3-(1-oxo-2-isohexenyl)-4-phenyl-2-oxazolidinone (**2.3**), prepared from precursor **2.4** as shown in Scheme 2.3, was tested, and it was found that it could react with a variety of aromatic Grignard reagents, including the highly sterically hindered 2′,6′-dimethylphenyl magnesium bromide under mild conditions as shown in Scheme 2.4.

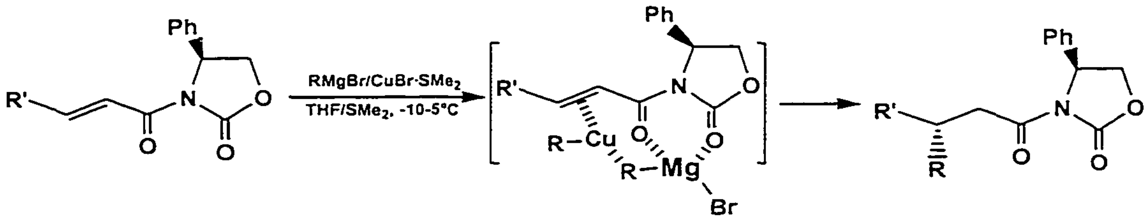

Scheme 2.2. Asymmetric Michael addition.

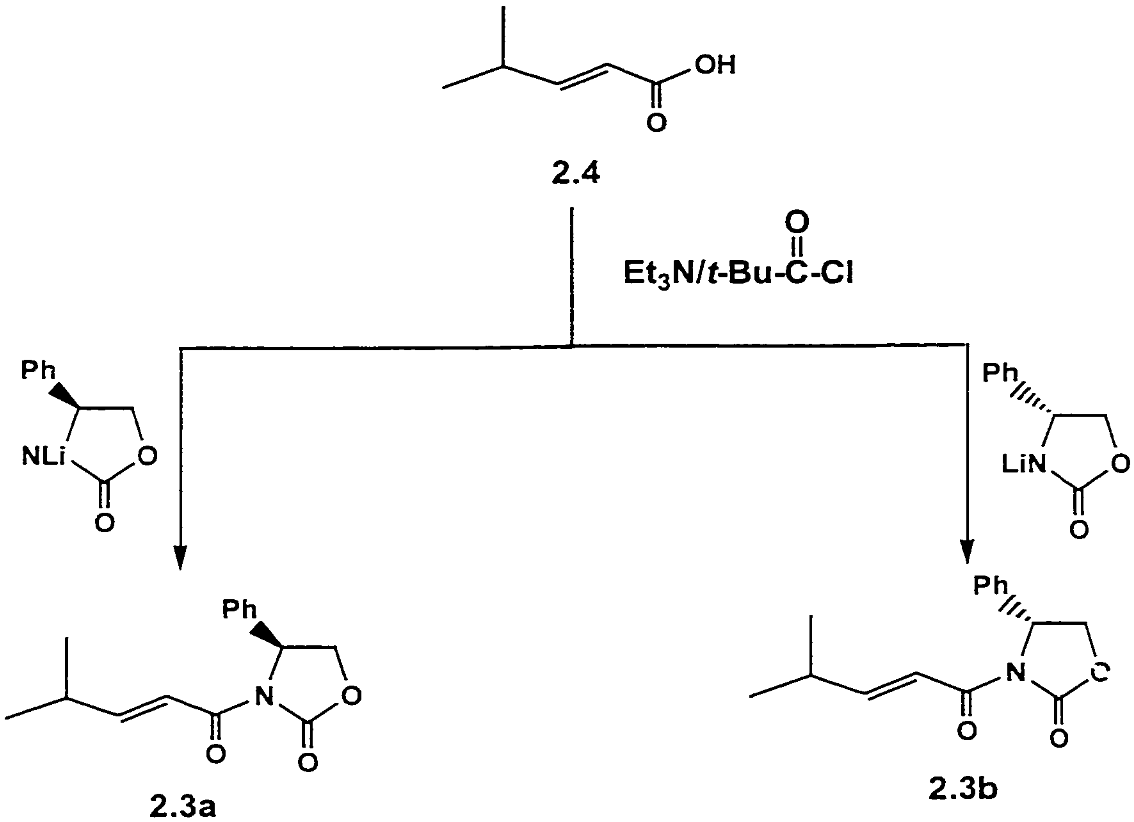

Scheme 2.3. Synthesis of β-isopropyltyrosine (1)

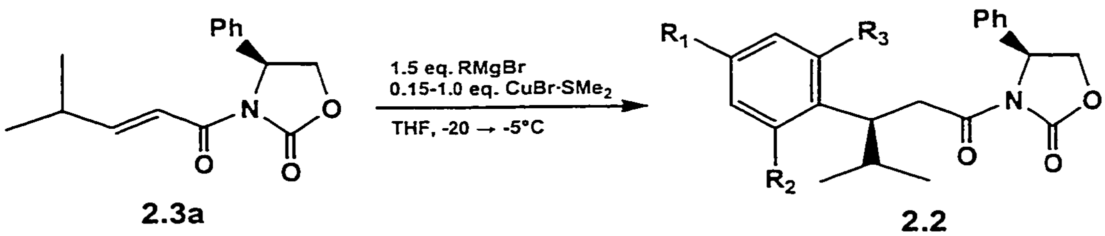

Scheme 2.4. Diastereoselective Michael addition of **2.3a**.

As compared to the previously reported reaction conditions,[93,101-104] we have found that the reactions of phenyl or substituted phenyl Grignard reagents only require catalytic amounts of CuBr·SMe$_2$ and no dimethyl sulfide as co-solvent. However, the para-methoxylated phenyl Grignard reagents needed one equivalent of CuBr·SMe$_2$ to secure reaction completion at a reasonable rate. Otherwise, 1,2-addition was observed, and even became the major reaction pathway. The reason why phenyl and para-methoxyphenyl Grignard reagents require different amounts of Cu(I) catalyst for 1,4-conjugate addition is not clear, and demands further investigation. In any case, all products were obtained in good to excellent yields with high optical purity (Table 2.3).

Table 2.3. Diastereoselective syntheses of β-aryl isohexanoic acid derivatives.

Entry	R_1	R_2	R_3	Yield[a]	de[b]	$\Delta\nu$(Hz)[c]
2.2a	H	H	H	82%	>90%	57.2
2.2b	OCH_3	H	H	97%	>90%	56.8
2.2c	OCH_3	CH_3	H	94%	>90%	69.9
2.2d	H	CH_3	CH_3	68%	>90%	98.9
2.2e	OCH_3	CH_3	CH_3	86%	>90%	98.6

[a] The yields were calculated from the weight of product after column chromatography purification; [b] The de was determined from ^{1}H NMR of crude product, de > 90% means that no diastereomer was observed by ^{1}H NMR; [c] $\Delta\nu$ is the chemical shift difference between the two methyl groups of the β–isopropyl group (250 MHz field).

An X-ray crystal structure of the compound (4*S*,3′*S*)-3-[3′-(2,6-dimethyl-4-methoxyphenyl)isohexanyl]-4-phenyl-2-oxazolidinone (**2.2e**) has been determined and is shown in Fig. 2.4. These results suggested that in the Michael reaction, the stereochemistry of the β-carbon was presumably induced from the *si*-face because the *re*-

face was shielded by the phenyl ring of the chiral auxiliary.[105] The chemical shift differences (Δν) of the two methyl groups of the β-isopropyl function could be used to assess the degree of constraint in these β-aryl isohexanoic acid derivatives. As seen in Table 2.3, Δν increases with the number of methyl substituents on the aromatic ring. Compounds **2.2d** and **2.2e** have the largest Δν values and compounds **2.2a** and **2.2b**, the smallest Δν values. The *para*-methoxyl substituent on the aromatic ring has no effect on Δν values. Thus, the presence of the two methyl groups on the phenyl ring and the β-isopropyl group produces torsional constraints, which greatly enhance the rigidity of β-aryl isohexanoic acid derivatives, which are very important precursors for the preparation of β-isopropyl aromatic amino acids.

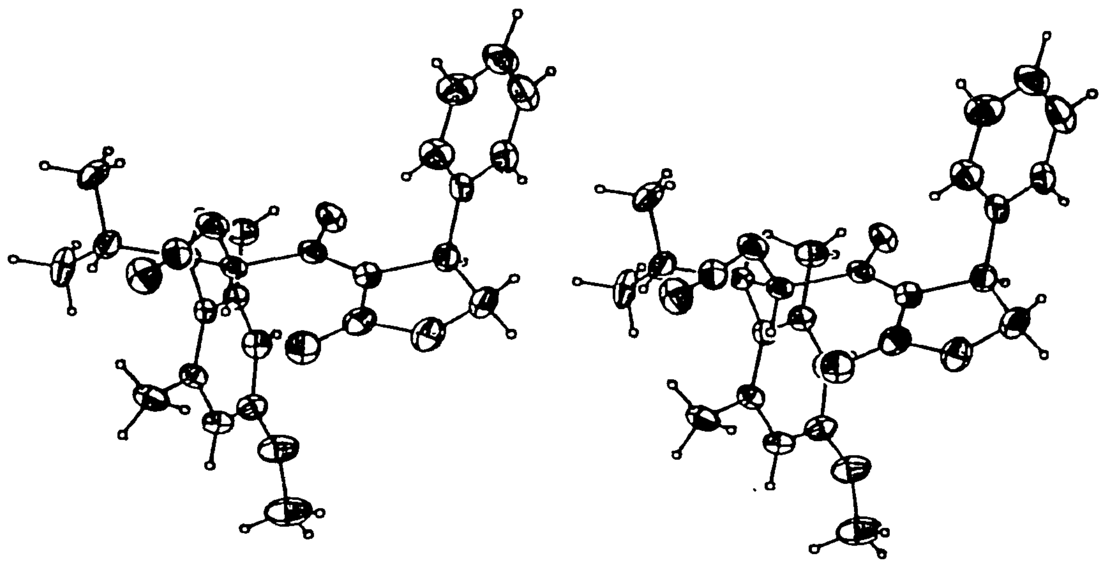

Fig. 2.4. Stereoview of the crystal structure of (4*S*, 3'*S*)-3-[3'-(2,6-dimethyl-4-methoxyphenyl)isohexanyl]-4-phenyl-2-oxazolidinone **2.2e**.

From key intermediate **2.2**, various β-isopropylaromatic amino acids become fairly easy to access with further 3- to 4-step modifications. Further transformation was exemplified by the total synthesis of all four stereoisomers of β-isopropyltyrosine.

Synthesis of β-isopropyltyrosine (β-*i*-PrTyr). The synthesis started from isohexenoic acid **2.4** (Scheme 2.3), which was coupled with enantiopure (4*R*)- or (4*S*)-4-phenyloxazolidinone to yield (4*R*)- or (4*S*)-4-phenyl-3-isohexenyl-2-oxazolidinone (2.3a and 2.3b) via the mixed anhydride method. Michael addition to the chiral Michael acceptor **2.3a** or **2.3b** produced β-4-methoxyphenyl isohexanoic acid derivatives **2.5a** and **2.5b** (Scheme 2.5).

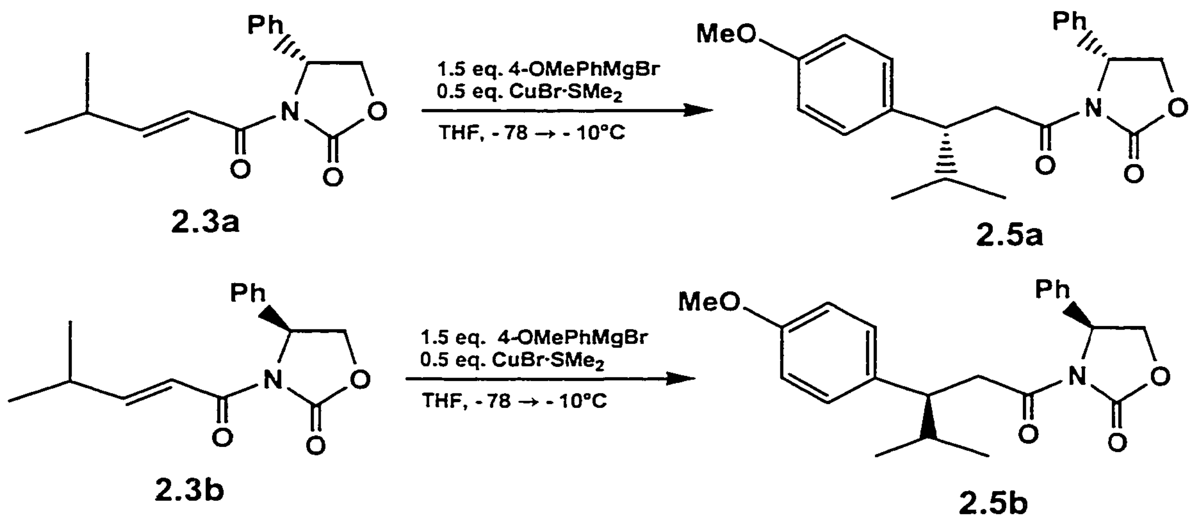

Scheme 2.5. Synthesis of β-isopropyltyrosine (2).

Introduction of the azido group to **2-5a** and **2-5b** was accomplished (Scheme 2.6) either directly by electrophilic azidation with trisyl azide,[95] or indirectly by bromination with NBS followed by S_N2 substitution with tetramethylguanidinium azide[106] to give α-azido products with opposite configurations at the α-position. As illustrated in Scheme

2.6, intermediate **2.5a** was converted into azido compounds **2.7a** and **2.7b** by these methods. In both cases the stereoselectivity was excellent (>90% de) in 75-85% yields. The other two stereoisomers were obtained from intermediate **2.5b** by the same methodology.

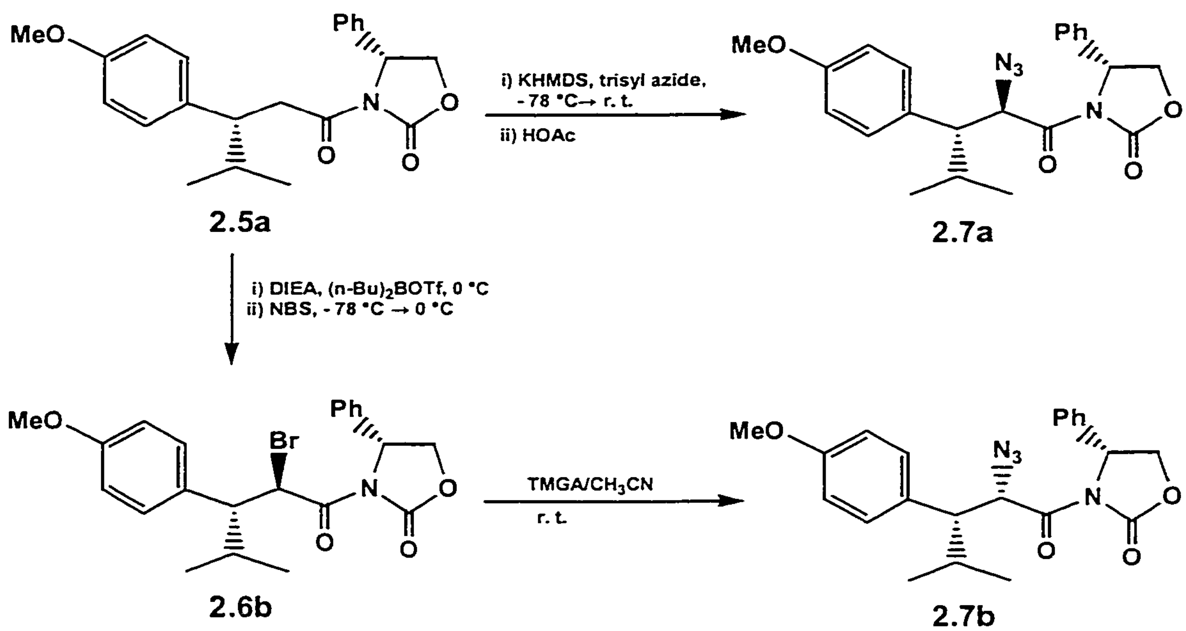

Scheme 2.6. Synthesis of β-isopropyltyrosine (3).

No diastereoisomers were detected by ^{1}H NMR in the crude azidation products in all cases, which indicated that the bulky β-isopropyl group does not have any effect on the chiral induction of the α-azido group. It suggested that in the asymmetric synthesis, the β-isopropyl and α-bromo groups were both induced from the Re-face, presumably because the Si-face was shielded by the phenyl ring of the oxazolidinone in the transition state of Michael reaction and bromination, and the bulky isopropyl group did not have any effect on the chiral induction of the α-bromo group.

Further transformations are exemplified with intermediate **2.7a** (Scheme 2.7). Azido acid **2.8a** was obtained by hydrolysis with recovery of the chiral auxiliary.[93,101-103]

No epimerization at the α-carbon was detected in any case. The hydrogenolysis of azido acid **2.8a** in the presence of 10% palladium/carbon in mixed solvents of HOAc and water (2:1, v/v) or EtOH containing 5% 2N HCl yielded the amino acid hydrochloride **2.9a**. Finally, the methoxy group was removed either by trifluoromethane sulfonic acid and thioanisole in TFA, or by NaI in 47% hydrobromic acid[107] to yield β-isopropoyltyrosine **2.10a**. Using the same methodology the other three stereoisomers **2.10b** to **2.10d** were synthesized.

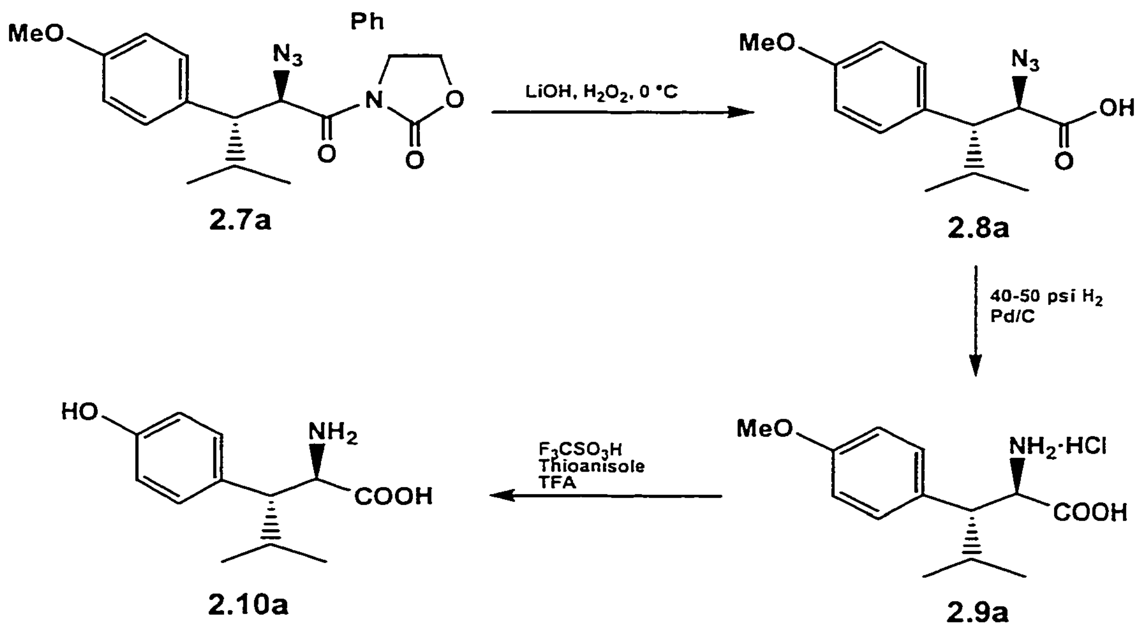

Scheme 2.7. Synthesis of β-isopropyltyrosine (4).

2.4 EXPERIMENTAL

General. All reagents, unless otherwise noted, were purchased from Aldrich Chemical Co. and were used without further purification. Triisopropylsulfonyl azide and tetramethylguanidinium azide were synthesized as described in literature.[106] The following solvents were freshly distilled and stored under argon prior to use: THF from potassium/benzophenone, CH_2Cl_2 from CaH_2. All reactions, unless otherwise noted, were carried out under the protection of nitrogen; the reaction temperatures listed are the bath temperatures. Reaction containers were flame dried under vacuum before use if necessary. Melting points were taken on a Thomas Hoover melting point apparatus. ^{1}H and ^{13}C NMR spectra were recorded on a Bruker AM 250 (operating at 250.0 and 62.9 MHz) spectrometer, using TMS or D_2O (4.66 ppm downfield from TMS) as internal standard or $CDCl_3$ (77.0 ppm downfield from TMS) as internal standard for ^{13}C NMR. Optical rotations were taken on an Autopol III polarimeter using a 1.0 dm cell. Flash column chromatography was performed using EM silica gel. Solvents for chromatography were used without further purification. Analytical TLC was performed on Merck precoated Kieselgel 60 F-254 plates with the following solvent systems (v/v): **(I)** EtOAc/hexanes (3/7), **(II)** EtOAc/hexanes/HOAc(30/70/1), **(III)** $CH_3CN/CH_3OH/H_2O$ (4/1/1). Detection was made using I_2, ninhydrin, or UV light. A jacketed column with an inside diameter of 1 inch and length of 18 inches purchased from ACE Glass was used for ion-exchange chromatography. Elemental analysis was done by Desert Analytics Co., Tucson, Arizona. High resolution mass spectra were obtained on a JEOL JMS-HX110 Mass Spectrometer, Mass Spectroscopy Facility, Department of Chemistry, University of Arizona.

General procedure for 3-(2′-isohexenyl)-4-phenyl-2-oxazolidinone (2.3a,b)

A solution of (2*E*)-isohexenoic acid (**2.4**, 6.85 g, 60 mmol) in THF (250 mL) was stirred under N_2 at –78 °C for 15 min, and triethylamine (6.07 g, 60 mmol) was added via a syringe followed by trimethylacetyl chloride (7.24 g, 60 mmol). The resulting suspension was stirred at –78 °C for 15 min, 0 °C for 1 h, and then at – 78 °C for 15 min before being transferred via cannula into a slurry of lithium 4-phenyl-2-oxazolidinone at 0 °C, which was prepared 10 min in advance at –78 °C by addition of *n*-butyllithium (37.5 mL, 60 mmol) into a solution of 4-phenyl-2-oxazolidinone (9.79 g, 50 mmol) in THF (150 mL) at –78 °C. The resulting slurry was stirred at –78 °C for 1 h and room temperature for 2 h. The reaction was quenched with saturated ammonium chloride (200 mL). The organic phase was separated. A small amount of water was added to the aqueous phase to dissolve solid, and the solution was extracted with ethyl acetate (2 x 75 mL). The combined organic phase was washed with saturated aqueous sodium bicarbonate (2 x 100 mL), brine (100 mL) and water (100 mL), dried over anhydrous magnesium sulfate, rotary evaporated, and the crude product was purified by recrystallization from ethyl acetate and hexanes to give the pure product.

3(2′*E*), 4(*R*)-3-(4-Methyl-1′-oxo-2′-pentenyl)-2-oxazolidinone (2.3a)

Yield 92.6 %, white solid, m.p. 103-104 °C, $[\alpha]_D^{22}$= -103.4 (c 1.07, $CHCl_3$). IR (KBr, cm^{-1}): 3036, 2962, 1775, 1682, 1630m 1391, 1352, 1213, 713. ^{1}H NMR (δ): 7.42-7.01 (m, 7H, aromatic protons and –CH=CH-), 5.50 (dd, J=13.9 Hz, 1H, oxazolidinone PhCH-), 4.68 (t, 1H, J=10.6 Hz, oxazolidinone, -H*CH*-), 4.28 (dd, J=14.2, 6.2 Hz, 1H, oxazolidinone, -*H*CH-), 2.51 (m, 1H, -*CH*(CH_3)$_2$), 1.07 (d, J=11.1 Hz, 6H, -CH(CH_3)$_2$). ^{13}C NMR (δ): 164.9, 158.1, 153.7, 139.1, 129.3, 128.5, 125.7, 117.6, 70.4, 57.2, 31.7, 21.4, 21.3. Anal. For $C_{15}H_{18}O_3N$: Calcd C, 69.48; H, 6.61; N, 5.40. Found C, 69.64; H, 6.57; N, 5.36.

3(2′*E*), 4(*S*)-3-(4′-Methyl-1′-oxo-2′-pentenyl)-2-oxazolidinone (2.3b)

Yield 91.3 %, white solid, m.p. 103.5-104 °C, $[\alpha]_D^{22}$ = -103.8 (c 1.07, $CHCl_3$). IR (KBr, cm^{-1}): 3017, 2964, 1774, 1683, 1636, 1394, 1361, 1212, 712. ^1H NMR (δ,): 7.39-7.01 (m, 7H, aromatic protons and –CH=CH-), 5.49 (dd, J=13.9, 6.2 Hz, 1H, oxazolidinone PhCH-), 4.70 (t, 1H, J=14.0 Hz, oxazolidinone, -*H*CH-), 4.29 (dd, J=14.1, 6.0 Hz, 1H, oxazolidinone, -HC*H*-), 2.51 (m, 1H, -*CH*(CH_3)$_2$), 1.07 (d, J=11.0 Hz, 6H, -CH(CH_3)$_2$). ^{13}C NMR (δ): 164.9, 158.0, 153.7, 139.1, 129.1, 128.0, 125.9, 117.6, 69.8, 57.7, 31.4, 21.2, 21.1. Anal. For $C_{15}H_{18}O_3N$: Calcd C, 69.48; H, 6.61; N, 5.40. Found C, 69.46; H, 6.57; N, 5.53.

General procedure for Michael addition reaction

To a mixture of 4-OmePhMgBr and copper (I) bromide-dimethyl sulfide complex (5.15 g, 25 mmol) in THF (80 mL) at –78 °C was added dropwise a solution of **2.3a** or **b** (12.97 g, 50 mmol) in THF (100 mL) under N_2. The resulting mixture was stirred vigorously at –78 °C for 15 min and 0 °C for 2 h, then slowly warmed to room temperature during 1 h. The reaction was quenched by addition of saturated ammonium chloride (120 mL). The organic phase was separated and the aqueous phase was extracted with ether (2 x 40 mL). The combined organic phase was washed with brine (2 x 50 mL) and water (50 mL), dried over anhydrous magnesium sulfate, and rotary evaporated to give crude **2.5a** or **b** which was purified by column chromatography.

3(3′*R*), 4(*R*)-3-[3′-(4′-Methoxyphenyl)-4′-methyl-1′-oxo-2′-pentanyl]-4-phenyl-2-oxazolidinone (2.5a)

Yield 81.4 %, colorless needles, m.p. 82-84 °C, $[\alpha]_D^{22}$ = -55.5 (c 1.06, $CHCl_3$). IR (KBr, cm^{-1}): 3027, 2950, 1788, 1702, 1392, 1364, 1327, 1187, 709. ^1H NMR (δ): 7.21-

6.74 (m, 9H, aromatic protons), 5.32 (dd, J=14.0, 6.5 Hz, 1H, oxazolidinone PhCH-), 4.56 (t, 1H, J=14.1 Hz, 1H, oxazolidinone, -HCH-), 4.09 (dd, J=14.0, 6.5 Hz, oxazolidinone, -*H*CH-), 3.79 (s, 3H, $-OCH_3$), 3.76 (dd, J=16.6, 5.9 Hz, 1H, $-C_{\alpha}H-$), 3.06 (dd, J=24.8, 8.2 Hz, 1H, $-C_{\alpha}H-$), 2.86 (m, 1H, $-C_{\beta}H-$), 1.83 (m, 1H, $-CH(CH_3)_2$), 0.95 (d, J=10.7 Hz, 3H, $-CH_3$), 0.73 (d, J=10.7 Hz, 3H, $-CH_3$). ^{13}C NMR (δ): 172.1, 157.9, 153.6, 138.5, 134.4, 129.3, 128.8, 128.0, 125.1, 113.3, 69.6, 57.4, 55.0, 48.1, 38.2, 33.3, 20.7, 20.1. Anal. For $C_{22}H_{25}O_4N$: Calcd C, 71.91; H, 6.86; N, 3.81. Found C, 71.92; H, 6.92; N, 3.82.

3(3´*S*), 4(*S*)-3-[3´-(4´-Methoxyphenyl)-4´-methyl-1´-oxo-2´-pentanyl]-4-phenyl-2-oxazolidinone (2.5b)

Yield 85.8 %, colorless needles, m.p. 85-86 °C, $[\alpha]_D^{22}$ = -54.7 (c 1.02, $CHCl_3$). IR (KBr, cm^{-1}): 3030, 2950, 1777, 1709, 1392, 1510, 1387, 1357, 1240,1177, 701. ^1H NMR (δ): 7.24-6.74 (m, 9H, aromatic protons), 5.32 (dd, J=13.9 Hz, 6.5 Hz, 1H, oxazolidinone PhCH-), 4.60 (t, 1H, J=14.0 Hz, 1H, oxazolidinone, -*H*CH-), 4.12 (dd, J=14.1, 6.5 Hz, 1H, oxazolidinone, -H*CH*-), 3.82 (s, 3H, $-OCH_3$), 3.74 (dd, J=16.5Hz, 5.9 Hz, 1H, $-C_{\alpha}H-$), 3.09 (dd, J=24.9 Hz, 8.2 Hz, 1H, $-C_{\beta}H-$), 2.88 (m, 1H, $-C_{\beta}H-$), 1.85 (m, 1H, $-CH(CH_3)_2$), 0.96 (d, J=10.6 Hz, 3H, $-CH_3$), 0.74 (d, J=10.6 Hz, 3H, $-CH_3$). ^{13}C NMR (δ): 172.1, 157.9, 153.6, 138.5, 134.4, 129.3, 128.8, 128.0, 125.1, 113.3, 69.6, 57.4, 55.0, 48.1, 38.2, 33.3, 20.7, 20.2. HRMS for $C_{22}H_{26}O_4N$: $[M+H]^+$ (Calcd 368.1862. Found 368.1857).

General procedure for direct azidation of N-acyloxazolidinones 2.5a,b

A solution of N-acyloxazolidinones **2.5a** or **b** (7.37 g, 20 mmol) in THF (50 mL) was stirred at –78 °C under N_2. A precooled solution of KHMDS (60mL, 1M, 30 mmol) in THF (30 mL) was added via cannula. The resulting mixture was stirred at –78 °C for 30 min. A precooled solution of trisyl azide (9.28 g, 30 mmol) in THF (30 mL) was added via cannula. The reaction was stirred at –78 °C for 15 min and then quenched by addition of acetic acid (5.5 mL, 4.6 eq.). The reaction flask was immersed into a water bath (30-40 °C) for 35 min. Brine (100 mL) was added and the organic phase was separated. The aqueous phase was extracted with ether (2 x 30 mL). The combined organic phase was washed with brine (2 x 80 mL) and water (2 x 80 mL), and dried over anhydrous magnesium sulfate. Removal of the solvents gave the crude **2.7a** or **b** as light yellow oil, which was purified by column chromatography.

3(2′*R*, 3′*R*), 4(*R*)-3-[2′-Azido-3′-(4′-methoxyphenyl)-4′-methyl-1′-oxo-2′-pentanyl]-4-phenyl-2-oxazolidinone (2.7a)

Yield 84.8 %, colorless oil, $[\alpha]_D^{22}$ = -56.4 (c 0.11, $CHCl_3$). IR (film, cm^{-1}): 3031, 2958, 2109, 1777, 1708, 1392, 1510, 1383, 1247, 1037, 698. ^1H NMR (δ): 7.37-6.77 (m, 9H, aromatic protons), 5.65 (d, J=11.3 Hz, 1H, -C_αH-), 5.22 (dd, J=13.4, 5.0 Hz, 1H, oxazolidinone, PhCH-), 4.73 (t, J=4.8 Hz, 1H, oxazolidinone, -H*CH*-), 4.34 (dd, J=14.1 Hz, 4.8 Hz, 1H, oxazolidinone, -*H*CH-), 3.80 (s, 3H, OCH_3), 2.96 (t, J=11.9 Hz, 1H, -C_βH-), 2.05 (m, 1H, -*CH*$(CH_3)_2$), 1.04 (d, J=10.6 Hz, 3H, -CH_3), 0.75 (d, J=10.7 Hz, 3H, -CH_3). ^{13}C NMR (δ): 168.7, 158.7, 153.3, 138.2, 130.1, 130.0, 129.2, 128.9, 125.7, 113.6, 70.5, 62.7, 58.1, 55.1, 52.2, 30.0, 20.9, 20.0. HRMS for $C_{22}H_{25}O_4N_4$: $[M+H]^+$ (Calcd 409.1876. Found 409.1867).

3(2′*S*, 3′*S*), 4(*S*)-3-[2′-Azido-3′-(4′-methoxyphenyl)-4′-methyl-1′-oxo-2′-pentanyl]-4-phenyl-2-oxazolidinone (2.7c)

Yield 86.5 %, colorless oil, $[\alpha]_D^{22} = +63.3$ (c 0.12, $CHCl_3$). IR (film, cm^{-1}): 3031, 2958, 2109, 1778, 1708, 1392, 1510, 1381, 1247, 1037, 698. ^{1}H NMR (δ): 7.36-6.75 (m, 9H, aromatic protons), 5.67 (d, J=11.3 Hz, 1H, -C_αH-), 5.21 (dd, J=13.4, 5.0 Hz, 1H, oxazolidinone, PhCH-), 4.71 (t, J=13.9 Hz, oxazolidinone, -*H*CH-), 4.31 (dd, J=10.1 Hz, 5.0 Hz, 1H, oxazolidinone, -H*CH*-), 3.81 (s, 3H, OCH_3), 2.97 (t, J=11.9 Hz, 1H, -C_βH-), 2.05 (m, 1H, -*CH*$(CH_3)_2$), 1.05 (d, J=10.6 Hz, 3H, -CH_3), 0.75 (d, J=10.6 Hz, 3H, -CH_3). ^{13}C NMR (δ): 168.7, 158.7, 153.3, 138.2, 130.1, 130.0, 129.1, 128.8, 125.6, 113.5, 70.5, 62.6, 57.4, 58.1, 52.2, 29.9, 20.9, 20.0. HRMS for $C_{22}H_{25}O_4N_4$: $[M+H]^+$ (Calcd 409.1876. Found 409.1883).

General procedure for asymmetric bromination of N-acyloxazolidinones 2.5a,b

A solution of N-acyloxazolidinones **2.5** (7.35 g, 20 mmol) in DCM (60 mL) was cooled to –78 °C with stirring under N_2, and diisopropylethylamine (3.10 g, 24 mmol) and dibutylborontriflate (7.4 mL, 1M, 22 mmol) were added via syringe. The light yellow solution was stirred at –78 °C for 15 min, 0 °C for 1 h and recooled to –78 °C for 15 min. The above solution was transferred to a precooled suspension of NBS (7.12 g, 40 mmol) in DCM (50 mL) via cannula. The resulting mixture was stirred at –78 °C for 1 h and 0 °C for 3 h. The reaction was quenched by addition of 0.5 N sodium bisulfite (100 mL). The organic phase was separated and the aqueous phase was extracted with DCM (2 x 50 mL). The combined organic phase was washed with brine (2 x 100 mL) and water (2 x 100 mL), dried over anhydrous magnesium sulfate and rotary evaporated to give crude which was purified by column chromatography.

3(2′*R*,3′*R*), 4(*R*)-3-[2′-Bromo-3′-(4′-methoxyphenyl)-4′-methyl-1′-oxo-2′-pentanyl]-4-phenyl-2-oxazolidinone (2.6a)

Yield 84.5 %, white solid, m.p. 171-173°C. $[\alpha]_D^{22}$ = +15.5 (c 0.86, $CHCl_3$). IR (KBr, cm^{-1}): 3029, 2963, 1781, 1722, 1384, 1345, 1229, 698. ^1H NMR (δ): 7.40-6.75 (m, 9H, aromatic protons), 6.28 (d, J=17.7Hz, 1H, -C_αH-), 5.48 (dd, J=14.3 Hz, 7.5 Hz, 1H, oxazolidinone, PhCH-), 4.78 (t, J=14.2 Hz, 1H, oxazolidinone, - H*CH*-), 4.32 (dd, J=14.4 Hz, 7.4 Hz, 1H, oxazolidinone, -H*CH*-), 3.80 (s, 3H, OCH_3), 3.32 (dd, J=17.8 Hz, 7.1Hz, 1H, -C_βH-), 1.99 (m, 1H, -*CH*$(CH_3)_2$), 0.83 (d, J=10.8 Hz, 3H, -CH_3), 0.75 (d, J=10.9 Hz, 3H, -CH_3). ^{13}C NMR (δ): 168.5, 157.9, 153.0, 138.5, 134.5, 129.3, 128.8, 128.0, 125.9, 125.1, 113.3, 69.6, 57.4, 55.1, 48.2, 33.3, 20.7, 17.4. HRMS for $C_{22}H_{25}O_4NBr$: $[M+H]^+$ (Calcd 446.0967. Found 446.0973).

3(2′*S*,3′*S*),4(*S*)-3-[2′-Bromo-3′-(4′-methoxyphenyl)-4′-methyl-1′-oxo-2′-pentanyl]-4-phenyl-2-oxazolidinone (2.6b)

Yield 78.8 %, white solid, m.p. 173-174°C. $[\alpha]_D^{22}$ = +14.5 (c 0.88, $CHCl_3$). IR (KBr, cm^{-1}): 3031, 2954, 1769, 1705, 1388, 1349, 1210, 699. ^1H NMR (δ): 7.40-6.83 (m, 9H, aromatic protons), 6.27 (d, J=17.7Hz, 1H, -C_αH-), 5.48 (dd, J=14.3 Hz, 7.4 Hz, 1H, oxazolidinone, PhCH-), 4.77 (t, J=14.2 Hz, 1H, oxazolidinone, - H*CH*-), 4.32 (dd, J=14.2 Hz, 7.4 Hz, 1H, oxazolidinone, -H*CH*-), 3.80 (s, 3H, OCH_3), 3.30 (dd, J=17.7 Hz, 7.1Hz, 1H, -C_βH-), 1.99 (m, 1H, -*CH*$(CH_3)_2$), 0.83 (d, J=10.8 Hz, 3H, -CH_3), 0.76 (d, J=11.0 Hz, 3H, -CH_3). ^{13}C NMR (δ): 172.1, 168.5, 157.9, 138.5, 134.5, 129.3, 128.8, 128.0, 125.1, 113.3, 69.6, 57.4, 55.1, 48.2, 38.2, 33.3, 20.7, 20.2. HRMS for $C_{22}H_{25}O_4NBr$: $[M+H]^+$ (Calcd 446.0967. Found 446.0951).

General procedure for azide displacement

2.6a, or **b** (6.25g, 15 mmol) and tetramethylguanidinium azide (3.56g, 22.5 mmol) were dissolved in acetonitrile (100 ml). The solution was stirred at room temperature for 12 h. The solids were filtered off, and the filtrate was evaporated by rotary evaporation. The crude **2.7b** or **d** was purified by silica gel chromatography.

3(2′*S*,3′*R*),4(*R*)-3-[2′-Azido-3′-(4′-methoxyphenyl)-4′-methyl-1′-oxo-2′-pentanyl]-4-phenyl-2-oxazolidinone (2.7b)

Yield 91.5 %, white solid, m.p. 173-174°C. $[\alpha]_D^{22} = -3.4$ (c 0.54, $CHCl_3$). IR (KBr, cm^{-1}): 3030, 2957, 2099, 1767, 1698, 1510, 1393, 1225, 1039, 701. ^1H NMR (δ): 7.17-6.48 (m, 9H, aromatic protons), 5.69 (d, J=18.5Hz, 1H, -$C_\alpha H$-), 5.34 (dd, J=14.1 Hz, 7.1 Hz, 1H, oxazolidinone, PhCH-), 4.63 (t, J=14.1 Hz, 1H, oxazolidinone, - H*CH*-), 4.07 (dd, J=12.9 Hz, 7.1 Hz, 1H, oxazolidinone, -H*CH*-), 3.83 (s, 3H, OCH_3), 3.08 (dd, J=18.4 Hz, 11.9 Hz, 1H, -$C_\beta H$-), 2.26 (m, 1H, -*CH*(CH_3)$_2$), 0.91 (d, J=11.0 Hz, 3H, -CH_3), 0.79 (d, J=10.9 Hz, 3H, -CH_3). ^{13}C NMR (δ): 168.7, 158.7, 153.2, 138.1, 131.3, 129.4, 128.6, 128.5, 125.5, 114.0, 70.3, 59.2, 58.1, 55.6, 51.9, 29.0, 21.6, 17.6. HRMS for $C_{21}H_{25}O_4N_4$: $[M+H]^+$ (Calcd 409.1875. Found 409.1867).

3(2′*R*,3′*S*),4(*S*)-3-[2′-Azido-3′-(4′-methoxyphenyl)-4′-methyl-1′-oxo-2′-pentanyl]-4-phenyl-2-oxazolidinone (2.7d)

Yield 87.3 %, white solid, m.p. 167-169°C. IR (KBr, cm^{-1}): 3030, 2956, 2098, 1767, 1697, 1510, 1392, 1225, 1039, 701. ^1H NMR (δ): 7.20-6.48 (m, 9H, aromatic protons), 5.69 (d, J=18.4Hz, 1H, -$C_\alpha H$-), 5.34 (dd, J=14.2 Hz, 7.1 Hz, 1H, oxazolidinone, PhCH-), 4.63 (t, J=14.1 Hz, 1H, oxazolidinone, - H*CH*-), 4.07 (dd, J=14.1 Hz, 7.0 Hz, 1H, oxazolidinone, -H*CH*-), 3.83 (s, 3H, OCH_3), 3.08 (dd, J=18.4 Hz, 6.7 Hz, 1H, -$C_\beta H$-

), 2.26 (m, 1H, -*CH*(CH_3)$_2$), 0.91 (d, J=11.0 Hz, 3H, -CH_3), 0.79 (d, J=10.9 Hz, 3H, -CH_3). ^{13}C NMR (δ): 168.7, 158.7, 153.2, 138.1, 131.3, 129.1, 129.4, 128.6, 128.5, 125.5, 114.0, 70.3, 59.2, 58.1, 55.6, 51.9, 29.0, 21.6, 17.6. HRMS for $C_{22}H_{25}O_4N_4$: $[M+N]^+$ (Calcd 409.1876. Found 409.1878).

General procedure for hydrolysis of azido compounds 2.7

To a solution of azido compound **2.7** (4.08 g, 10 mmol) in THF (120 mL) was added water (40 mL). The solution was stirred at 0 °C for 15 min, and 30% H_2O_2 (6.8 mL, 6 equiv.) was added dropwise followed by dropwise addition of lithium hydroxide (0.92 g, 22 mmol) in water (15 mL). The resulting mixture was stirred at 0 °C for 4 h. The reaction was quenched by addition of saturated sodium sulfite (60 mL) and stirred at room temperature for 30 min. The aqueous phase was separated and extracted with DCM (3 x 40 mL) for recovery of auxiliary, then acidified with 6N HCl to pH=1, extracted with DCM (3 x 40 mL). The combined organic phase was dried over anhydrous magnesium sulfate and rotary evaporated to give crude **2.8**, which was used in the next step directly.

(2*R*,3*R*)-2-Azido-3-(4′-methoxyphenyl)-4-methylpentanoic acid (2.8a)

Light yellow oil. IR (KBr, cm^{-1}): 3500-2500, 2110, 1712, 1608, 1510, 1385, 1367, 1249, 1034, 830. ^{1}H NMR (δ): 10.9 (s, br, 1H, COOH), 7.12 (d, J=10.8 Hz, 2H, aromatic protons), 6.82 (d, J=10.8 Hz, 2H, aromatic protons), 4.49 (d, J=8.3 Hz, 1H, -C_αH-), 3.79 (s, 3H, -OCH_3), 2.76 (dd, J=15.1 Hz, 8.3 Hz, 1H, -C_βH-), 2.09 (m, 1H, -CH(CH_3)$_2$), 1.07 (dd, J=10.5 Hz, 3H, -CH_3), 0.72 (d, J=10.9 Hz, 3H, -CH_3). ^{13}C NMR (δ): 175.6, 158.6, 130.2, 129.8, 129.0, 113.4, 64.0, 55.1, 53.2, 29.4, 20.9, 20.4.

(2*S*,3*S*)-2-Azido-3-(4′-methoxyphenyl)-4-methylpentanoic acid (2.8b)

Light yellow oil. IR (KBr, cm^{-1}): 3500-2500, 2110, 1712, 1608, 1510, 1385, 1307, 1249, 1035, 830. ^1H NMR (δ): 10.9 (s, br, 1H, COOH), 7.13 (d, J=13.9 Hz, 2H, aromatic protons), 6.81 (d, J=14.0 Hz, 2H, aromatic protons), 4.49 (d, J=8.3 Hz, 1H, -$C_\alpha H$-), 3.79 (s, 3H, -OCH_3), 2.76 (dd, J=15.0 Hz, 8.3 Hz, 1H, -$C_\beta H$-), 2.10 (m, 1H, -$CH(CH_3)_2$), 1.06 (dd, J=10.5 Hz, 3H, -CH_3), 0.72 (d, J=10.6 Hz, 3H, -CH_3). ^{13}C NMR (δ): 175.6, 158.6, 130.2, 129.8, 129.0, 113.4, 64.0, 55.1, 53.2, 29.4, 20.9, 20.4.

(2*S*,3*R*)-2-Azido-3-(4′-methoxyphenyl)-4-methylpentanoic acid (2.8c)

Light yellow oil. IR (KBr, cm^{-1}): 3500-2500, 2109, 1709, 1608, 1510, 1385, 1367, 1249, 1034, 830. ^1H NMR (δ): 10.3 (s, br, 1H, COOH), 7.08 (d, J=13.8Hz, 2H, aromatic protons), 6.82 (d, J=13.9 Hz, 2H, aromatic protons), 4.14 (d, J=11.7 Hz, 1H, -$C_\alpha H$-), 3.79 (s, 3H, -OCH_3), 2.87 (t, J=11.7 Hz, 1H, -$C_\beta H$-), 2.25 (m, 1H, -$CH(CH_3)_2$), 0.94 (d, J=10.7 Hz, 3H, -CH_3), 0.77 (d, J=10.9 Hz, 3H, -CH_3).

(2*R*,3*S*)-2-Azido-3-(4′-methoxyphenyl)-4-methylpentanoic acid (2.8d)

Light yellow oil. IR (KBr, cm^{-1}): 3500-2500, 2109, 1709, 1608, 1510, 1385, 1367, 1249, 1034, 830. ^1H NMR (δ): 10.3 (s, br, 1H, COOH), 7.08 (d, J=15.3 Hz, 2H, aromatic protons), 6.82 (d, J=13.9 Hz, 2H, aromatic protons), 4.14 (d, J=11.7 Hz, 1H, -$C_\alpha H$-), 3.79 (s, 3H, -OCH_3), 2.87 (t, J=11.7 Hz, 1H, -$C_\beta H$-), 2.27 (m, 1H, -$CH(CH_3)_2$), 0.93 (d, J=10.7 Hz, 3H, -CH_3), 0.77 (d, J=10.8 Hz, 3H, -CH_3).

General procedure for reduction of azido acid 2.8

To a solution of azido acid **2.8** (2.07 g, 8 mmol) in methanol (50 mL) and 6 N HCl (2 mL) in a hydrogenation vessel was added 10% Pd/C (0.3 g). The reaction vessel was emptied, refilled with hydrogen three times, and shaken under 40-50 psi H_2 for 24 h. The catalyst was filtered off and washed with methanol. The solvent was removed by rotary evaporation. The residue was dissolved in 6N HCl (6 mL) and rotary evaporated to give crude **2.9**, which was used in the next step directly.

(2*R*,3*R*)-2-Amino-3-(4′-methoxyphenyl)-4-methylpentanoic acid (2.9a)

Yield 97.8 %, white solid, $[\alpha]_D^{22}$ = -11.7 (c 1.04, $CHCl_3$). IR (KBr, cm^{-1}): 3500-2500, 1736, 1608, 1512, 1388, 1368, 1251, 1034, 835. ^1H NMR (δ): 6.98 (d, J=10.7 Hz, 2H, aromatic protons), 6.78 (d, J=10.7 Hz, 2H, aromatic protons), 4.19 (d, J=8.9 Hz, 1H, -$C_\alpha H$-), 3.60 (s, 3H, -OCH_3), 2.84 (dd, J=14.6 Hz, 8.9 Hz, 1H, -$C_\beta H$-), 1.96 (m, 1H, -*CH*(CH_3)$_2$), 0.79 (d, J=10.5 Hz, 3H, -CH_3), 0.58 (d, J=11.2 Hz, 3H, -CH_3). ^{13}C NMR (δ): 171.9, 158.4, 130.4, 127.8, 114.4, 55.5, 55.3, 51.8, 27.6, 20.1, 19.3. HRMS for $C_{13}H_{20}O_3N$: $[M+H]^+$ (Calcd 238.1443. Found 238.1445).

(2*S*,3*S*)-2-Amino-3-(4′-methoxyphenyl)-4-methylpentanoic acid (2.9b)

Yield 91.7 %, white solid, $[\alpha]_D^{22}$ = +12.0 (c 1.04, $CHCl_3$). IR (KBr, cm^{-1}): 3500-2500, 1729, 1608, 1511, 1386, 1249, 1033, 834. ^1H NMR (δ): 6.98 (d, J=14.0 Hz, 2H, aromatic protons), 6.79 (d, J=13.9 Hz, 2H, aromatic protons), 4.18 (d, J=9.0 Hz, 1H, -$C_\alpha H$-), 3.60 (s, 3H, -OCH_3), 2.84 (dd, J=14.6 Hz, 8.7 Hz, 1H, -$C_\beta H$-), 1.97 (m, 1H, -CH(CH_3)$_2$), 0.79 (d, J=10.5 Hz, 3H, -CH_3), 0.59 (d, J=10.5 Hz, 3H, -CH_3). ^{13}C NMR (δ): 171.9, 158.4, 130.4, 127.8, 114.4, 55.5, 55.3, 51.8, 27.6, 20.1, 19.3. HRMS for $C_{13}H_{20}O_3N$: $[M+H]^+$ (Calcd 238.1443. Found 238.1442).

(2*S*,3*R*)-2-Amino-3-(4′-methoxyphenyl)-4-methylpentanoic acid (2.9c)

Yield 96.3 %, white solid. IR (KBr, cm^{-1}): 3500-2500, 1729, 1608, 1511, 1386, 1249, 1033, 834. ^1H NMR (δ): 6.96 (d, J=14.1 Hz, 2H, aromatic protons), 6.76 (d, J=14.1 Hz, 2H, aromatic protons), 4.22 (d, J=8.9 Hz, 1H, -C_αH-), 3.60 (s, 3H, -O*CH*$_3$), 2.43 (dd, J=16.2 Hz, 7.6 Hz, 1H, -C_βH-), 2.14 (m, 1H, -CH(CH_3)$_2$), 0.94 (d, J=10.2 Hz, 3H, -CH_3), 0.47 (d, J=10.6 Hz, 3H, -CH_3). ^{13}C NMR (δ): 171.9, 158.5, 130.4, 129.2, 114.2, 55.3, 55.1, 53.9, 28.9, 20.6, 20.4. HRMS for $C_{13}H_{20}O_3N$: $[M+H]^+$ (Calcd 238.1443. Found 238.1438).

(2*R*,3*S*)-2-Amino-3-(4′-methoxyphenyl)-4-methylpentanoic acid (2.9d)

Yield 95.9 %, white solid. IR (KBr, cm^{-1}): 3500-2500, 1730, 1609, 1511, 1387, 1249, 1034, 833. ^1H NMR (δ): 6.96 (d, J=12.4 Hz, 2H, aromatic protons), 6.77 (d, J=12.3 Hz, 2H, aromatic protons), 4.25 (d, J=5.7 Hz, 1H, -C_αH-), 3.60 (s, 3H, -O*CH*$_3$), 2.46 (dd, J=16.1 Hz, 7.5 Hz, 1H, -C_βH-), 2.16 (m, 1H, -*CH*(CH_3)$_2$), 0.95 (d, J=10.3 Hz, 3H, -CH_3), 0.47 (d, J=10.4 Hz, 3H, -CH_3). ^{13}C NMR (δ): 171.9, 158.5, 130.4, 129.2, 114.2, 55.3, 55.1, 53.9, 28.9, 20.6, 20.4. HRMS for $C_{13}H_{20}O_3N$: $[M+H]^+$ (Calcd 238.1443. Found 238.1449).

General procedure for demethylation

Method I. Amino acid chloride **2.9a** (14.5 g, 5.3 mmol) was dissolved in trifluoroacetic acid (60 mL). The solution was cooled to –4 °C, thioanisole (4.61 g, 7 eq.) was added and stirred for 10 min, and then trifluoromethanesulfonic acid (11.9 g, 15 eq.) was added via a syringe. The light yellow cloudy solution was stirred at 0 °C for 4 h. Volatiles were removed by rotary evaporation. The residue was dissolved in water (150 mL) and extracted with DCM (2 x 30 mL). The aqueous phase was loaded on an ion-exchange column (2.5 x 46 cm) with Amberlite IR-120 (H^+) resin. The column was washed with 2:3 ($NH_3{\bullet}H_2O:H_2O$) ammonia solution. Fractions containing the product were combined, evaporated to remove excess ammonia and water, frozen and lyophilized to give final amino acid **2.10a**.

Method II. To an amino acid chloride **2.9b** (1.37g, 5.0 mmol) in hydrobromic acid (48%, 70 mL) was added sodium iodide. The solution was stirred at 90 °C for 3 h. Volatiles were removed by rotary evaporation. The residue was dissolved in water (50 mL) and extracted with ethyl acetate (2 x 30 mL). The aqueous phase was loaded on an ion-exchange column (2.5 x 46 cm) with Amberlite IR-120 (H^+) resin. The column was washed with 2:3 ($NH_3{\bullet}H_2O:H_2O$) ammonia solution. Fractions containing the product were combined, evaporated to remove excess of ammonia and water, frozen and lyophilized to give final amino acid **2.10b**.

(2*R*,3*R*)-2-Amino-3-(4′-methoxyphenyl)-4-methylpentanoic acid (2.10a)

Yield 92.3 %, white solid, m.p. 235°C decomposed. $[\alpha]_D^{22}$ = -16.4 (c=0.56, 1N HCl). IR (KBr, cm^{-1}): 3500-2500, 1650, 1611, 1581, 1512, 1400, 1345, 1248, 832. ^1H NMR (D_2O, δ): 6.88 (d, J=5.64 Hz, 2H, aromatic protons), 6.67 (d, J=8.45 Hz, 2H, aromatic protons), 3.87 (d, 1H, J=5. 57 Hz, 1H, $-C_{\alpha}H$), 2.69 (m, 3H, $-C_{\beta}H$), 1.94 (m, 1H, $CH(CH_3)_2$), 0.79 (d, J=6.55 Hz, 3H, $-CH_3$), 0.59 (d, J=6.47 Hz, 3H, $-CH_3$). HRMS for $C_{12}H_{18}O_3N$: $[M+H]^+$ (Calcd 224.1287. Found 224.1288).

(2*S*,3*S*)-2-Amino-3-(4′-methoxyphenyl)-4-methylpentanoic acid (2.10b)

Yield 76.2 %, white solid, m.p. 230°C decomposed. $[\alpha]_D^{22}$ = +15.2 (c=0.57, 1N HCl). IR (KBr, cm^{-1}): 3500-2500, 1649, 1612, 1581, 1511, 1401, 1345, 1248, 832. ^1H NMR (D_2O, δppm): 6.89 (d, J=10.51 Hz, 2H, aromatic protons), 6.70 (d, J=10.31 Hz, 2H, aromatic protons), 3.86 (d, 1H, J=5.53 Hz, 1H, -C$_\alpha$H), 2.69 (m, 3H, -C$_\beta$H), 1.94 (m, 1H, *CH*(CH$_3$)$_2$), 0.78 (d, J=6.53 Hz, 3H, -CH$_3$), 0.58 (d, J=6.61 Hz, 3H, -CH$_3$). HRMS for $C_{12}H_{18}O_3N$: $[M+H]^+$ (Calcd 224.1287. Found 224.1292).

(2*S*,3*R*)-2-Amino-3-(4′-methoxyphenyl)-4-methylpentanoic acid (2.10c)

Yield 89.8 %, white solid, m.p. 235°C decomposed. $[\alpha]_D^{22}$ = +5.3 (c=0.55, 1N HCl). IR (KBr, cm^{-1}): 3500-2500, 1610, 1585, 1511, 1409, 1387, 1248, 840. ^{1}H NMR (D_2O, δ): 6.88 (d, J=8.57 Hz, 2H, aromatic protons), 6.63 (d, J=8.52 Hz, 2H, aromatic protons), 3.94 (d, 1H, J=4.67 Hz, -C$_\alpha$H-), 2.37 (dd, J=16.0 Hz, 7.3 Hz, 1H, -C$_\alpha$H), 2.15 (m, 1H, *CH*(CH$_3$)$_2$), 0.92 (d, J=6.35 Hz, 3H, -CH$_3$), 0.45 (d, J=6.65 Hz, 3H, CH$_3$). HRMS for $C_{12}H_{18}O_3N$: $[M+H]^+$ (Calcd 224.1287. Found 224.1284).

(2*R*,3*S*)-2-Amino-3-(4′-methoxyphenyl)-4-methylpentanoic acid (2.10d)

Yield 92.3%, white solid, m.p. 230°C decomposed. $[\alpha]_D^{22}$ = -5.1 (c=0.74, 1N HCl). IR (KBr, cm^{-1}): 3500-2500, 1610, 1585, 1511, 1409, 1387, 1247, 840. ^{1}H NMR (D_2O, δ): 6.88 (d, J=8.62 Hz, 2H, aromatic protons), 6.63 (d, J=7.30 Hz, 2H, aromatic protons), 3.93 (d, 1H, J=4.47 Hz, -C$_\alpha$H), 2.35 (m, 1H, -C$_\beta$H), 2.15 (m, 1H, *CH*(CH$_3$)$_2$), 0.92 (d, J=6.20 Hz, 3H, CH$_3$), 0.45 (d, J=6.44 Hz, 3H, CH$_3$). HRMS for $C_{12}H_{18}O_3N$: $[M+H]^+$ (Calcd 224.1287. Found 224.1283).

Chapter 3

DE NOVO DESIGN AND STEREOSELECTIVE SYNTHESIS OF CONFORMATIONALLY CONSTRAINED REVERSE TURN DIPEPTIDE MIMETICS

3.1 INTRODUCTION

Our knowledge of how receptor-ligand interactions are manifested in biological changes often is very incomplete. A central goal in peptide and protein research is the development of systematic, predictive approaches to the design of peptidomimetics with specific conformational and topographical properties in order to obtain insights into the bioactive conformation of the native peptide on interaction with its receptor. Important peptide mediators of biological information transduction such as hormones and neurotransmitters have great potential for medical applications, but often have inherent drawbacks such as high degrees of flexibility, biodegradability, and lack of receptor selectivity, which can complicate their use as drugs. Conformational constraints play an important role in rational design of peptides and peptide mimetics that can overcome these problems.[10,12] Conformationally constrained peptides are often more stable, more selective and have fewer side effects.

De novo design is design of new compounds on the basis of proved or proposed pharmacophores. The "secondary structure approach" to *de novo* design of peptidomimetics is guided by the simple elegance which nature has employed in the molecular architecture of proteins.[21] Of the three major types of secondary structural motifs (α-helices, β-sheets and reverse turns), reverse turns offer the significant synthetic advantage that they are relatively compact, and of such a size that, in principle, they can be more readily mimicked by conformational constraint, or by use of more rigid small organic molecules.[108] The surface localization of reverse turns and the predominance of reverse turn residues containing potentially critical pharmacophoric information strongly support the hypothesis that reverse turns play critical roles in peptide-receptor interaction. Since side chains are often extremely important in molecular recognition events, an ideal reverse turn mimetic should have the following characteristics: proper backbone geometry (relatively rigid scaffold); proper side chain orientation; synthetically accessibility.

β-Turns (Fig. 3.1) are formed by tetrapeptide sequences, which in most cases have a 10-membered intramolecularly H-bonded ring. β-Turns are classified by the φ and ψ angles of the i+1 and i+2 residues, while the distance between Cα (i) and Cα(i+3) varies from 4 to 7 Å.

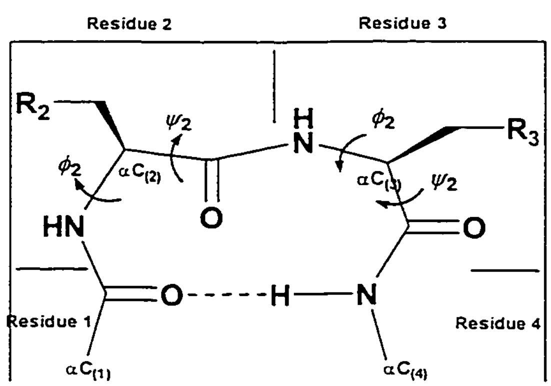

Turn type	ϕ_2	ψ_2 (degrees)	ϕ_3	ψ_3
I	-60	-30	-90	0
I'	60	30	90	0
II	-60	120	80	0
II'	60	-120	-80	0
III	-60	-30	-60	-30
III'	60	30	60	30
V	-80	80	80	-80
V'	80	-80	-80	80

Fig. 3.1. Definition and classification of β-turns

Though quite a few successes have been reported in obtaining mimetics which can force or stabilize β-turns,[109-117] very little success has been obtained in incorporating such mimetics into the agonist active site of peptide hormone or neurotransmitter ligands, due to the lack of appropriately positioned side chain groups. In the event of molecular recognition, the peptide backbone serves as a scaffold for the key side chain groups involved in the interaction. The side chain moieties involved directly in the binding are critical for the interaction. Their 3D architecture (topography) and stereoelectronic properties provide the critical complementary shape and chemical properties that favor efficient molecular recognition. In order to truly mimic the backbone conformation and side chain orientation of different types of β-turns, a synthetic strategy requires stereocontrolled introduction of a minimum of four asymmetric centers, with different backbone geometry and side chain topography. Here we report our efforts to fulfil all the aforementioned criteria.

α-Melanotropin Ligands

α-Melanotropin (α-melanocyte-stimulating hormone, α-**MSH**, Ac-Ser^1-Tyr-Ser-Met-Glu^5-His-Phe-Arg-Trp-Gly^{10}-Lys-Pro-Val-NH_2) belongs to the family of melanotropin peptides derived by the post-translational processing of the proopiomelanocortin (POMC) gene.[118] Many biological activities have been attributed to this peptide hormone. Both peripheral and central nervous system activities related to α-**MSH** include cognitive effects related to learning, memory and attention,[119,120] analgesic effects,[120] modulation of body temperature,[121] role in fetal development and parturition,[122] and immunomodulatory effects.[123] The most recognized biological activity of α-**MSH** is its role in regulating skin pigmentation.[124] Melanotropic peptides mediate their actions through melanocortin receptors (MCRs) that are restricted to certain cells.[125]

Presently, five distinct MCRs have been cloned and found to have different tissue expression patterns: MC1R, MC2R, MC3R, MC4R, and MC5R.[126-136]

These multiple physiological effects have made α-**MSH** the target of extensive structure-activity studies.[137-140] The Hruby group has designed and synthesized over 1000 analogues of α-**MSH** and have determined the minimal fragment of the native peptide needed for biological activity. Specifically, using the classical frog and lizard skin bioassays, it was determined that the minimal fragment of α-**MSH** required for agonist activity is its central tetrapeptide sequence, His^6-Phe^7-Arg^8-Trp^9, as exemplified by the analogue Ac-His-Phe-Arg-Trp-NH_2.[141] Both *N*- and *C*-terminal amino acid extension of the central tetrapeptide sequence increased potency to match that of α-**MSH**, as exemplified by Ac- α-$\mathbf{MSH}_{4\text{-}11}$-$NH_2$ on the lizard skin bioassay and by Ac-α-$\mathbf{MSH}_{4\text{-}12}$-$NH_2$ on the frog skin bioassay.[137] The replacement of the Met oxidizable side chain with the oxidatively stable amino acid Nle (an isostere of Met) resulted in a 10-fold enhancement of the biological activity of the native peptide. Replacement of *L*-Phe^7 with *D*-Phe^7 further enhanced the biological activity of α-**MSH**.[142,143] These studies led to the development of Ac-[Nle^4,$Dphe^7$]α-**MSH** (**MT-I**), which is 3-100 times more potent than α-**MSH** in assays of various types.[142] Substitution of a *D*-Phe residue makes this peptide resistant to proteolytic degradation, leading to a longer duration of action.

The biologically active conformation of α-**MSH** at the MC1R consists of a β-turn in the vicinity of the *D*-Phe residue, as determined by molecular modeling and conformational calculations on this peptide.[64,65] Further, the Met^4 and Gly^{10} residues were relatively close to each other in the parent compound. This bioactive conformation was first shown to be possible by the design and study of the macrocyclic analogue Ac-*c*[Cys^4, Cys^{10}]α-$\mathbf{MSH}_{1\text{-}13}$-$NH_2$, which proved to be a superpotent compound, being 10 to 20 times more potent than the native α-**MSH** hormone in the frog skin bioassay.[144]

Several conclusions were drawn from this series of cyclic α-**MSH** analogues: 1) cyclization between positions 4 (Met) and 10 (Gly) by isosteric replacement with cysteine enhanced the melanocyte dispersion activity by not less than 10 times in frog skin and two times in the lizard skin bioassay; 2) substitution of Phe^{7} with *D*-Phe^{7} in these cyclic analogues causes double the activity in frog skin and four times the activity in lizard skin bioassay; 3) the presence of Lys at position 11 always gave more active analogues than those without it; and 4) reduction and expansion of the ring size of the disulfide bridge from a 23-membered ring caused severe reduction in the biological potency of the resultant analogue.[137,144] However, these cyclic compounds were not potent in mammalian systems. NMR results and molecular modeling showed that the Lys^{11} and Glu^{5} side chains do not form a salt bridge to stabilize a secondary structure, but if Lys^{10} is substituted for Gly^{10}, the residues Lys^{10} and Glu^{5} are well disposed to form a stable salt bridge.

Following up on this information, a number of linear, cyclic and bicyclic second generation α-**MSH** analogues were synthesized and tested[65,144-150] including the cyclic lactam analogue Ac-*c*[Nle^{4},Asp^{5},Dphe^{7},Lys^{10}]α-**MSH**(4-10)-NH$_2$ (**MT-II**).[66,151] This peptide is about 100 times more potent in the lizard skin and in the mammalian assay systems and has become the lead molecule for extensive studies to optimize and identify the bioactive conformations of α-**MSH**.[151-155] In addition highly potent antagonists have been discovered.[154]

Table 3.1. Comparative biological properties of **MT-I** and **MT-II**.

α-MSH : Ac-Ser-Tyr-Ser-Met-Glu-***His-Phe-Arg-Trp***-Gly-Lys-Pro-Val-NH$_2$
MT-I : Ac-Ser-Tyr-Ser-Nle-Glu-***His-D-Phe-Arg-Trp***-Gly-Lys-Pro-Val-NH$_2$

MT-II : Ac-Nle-Asp-***His-D-Phe-Arg-Trp***-Lys-NH$_2$

	Relative Potency	
	Frog skin	Lizard skin
α-MSH	1.0	1.0
MT- I	60.0	5.0
MT – II	0.8	90.0

Oxytocin Analogues

Oxytocin, H-Cys-Tyr-Ile-Gln-Asn-Cys-Pro-Leu-Gly-NH_2 (**OT**), is a neurohypophyseal hormone physiologically important for its milk-ejecting and uterine-contracting activity in mammals. **OT** was the first peptide hormone whose primary structure was determined and proven by total synthesis.[156] Intensive structure-activity relationship studies carried out for four decades have resulted in several hundred analogues of **OT**.[157,158]

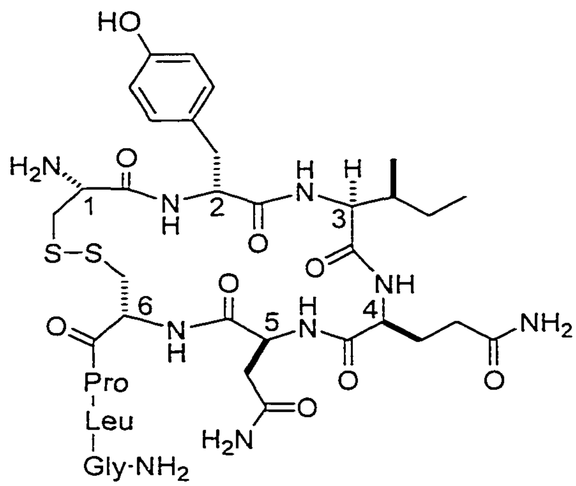

Fig. 3.2. Oxytocin

The 3D structure of oxytocin and the structurally related neurohypophyseal hormone vasopressin (**VP**) have been extensively investigated both by experimental and by theoretical methods.[159-161] Since the first model of solution conformation of **OT** was proposed by Urry and Walter,[162] several molecular mechanics[163-166] and molecular dynamics[167-169] studies have been aimed at determining low-energy conformations and at evaluating conformational mobility of neurohypophyseal hormones. Although a broad variety of models have been suggested for **OT**,[159-166] most researchers were in agreement that a conformation with a β–turn at positions 3 and 4, and with a reverse turn at positions 7 and 8, might be responsible for the uterotonic activity of **OT** and its analogues. This type of conformation was found also in the crystal structure of the potent **OT** agonist deaminooxytocin.[170] Extensive electrostatically driven Monte Carlo simulations *in vacuo* and with a solution-shell model have shown[171] that, despite restrictions imposed by the 20-membered disulfide ring, the **OT** molecule retains considerable conformational mobility, and energy preferences for several quite different types of conformations of **OT** are possible depending on the environment. This flexibility of the disulfide ring was probably the reason for different models of solution and receptor-bound conformations proposed for neurohypophyseal hormones in earlier studies.[162-166]

Inhibitors of the uterotonic activity of **OT** have been traditionally produced by introduction of bulky β-carbon substituents into position 1 and/or by substitution of L-tyrosine in position 2 of **OT** and VP with an aromatic D-amino acid.[172] Bulky β-carbon substituents in position 1 were shown to constrain the conformational mobility of the disulfide bridge moiety of **OT** and VP.[173] Nevertheless, both theoretical calculations and NMR studies showed[174,175] that substantial conformational mobility of the 20-membered disulfide ring was retained despite the additional conformational constraints imposed by substitutions in position 1.

A novel class of bicyclic antagonists of **OT** (**OT**-BC) have been prepared by amide bond cyclization between side chains in positions 4 and 8 of the amino acid sequence of a super-potent agonist deaminooxytocin ([Mpa1]**OT**), which resulted in the primary structure:

Xxx-Tyr-Ile-Glu-Asn-Cys-Pro-Lys-Gly-NH_2

where Xxx is β′-mercaptopropionic acid ([Mpa^1]**OT**-BC)[176] or β′-mercapto-β,β-dimethylpropionic acid ([*D*-Pen^1]**OT**-BC).[177] Discovery of these potent, conformationally restrained antagonists with pA_2 = 8.2 and 8.74, respectively,[176,177] presents a unique opportunity to investigate conformational features responsible for the uterine receptor binding of oxytocin antagonists. Extensive conformational analysis of **OT**-BC was first performed[178] with the ECEPP/2 force field,[179,180] using an elaborate build-up procedure. Low-energy conformations found for the bicyclic analogues were classified into several conformational families and compared to low-energy conformations of several monocyclic antagonists of **OT** with β-carbon substituents in position 1 of the disulfide ring. Three types of 3D structure which showed a good overlap with the monocyclic antagonists were suggested as tentative models of binding conformations of **OT**-BC to the uterine receptor of **OT**.[178] These models differ mainly by the location of a type I or type III β-turn at residues 2,3 (model 1), 3,4 (model 2), or 4,5 (model 3) of the disulfide ring. A dynamic model of solution structure of the two bicyclic analogues has been proposed as a result of the combined NMR and MD studies, and the SARs of oxytocin antagonists were discussed in connection with the solution conformation of **OT**-BC.[181]

The proposed 3D model is characterized by a type III β-turn located at the Tyr^2-Ile^3 residues and by the *cis*-amide bond between Cys^6 and Pro^7, which induces a reverse turn in the C-terminal moieties of the bicyclic peptides. The disulfide bridge and the lactam bridge moieties of two analogues are relatively flexible with respect to the constrained backbone conformation. The solution structure of **OT**-BC differs considerably from the crystal structure of deaminooxytocin[170] and from the solution structure proposed for **OT** analogues.[162] This fact confirms the hypothesis[182] that agonists and competitive antagonists of **OT** may interact somewhat differently with the uterine receptor of **OT**. This proposed model is generally consistent with structure-activity relationships of **OT** antagonists. In particular, a β-turn-like conformation in the N-terminal part seems to be the common feature of all potent **OT** antagonists that may be stabilized by substitution of Tyr^2 with a D-amino acid. A good overlap of a non-peptide antagonist of **OT** with the Tyr^2-Ile^3 dipeptide of **OT**-BC suggests that this moiety is responsible for a specific binding of antagonists to the **OT** receptor. Although this study has revealed a constrained, specifically folded conformation in the C-terminal part of **OT**-BC, the role of this moiety in the antagonist-receptor binding is still unclear. Further modifications in the C-terminal sequence of **OT**-BC are necessary to determine whether this moiety contributes to the high uterine receptor affinity of the bicyclic antagonists. In addition, the proposed 3D model does not specify the putative receptor-bound conformations for the Tyr^2 and Asn side chains. Both NMR data and MD simulations suggest considerable conformational mobility of these side chains in solution. A systematic substitution of these residues with topographically constrained analogues may reveal the side chain conformations recognized by the **OT** receptor and will contribute to the development of more exact models for the receptor-bound conformations of **OT** antagonists. The proposed solution structure of **OT**-BC presents a good template for such conformationally directed modifications and for *de novo* design of peptide and non-peptide antagonists of oxytocin.

3.2 RESULTS AND DISCUSSION

As we have discussed, extensive SAR studies on the peptide hormones/neurotransmitters α-**MSH**, oxytocin and their analogues have been done in the Hruby group.[140,183,184] Molecular dynamics simulations, molecular mechanics calculations, and NMR studies of selected potent analogues[155,181,182] have showed that in the low energy conformation, certain types of β-turns are preferred. Conformationally constrained bicyclic dipeptide mimetic scaffolds, such as template **3.1** (Fig. 3.3), can provide at least 16 stereoisomers with different backbone geometry and side chain orientation, which will greatly help us to study the bioactive conformation.

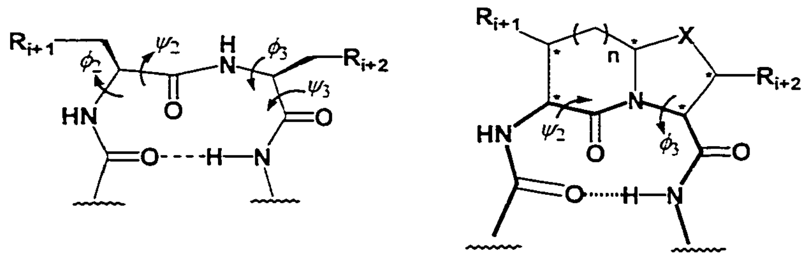

Type I β-turn **3.1**

Fig. 3.3. Conformationally constrained β-turn mimetics.

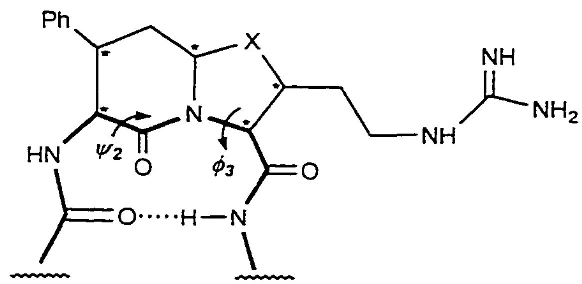

Fig. 3.4. A conformationally fixed prototype mimetic of the *Phe-Arg* portion of α-**MSH**.

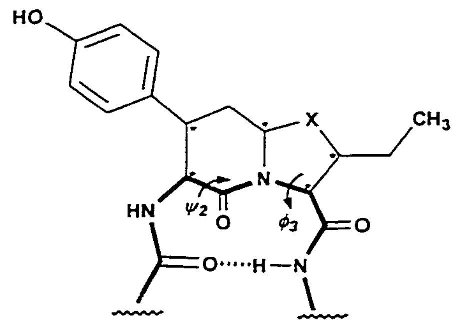

Fig. 3.5. Proposed β-turn dipeptide mimetic of oxytocin.

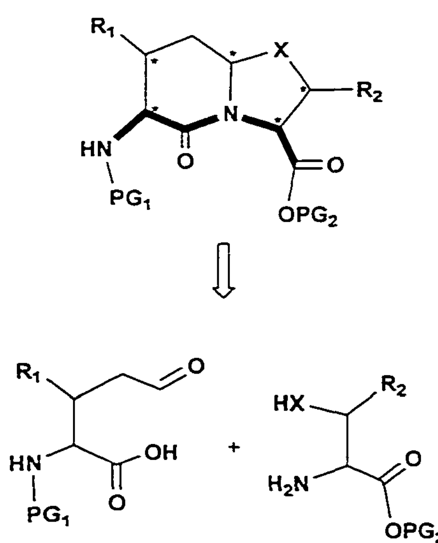

Scheme 3.1. Retrosynthetic analysis.

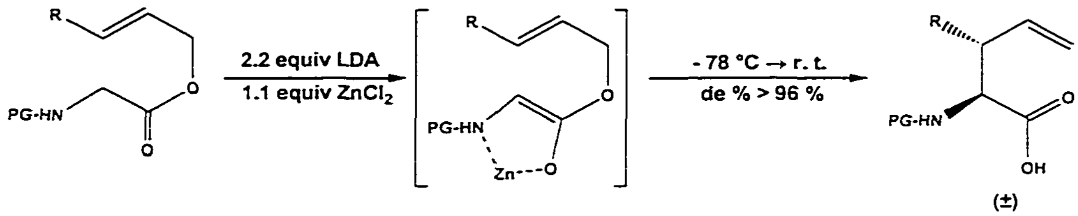

Scheme 3.2. A highly diastereoselective Claisen rearrangement.[185]

Our synthesis begins with esterification of *N*-Cbz-glycine (**3.2**) to the amino acid ester **3.4**[186] (Scheme **3.3**). A highly diastereoselective Claisen rearrangement of **3.4** generated a pair of diastereopure β-vinyl phenylalanines (**3.5**).[187] The related literature procedure only gave moderate yields (~60%), but when refluxing conditions were applied after warming to room temperature, a 78.5% yield was obtained. Formylation of **3.5** with a catalytic amount of *p*-TsOH in benzene gave 5-oxazolidinone **3.6**.

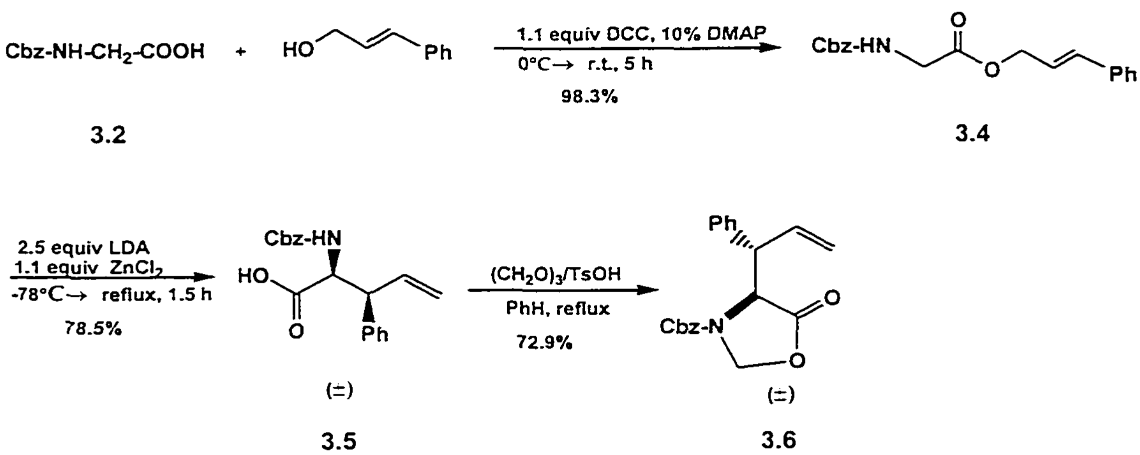

Scheme 3.3. Synthesis of [5.5]-bicyclic reverse turn mimetics (1).

Further transformation by one-pot hydroboration-oxidation was unsuccessful (Scheme 3.4).

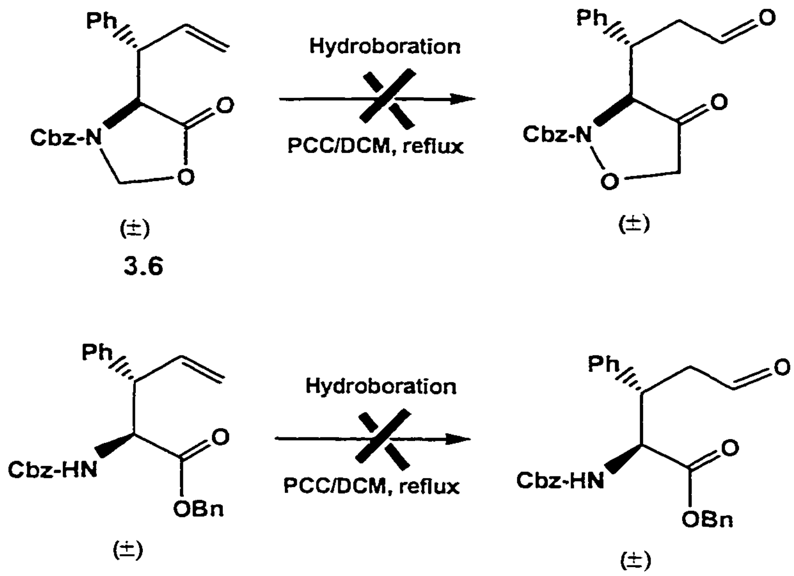

Scheme 3.4. One-Pot hydroboration/oxidation.

Oxidative cleavage of **3.5** gave γ-hydroxy-γ-lactone **3.7** (Scheme 3.5). Although intermediate **3.7** was not purified before further reactions, its monomethyl (**3.8**) and trimethyl (**3.9**) derivatives were characterized (Scheme 3.6). To a solution of **3.7** in MeOH, was added a catalytic amount of concentrated HCl. The solution was stirred at room temperature until equilibrium was reached. A 1:9 ratio of derivatives **3.8**/**3.9** was determined by ^{1}H-NMR.

Condensation of **3.7** with L-cysteine methyl ester in EtOH gave a mixture of monocyclic amino acids **3.10**[115] (Scheme 3.5), which were cyclized with DCC/HOBt in dichloromethane without further purification. Compounds **3.11** and **3.12** were separated by flash chromatography (EtOAc/Hexanes 1:4 to 1:3). Their stereochemistry was assigned by 1D transient nOe experiments and confirmed by X-ray diffraction analysis.

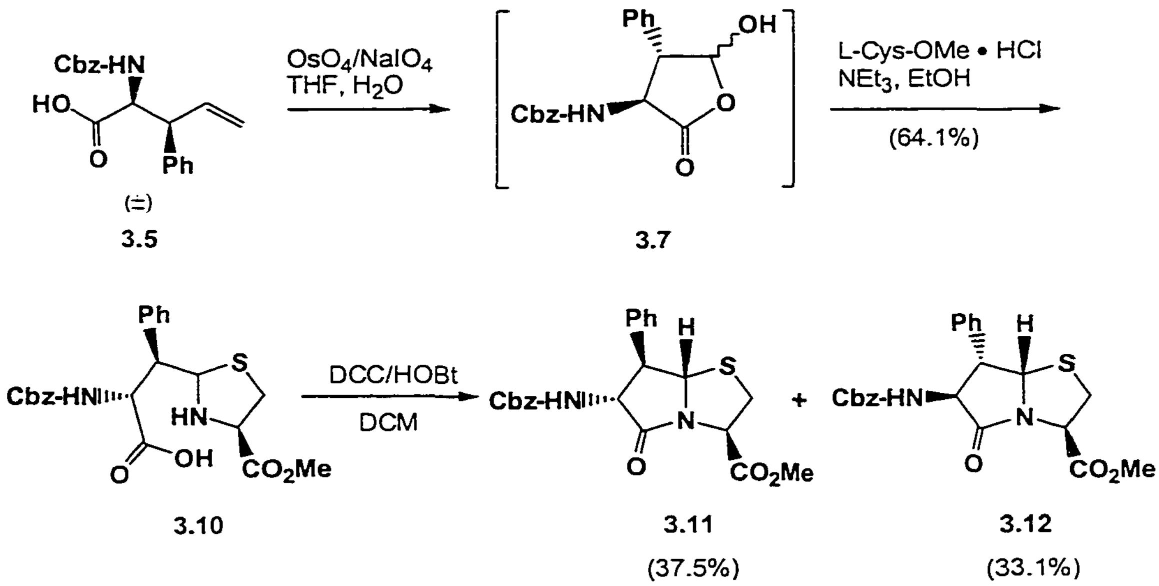

Scheme 3.5. Synthesis of [5.5]-bicyclic reverse turn mimetics (2).

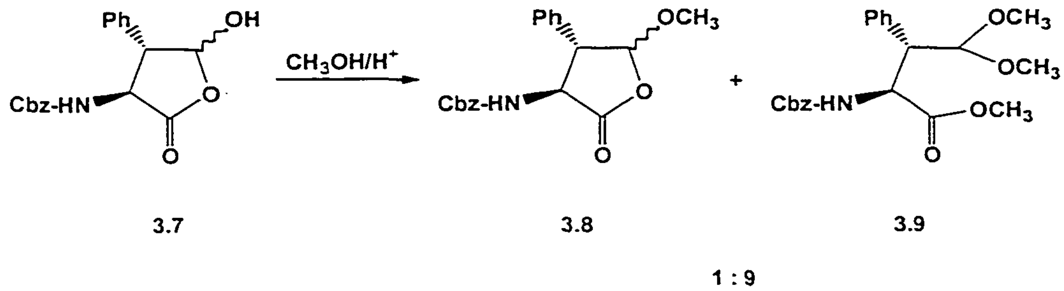

Scheme 3.6. Derivatization of γ-hydroxy-γ-lactone **3.7**.

The X-ray crystal structure of compound **3.11** is shown in Fig. 3.5. Thus we have succeeded in incorporating a phenyl group into a template which mimics a phenylalanine side chain at the *i*+1 position of a β-turn.

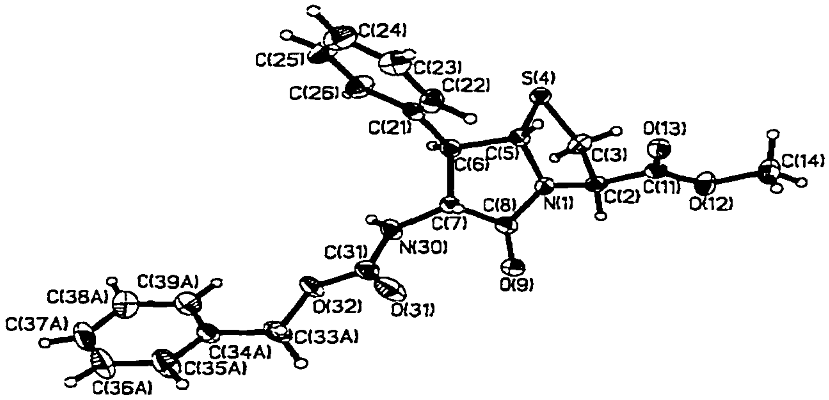

Fig. 3.6. Crystal structure of (2*R*,5*S*,6*R*,7*R*)-methyl 1-aza-7-(*N*-benzyloxycarbonylamino)-8-oxo-6-phenyl-4-thia-bicyclo[*5.5.0*]octane-2-carboxylate (**3.11**).

A Monte Carlo conformational search (MacroModel 6.0, Amber force field, aqueous environment) showed that in the lowest energy conformation, the ψ_2 and ϕ_3 values are quite close to the values of the solid state (Table 3.2), which indicates that these two tortional angles are very well constrained.

Table 3.2. Comparison of dihedral angles ψ_2 and ϕ_3.

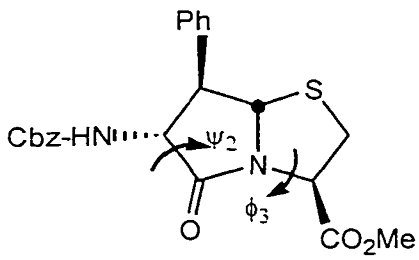

	ψ_2	ϕ_3
Crystal Structure	151.9°	-125.9°
Lowest Energy Conformation	145.0°	-138.1°

In order to incorporate an i+2 side chain into this [5.5]-bicyclic template, intermediate **3.5** was coupled with *L*-threonine methyl ester to form diastereomers **3.13** and **3.14** (Scheme 3.7). Oxidative cleavage gave a mixture of γ-hydroxy lactams, which were cyclized in dry dichloromethane with catalytic amounts of TFA and 3A molecular sieves to give compounds **3.15** and **3.16**. After separation by flash chromatography (EtOAc/Hexanes 1:4 to 1:3), the stereochemistry of **3.15** and **3.16** was assigned by 1D transient nOe experiments.

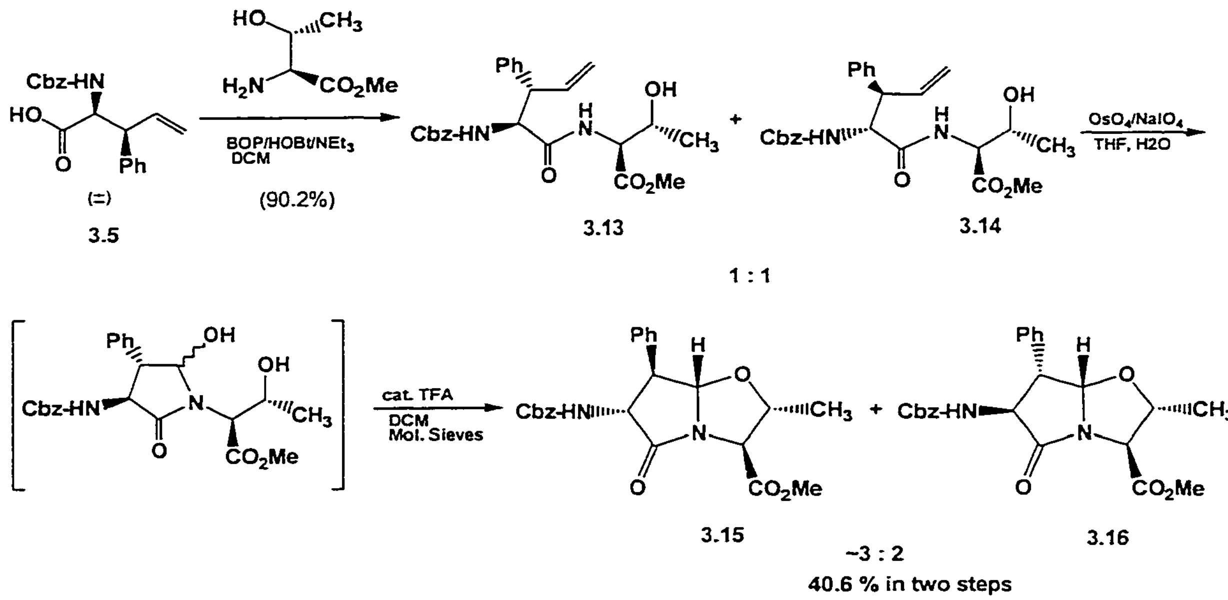

Scheme 3.7. Synthesis of [5.5]-bicyclic reverse turn mimetics (2).

In conclusion, a concise and straightforward five-step synthesis of [5.5]-bicyclic reverse turn dipeptide mimetic scaffolds with side chain functionality at the i+1 and i+2 positions has been developed. In the bicyclic structure, two dihedral angles (ψ_2 and ϕ_3) are greatly restricted. Further development of the synthesis will enable us to prepare various types of reverse turns with different backbone geometry and side chain topography. Incorporating these conformationally and topographically constrained scaffolds into peptides will help us to understand the bioactive conformation of the parent peptides. Due to its convergent nature, this synthesis also has the potential to be applied to both solid phase chemistry and combinatorial chemistry, which is under investigation.

3.3 FUTURE WORK

[6.5]-Bicyclic scaffold

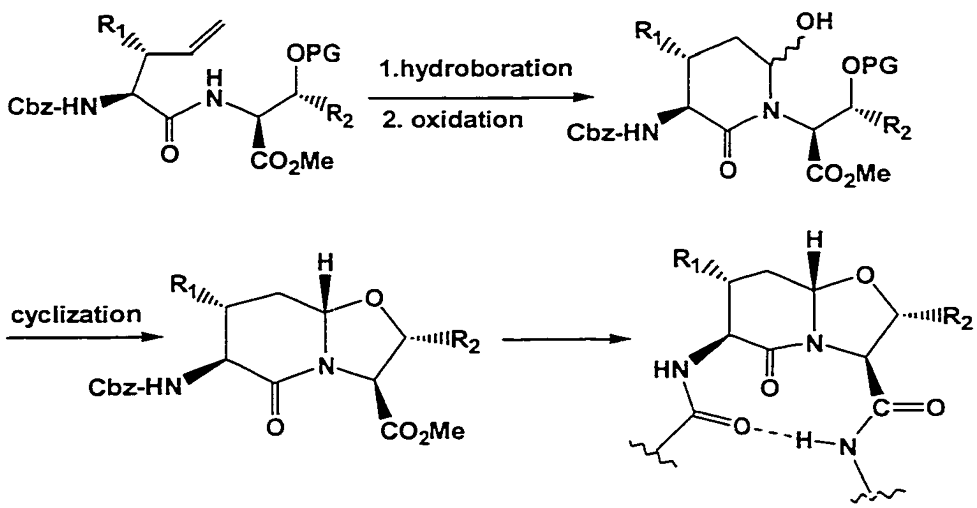

Scheme 3.8. A [6.5]-bicyclic scaffold.

[5.6]-Bicyclic scaffold

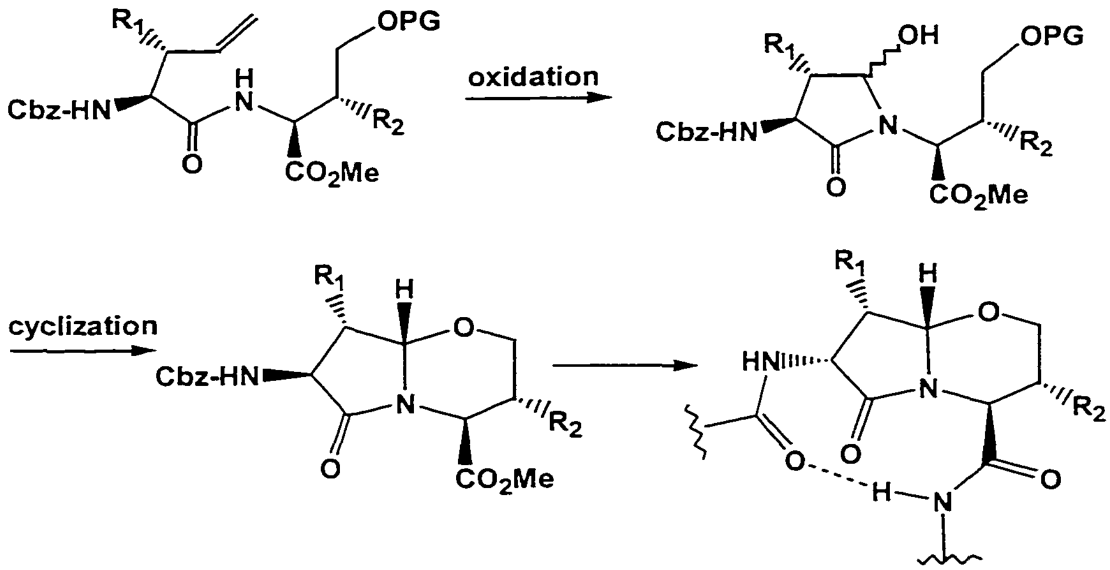

Scheme 3.9. A [5.6]-Bicyclic scaffold.

8-Membered monocyclic scaffold

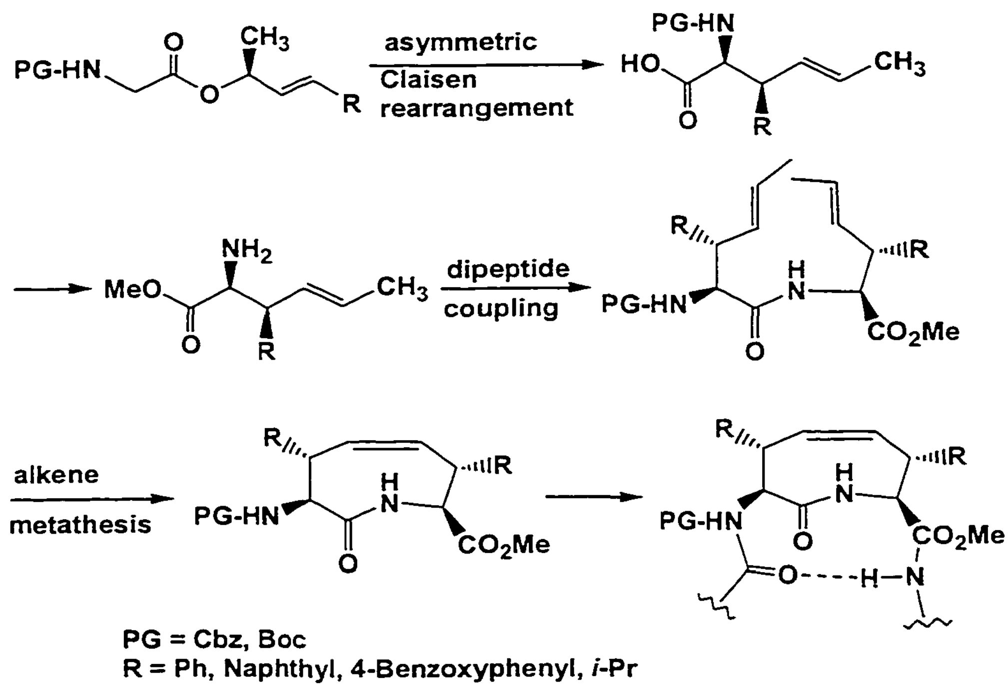

Scheme 3.10. An 8-Membered monocyclic scaffold.

Catalytic asymmetric reduction to prepare chiral secondary alcohol (Scheme 3.11)

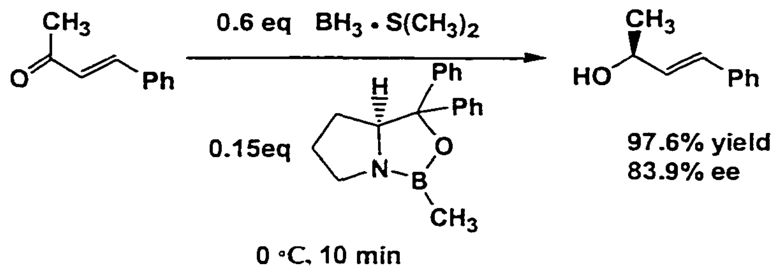

Scheme 3.11. Catalytic asymmetric hydroboration.

3.4 EXPERIMENTAL

General. ^{1}H and ^{13}C NMR were performed on a Bruker DRX-500 (500.130 MHz) spectrometer and a Bruker AM-250 (250.133 MHz) spectrometer using TMS and $CDCl_3$ as internal standards. High Resolution Mass Spectra (HRMS) were recorded on a JEOL HX110A instrument. Optical rotations were measured on a JASCO P-1020 polarimeter. Melting points (mp) are uncorrected and were obtained on a Thomas-Hoover apparatus in open capillaries. All reagents and solvents, unless otherwise stated, were bought from Aldrich Chemical Co. and used as received. The following solvents were freshly distilled and stored under nitrogen prior to use: THF from potassium/benzophenone, CH_2Cl_2 from CaH_2. Analytical TLC was performed on Merck precoated Kieselgel 60 F-254 plates with the following solvent systems (v/v): **(I)** EtOAc/hexanes (3/7), **(II)** EtOAc/hexanes/HOAc(30/70/1). Detection was made using I_2, ninhydrin, or UV light. Unless otherwise stated, yields refer to isolated yields of products of greater than 95% purity as estimated by ^{1}H-NMR spectroscopy.

General Procedure for Esterification

To a solution of Cbz-Gly-OH **3.2** (30 g, 143.4 mmol) in THF (200 mL), cinnamyl alcohol (17.85 g, 130.3 mmol) was added with stirring, followed by DMAP (1.61 g, 13.0 mmol). The mixture was cooled to 4 °C (ice water) and DCC (29.9 g, 143.4 mmol) in THF (50 mL) was added dropwise. The resulting solution was stirred at 4 °C for 5 min, then at room temperature overnight. TLC (EtOAc/Hexanes 2:3) showed no cinnamyl alcohol left. The white precipitate (DCU) was filtered out. The solution was rotary evaporated, dissolved in 200 mL ether, washed with 5% HOAc (2 x 150 mL), water (200 mL), sat. $NaHCO_3$ (2 x 150 mL), and dried over anhydrous $MgSO_4$. After filtration and rotary evaporation, the crude brownish oil was crystallized from hexanes to give white needles of **3.4** (41.77 g, 98.3 %).

N-Cbz-Glycine cinnamyl ester (3.4)

Yield: (98.3%); mp 66.5-67 °C. ^{1}H-NMR ($CDCl_3$) δ 4.04 (2H, d, J = 5.6 Hz), 4.81 (2H, d, J = 6.5 Hz), 5.14 (2H, s), 5.27 (1H, m), 6.28 (1H, dt, J = 13.1, 6.5 Hz), 6.67 (1H, d, J = 16.0 Hz), 7.26-7.41 (10H, m).

General Procedure for Claisen Rearrangement

To a 500 mL flame-dried two-necked round bottom flask equipped with a condenser, a pressure-equalizing funnel and a magnetic stirring bar, allylic ester **3.4** (9.15 g, 28.1 mmol) was added under N_2, followed by zinc chloride (15.5 mL, 30.9 mmol, 2.0M, in THF) and 150 mL freshly distilled THF. The slightly cloudy solution was cooled to –78 °C. Pre-cooled, freshly prepared LDA (72.6 mmol) in 100 mL THF was added via cannula. The cloudy yellow solution was warmed to room temperature, then refluxed for 1.5 h. The resulting orange solution was diluted with 150 mL anhydrous ether, hydrolyzed with 1N HCl at 4 °C (ice water) to pH = 1 (~200 mL HCl solution needed). Then the ether layer was extracted with 1N NaOH (3 x 100 mL). Acidification of the aqueous layer at 4 °C with 6N HCl to pH = 2, followed by extraction with ether (3 x 100 mL) and rotary evaporation gave 8.46 g brownish sticky oil. Crystallization from hexanes gave **3.5** (7.18 g, 78.5 % yield) as a light yellow solid.

(2*SR*,3*SR*) N-Cbz-β-Vinylphenylalanine (3.5)

^{1}H-NMR (CDCl3) δ 3.89 (1H, ABX, J_{AX} = 7.0 Hz, J_{AB} = 6.5 Hz), 4.79 (1H, ABX, J_{AX} = 8.5 Hz, J_{AB} = 6.5 Hz), 5.07-5.32 (4H, m), 6.10 (1H, m), (1H, m), 7.19-7.37 (10H, m).

Procedure for Oxidative Cleavage

A 100 mL round bottom flask with magnetic stirring bar was charged with **3.5** (1 g, 3.07 mmol) and 45 mL THF/H_2O (v/v 2:1). To the clear solution was added OsO_4 (40 mg, 0.15 mmol). After 5 min, $NaIO_4$ (1.67 g, 7.68 mmol) was added in batches to the dark solution over a period of 10 min. After stirring for 24 h, the white precipitate was filtered. The solution was rotary evaporated, then partitioned between ether (30 mL) and sat. $NaHCO_3$ (70 mL). The aqueous layer was acidified with 6N HCl to pH = 1 and extracted with EtOAc (3 x 80 mL). The combined organic solution was dried over anhydrous $MgSO_4$, rotary evaporated, and dried under vacuum to give **3.7** (0.98 g, 98% crude yield) as a pale yellow oil.

γ-Hydroxy-γ-lactone 3.7

^{1}H-NMR ($CDCl_3$) δ 3.65 (1H, m), 4.72 (1H, m), 5.02 (2H, s), 5.84 (1H, m), 7.26-7.36 (10H, m), ^{13}C-NMR ($CDCl_3$) δ 25.5, 29.6, 59.7, 64.3, 67.1, 67.6, 70.9, 117.8, 127.3, 127.8, 128.1, 128.3, 128.7, 128.8, 128.9, 129.1, 129.3 129.7, 134.8, 170.2, 197.5.

Procedure for Condensation with L-Cys-OMe

3.7 (0.98 g, 2.99 mmol) in 15 mL 95% EtOH was cooled to –20 °C (*i*-PrOH/dry ice), then $KHCO_3$ (300 mg, 3.0 mmol) in water (15 mL) was added, followed by *L*-Cys-OMe·HCl (524.4 mg, 3.0 mmol). The pH was adjusted to 6.5 with 2% $KHCO_3$. After stirring for 12 h, the reaction mixture was condensed to half of the volume, and the pH was adjusted to 6 with 1N HCl. Extraction with EtOAc (3 x 80 mL) with readjustment of the pH to 6 between extractions gave combined extracts which were dried over $MgSO_4$, followed by rotary evaporation to give **3.10** (0.63 g, 64.1% crude yield) as alight yellow oil. Intramolecular condensation of **3.10** with DCC/HOBt gave a mixture of **3.11** and **3.12**, which was separated by flash chromatography (EtOAc/Hexanes v/v 1:4 to 1:3). A needle of **3.11** was submitted for X-ray crystal diffraction analysis.

[5.5]-Bicyclic 3.11

^{1}H-NMR ($CDCl_3$) δ 3.31-3.35 (2H, m), 3.64 (1H, m), 3.74 (3H, s), 4.86 (1H, m), 5.01 (2H, m), 5.09-5.10 (1H, m), 5.30 (1H), 5.59 (2H, d, J = 8.5 Hz,), 7.23-7.31 (10H, m). $[M+H]^+$ 427.1.

[5.5]-Bicyclic 3.12

^{1}H-NMR ($CDCl_3$) δ 3.30-3.37 (2H, m), 3.68 (1H, m), 3.76 (3H, s), 4.83 (1H, m), 5.03 (2H, m), 5.07-5.11 (1H, m), 5.30 (1H), 5.57 (2H, d, J = 8.5 Hz), 7.21-7.32 (10H, m). $[M+H]^+$ 427.1.

Procedure for Dipeptide Coupling

3.5 (1 g, 3.07 mmol) in 20 mL DCM, was added BOP (1.5 g, 3.4 mmol), HOBt (0.46 g, 3.4 mmol), *L*-Thr-OMe•HCl (0.58 g, 3.4 mmol). The resulting solution was cooled to 4 °C (ice water), followed by dropwise addition of NEt_3 (1.08 mL, 7.67 mmol). After stirring at room temperature overnight and rotary evaporation, the residue was dissolved with EtOAc (100 mL), washed with 1N HCl, water, sat. $NaHCO_3$, water, and dried over $MgSO_4$. Hexanes/acetone (v/v 2:1) as eluent gave a 1:1 mixture (^{1}H NMR) of **3.13** and **3.14** (1.22 g, 90.2%).

Dipeptide 3.13 and 3.14

^{1}H-NMR ($CDCl_3$) δ 1.10, 1.15 (3H, d, J = 6.0 Hz), 3.65, 3.67 (3H, s), 3.85 (1H, m), 4.21 (dd, J = 4.5 Hz), 4.43-4.45, 4.48-4.50 (1H, m), 4.75-4.78 (1H, m), 4.92-5.09 (4H, m), 6.16-6.23 (1H, m), 6.41 (dd, J = 8.0 Hz), 7.17-7.35 (10H, m), 7.50 (1H, dd, J = 6.5 Hz). $[M+H]^+$ 441.3.

Procedure for Oxidative Cleavage of 3.13 and 3.14 and Cyclization to Prepare 3.15 and 3.16

To a 1:1 mixture of **3.13** and **3.14** (0.5 g, 1.135 mmol) in THF/water (21 mL, v/v 2:1), OsO_4 (15 mg, 0.057 mmol) was added. After 5 min, under vigorous stirring, $NaIO_4$ (0.74 g, 3.4 mmol) was added in batches over 15 min. After stirring at room temperature for 2 h, the reaction mixture was filtered. The precipitate was washed with EtOAc. After rotary evaporation, the residue was dissolved in EtOAc (50 mL), washed with brine, dried over $MgSO_4$. Rotary evaporation gave 0.58 g of light yellow oil. Drying under vacuum afforded an off-white powder (0.53 g). DCM (10 mL) and 3A molecular sieves were added, followed by 10 μL TFA. The reaction mixture was stirred at room temperature overnight. Flash chromatography (EtOAc/Hexanes 1:4 to 1:3) separated **3.15** and **3.16** (40.6 % in two steps). The stereochemistry of **3.15** and **3.16** was determined by 1D transient nOe NMR experiments.

[5.5]-Bicyclic 3.15

^{1}H-NMR (CD_3COCD_3) δ 1.48 (3H, d, J = 6.0 Hz), 3.66 (1H, dd, J = 11.5, 5.0 Hz), 3.75 (3H, s), 4.13 (1H, d, J = 6.5 Hz), 4.37 (1H, m), 4.98 (1H, dd, J = 11.5, 9.5 Hz), 5.07 (2H, AB, J = 17.5, 13.0 Hz), 5.28(1H, d, J = 5.5 Hz), 6.94 (1H, d, J = 9.0 Hz), 7.27-7.34 (10H, m). HRMS (FAB) $[M+H]^+$ calcd. for $C_{23}H_{24}N_2O_6$ 424.1634, found 424.1634.

[5.5]-Bicyclic 3.16

^{1}H-NMR (CD_3COCD_3) δ 1.39 (3H, d, J = 6.0 Hz), 3.77 (3H, s), 3.94 (1H, dd, J = 10.5, 5.0 Hz), 4.19 (1H, m), 4.37 (1H, m), 4.65 (1H, dd, J = 9.5 Hz), 5.07 (2H, AB J = 16.5, 12.5 Hz), 5.26(1H, d, J = 5.0 Hz), 7.03 (1H, d, J = 8.5 Hz), 7.29-7.41 (10H, m). HRMS (FAB) $[M+H]^+$ calcd. for $C_{23}H_{24}N_2O_6$ 424.1634, found 424.1638.

Chapter 4

CONVENIENT ASYMMETRIC SYNTHESIS OF ENANTIOPURE *TRANS*-CINNAMYLGLYCINE AND -α-ALANINE

4.1 INTRODUCTION

Systematic studies conducted by our group into the chemical-physical basis for peptide-mediated biological information transfer, as a function of topographical properties and three-dimensional structure of peptides, has led to a uniquely fruitful approach to the *de novo* design of peptides via rational introduction of global and local constraints to the peptide's geometry.[10,12,13,19] Since phenylalanine (Phe) often plays a pivotal role as a pharmacophore element in biologically active peptides and proteins, much attention had been paid by us[188-192] and others[193-201] to the development of sterically constrained analogues of this essential amino acid and related tyrosine (Tyr) analogues to be used as building blocks in the rational design of peptide and proteins. Our efforts in this field resulted in the discovery of β-methyl-2′,6′-dimethyl tyrosine (TMT),[93] used as a key structural unit in the design and synthesis of numerous bioactive peptides, some of which have potential medicinal applications.[79,202] Thus, while the pattern of steric substitution on the Phe moiety in peptides has been extensively studied, little is known about the possibility of modifying biological activity of Phe-containing peptides by altering the distance between the pharmacophoric phenyl ring and the α-stereogenic carbon in the original Phe molecule. To pursue this opportunity we chose (*S*)-*trans*-cinnamylglycine (**4.1**) and -α-alanine (**4.2**, Fig. 4.1) as first, most interesting targets. In this chapter, a convenient asymmetric method for preparing these amino acids on a multi-gram scale is described.

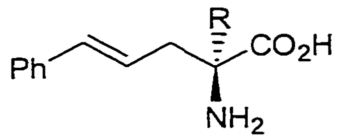

4.1 R = H
4.2 R = CH_3

Fig. 4.1. (*S*)-*trans*-Cinnamylglycine and -α-alanine.

4.2 RESULTS AND DISCUSSION

A literature search for enantiomerically pure *trans*-cinnamyl derivatives of glycine **4.1** and α-alanine **4.2** revealed that these amino acids have been prepared by traditional approaches such as biocatalytic resolution of the corresponding racemates[203] or elaboration of enantiomerically pure glutamic acid derivatives.[204] More recent and methodologically straightforward methods involved the asymmetric alkylation of chiral equivalents of nucleophilic glycine and alanine, respectively. For instance, reactions between *trans*-cinnamyl bromide and lithium enolates of *c*-(*S*)-Val-Gly or Ala *bis*-lactim ethers,[205-208] or (2*S*,4*S*)-2-ferrocenyl-3-pivaloyl-4-methyl-1,3-oxazolidin-5-one[209] were shown to afford the corresponding derivatives of the target amino acids **4.1** and **4.2** in high chemical yield and excellent diastereoselectivity. In contrast, asymmetric cinnamylation of (6*S*)- or (6*R*)-6-methylmorpholine-2,5-dione derivatives was less successful, giving rise to the desired diastereomeric products in less than 75% de.[210] An efficient catalytic asymmetric hydrogenation of the corresponding enamide furnishing *trans*-cinnamylglycine (98.6% ee) also has been reported.[211] However, an apparent disadvantage of this method for large scale synthesis would be the high-pressure (90 psi) reduction protocol. One more approach to the stereochemically defined *trans*-cinnamylglycine (**4.1**) via asymmetric Claisen rearrangement of chelated enolates of chiral *N*-protected glycine allyl esters[212] should be mentioned.

In our experience, Ni (II)-complexes of the chiral Schiff bases of glycine or alanine[213-225] with (*S*)-*o*-[*N*-(*N*-benzylprolyl)amino]benzophenone (BPB), as chiral equivalents of nucleophilic glycine **4.3** and alanine **4.4** (Fig. **4.2**), provide a generally more practical solution for the asymmetric homologation of these simple amino acids than the above-mentioned methods.[203-212] Apparent synthetic advantages of Ni (II)-complexes **4.3** and **4.4** over other known and well-tried chiral equivalents of nucleophilic glycine and alanine are the readily availability of **4.3** and **4.4** even on kilogram scales[226] (Scheme **4.1**) and recyclability. Another reason is the simple experimental procedure for the corresponding asymmetric alkylation step (no air- or moisture-sensitive reagents; easy monitoring with TLC; easy work-up and purification procedures). Therefore, we decided to study the reactions of Ni (II)-complexes **4.3** and **4.4** with *trans*-cinnamyl halides to develop a practical large-scale asymmetric synthesis of the target amino acids.

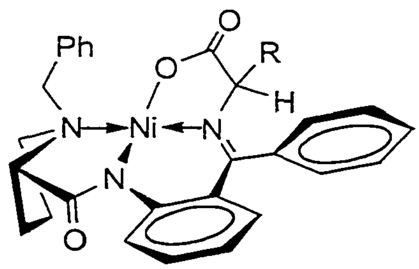

4.3 R = H
4.4 R = CH_3

Fig. 4.2. Chiral Ni(II) complex.

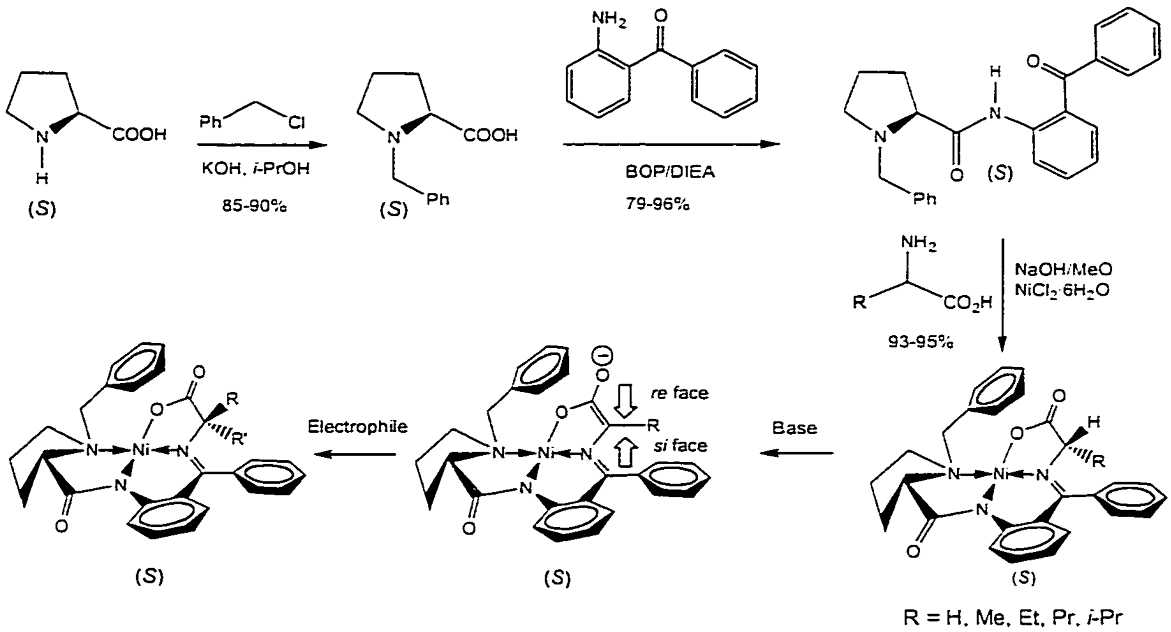

Scheme 4.1. Preparation and nucleophilic reaction of chiral Ni(II) complex.

Synthesis of (*S*)-trans-cinnamylglycine (4.1). Since the reactivity of cinnamyl halides was expected to be similar to that of benzyl/allyl halides, we decided to use initially the conditions used previously for the corresponding benzylation/allylation of glycine complex (*S*)-**4.3**.[227,228] The reaction of complex (*S*)-**4.3** with *trans*-cinnamyl bromide **4.5a** was conducted in DMF solution at room temperature in oxygen-free atmosphere (N_2) using powdered KOH as a base and 1/1.5 ratio of the starting (*S*)-**4.3** and **4.5a**, respectively (Scheme 4.2). The exothermic reaction was completed in less than 5 min giving rise in high chemical yield to a mixture of products **4.6-4.8** in a ratio of 24.4/1.0/13.1, respectively (Table 4.1, entry 1). All three products were isolated in diastereomerically pure form by column chromatography and completely characterized. Based on the NMR spectra, compounds **4.6** and **4.7** were found to be the diastereomeric derivatives of *trans*-cinnamylglycine, while complex **4.8** showed data consistent with the corresponding *bis*-cinnamylation product. Investigation of the chiroptical properties of complexes **4.6** and **4.7** allowed us to assign the absolute configuration of the corresponding *trans*-cinnamylglycine moieties as *S* and *R*, respectively. It has been demonstrated[213-225] that CD and ORD spectra of Ni (II)-complexes of this type in neutral solutions exhibit two maxima in the region of metal d-d transition (Cotton effects at 450 and 550 nm). In the ORD spectra, the sign of Cotton effects in this region strictly depends upon the conformation of the polycyclic system of chelate rings. Thus, in the case of complexes containing α-monosubstituted α-amino acid, the pseudoaxial orientation of the amino acid side chain, corresponding to an α-(*L*) configuration of an α-amino acid, causes a Cotton effect with a positive sign at the 500-700 nm region and a negative sign at 400-450 nm. On the other hand, a pseudoequatorial orientation of the amino acid side chain brings about opposite signs of the Cotton effects at 400-450 (positive) and at the 500-700 nm (negative) region. As established in numerous studies, this general trend is not influenced by the structure and nature of the α-amino acid side chain, and the configuration of other stereogenic centers that may be within it. ^{1}H-NMR spectra of the complexes containing α-(*L*)- and α-(*D*)-amino acids are also very characteristic featuring substantial difference in chemical shifts of aromatic and methylene protons of the (*N*-benzyl)proline moiety.

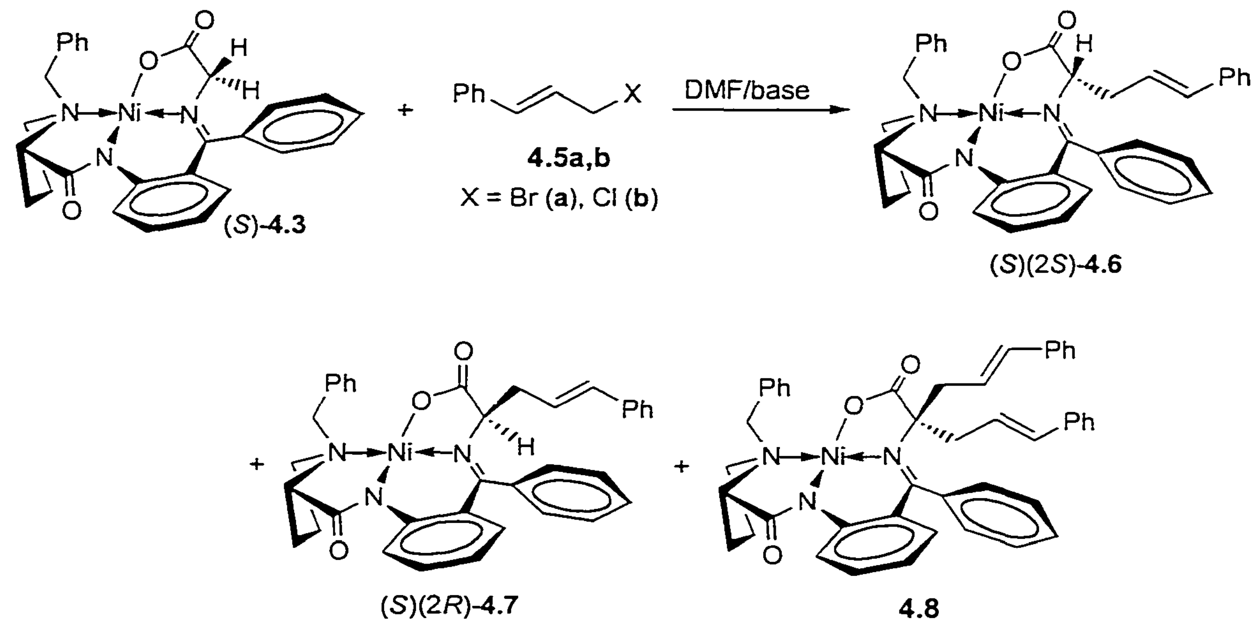

Scheme 4.2. Nucleophilic substitution of chiral Ni(II) complex.

Table 4.1. The reactions of Ni(II)-complex with *trans*-cinnamyl halides.[a]

entry	a,b	ratio	base	t, °C	time	ratio[b] 2*S*	2*R*	*bis*-	yield[c] (%)
1	a	1.0/1.5	KOH	r.t.	5 min	24.4	1.00	13.1	95.1
2	a	1.0/2.3	KOH	r.t.	1 hr	1.00	0.00	20.0	96.8
3	a	1.0/1.1	K_2CO_3	r.t.	*d*	4.50	1.00	0.00	87.4
4	b	1.0/1.0	KOH	4	10 min	26.5	1.00	1.30	95.4

[a] All reactions conducted in DMF under an inert atmosphere. [b] Ratio of diastereomers determined by ^{1}H NMR analysis of crude reaction mixtures. [c] Combined yield of all listed products. [d] Overnight.

The results obtained suggested that while the ratio of (*S*)-**4.6** and (*R*)-**4.7** diastereomers (92% de) is synthetically meaningful, the *bis*-cinnamylation side reaction would compromise large-scale preparative use of the method. Indeed, the *bis*-cinnamylation product **4.8** could be readily obtained as the major reaction product using 2.3 moles excess of bromide **4.5a** (Table 4.1, entry 2). We reasoned that the unwanted *bis*-cinnamylation reaction could be suppressed by using a less powerful base or a less reactive cinnamyl halide.

Application of K_2CO_3 in place of KOH dramatically decreased the reaction rate, taking more than 12 h at room temperature to reach 95% conversion of starting complex (*S*)-**4.3**. While our expectation was satisfied and not even trace amount of *bis*-**4.8** was detected in the reaction mixture, the ratio of (*S*)-**4.6** and (*R*)-**4.7** diastereomers was disappointedly low (entry 3). The absence of *bis*-**4.8** in this reaction might imply that K_2CO_3 as a base is ineffective in generating the corresponding enolates from the primary products (*S*)-**4.6** and (*R*)-**4.7**, and consequently, the observed stereochemical outcome is kinetically controlled. Indeed, treatment of the 4.5/1 mixture of (*S*)-**4.6** and (*R*)-**4.7**, with KOH in DMF solution resulted in a fast epimerization of the diastereomers to afford products (*S*)-**4.6** and (*R*)-**4.7** in a thermodynamically controlled ratio of 27/1, respectively. After a series of additional experiments, we found that the less reactive cinnamyl chloride **4.5b** in combination with KOH as a base provides a synthetically acceptable solution. The reaction of complex (*S*)-**4.3** with **4.5b** conducted at 4 °C gave a mixture of (*S*)-**4.6**, (*R*)-**4.7** and *bis*-**8** in a ratio of 26.5/1.0/1.3, respectively (entry 4). The same stereochemical outcome was reliably observed on gram and multi-gram scales.

Decomposition of the diastereomerically pure (*S*)-**4.6** under standard conditions[213-225] afforded the target amino acid (*S*)-**4.1** along with 94% recovery of the chiral ligand (*S*)-**4.9**, which was readily converted back to glycine complex (*S*)-**4.3** (Scheme 4.3). It is important to note that cinnamylglycine (*S*)-**4.1** was found to be extremely hydrophobic, necessitating application of a mixture of NH_4OH/EtOH as an eluent to isolate (*S*)-**4.1** from a cation-exchange column.

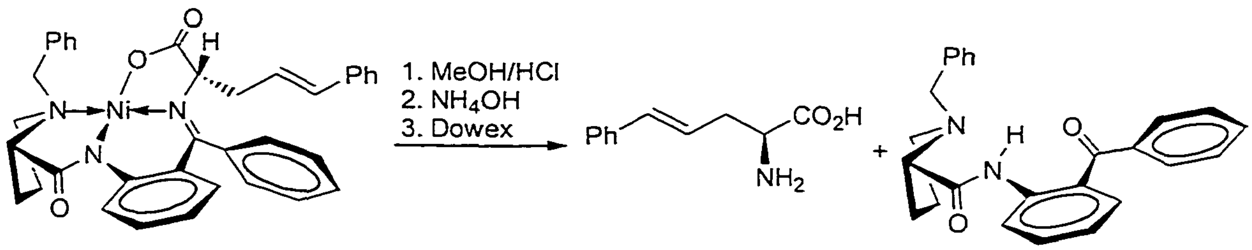

Scheme 4.3. Decomposition of Ni (II)-complex.

Synthesis of (*S*)-α-trans-cinnamyl-α-alanine (4.2). Since cinnamylation of alanine complex **4.4** cannot be accompanied by the problematic side reactions encountered in the case of glycine complex (*S*)-**4.3**, we used the more reactive *trans*-cinnamyl bromide and KOH as a base. Alanine complex **4.4** was prepared and used as a mixture of (*S*)(2*S*) and (*S*)(2*R*) diastereomers in a ratio of 10/1, respectively. As one can assume, the homologation of complex **4.4** occurs via formation of the corresponding enolate, and thus the initial diastereomeric composition of starting **4.4** does not influence the stereochemical outcome of the corresponding alkylation/benzylation/allylation reactions.[213-225] Having conducted a series of reactions between alanine complex (*S*)(2*S*,*R*)-**4.4** and **4.5a** varying the reaction temperature and ratio of the starting compounds, we found that the best synthetic result could be obtained using a 1/1.1 ratio of (*S*)(2*S*,*R*)-**4.4** to **4.5a**, respectively, at 4 °C (Scheme 4.4). Under these reaction conditions the cinnamylation of complex (*S*)(2*S*,*R*)-**4.4** was completed in 30 min, affording **4.10** in high chemical yield. Analysis of the crude reaction mixture by ^{1}H-

NMR revealed trace amounts of some byproducts formed in less than 2% yield. Based on its spectral data and chiroptical properties, the absolute configuration of **4.10** was determined to be (*S*)(2*S*). Attempts to isolate the corresponding (2*R*)-diastereomer among the minor products were not successful. It is interesting to note that the diastereoselectivity obtained in this reaction (>98% de) is better than that reported for the benzylation/allylation (90-92% de) of complex **4.4**.[213-225]

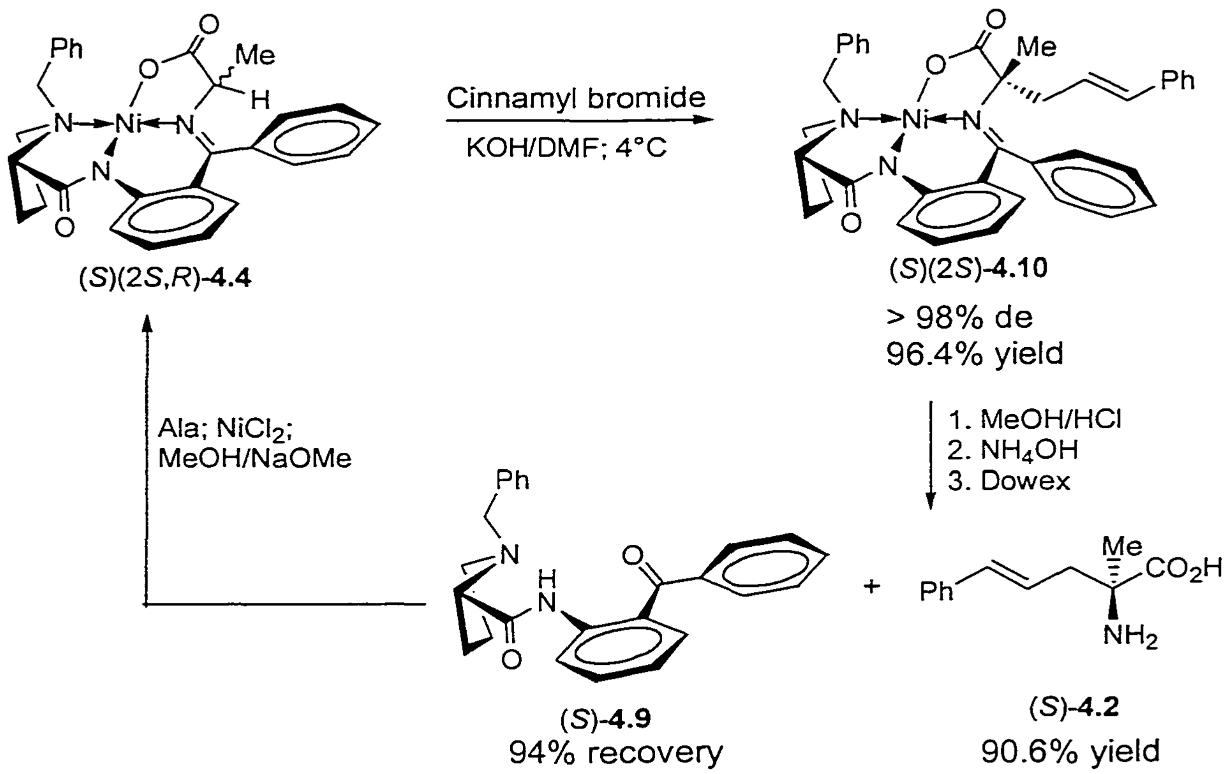

Scheme 4.4. Synthesis of (*S*)-α-cinnamylalanine and recovery of chiral ligand.

Decomposition of product (*S*)(2*S*)-**4.10** (Scheme 4.4) afforded the target (*S*)-α-*trans*-cinnamyl-α-alanine (**4.2**) as well as chiral ligand (*S*)-**4.9** which was recycled to give the starting alanine complex (*S*)(2*S*,*R*)-**4.4**. As with the glycine derivative (*S*)-**4.1**, the amino acid (*S*)-**4.2** was found to be highly hydrophobic. However its purification to the analytically pure state was readily achieved by recrystallization from water-ethanol.

In conclusion, we have demonstrated that enantiomerically pure (*S*)-*trans*-cinnamylglycine (**4.1**) and (*S*)-α-*trans*-cinnamyl-α-alanine (**4.2**) can be readily prepared via reaction of Ni (II)-complexes of glycine and alanine respectively, with cinnamyl halides (Cl, Br). Inexpensive and readily available reagents and solvents are used, including a recyclable chiral ligand, (*S*)-**4.9**. The simplicity of the experimental procedures and high stereochemical outcome make this method synthetically attractive for preparing the target amino acids on multi-gram scales.

4.3 EXPERIMENTAL

General. ^{1}H and ^{13}C NMR were performed on a Bruker DRX-500 (500.130 MHz) spectrometer and a Bruker AM-250 (250.133 MHz) spectrometer using TMS and $CDCl_3$ as internal standards. High Resolution Mass Spectra (HRMS) were recorded on a JEOL HX110A instrument. Optical rotations were measured on a JASCO P-1020 polarimeter. Melting points (mp) are uncorrected and were obtained on a Thomas-Hoover apparatus in open capillaries. All reagents and solvents, unless otherwise stated, are commercially available and were used as received. Synthesis of the Ni (II)-complex of the Schiff base of (*S*)-BPB and glycine (*S*)-**4.1** was accomplished by a literature procedure.[227,228] Unless otherwise stated, R_f values were taken using ethyl acetate/acetone (20:1) as an eluting system. Unless otherwise stated, yields refer to isolated yields of products of greater than 95% purity as estimated by ^{1}H- and ^{13}C-NMR spectroscopy. All new compounds were characterized by ^{1}H-, ^{13}C-NMR and HRMS.

General Procedure for the Reactions of Complexes (*S*)-4.3 and (*S*)(2*S*,*R*)-4.4 with Cinnamyl Halides 4.5a and 4.5b

To a solution of complex **4.3** or **4.4** (10 mmol) in DMF (45 mL) at 4 °C (ice water) under oxygen-free atmosphere, KOH powder (100 mmol) was added with stirring. The mixture was warmed to room temperature and *trans*-cinnamyl halide **4.5a** or **4.5b** in DMF (4 mL) was added dropwise. The course of the reaction was monitored by TLC (SiO_2). Each sample was quenched with 5% aqueous acetic acid and the products were extracted with chloroform before being applied to the TLC plate. Upon disappearance of the starting **4.3** or **4.4**, the reaction mixture was poured into icy 5% acetic acid aqueous solution (200 mL) and stirred with a glass bar to initiate crystallization. The crystalline product was filtered off, thoroughly washed with water and dried *in vacuo* to afford the corresponding diastereomeric products. In the case of complex (*S*)-**4.3**, resulting complexes **4.6-4.8** were isolated by flash chromatography on silica gel using acetone/ethyl acetate (1:20) as an eluent, to afford diastereomerically pure **4.8** (emerges first), **4.6** (emerges second), and **4.7** (emerges last). Yields, ratios of starting compounds (*S*)-**4.3** and **4.5a**, **4.5b**, and products **4.6-4.8** are shown in Table 4.1. Alanine derivative (*S*)(2*S*)-**4.10** was purified prior to decomposition on a short silica gel column using acetone/ethyl acetate (1:20) as an eluent.

Ni (II) complex of Schiff base of (*S*)-BPB and (*S*)-*trans*-cinnamylglycine (4.6)

R_f = 0.30. mp 129-130 °C. $[\alpha]_D^{25}$ = 2695° (*c* 0.0302, $CHCl_3$). ^{1}H-NMR ($CDCl_3$) δ 1.52-1.58 (1H, m), 1.97 (1H, ddd, *J* = 17.0, 10.5, 6.5 Hz), 2.13-2.21 (1H, m), 2.24-2.30 (1H, m), 2.48, 2.64 (2H, ABXY, J_{AB} = 14.0 Hz, J_{AX} = 7.0 Hz, J_{AY} = 4.0 Hz, J_{BX} = 7.0 Hz, J_{BY} = 6.0 Hz), 2.82-2.91 (1H, m), 3.31 (1H, dd, *J* = 10.5 , 7.0 Hz), 3.43 (1H, ddd, *J* = 10.0, 6.5, 3.0 Hz), 3.51, 4.35 (2H, AB, *J* = 12.5 Hz), 4.14 (1H, dd, *J* = 6.0, 4.0 Hz), 6.54, 6.72 (2H, ABXY, J_{AB} = 15.5 Hz, J_{AX} = J_{AY} = 7.5 Hz), 6.65-6.69 (2H, m), 6.99 (1H, m), 7.13-7.19 (2H, m), 7.23-7.34 (6H, m), 7.43-7.48 (3H, m), 7.50-7.57 (2H, m), 8.02-8.03 (2H, m), 8.20 (1H, part of AB, J = 9.0 Hz). ^{13}C-NMR ($CDCl_3$) δ 23.2, 30.7, 37.7, 57.2, 63.2, 70.3, 70.6, 120.6, 123.5, 123.5, 126.3, 126.6, 127.1, 127.7, 127.9, 128.5, 128.8, 128.9, 129.0, 129.8, 131.5, 132.3, 133.2, 133.3, 134.1, 134.7, 137.0, 139.2, 142.7, 171.0, 178.9, 180.4. HRMS (FAB) $[M+H]^+$ calcd. for $C_{36}H_{33}N_3NiO_3$ 614.1954, found 614.1964.

Ni (II) complex of Schiff base of (*S*)-BPB and (*R*)-*trans*-cinnamylglycine (4.7)

R_f = 0.25. mp 202.0-202.5 °C. $[\alpha]_D^{25}$ = -1329° (*c* 0.0256, CHCl3). ^{1}H-NMR (CDCl3) δ 1.20-1.32 (1H, m), 1.58-1.69 (2H, m), 2.01-2.04 (1H, m), 2.35-2.42 (1H, m), 2.57-2.63 (1H, m), 3.40 (1H, dd, J = 9.5, 3.5 Hz), 3.81, 4.37 (2H, AB, J = 13.5 Hz), 3.99-4.02 (1H, m), 4.05-4.14 (2H, m), 6.55, 6.74 (2H, ABXY, J_{AB} = 15.8 Hz, J_{AX} = J_{AY} = 7.6 Hz), 6.74, 6.80 (2H, AB, J = 8.0 Hz), 7.06-7.11 (1H, m), 7.18-7.36 (7H, m), 7.44-7.45 (3H, m), 7.48-7.52 (5H, m), 8.52 (1H, d, J = 8.5 Hz). ^{13}C-NMR ($CDCl_3$) δ 23.5, 31.1, 37.9, 56.5, 61.1, 68.7, 70.8, 120.7, 123.6, 124.1, 126.1, 126.5, 127.0, 127.6, 128.0, 128.6, 128.8, 129.2, 129.8, 131.8, 132.1, 132.6, 133.7, 134.2, 134.7, 137.2, 143.1, 171.1, 178.9, 182.2. HRMS (FAB) $[M+H]^+$ calcd. for $C_{36}H_{33}N_3NiO_3$ 614.1954, found 614.1948.

Ni (II) complex of Schiff base of (*S*)-BPB and *bis*-(*trans*-cinnamyl)glycine (4.8)

R_f = 0.52. mp 194-195 °C. $[\alpha]_D^{25}$ = 2102° (*c* 0.0245, CHCl3). ^{1}H-NMR ($CDCl_3$) δ 1.40-1.43 (1H, m), 1.90 (1H, ddd, J =17.0, 11.0, 6.5 Hz), 2.12-2.17 (2H, m), 2.42, 2.63 (2H, ABX, J_{AB} = 14.5 Hz, J_{AX} = 9.0 Hz, J_{BX} = 5.5 Hz), 2.57, 2.72 (2H, ABX, J_{AB} = 15.5 Hz, J_{AX} = 6.5 Hz, J_{BX} = 7.0 Hz), 2.60-2.70 (1H, m), 3.24-3.70 (1H, t, J = 8.5 Hz), 3.31, 4.30 (2H, AB, J = 12.5 Hz), 3.54-3.57 (1H, m), 6.19, 6.56 (2H, ABXY, J_{AB} = 15.0 Hz,

$J_{AX} = J_{AY}$ = 7.0 Hz), 6.63, 6.73 (2H, ABXY, J_{AB} = 15.0 Hz, $J_{AX} = J_{AY}$ = 8.0 Hz), 6.97 (1H, ddd, J = 15.5, 8.5, 6.0 Hz), 7.06-7.17 (5H, m), 7.23-7.29 (2H, m), 7.33-7.37 (3H, m), 7.46-7.58 (7H, m), 7.81 (1H, d, J = 8.5 Hz), 8.12 (2H, d, J = 7.5 Hz). ^{13}C-NMR ($CDCl_3$) δ 22.8, 30.7, 41.4, 43.3, 58.4, 64.2, 70.6, 82.3, 120.6, 123.4, 124.1, 126.3, 126.5, 127.2, 127.5, 127.6, 127.7, 128.1, 128.6, 128.7, 128.8, 129.8, 131.3, 131.4, 133.0, 133.9, 134.2, 134.6, 136.5, 137.1, 137.2, 141.6, 172.8, 180.6, 180.8. HRMS (FAB) $[M+H]^+$ calcd. for $C_{45}H_{41}N_3NiO_3$ 730.2580, found 730.2601.

Ni (II) complex of Schiff base of (*S*)-BPB and (*S*)-α-*trans*-cinnamyl-α-alanine (4.10)

Starting from 5.0 g of (*S*)(2S,R)-**4.4**, 5.80 g (94.6%) of **4.10** was obtained. R_f = 0.40. mp 123-124 °C. $[\alpha]_D^{25}$ = 2192° (*c* 0.0262, $CHCl_3$). ^{1}H-NMR ($CDCl_3$) δ 1.26 (3H, s), 1.41-1.47 (1H, m), 1.89-1.95 (1H, ddd, J = 17.2, 10.7, 6.5 Hz), 2.07-2.23 (2H, m), 2.57-2.68 (3H, m), 3.27 (1H, dd, J = 10.0, 7.0 Hz), 3.49 (1H, ddd, J = 10.0, 6.5, 2.5 Hz), 3.61, 4.39 (2H, AB, J = 13.0 Hz), 6.61-6.68 (3H, m), 6.92 (1H, ddd, J = 15.5, 9.0, 6.5 Hz), 7.09-7.14 (2H, m), 7.23-7.26 (2H, m), 7.31-7.38 (5H, m), 7.41-7.45 (1H, m), 7.48-7.53 (4H, m), 8.04 (2H, t, J = 7.0 Hz). ^{13}C-NMR ($CDCl_3$) δ 22.9, 29.4, 30.5, 43.7, 57.3, 63.4, 70.1, 78.5, 120.6, 123.8, 124.0, 126.5, 127.0, 127.5, 127.7, 128.0, 128.5, 128.6, 128.8, 128.9, 129.5, 130.6, 131.6, 133.3, 133.4, 134.5, 136.6, 137.1, 141.9, 172.6, 180.4, 181.7. HRMS (FAB) $[M+H]^+$ calcd. for $C_{37}H_{35}N_3NiO_3$ 628.2110, found 628.2096.

General Procedure for Decomposition of complexes (*S*)(2*S*)-(4.6) and (*S*)(2*S*)-(4.10); Isolation of (*S*)-trans-cinnamylglycine (4.1) and (*S*)-α–trans-cinnamyl-α-alanine (4.2) and Recovery of Chiral Ligand (S)-4.9

A solution of diastereo- and enantiomerically pure complex (*S*)(2*S*)-(**4.6**) or (*S*)(2*S*)-(**4.10**) (10 mmol) in MeOH (15 mL) was added dropwise to a mixture of aqueous 3 *N* HCl and MeOH (1:1) (70 mL) at 70 °C with stirring. Upon disappearance of the red color of the starting complex, the reaction mixture was evaporated and dried *in vacuo* to dryness. Conc. $NH_3{\cdot}H_2O$ (45 mL) was added, followed by extraction with $CHCl_3$ (40 mL). The $CHCl_3$ extract was dried over $MgSO_4$ and evaporated and dried *in vacuo* to afford (94.8-97.3 %) of free (*S*)-**4.9**. The aqueous solution was evaporated and dried *in vacuo*, dissolved in water/EtOH (1:1) and loaded on Dowex 50X2 100 cation-exchange resin. Elution of the column with 10% $NH_3{\cdot}H_2O$/EtOH (1:1) and subsequent evaporation gave the target amino acids (*S*)-**4.1** and (*S*)-**4.2**.

(*S*)-*trans*-Cinnamylglycine (4.1)

Yield: (90.2%); mp. 238-239 °C (dec.). $[\alpha]_D^{25} = -30.7°$ (*c* 0.11, MeOH), –18.3° (*c* 0.57, *1* N HCl); literature[229] mp. 197-200 °C. $[\alpha]_D^{25} = -18.7°$, (*c* 1, *1* N HCl). ^{1}H-NMR (CD_3OD/D_2O) δ 2.75, 2.83 (2H, ABXY, J_{AB}= 15.0 Hz, $J_{AX} = J_{AY}$ = 7.5 Hz, $J_{BX} = J_{BY}$ = 6.0 Hz), 3.78 (1H, dd, J = 7.5 Hz, 5.0 Hz), 6.21, 6.62 (2H, ABXY, J_{AB} = 15.0 Hz, $JAX = JAY$ = 7.5Hz), 7.24-7.27 (1H, m), 7.32-7.35 (2H, m), 7.43-7.44 (2H, m). ^{13}C-NMR (CD_3OD/D_2O) δ 35.4, 55.5, 123.9, 127.3, 128.8, 129.7, 135.8, 137.8, 174.4. HRMS(FAB) $[M+H]^+$ calcd. for $C_{11}H_{13}NO_2$ 192.1025, found 192.1032.

(*S*)-α-*trans*-Cinnamyl-α-alanine (4.2)

Yield: (90.6 %); mp. 249-250 °C (dec.). $[\alpha]_D^{25}$ = -12.9° (*c* 0.51, MeOH); literature[209] mp 241-245 °C. $[\alpha]_D^{21}$ = 13.1° (*R* enantiomer, *c* 0.4, MeOH). ^{1}H-NMR (CD_3COCD_3/ D_2O) δ 1.49 (3H, s), 2.61, 2.77 (2H, ABX, J_{AB} = 14.5 Hz, J_{AX} = 8.5 Hz, J_{BX} = 6.5 Hz), 6.19, 6.54 (2H, ABX, J_{AB} = 15.5 Hz, J_{AX} = J_{AY} = 7.5 Hz), 7.13-7.16 (1H, m), 7.22-7.25 (2H, m), 7.35-7.36 (2H, m). ^{13}C-NMR (CD_3OD/D_2O) δ 22.6, 41.3, 61.7, 123.6, 127.0, 128.1, 129.1, 135.6, 137.6, 175.6. HRMS(FAB) $[M+H]^+$ calcd. for $C_{12}H_{15}NO_2$ 206.1181, found 206.1181.

STRUCTURAL REPORT

WQ01 990103 $C_{22}H_{22}N_2O_5S$

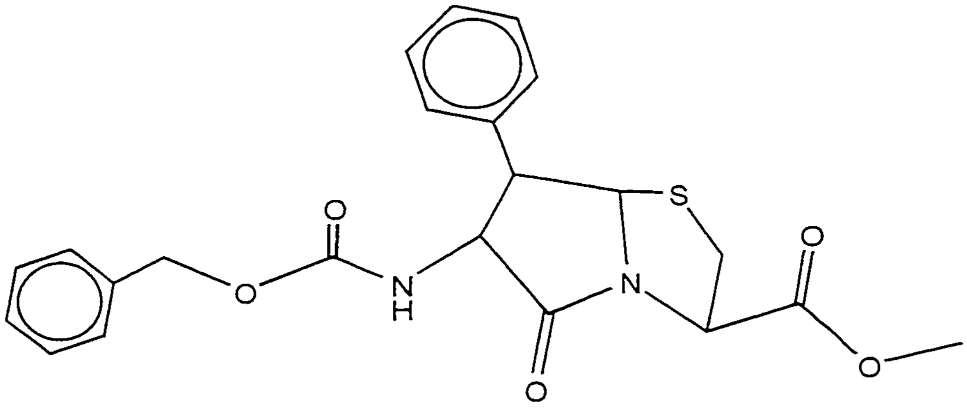

Report prepared for:

Wei Qiu and Prof. Victor Hruby
University of Arizona

April 7, 1999

Report prepared by:

Michael D. Carducci, Ph.D.

Molecular Structure Laboratory
Department of Chemistry
University of Arizona
1306 E. University
Tucson, Arizona 85721

NOTES

This written report is accompanied by an electronic Crystallographic Information File (CIF) which should be supplied to any journal publishing these results. It contains calculated distances and angles beyond those in the attached tables and all needed crystallographic information for generating other needed results. With modifications it is suitable for electronic submission to Acta Crystallographica Section C as a structure report. Observed and calculated structure factors are in the file fofc. Publications arising from this report must either 1) include the preparer(s) as coauthors when significant contributions were made and/or 2) acknowledge the Molecular Structure Laboratory and NSF grant CHE9610374 which provided the diffractometer. A copy of any paper reporting these results should be provided to MSL after publication.

EXPERIMENTAL

A colorless plate of $C_{22}H_{22}N_2O_5S$ having approximate dimensions of 0.034 x 0.238 x 0.289 mm was mounted on a glass fiber in a random orientation. Examination of the crystal on a Bruker SMART 1000 CCD detector X-ray diffractometer at 170(2)K and a power setting of 50KV, 40mA showed measurable diffraction to at least theta = 20.2deg. Data were collected on the SMART1000 system using graphite monochromated Mo Kα radiation (λ=0.71073Å).

Cell constants and an orientation matrix for integration were determined from reflections obtained in three orthogonal 5 deg wedges of reciprocal space. A total of 2592 frames at 1 detector setting covering 0 < 2theta < 61 deg were collected, having an omega scan width of 0.15 and an exposure time of 10 seconds. The frames were integrated using the Bruker SAINT software package's narrow frame algorithm. A total of 15112 reflections were integrated and retained of which 5798 were unique (<redundancy> = 2.6, Rint = 9.1%, Rsig = 22.6%). Of the unique reflections, 2592 (44.7%) were observed >2σ(I). The final Orthorhombic cell parameters of a = 9.5765(12)Å, b = 40.171(5)Å, c = 5.3387(7)Å, alpha = 90°, beta = 90°, gamma = 90°, volume = 2053.8(5) $Å^3$ are based on the refinement of the XYZ-centroids of 2158 reflections with I > 10 σ(I) covering the range of 2.03 < theta < 20.2. Empirical absorption and decay corrections were applied using the program SADABS. The absorption coefficient is 0.195 mm-1, Tmin = 0.817057, and Tmax = 0.980763. For Z = 4 and F.W. = 426.48 the calculated density is 1.379g/cm3. Systematic absences and intensity statistics indicate the space group to be $P2_12_12$ (#18) which was consistent with refinement.

The structure was solved using SHELXS in the Bruker SHELXTL (Version 5.0) software package[1]. Refinements were performed using SHELXL and illustrations were made using XP. Solution was achieved utilizing direct methods followed by Fourier synthesis. Hydrogen atoms were added at idealized positions, constrained to ride on the atom to which they are bonded and given thermal parameters equal to 1.2 or 1.5 times Uiso of that bonded atom. The final anisotropic full-matrix least squares refinement based on F^2 of all reflections converged (maximum shift/esd = 0.016) at R1 = 0.1458, wR2 = 0.0810 and goodness-of-fit = 0.748. "Conventional" refinement indices using the 2592 reflections with F > 4 sigma(F) are R1 = 0.0493, wR2 = 0.0673. The model consisted of 308 variable parameters, 88 constraints and 6 restraints. One of the phenyl groups had a 90° rotational disorder The refined populations of each orientation was 50% The exact value for orientation A is 0.50126 (0.00259). The 1 and 4 positions were constrained to be the same and both orientations were constrained to have flat rings. There were no correlation coefficients greater than 0.50. The highest peak on the final difference map was 0.353 e/A^3 located 0.04 A from S4. The lowest peak on the final difference map was -0.258 e/A^3 located 0.49 A from S4. Scattering Factors and anomalous dispersion were taken from International Tables Vol C Tables 4.2.6.8 and 6.1.1.4.

This compound crystalizes in a polar/chiral/non-centrosymetric space group. The absolute configuration was determined by refinement of the Flack x parameter. Flack x parameter = -0.10(9). Expected values are 0 (within 3 esd's) for correct and +1 for inverted absolute structure.

STRUCTURE

The title compound crystallizes as discrete molecules. Hydrogen bonding between the amide fragments in adjacent molecules forms infinite chains along the c axis. The phenyl disorder arises from adjacent molecules in the a direction not having enough room to maintain the same phenyl rotation. This could lead to short range order in which the phenyl orientations alternate approximating a doubled cell. Some evidence of a doubling of the cell in the c direction was found as weak low angle reflections indexed at half integer values. Integration and solution in this doubled isomorphic subgroup lead to a poorer solution with two molecules in the asymmetric unit and no resolution to the phenyl disorder.

FIGURES

Fig. WQ01_1 An ORTEP rendering of the molecule with 50% probability ellipsoids and artificially reduced hydrogens. Both disordered phenyl positions are shown.

Fig. WQ01_2 An ORTEP rendering of the molecule with 50% probability ellipsoids and artificially reduced hydrogens. One disordered phenyl position (A) is shown.

Fig. WQ01_3 An ORTEP rendering of the molecule with 50% probability ellipsoids and artificially reduced hydrogens. One disordered phenyl position (B) is shown.

Fig. WQ01cellA A ball and stick unit cell packing diagram looking along the a axis. Only disordered phenyl position A is drawn.

Fig. WQ01cellC A ball and stick unit cell packing diagram looking along the c axis. Only disordered phenyl position A is drawn.

Fig. WQ01dcellA A ball and stick unit cell packing diagram looking along the a axis. Both disordered phenyl positions are drawn.

Fig. WQ01dcellC A ball and stick unit cell packing diagram looking along the c axis. Both disordered phenyl positions are drawn.

EQUATIONS

$R_{int} = \sum |Fo^2 - \langle Fo^2 \rangle| / \sum [Fo^2]$

$R_{sig} = \sum[\sigma(Fo^2)]/\sum[Fo^2]$

$R_1 = \Sigma||Fo|-|Fc||/\sum|Fo|$

$wR_2 = \{\sum[w(Fo^2-Fc^2)^2]/\sum[w(Fo^2)^2]\}^{1/2}$

$w=1/[\sigma^2(Fo^2)+(0.0211P)^2+0.00P]$ where $P=(Fo^2+2Fc^2)/3$

$GOF = S = \{\sum[w(Fo^2-Fc^2)^2]/(n-p)\}^{1/2}$

REFERENCES

Shelxl97, Sheldrick, G.M. (1997).

Bruker (1997) SAINT Reference Manual Version 5.0, Bruker AXS Inc., Madison, Wisconsin, USA.

Bruker (1997) SHELXTL Reference Manual Version 5.0, Bruker AXS Inc., Madison, Wisconsin, USA.

Bruker (1997) SMART Reference Manual Version 5.0, Bruker AXS Inc., Madison, Wisconsin, USA.

Table 1. Crystal data and structure refinement for wq01.

Identification code	wq01	
Empirical formula	$C_{22} H_{22} N_2 O_5 S$	
Formula weight	426.48	
Temperature	170(2) K	
Wavelength	0.71073 Å	
Crystal system	Orthorhombic	
Space group	P2(1)2(1)2	
Unit cell dimensions	a = 9.5765(12) Å	a= 90°.
	b = 40.171(5) Å	b= 90°.
	c = 5.3387(7) Å	g = 90°.
Volume	2053.8(5) $Å^3$	
Z	4	
Density (calculated)	1.379 Mg/m^3	
Absorption coefficient	0.195 mm^{-1}	
F(000)	896	
Crystal size	0.289 x 0.238 x 0.034 mm^3	
Theta range for utilized data	2.03 to 30.48°.	
Limiting Indices	-13<=h<=12, -57<=k<=50, -6<=l<=7	
Reflections utilized	15112	
Independent reflections	5798 [R(int) = 0.0906]	
Completeness to theta = 30.48°	94.7 %	
Absorption correction	Empirical (SADABS)	
Max. and min. transmission	0.980763 and 0.817057	
Refinement method	Full-matrix least-squares on F^2	
Data / restraints / parameters	5798 / 6 / 308	
Goodness-of-fit on F^2	0.748	
Final R indices [I>2sigma(I)]	R1 = 0.0493, wR2 = 0.0673	
R indices (all data)	R1 = 0.1458, wR2 = 0.0810	
Absolute structure parameter	-0.10(9)	
Largest diff. peak and hole	0.353 and -0.258 e.$Å^{-3}$	
RMS difference density	0.051e.$Å^{-3}$	

Table 2. Atomic coordinates (x 10^4) and equivalent isotropic displacement parameters ($Å^2$x 10^3) for wq01.

	x	y	z	U(eq)
N(1)	-5903(2)	-2084(1)	-6050(4)	20(1)
C(2)	-5542(3)	-2411(1)	-5071(5)	22(1)
C(3)	-5886(3)	-2393(1)	-2270(5)	26(1)
S(4)	-7450(1)	-2134(1)	-2003(1)	24(1)
C(5)	-7185(3)	-1940(1)	-5087(5)	20(1)
C(6)	-6895(3)	-1562(1)	-5117(5)	20(1)
C(7)	-5822(3)	-1531(1)	-7231(6)	21(1)
C(8)	-4992(3)	-1857(1)	-7038(5)	24(1)
O(9)	-3797(2)	-1906(1)	-7698(4)	33(1)
C(11)	-6426(3)	-2677(1)	-6367(5)	21(1)
O(12)	-5827(2)	-2974(1)	-6100(4)	30(1)
O(13)	-7515(2)	-2624(1)	-7389(3)	26(1)
C(14)	-6609(3)	-3249(1)	-7200(6)	37(1)
C(21)	-8167(3)	-1345(1)	-5329(5)	22(1)
C(22)	-9132(3)	-1387(1)	-7233(6)	29(1)
C(23)	-10310(3)	-1187(1)	-7384(6)	33(1)
C(24)	-10541(3)	-942(1)	-5638(6)	40(1)
C(25)	-9579(3)	-896(1)	-3738(6)	41(1)
C(26)	-8403(3)	-1093(1)	-3581(6)	33(1)
N(30)	-4969(2)	-1236(1)	-7065(5)	27(1)
C(31)	-4493(3)	-1079(1)	-9115(6)	26(1)
O(31)	-4730(2)	-1158(1)	-11252(4)	41(1)
O(32)	-3719(2)	-809(1)	-8458(4)	29(1)
C(33A)	-3159(3)	-623(1)	-10539(6)	37(1)
C(34A)	-2829(3)	-272(1)	-9702(6)	28(1)
C(35A)	-2749(6)	-46(1)	-11618(12)	44(2)
C(36A)	-2538(7)	284(1)	-11063(12)	45(2)
C(37A)	-2275(5)	381(1)	-8398(8)	63(1)
C(38A)	-2584(8)	159(1)	-6724(12)	42(2)
C(39A)	-2807(6)	-181(1)	-7292(12)	33(2)
C(33B)	-3159(3)	-623(1)	-10539(6)	37(1)
C(34B)	-2829(3)	-272(1)	-9702(6)	28(1)
C(35B)	-3800(7)	-35(2)	-9021(14)	62(3)
C(36B)	-3424(8)	286(2)	-8240(17)	54(2)
C(37B)	-2275(5)	381(1)	-8398(8)	63(1)
C(38B)	-1067(7)	151(2)	-8789(13)	48(2)
C(39B)	-1434(7)	-171(2)	-9498(13)	46(2)

U(eq) is defined as one third of the trace of the orthogonalized U^{ij} tensor.

Table 3. Bond lengths [Å] and angles [°] for ¬wq01.

N(1)-C(8)	1.368(3)	C(35A)-C(36A)	1.374(7)
N(1)-C(5)	1.452(3)	C(35A)-H(35A)	0.9500
N(1)-C(2)	1.455(3)	C(36A)-C(37A)	1.496(7)
C(2)-C(11)	1.529(4)	C(36A)-H(36A)	0.9500
C(2)-C(3)	1.533(4)	C(37A)-C(38A)	1.297(7)
C(2)-H(2A)	1.0000	C(37A)-H(37A)	0.9500
C(3)-S(4)	1.829(3)	C(38A)-C(39A)	1.415(7)
C(3)-H(3A)	0.9900	C(38A)-H(38A)	0.9500
C(3)-H(3B)	0.9900	C(39A)-H(39A)	0.9500
S(4)-C(5)	1.841(2)	C(35B)-C(36B)	1.402(8)
C(5)-C(6)	1.540(3)	C(35B)-H(35B)	0.9500
C(5)-H(5A)	1.0000	C(36B)-H(36B)	0.9500
C(6)-C(21)	1.504(3)	C(38B)-C(39B)	1.392(8)
C(6)-C(7)	1.532(3)	C(38B)-H(38B)	0.9500
C(6)-H(6A)	1.0000	C(39B)-H(39B)	0.9500
C(7)-N(30)	1.442(3)		
C(7)-C(8)	1.536(3)	C(8)-N(1)-C(5)	114.2(2)
C(7)-H(7A)	1.0000	C(8)-N(1)-C(2)	126.0(2)
C(8)-O(9)	1.213(3)	C(5)-N(1)-C(2)	115.7(2)
C(11)-O(13)	1.196(3)	N(1)-C(2)-C(11)	109.7(2)
C(11)-O(12)	1.332(3)	N(1)-C(2)-C(3)	104.9(2)
O(12)-C(14)	1.458(3)	C(11)-C(2)-C(3)	110.8(2)
C(14)-H(14A)	0.9800	N(1)-C(2)-H(2A)	110.4
C(14)-H(14B)	0.9800	C(11)-C(2)-H(2A)	110.4
C(14)-H(14C)	0.9800	C(3)-C(2)-H(2A)	110.4
C(21)-C(22)	1.385(4)	C(2)-C(3)-S(4)	106.15(17)
C(21)-C(26)	1.393(4)	C(2)-C(3)-H(3A)	110.5
C(22)-C(23)	1.385(3)	S(4)-C(3)-H(3A)	110.5
C(22)-H(22A)	0.9500	C(2)-C(3)-H(3B)	110.5
C(23)-C(24)	1.374(4)	S(4)-C(3)-H(3B)	110.5
C(23)-H(23A)	0.9500	H(3A)-C(3)-H(3B)	108.7
C(24)-C(25)	1.383(4)	C(3)-S(4)-C(5)	93.42(12)
C(24)-H(24A)	0.9500	N(1)-C(5)-C(6)	103.7(2)
C(25)-C(26)	1.380(4)	N(1)-C(5)-S(4)	105.23(16)
C(25)-H(25A)	0.9500	C(6)-C(5)-S(4)	116.90(18)
C(26)-H(26A)	0.9500	N(1)-C(5)-H(5A)	110.2
N(30)-C(31)	1.344(3)	C(6)-C(5)-H(5A)	110.2
N(30)-H(30A)	0.8800	S(4)-C(5)-H(5A)	110.2
C(31)-O(31)	1.207(3)	C(21)-C(6)-C(7)	116.1(2)
C(31)-O(32)	1.360(3)	C(21)-C(6)-C(5)	115.3(2)
O(32)-C(33A)	1.441(3)	C(7)-C(6)-C(5)	102.1(2)
C(33A)-C(34A)	1.512(4)	C(21)-C(6)-H(6A)	107.6
C(33A)-H(33A)	0.9900	C(7)-C(6)-H(6A)	107.6
C(33A)-H(33B)	0.9900	C(5)-C(6)-H(6A)	107.6
C(34A)-C(39A)	1.339(6)	N(30)-C(7)-C(6)	113.8(2)
C(34A)-C(35A)	1.370(6)	N(30)-C(7)-C(8)	113.8(2)

C(6)-C(7)-C(8)	103.1(2)	N(30)-C(31)-O(32)	110.5(3)
N(30)-C(7)-H(7A)	108.6	C(31)-O(32)-C(33A)	114.6(2)
C(6)-C(7)-H(7A)	108.6	O(32)-C(33A)-C(34A)	109.4(2)
C(8)-C(7)-H(7A)	108.6	O(32)-C(33A)-H(33A)	109.8
O(9)-C(8)-N(1)	127.3(3)	C(34A)-C(33A)-H(33A)	109.8
O(9)-C(8)-C(7)	127.4(2)	O(32)-C(33A)-H(33B)	109.8
N(1)-C(8)-C(7)	105.3(2)	C(34A)-C(33A)-H(33B)	109.8
O(13)-C(11)-O(12)	125.7(3)	H(33A)-C(33A)-H(33B)	108.2
O(13)-C(11)-C(2)	124.4(2)	C(39A)-C(34A)-C(35A)	122.3(4)
O(12)-C(11)-C(2)	109.8(2)	C(39A)-C(34A)-C(33A)	123.0(3)
C(11)-O(12)-C(14)	114.5(2)	C(35A)-C(34A)-C(33A)	114.1(3)
O(12)-C(14)-H(14A)	109.5	C(34A)-C(35A)-C(36A)	119.2(5)
O(12)-C(14)-H(14B)	109.5	C(34A)-C(35A)-H(35A)	120.4
H(14A)-C(14)-H(14B)	109.5	C(36A)-C(35A)-H(35A)	120.4
O(12)-C(14)-H(14C)	109.5	C(35A)-C(36A)-C(37A)	118.8(5)
H(14A)-C(14)-H(14C)	109.5	C(35A)-C(36A)-H(36A)	120.6
H(14B)-C(14)-H(14C)	109.5	C(37A)-C(36A)-H(36A)	120.6
C(22)-C(21)-C(26)	118.1(3)	C(38A)-C(37A)-C(36A)	116.0(4)
C(22)-C(21)-C(6)	121.7(3)	C(38A)-C(37A)-H(37A)	122.0
C(26)-C(21)-C(6)	120.2(3)	C(36A)-C(37A)-H(37A)	122.0
C(21)-C(22)-C(23)	121.1(3)	C(37A)-C(38A)-C(39A)	123.3(6)
C(21)-C(22)-H(22A)	119.5	C(37A)-C(38A)-H(38A)	118.3
C(23)-C(22)-H(22A)	119.5	C(39A)-C(38A)-H(38A)	118.3
C(24)-C(23)-C(22)	120.4(3)	C(34A)-C(39A)-C(38A)	118.3(5)
C(24)-C(23)-H(23A)	119.8	C(34A)-C(39A)-H(39A)	120.8
C(22)-C(23)-H(23A)	119.8	C(38A)-C(39A)-H(39A)	120.8
C(23)-C(24)-C(25)	119.1(3)	C(36B)-C(35B)-H(35B)	118.6
C(23)-C(24)-H(24A)	120.4	C(35B)-C(36B)-H(36B)	119.3
C(25)-C(24)-H(24A)	120.4	C(39B)-C(38B)-H(38B)	122.7
C(26)-C(25)-C(24)	120.8(3)	C(38B)-C(39B)-H(39B)	118.9
C(26)-C(25)-H(25A)	119.6		
C(24)-C(25)-H(25A)	119.6		
C(25)-C(26)-C(21)	120.5(3)		
C(25)-C(26)-H(26A)	119.7		
C(21)-C(26)-H(26A)	119.7		
C(31)-N(30)-C(7)	121.9(2)		
C(31)-N(30)-H(30A)	119.1		
C(7)-N(30)-H(30A)	119.1		
O(31)-C(31)-N(30)	125.6(3)		
O(31)-C(31)-O(32)	124.0(3)		

Symmetry transformations used to generate equivalent atoms:

Table 4. Anisotropic displacement parameters ($Å^2 x 10^3$) for wq01. The anisotropic displacement factor exponent takes the form: $-2\pi^2[h^2 a^{*2}U^{11} + ... + 2 h k a^* b^* U^{12}]$

	U^{11}	U^{22}	U^{33}	U^{23}	U^{13}	U^{12}
N(1)	20(1)	20(1)	20(1)	-1(1)	1(1)	1(1)
C(2)	15(2)	25(2)	26(2)	1(1)	1(1)	4(1)
C(3)	27(2)	29(2)	23(2)	-2(1)	-5(2)	5(1)
S(4)	26(1)	26(1)	21(1)	2(1)	3(1)	2(1)
C(5)	22(2)	22(1)	15(2)	2(1)	-2(1)	-3(1)
C(6)	23(2)	20(2)	18(2)	-3(1)	-1(1)	-4(1)
C(7)	23(2)	20(2)	21(2)	-2(1)	2(1)	-5(1)
C(8)	26(2)	32(2)	15(2)	-7(2)	1(2)	-8(1)
O(9)	28(1)	34(1)	39(1)	-6(1)	11(1)	-5(1)
C(11)	23(2)	24(2)	16(2)	2(1)	5(1)	2(1)
O(12)	32(1)	20(1)	37(1)	-5(1)	-10(1)	4(1)
O(13)	25(1)	26(1)	27(1)	-2(1)	-3(1)	2(1)
C(14)	45(2)	25(2)	41(2)	-9(2)	-5(2)	2(2)
C(21)	27(2)	21(2)	19(2)	5(1)	1(1)	-4(1)
C(22)	41(2)	24(2)	23(2)	0(2)	-1(2)	4(2)
C(23)	35(2)	39(2)	25(2)	4(2)	-3(2)	3(2)
C(24)	38(2)	43(2)	38(2)	5(2)	5(2)	13(2)
C(25)	45(2)	41(2)	38(2)	-13(2)	4(2)	14(2)
C(26)	36(2)	38(2)	24(2)	-7(2)	-4(2)	6(2)
N(30)	37(1)	24(1)	22(2)	-6(1)	3(1)	-15(1)
C(31)	25(2)	27(2)	26(2)	-1(2)	0(2)	-6(1)
O(31)	56(2)	45(1)	22(1)	0(1)	2(1)	-29(1)
O(32)	34(1)	24(1)	29(1)	3(1)	0(1)	-14(1)
C(33A)	44(2)	35(2)	32(2)	4(2)	8(2)	-14(2)
C(34A)	26(2)	25(2)	32(2)	3(2)	4(2)	-3(2)
C(35A)	64(5)	35(4)	33(4)	3(3)	-4(4)	-21(4)
C(36A)	66(5)	24(3)	44(4)	11(3)	-8(5)	-6(4)
C(37A)	96(4)	21(2)	73(3)	-6(2)	31(3)	-16(2)
C(38A)	48(4)	37(4)	41(4)	-2(3)	-7(5)	1(4)
C(39A)	32(4)	31(4)	36(4)	5(3)	-4(3)	-2(3)
C(33B)	44(2)	35(2)	32(2)	4(2)	8(2)	-14(2)
C(34B)	26(2)	25(2)	32(2)	3(2)	4(2)	-3(2)
C(35B)	24(4)	37(4)	125(8)	-12(5)	-2(5)	-10(4)
C(36B)	32(4)	33(4)	97(8)	-29(5)	4(5)	7(4)
C(37B)	96(4)	21(2)	73(3)	-6(2)	31(3)	-16(2)
C(38B)	30(4)	44(4)	72(6)	-13(4)	8(4)	-12(3)
C(39B)	32(4)	29(4)	75(6)	-6(4)	19(4)	7(3)

Table 5. Hydrogen coordinates (x 10^4) and isotropic displacement parameters ($Å^2$x 10^3) for wq01.

	x	y	z	U(eq)
H(2A)	-4525	-2457	-5323	26
H(3A)	-5101	-2293	-1330	32
H(3B)	-6065	-2619	-1594	32
H(5A)	-7984	-1994	-6224	23
H(6A)	-6414	-1505	-3513	24
H(7A)	-6328	-1528	-8869	25
H(14A)	-6097	-3457	-6939	55
H(14B)	-6727	-3210	-9000	55
H(14C)	-7528	-3264	-6401	55
H(22A)	-8985	-1555	-8457	35
H(23A)	-10962	-1220	-8702	40
H(24A)	-11351	-806	-5735	48
H(25A)	-9730	-726	-2527	50
H(26A)	-7748	-1057	-2271	39
H(30A)	-4753	-1157	-5577	33
H(33A)	-3847	-618	-11922	44
H(33B)	-2300	-732	-11162	44
H(35A)	-2838	-117	-13309	53
H(36A)	-2559	448	-12347	54
H(37A)	-1904	593	-7960	76
H(38A)	-2665	229	-5028	51
H(39A)	-2938	-340	-5996	40
H(33C)	-3847	-618	-11922	44
H(33D)	-2300	-732	-11162	44
H(35B)	-4762	-91	-9084	74
H(36B)	-4119	429	-7568	65
H(37B)	-2101	613	-8275	76
H(38B)	-125	219	-8570	58
H(39B)	-715	-327	-9855	55

Table 6. Torsion angles [°] for wq01.

C(8)-N(1)-C(2)-C(11)	-125.9(3)	C(3)-C(2)-C(11)-O(12)	-84.0(3)
C(5)-N(1)-C(2)-C(11)	78.1(3)	O(13)-C(11)-O(12)-C(14)	0.5(4)
C(8)-N(1)-C(2)-C(3)	115.1(3)	C(2)-C(11)-O(12)-C(14)	178.1(2)
C(5)-N(1)-C(2)-C(3)	-41.0(3)	C(7)-C(6)-C(21)-C(22)	65.7(3)
N(1)-C(2)-C(3)-S(4)	35.9(2)	C(5)-C(6)-C(21)-C(22)	-53.6(3)
C(11)-C(2)-C(3)-S(4)	-82.4(2)	C(7)-C(6)-C(21)-C(26)	-114.4(3)
C(2)-C(3)-S(4)-C(5)	-20.32(19)	C(5)-C(6)-C(21)-C(26)	126.2(3)
C(8)-N(1)-C(5)-C(6)	-10.4(3)	C(26)-C(21)-C(22)-C(23)	-0.8(4)
C(2)-N(1)-C(5)-C(6)	148.4(2)	C(6)-C(21)-C(22)-C(23)	179.0(3)
C(8)-N(1)-C(5)-S(4)	-133.75(19)	C(21)-C(22)-C(23)-C(24)	0.2(4)
C(2)-N(1)-C(5)-S(4)	25.1(2)	C(22)-C(23)-C(24)-C(25)	0.3(5)
C(3)-S(4)-C(5)-N(1)	-1.12(17)	C(23)-C(24)-C(25)-C(26)	-0.2(5)
C(3)-S(4)-C(5)-C(6)	-115.5(2)	C(24)-C(25)-C(26)-C(21)	-0.4(5)
N(1)-C(5)-C(6)-C(21)	154.0(2)	C(22)-C(21)-C(26)-C(25)	0.9(4)
S(4)-C(5)-C(6)-C(21)	-90.7(3)	C(6)-C(21)-C(26)-C(25)	-178.9(3)
N(1)-C(5)-C(6)-C(7)	27.2(2)	C(6)-C(7)-N(30)-C(31)	-147.3(3)
S(4)-C(5)-C(6)-C(7)	142.48(19)	C(8)-C(7)-N(30)-C(31)	35.0(3)
C(21)-C(6)-C(7)-N(30)	76.5(3)	C(7)-N(30)-C(31)-O(31)	1.3(5)
C(5)-C(6)-C(7)-N(30)	-157.2(2)	C(7)-N(30)-C(31)-O(32)	179.9(2)
C(21)-C(6)-C(7)-C(8)	-159.8(2)	O(31)-C(31)-O(32)-C(33A)	-1.4(4)
C(5)-C(6)-C(7)-C(8)	-33.5(2)	N(30)-C(31)-O(32)-C(33A)	179.9(2)
C(5)-N(1)-C(8)-O(9)	171.0(3)	C(31)-O(32)-C(33A)-C(34A)	158.1(2)
C(2)-N(1)-C(8)-O(9)	14.6(4)	O(32)-C(33A)-C(34A)-C(39A)	12.3(5)
C(5)-N(1)-C(8)-C(7)	-11.2(3)	O(32)-C(33A)-C(34A)-C(35A)	-158.9(3)
C(2)-N(1)-C(8)-C(7)	-167.6(2)	C(39A)-C(34A)-C(35A)-C(36A)	4.8(7)
N(30)-C(7)-C(8)-O(9)	-30.3(4)	C(33A)-C(34A)-C(35A)-C(36A)	176.1(5)
C(6)-C(7)-C(8)-O(9)	-154.0(3)	C(34A)-C(35A)-C(36A)-C(37A)	5.4(8)
N(30)-C(7)-C(8)-N(1)	151.9(2)	C(35A)-C(36A)-C(37A)-C(38A)	-15.6(9)
C(6)-C(7)-C(8)-N(1)	28.2(3)	C(36A)-C(37A)-C(38A)-C(39A)	16.1(10)
N(1)-C(2)-C(11)-O(13)	-21.8(4)	C(35A)-C(34A)-C(39A)-C(38A)	-5.0(8)
C(3)-C(2)-C(11)-O(13)	93.6(3)	C(33A)-C(34A)-C(39A)-C(38A)	-175.5(5)
N(1)-C(2)-C(11)-O(12)	160.6(2)	C(37A)-C(38A)-C(39A)-C(34A)	-6.5(11)

Symmetry transformations used to generate equivalent atoms:

Table 7. Hydrogen bonds for wq01 [Å and °].

D-H...A	d(D-H)	d(H...A)	d(D...A)	<(DHA)
N(30)-H(30A)...O(31)#1	0.88	2.31	3.127(3)	154.6

Symmetry transformations used to generate equivalent atoms:
#1 x,y,z+1

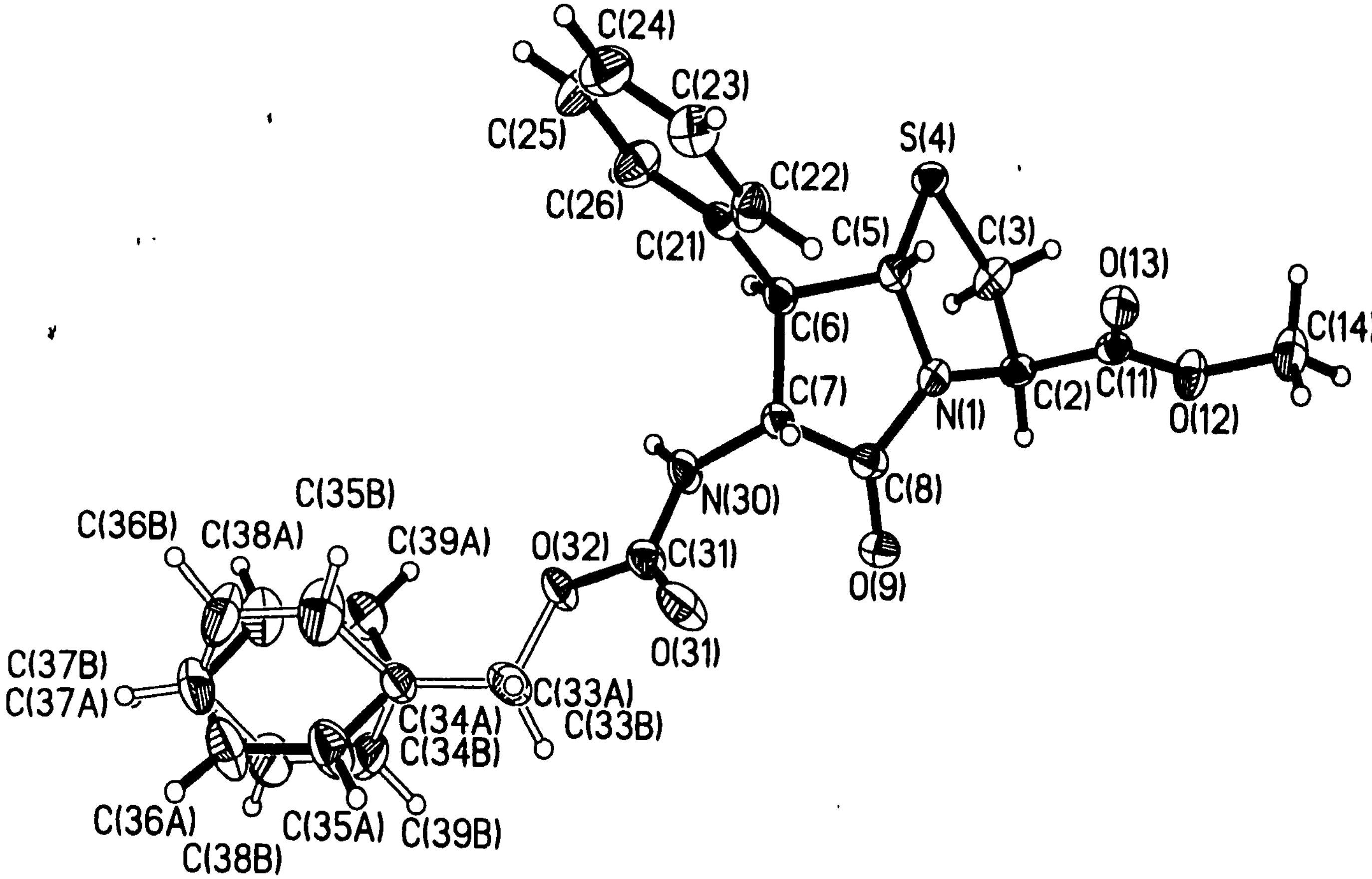
C(24)
C(23)
C(25)
S(4)
C(22)
C(26)
C(5)
C(3)
C(21)
O(13)
C(6)
C(14)
C(7)
C(2)
C(11)
N(1)
O(12)
C(35B)
N(30)
C(8)
C(36B)
C(38A)
C(39A)
O(32)
C(31)
O(9)
O(31)
C(37B)
C(37A)
C(33A)
C(34A)
C(33B)
C(34B)
C(36A)
C(35A)
C(39B)
C(38B)

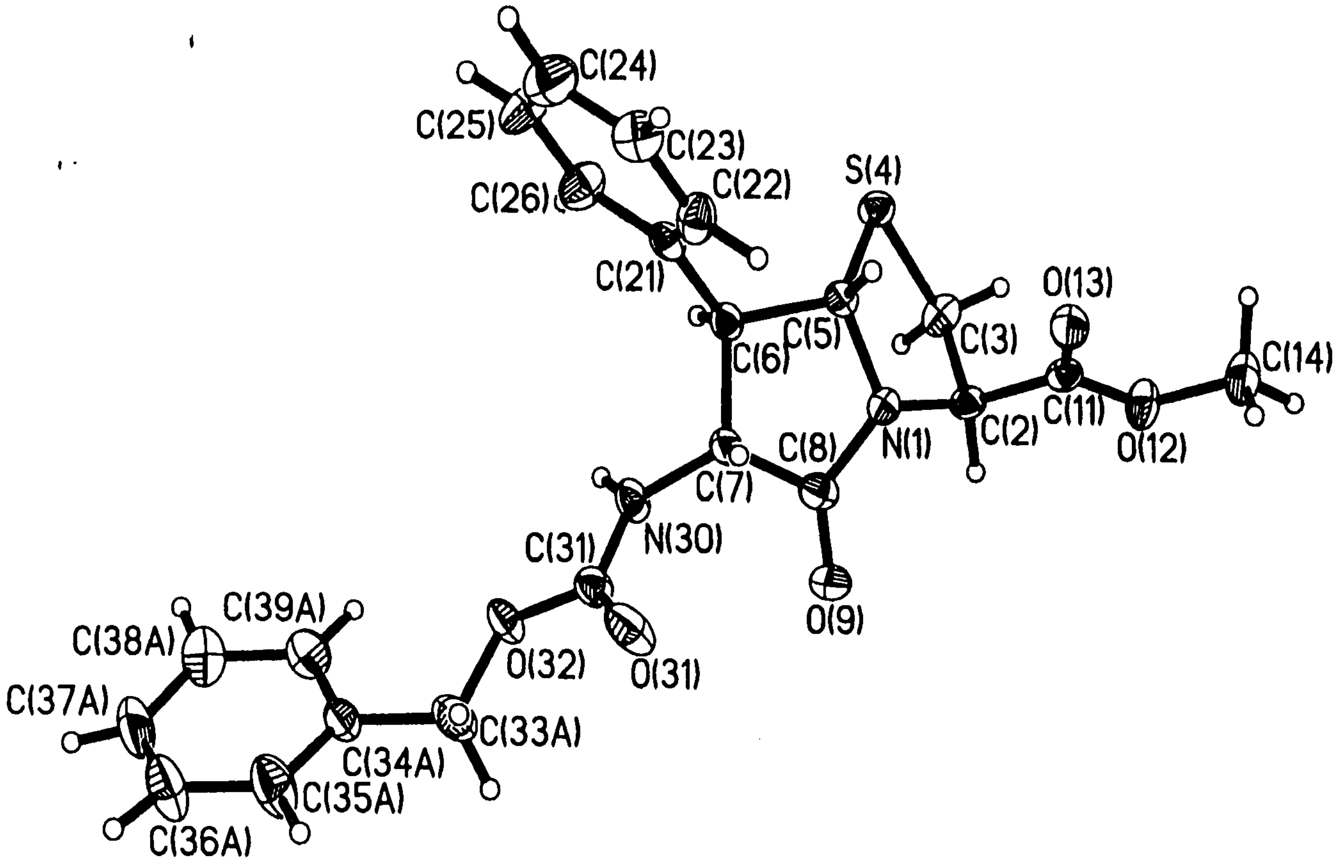
C(24)
C(25)
C(23)
C(22)
S(4)
C(26)
C(21)
O(13)
C(5)
C(3)
C(14)
C(6)
C(11)
C(8)
N(1)
C(2)
O(12)
C(7)
N(30)
C(31)
C(39A)
C(38A)
O(32)
O(9)
O(31)
C(37A)
C(33A)
C(34A)
C(35A)
C(36A)

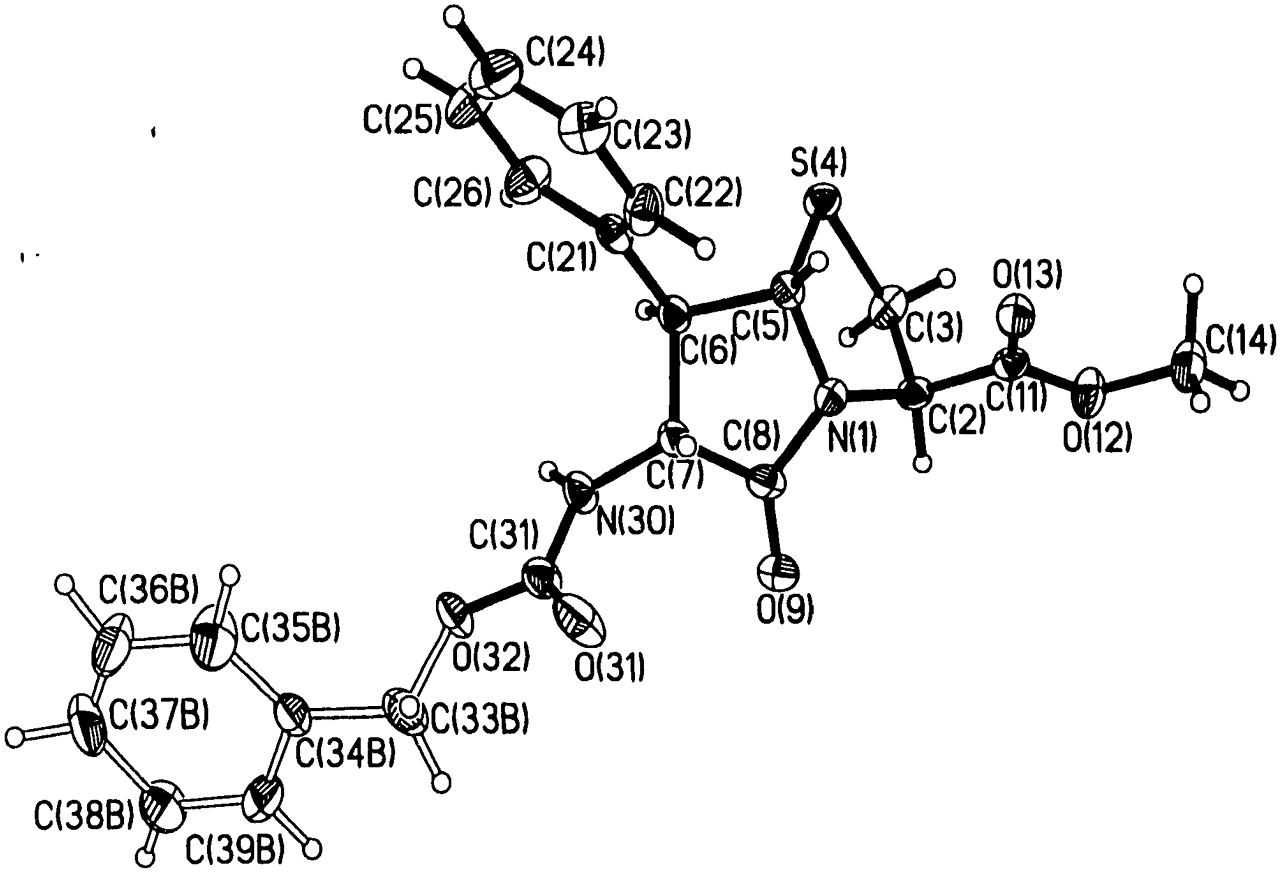
C(24)
C(25)
C(23)
S(4)
C(26)
C(22)
C(21)
O(13)
C(5)
C(3)
C(14)
C(6)
C(11)
C(2)
C(8)
N(1)
O(12)
C(7)
N(30)
C(31)
C(36B)
C(35B)
O(9)
O(32)
O(31)
C(37B)
C(34B)
C(33B)
C(38B)
C(39B)

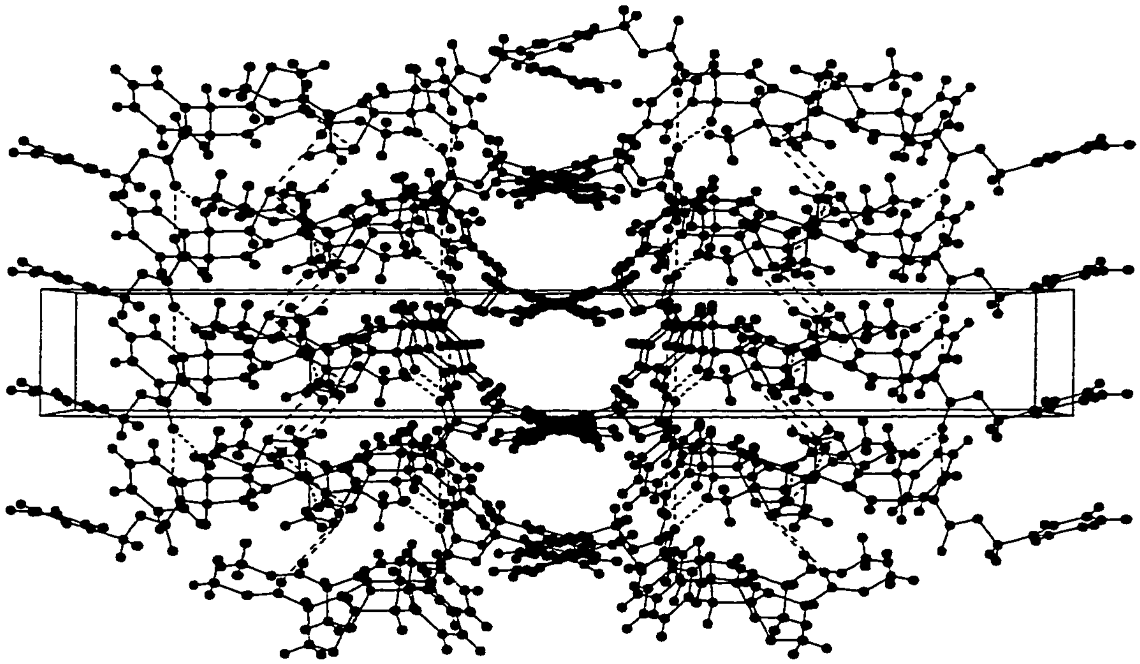

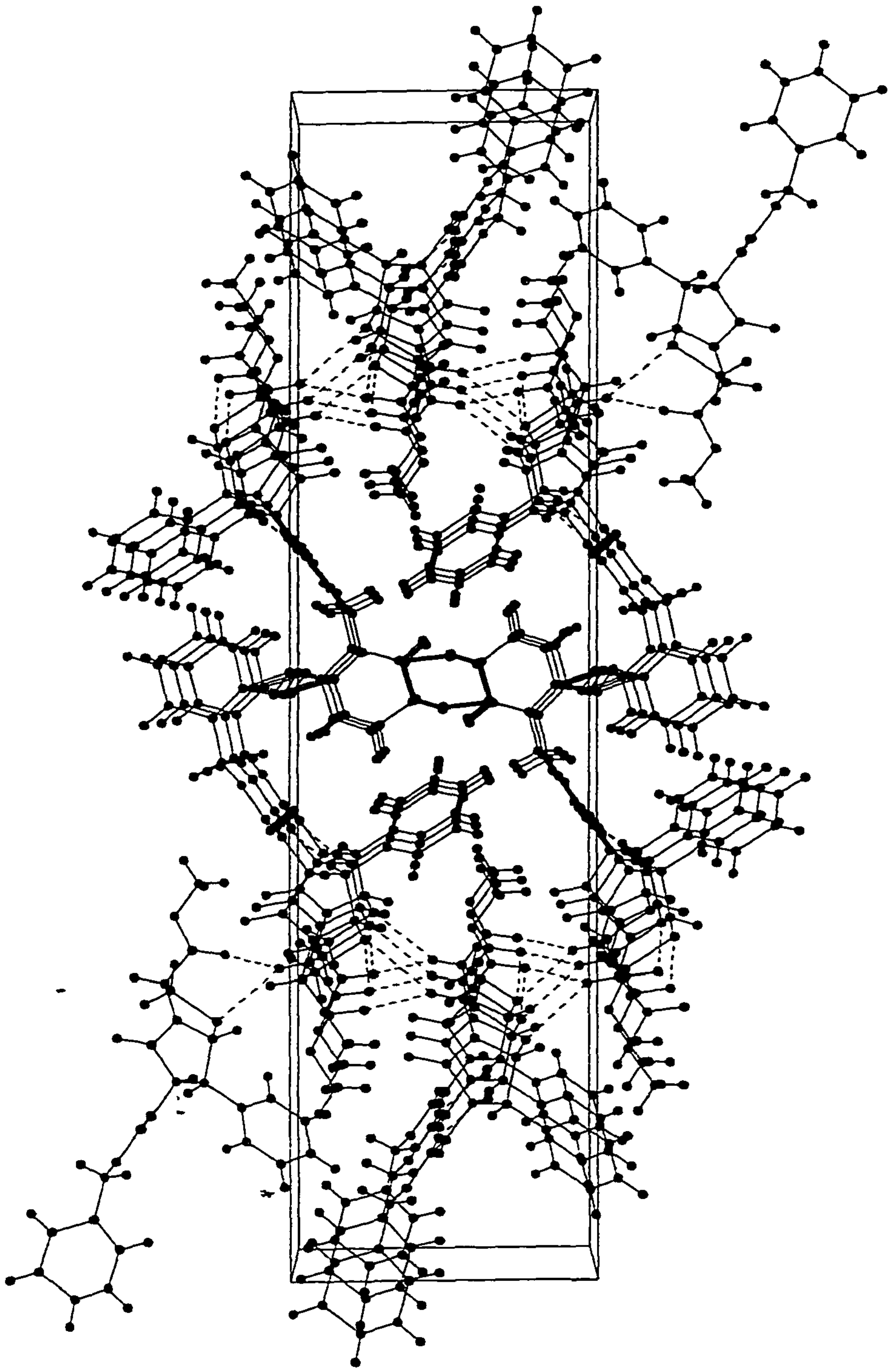

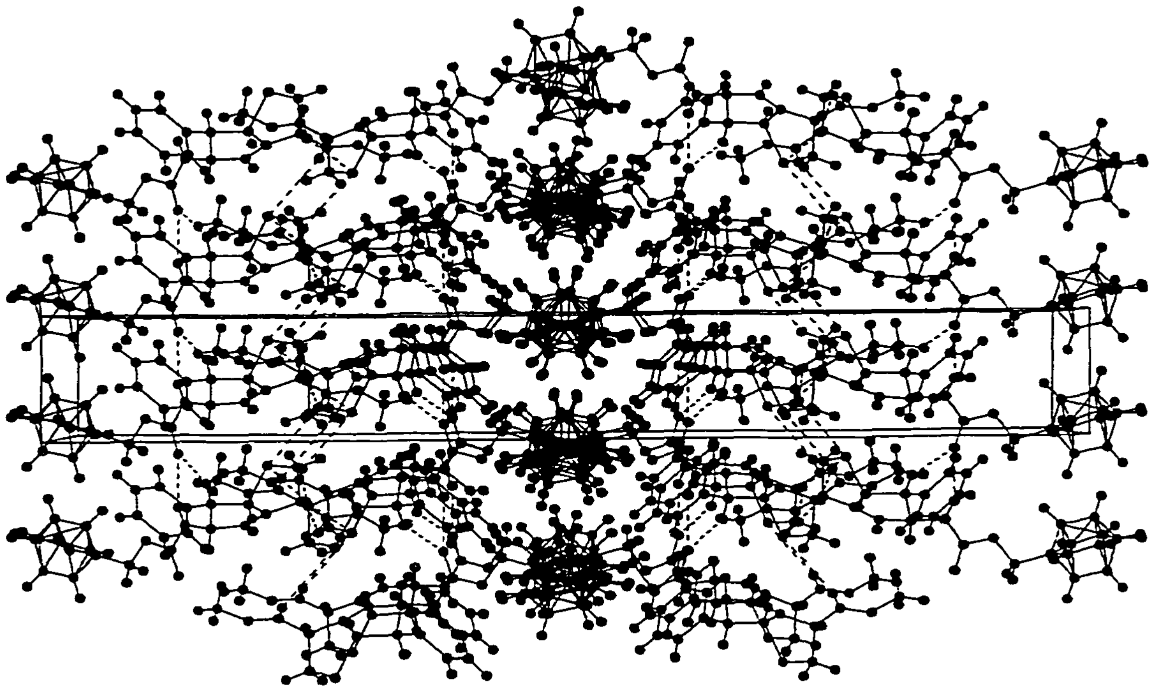

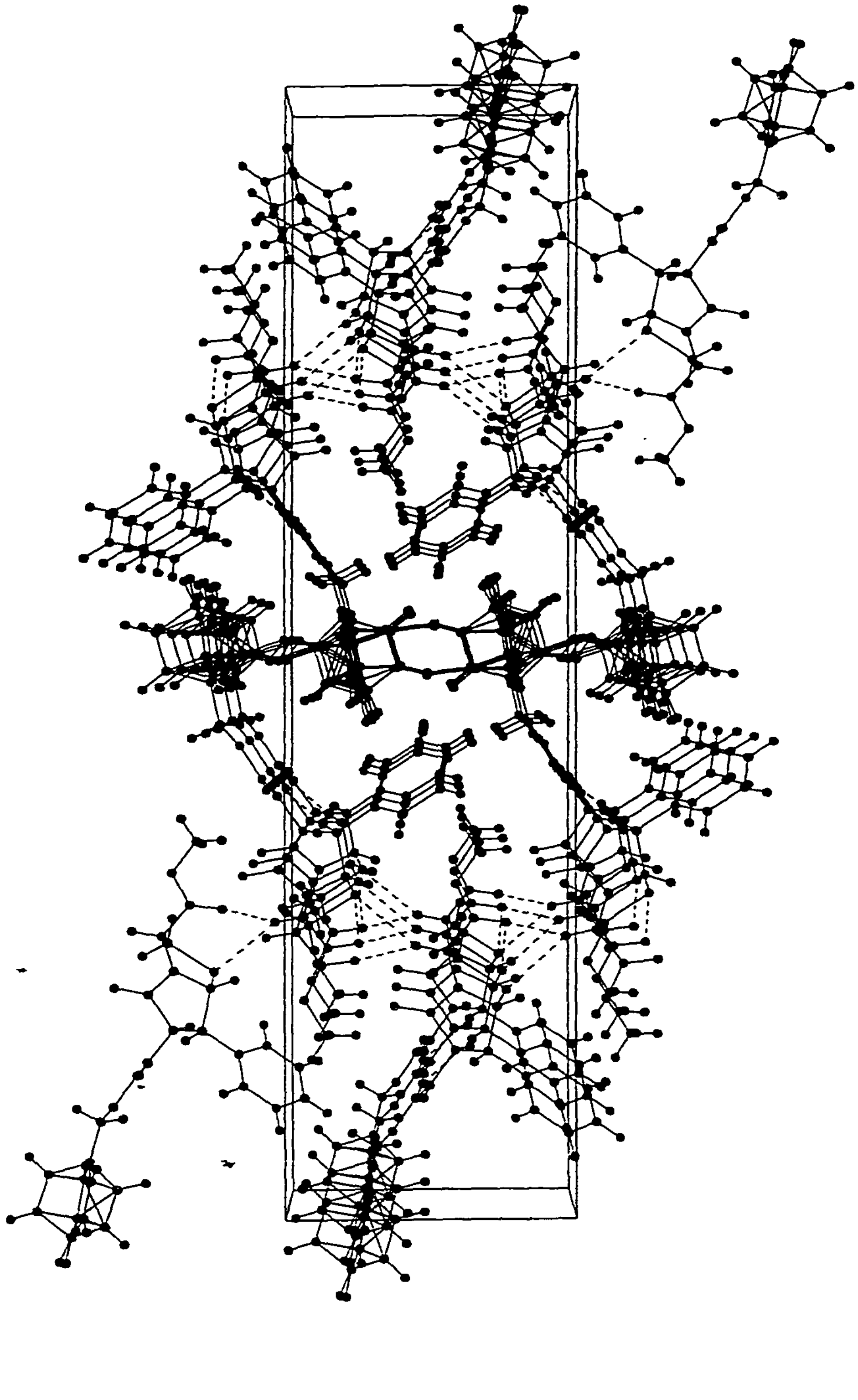

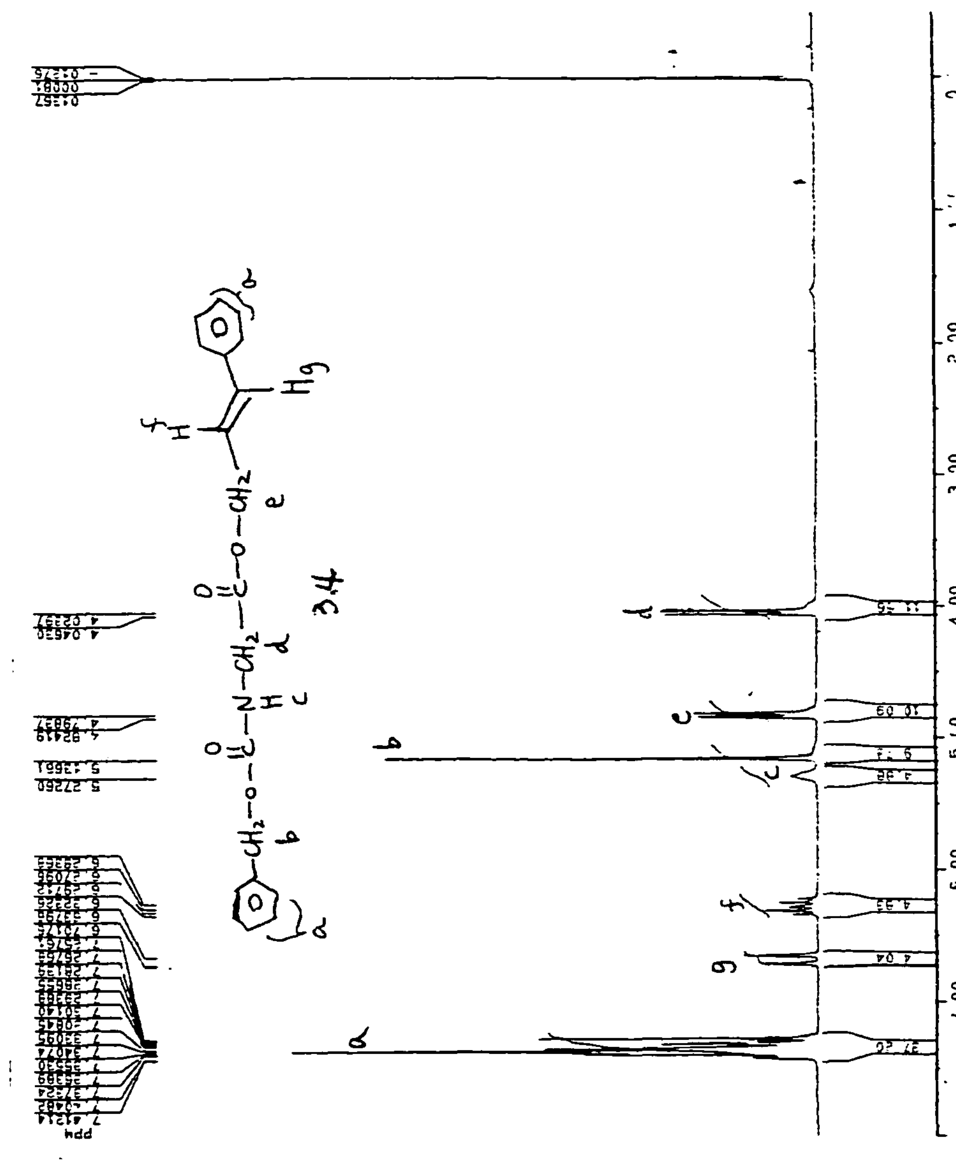

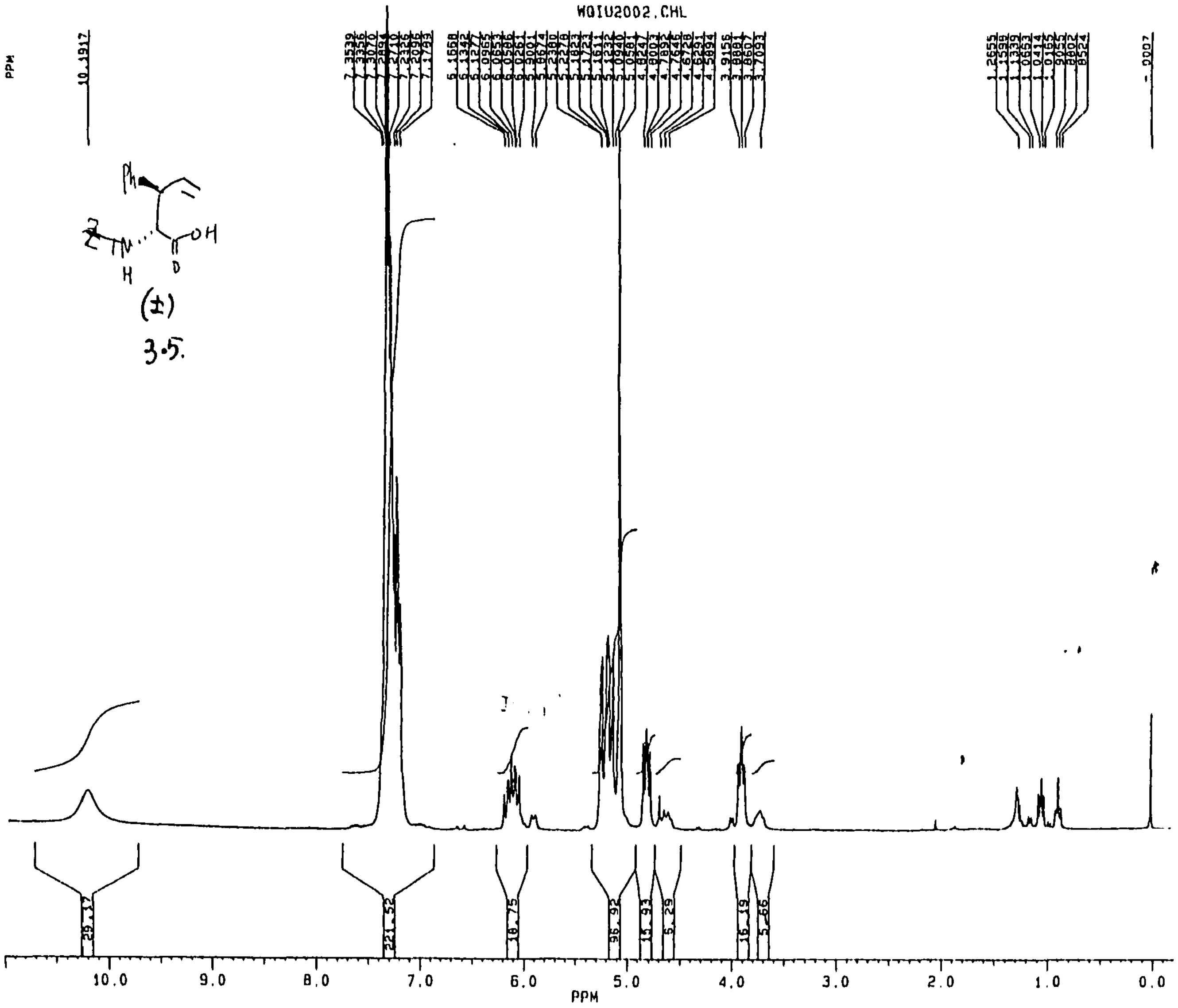
WQIU2002.CHL
PPM
(±)
3.5.
10.0
9.0
8.0
7.0
6.0
5.0
4.0
3.0
2.0
1.0
0.0
PPM

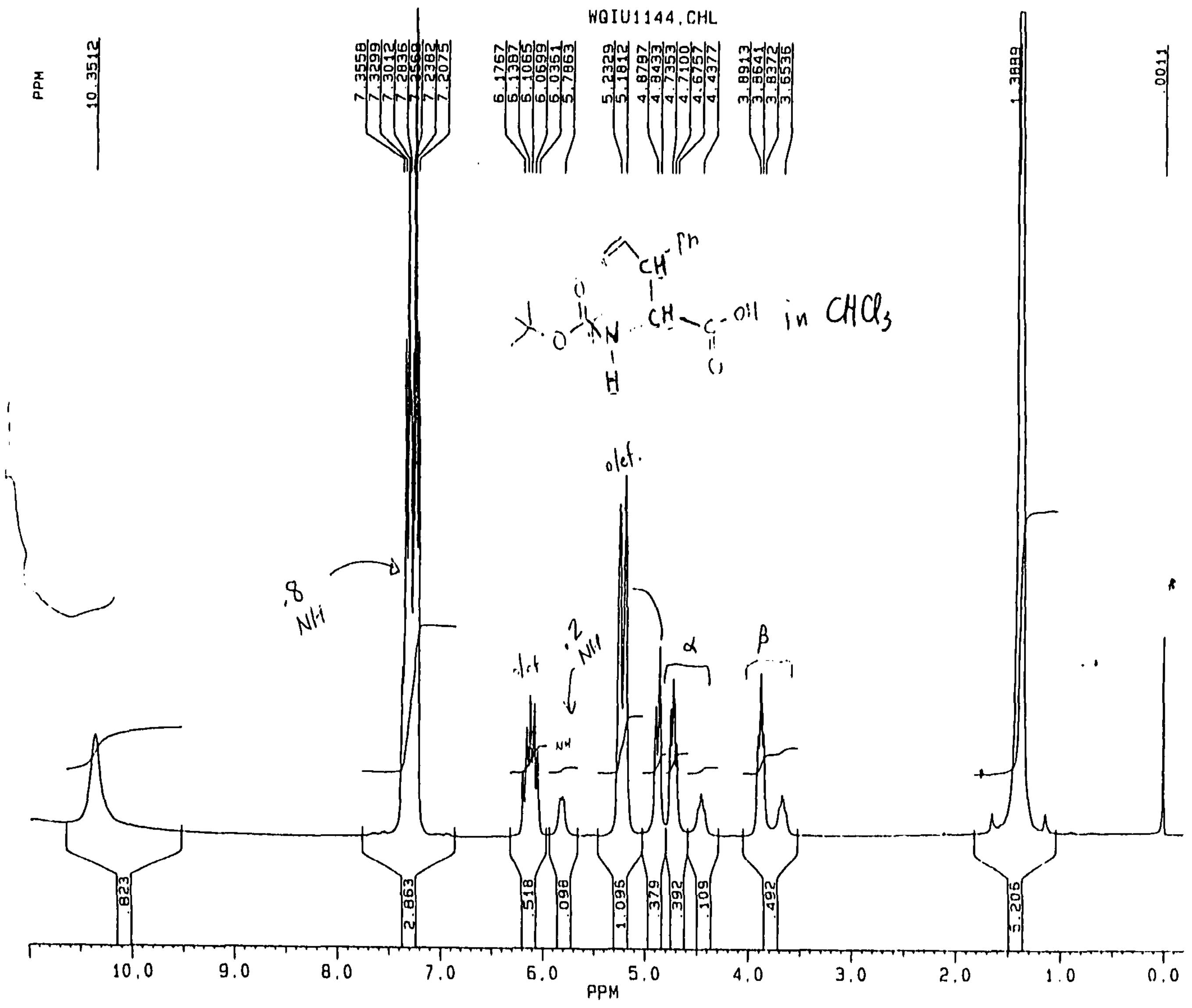

WQIU1144.CHL
PPM
10.3512
7.3558
7.3299
7.3012
7.2836
7.2569
7.2382
7.2075
6.1767
6.1387
6.1065
6.0699
6.0361
5.7863
5.2329
5.1812
4.8787
4.8433
4.7353
4.7100
4.6757
4.4377
3.8913
3.8641
3.8372
3.6536
1.3889
.0011
in $CHCl_3$
olef.
.8 NH
.2 NH
olef
NH
α
β
.823
2.863
.518
.098
1.095
.379
.392
.109
.492
5.205
10.0
9.0
8.0
7.0
6.0
5.0
4.0
3.0
2.0
1.0
0.0
PPM

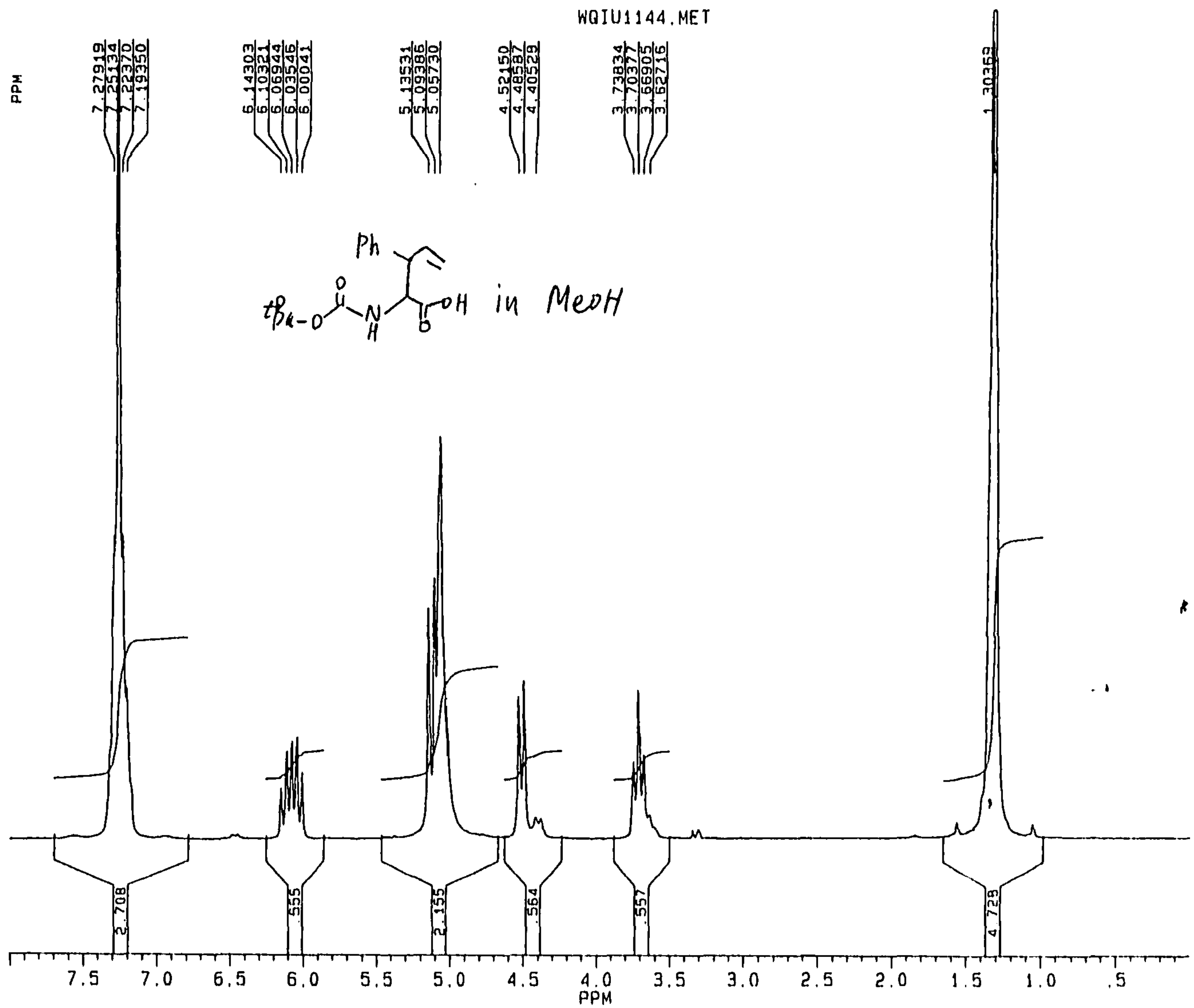

WQIU1144.MET
PPM
7.27919
7.25134
7.22370
7.19350
6.14303
6.10321
6.06944
6.03546
6.00041
5.13531
5.09386
5.05730
4.52150
4.48587
4.40529
3.73834
3.70377
3.66905
3.62716
1.30369
Ph
tBu-O
N
H
OH
O
in MeOH
2.708
.555
2.155
.564
.557
4.729
7.5
7.0
6.5
6.0
5.5
5.0
4.5
4.0
3.5
3.0
2.5
2.0
1.5
1.0
.5
PPM

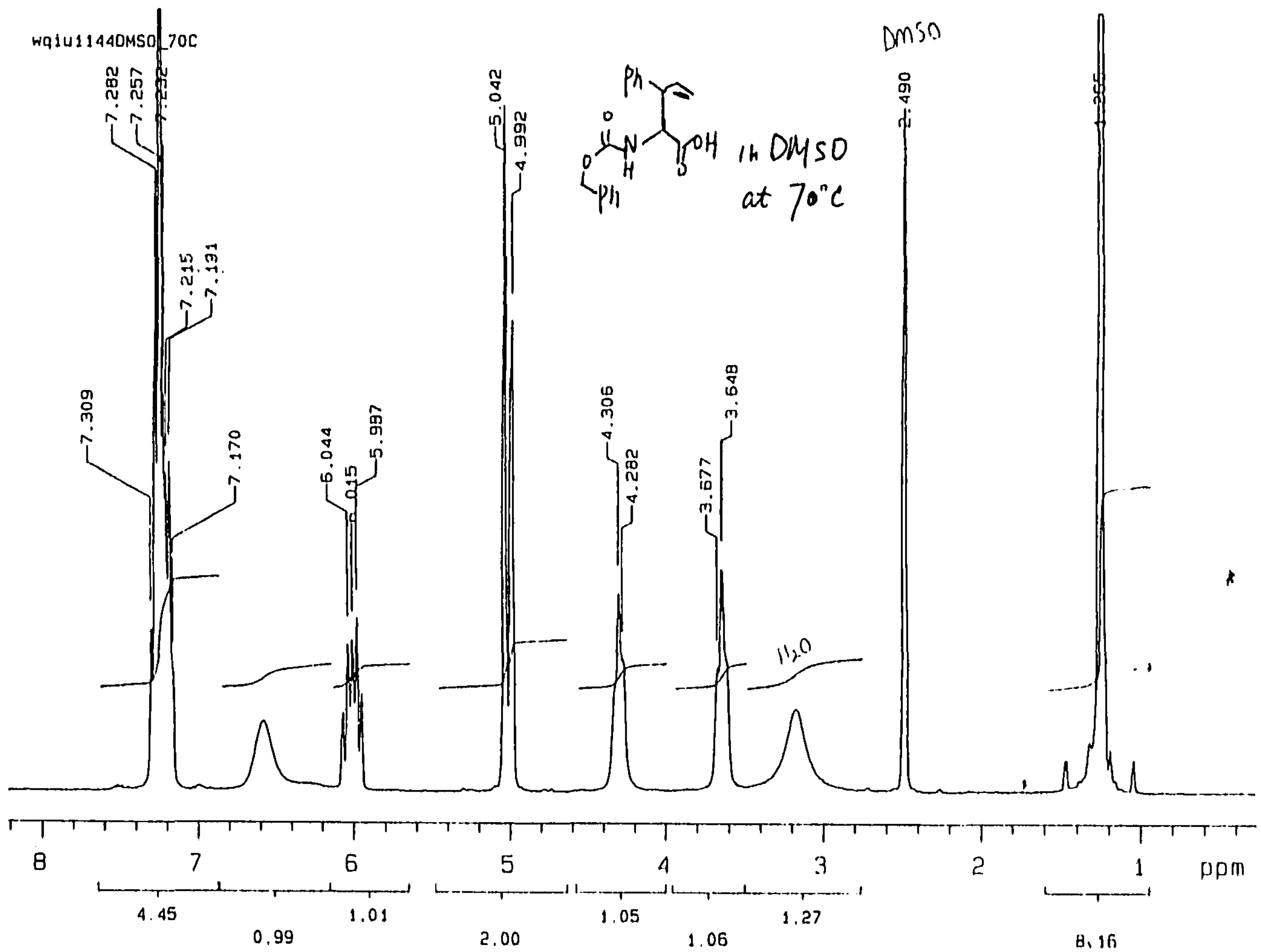
wqiu1144DMSO_70C
7.309
7.282
7.257
7.232
7.215
7.191
7.170
6.044
6.015
5.997
5.042
4.992
4.306
4.282
3.677
3.648
2.490
DMSO
H2O
Ph
O
N
H
OH
Ph
in DMSO
at 70°C
8
7
6
5
4
3
2
1
ppm
4.45
0.99
1.01
2.00
1.05
1.06
1.27
8.16

Claisen Rearr. Benzyl Ester

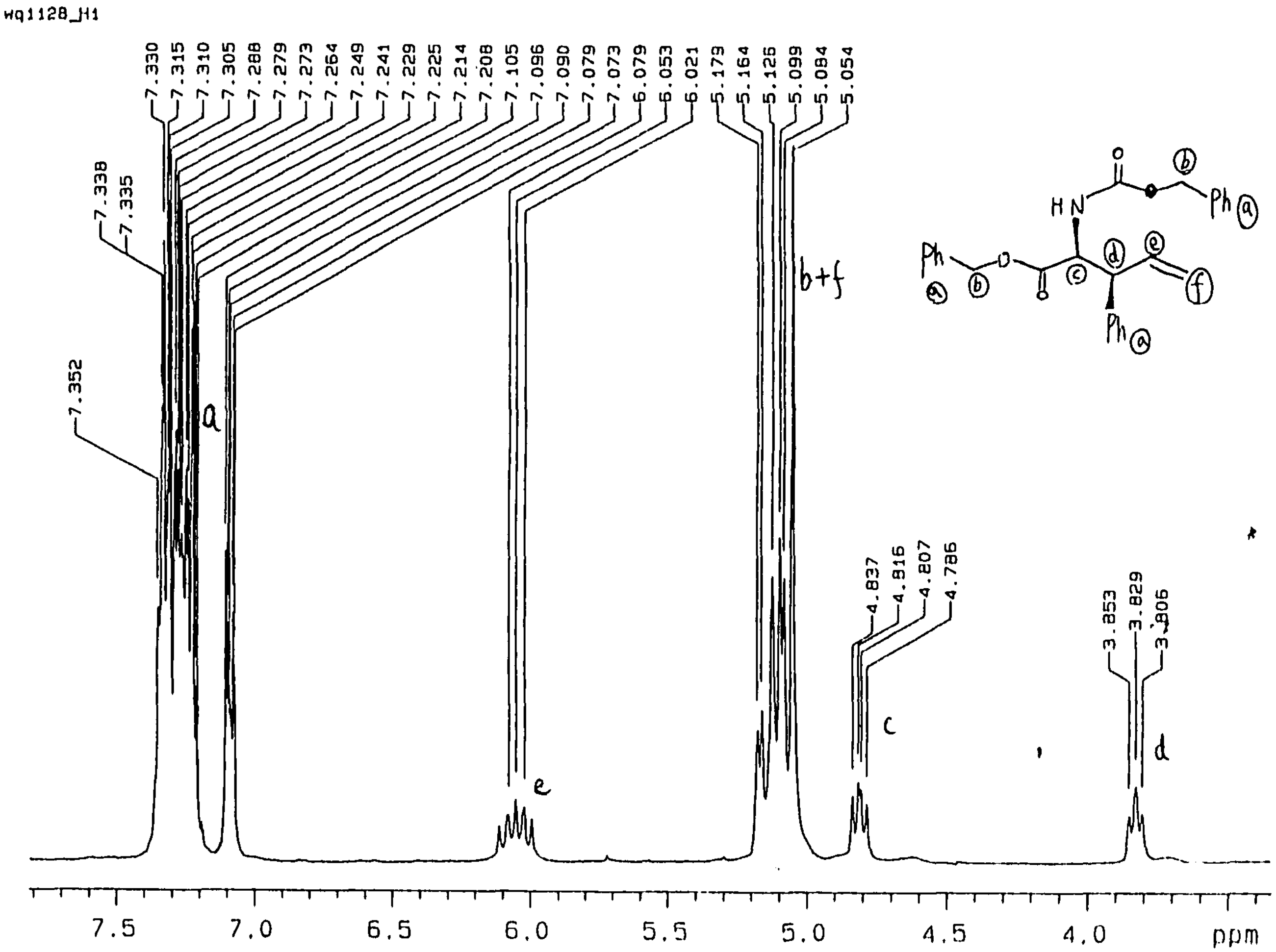

HECTOR of Claisen Rearr. Benzyl Ester

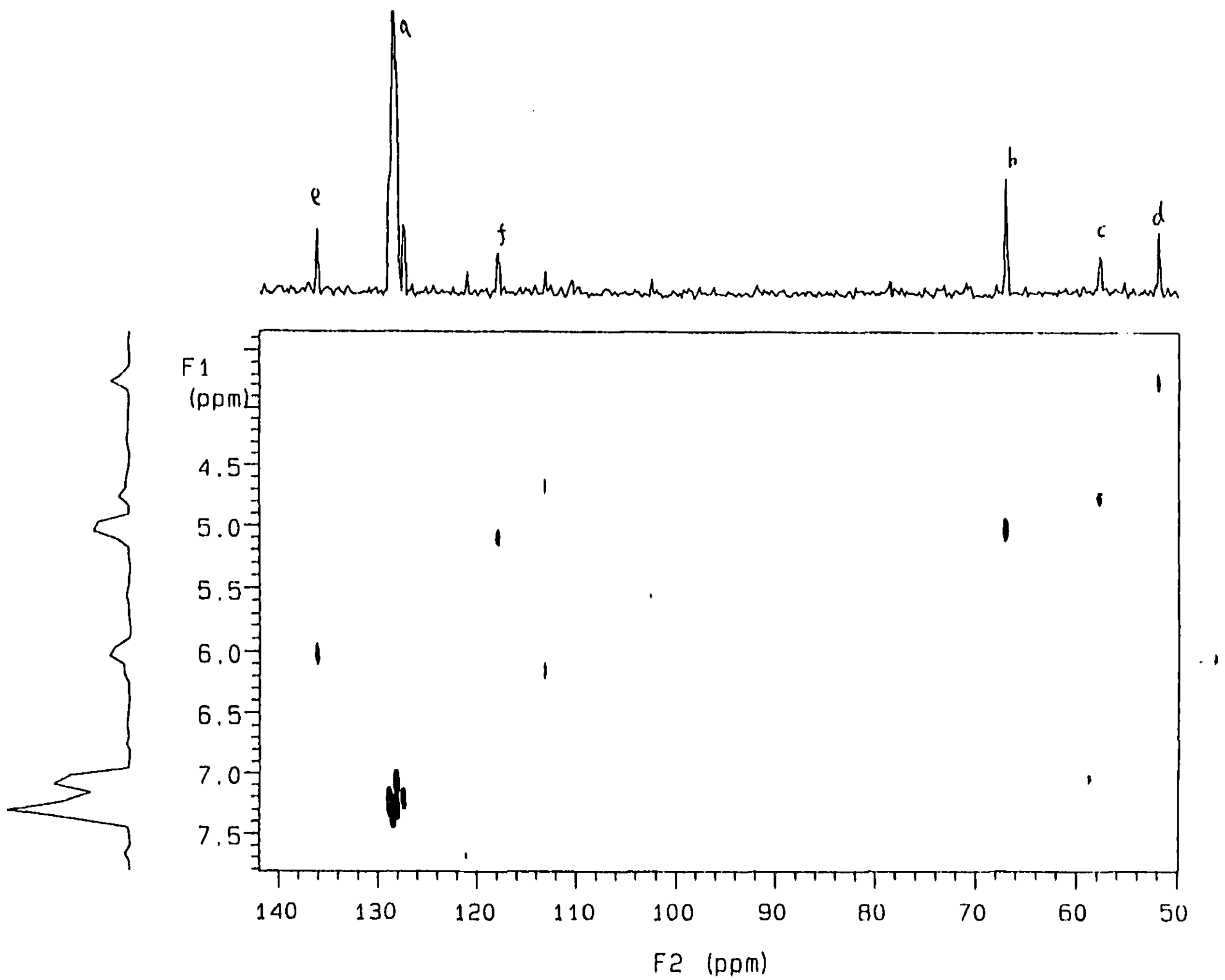

Claisen Rearrangement Bn ester

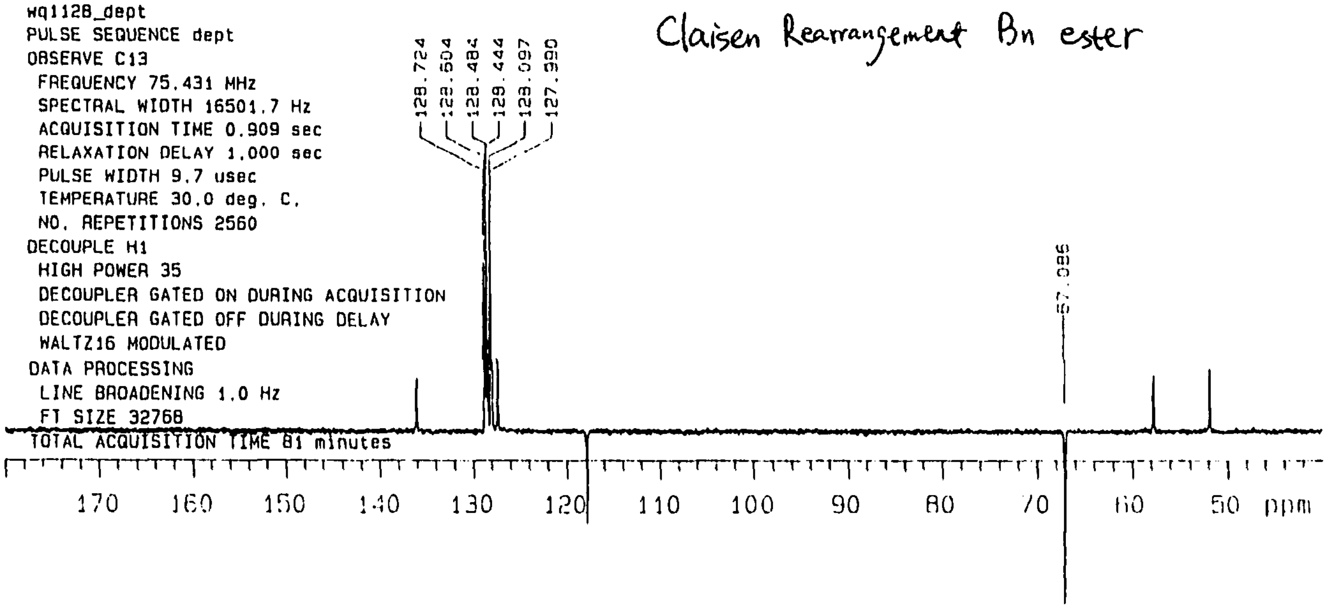

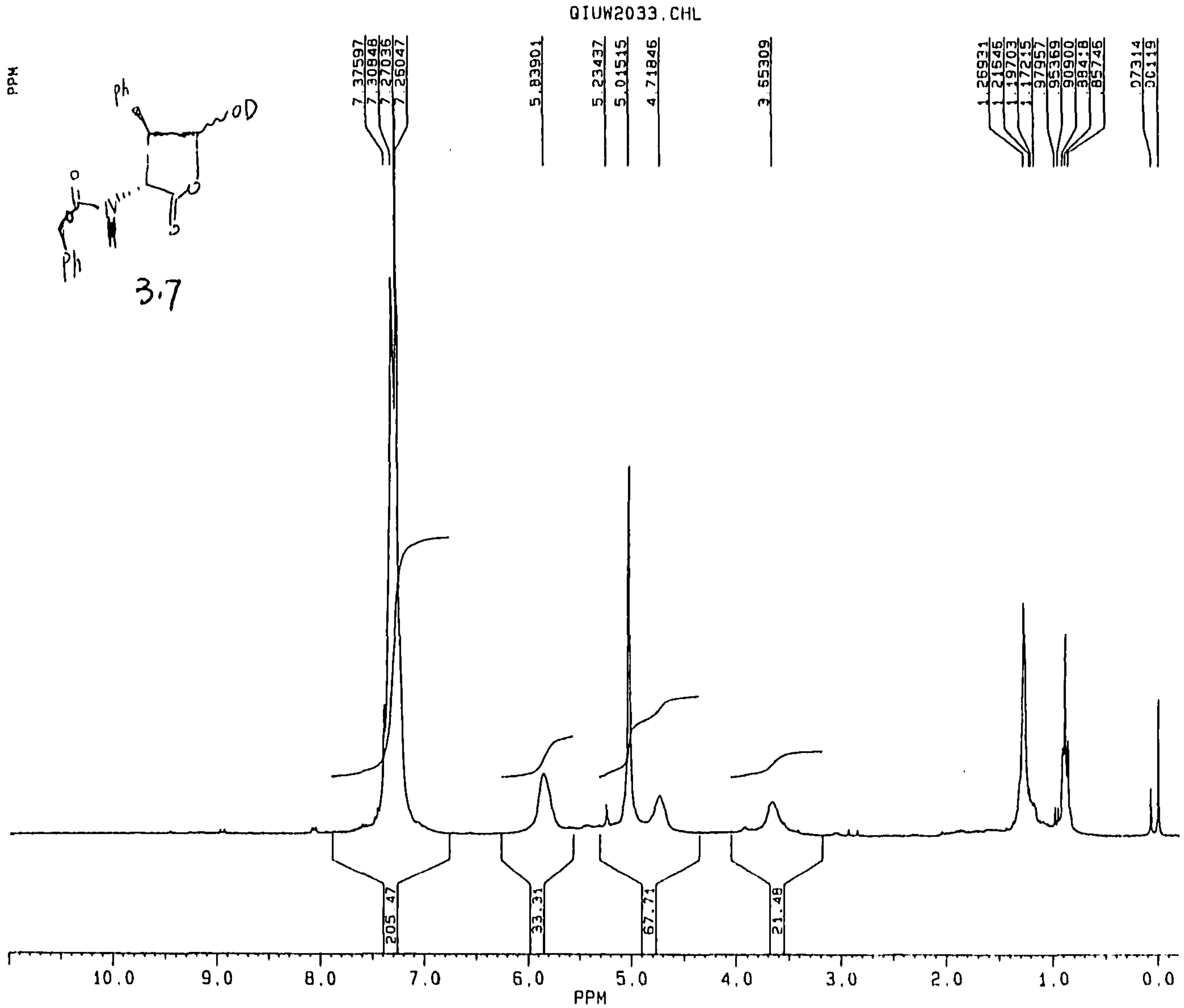
QIUW2033.CHL
PPM
Ph
OD
3.7
7.37597
7.30848
7.27036
7.26047
5.83901
5.23437
5.01515
4.71846
3.55309
1.26931
1.21546
1.19703
1.17215
.97957
.95369
.90900
.88418
.85746
.07314
.00119
205.47
33.31
67.71
21.48
10.0
9.0
8.0
7.0
6.0
5.0
4.0
3.0
2.0
1.0
0.0
PPM

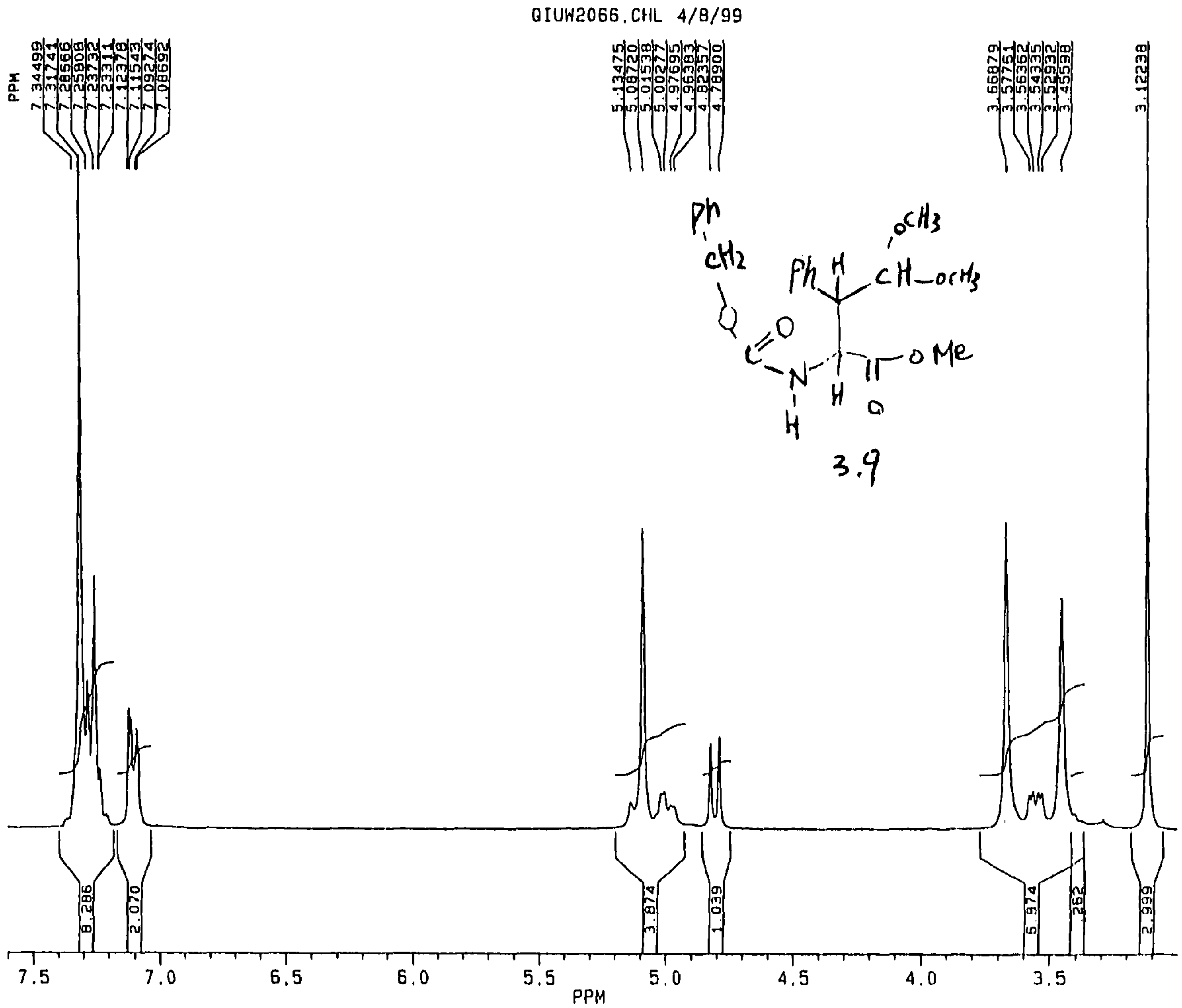
QIUW2066.CHL 4/8/99
PPM
7.34499
7.31741
7.28566
7.25808
7.23732
7.23311
7.12378
7.11543
7.09274
7.08692
5.13475
5.08720
5.01538
5.00277
4.97695
4.96383
4.82357
4.78900
3.66879
3.57751
3.56362
3.54335
3.52932
3.45598
3.12238
8.286
2.070
3.874
1.039
6.974
.262
2.999
7.5
7.0
6.5
6.0
5.5
5.0
4.5
4.0
3.5
PPM
3.9

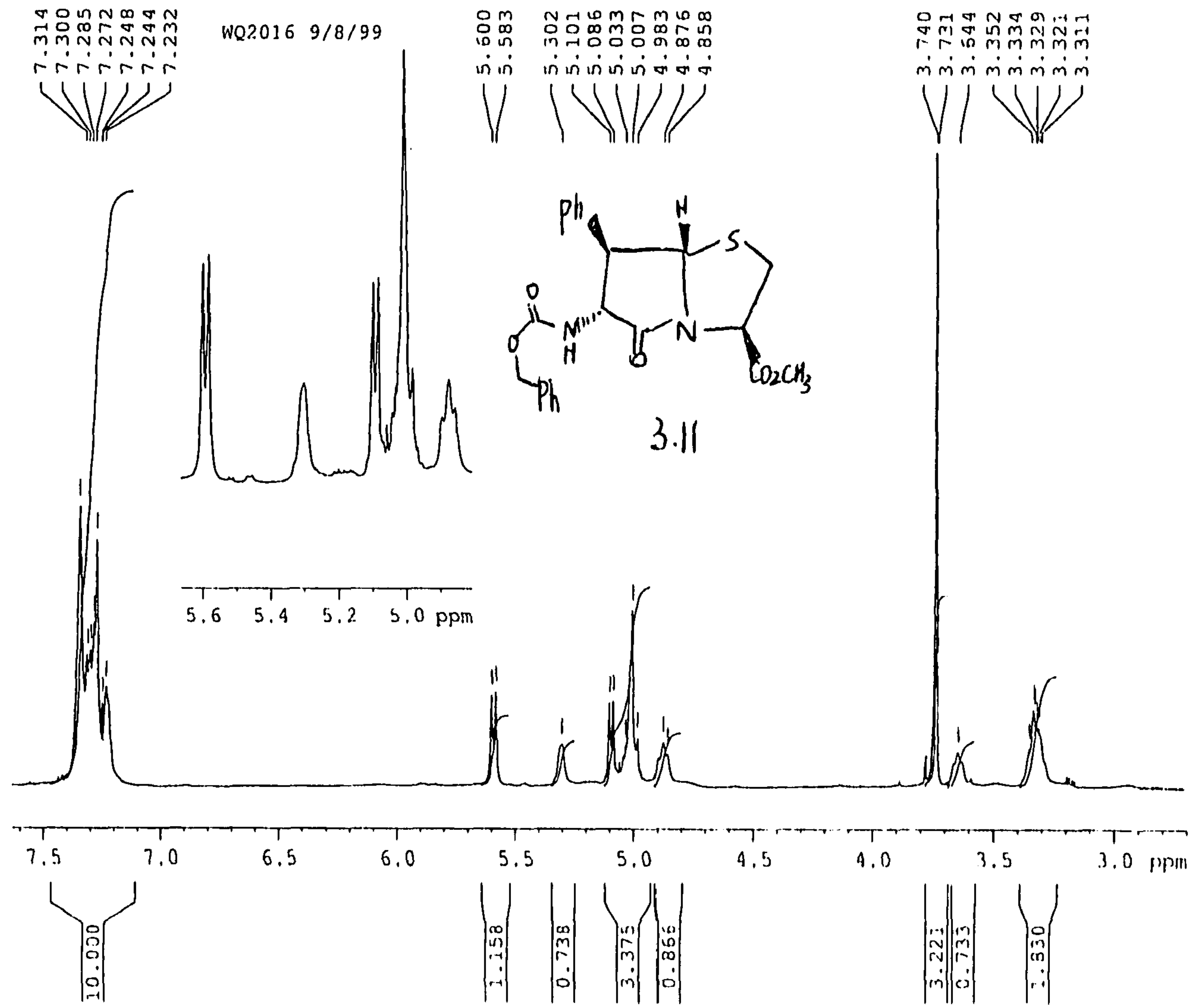
WQ2016 9/8/99
7.314
7.300
7.285
7.272
7.248
7.244
7.232
5.600
5.583
5.302
5.101
5.086
5.033
5.007
4.983
4.876
4.858
3.740
3.731
3.644
3.352
3.334
3.329
3.321
3.311
5.6 5.4 5.2 5.0 ppm
Ph
H
S
O
N
H
Ph
CO2CH3
3.11
7.5 7.0 6.5 6.0 5.5 5.0 4.5 4.0 3.5 3.0 ppm
10.000
1.158
0.738
3.375
0.866
3.221
0.733
1.830

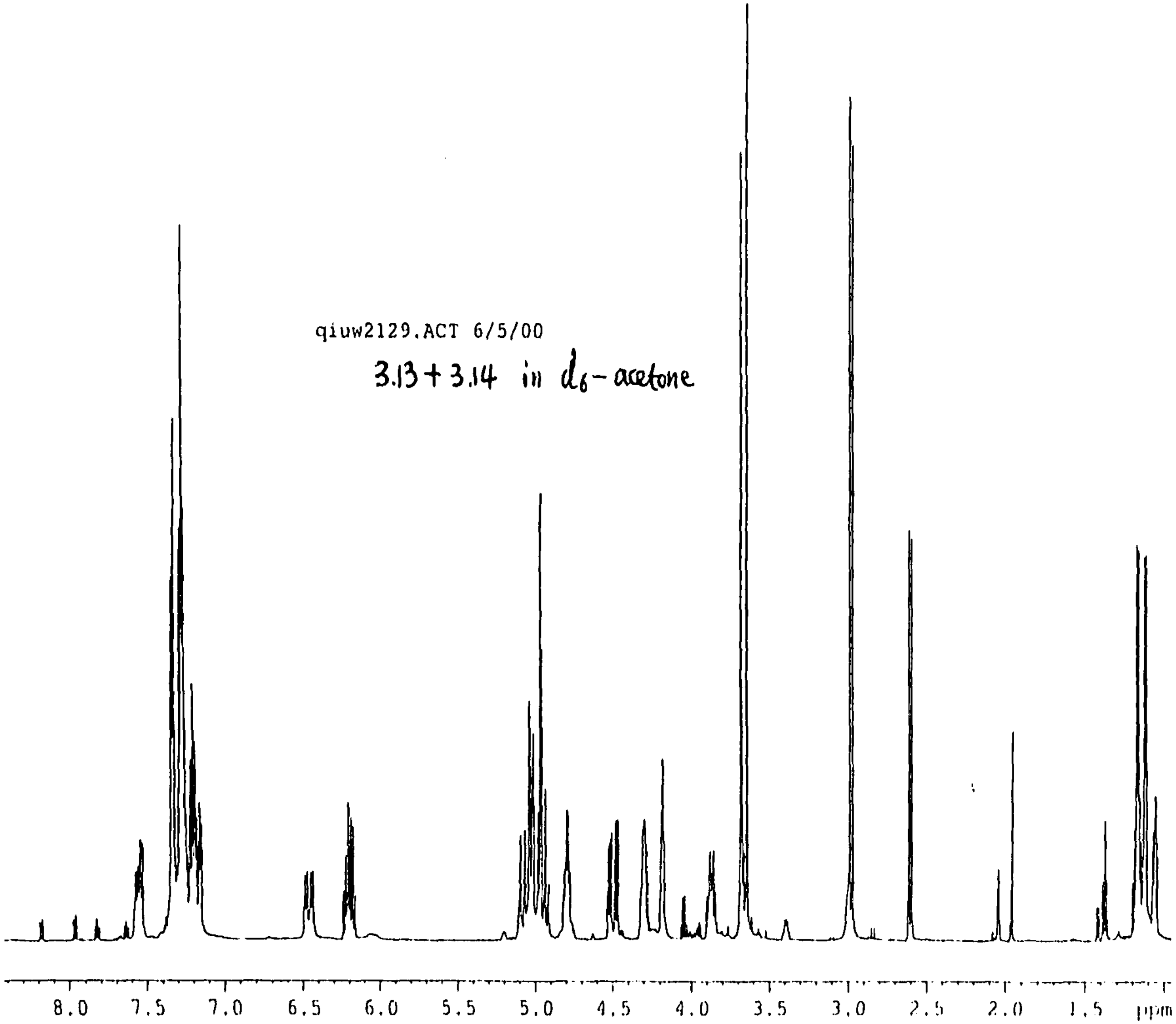
qiuw2129.ACT 6/5/00
3.13 + 3.14 in d_6-acetone
8.0 7.5 7.0 6.5 6.0 5.5 5.0 4.5 4.0 3.5 3.0 2.5 2.0 1.5 ppm

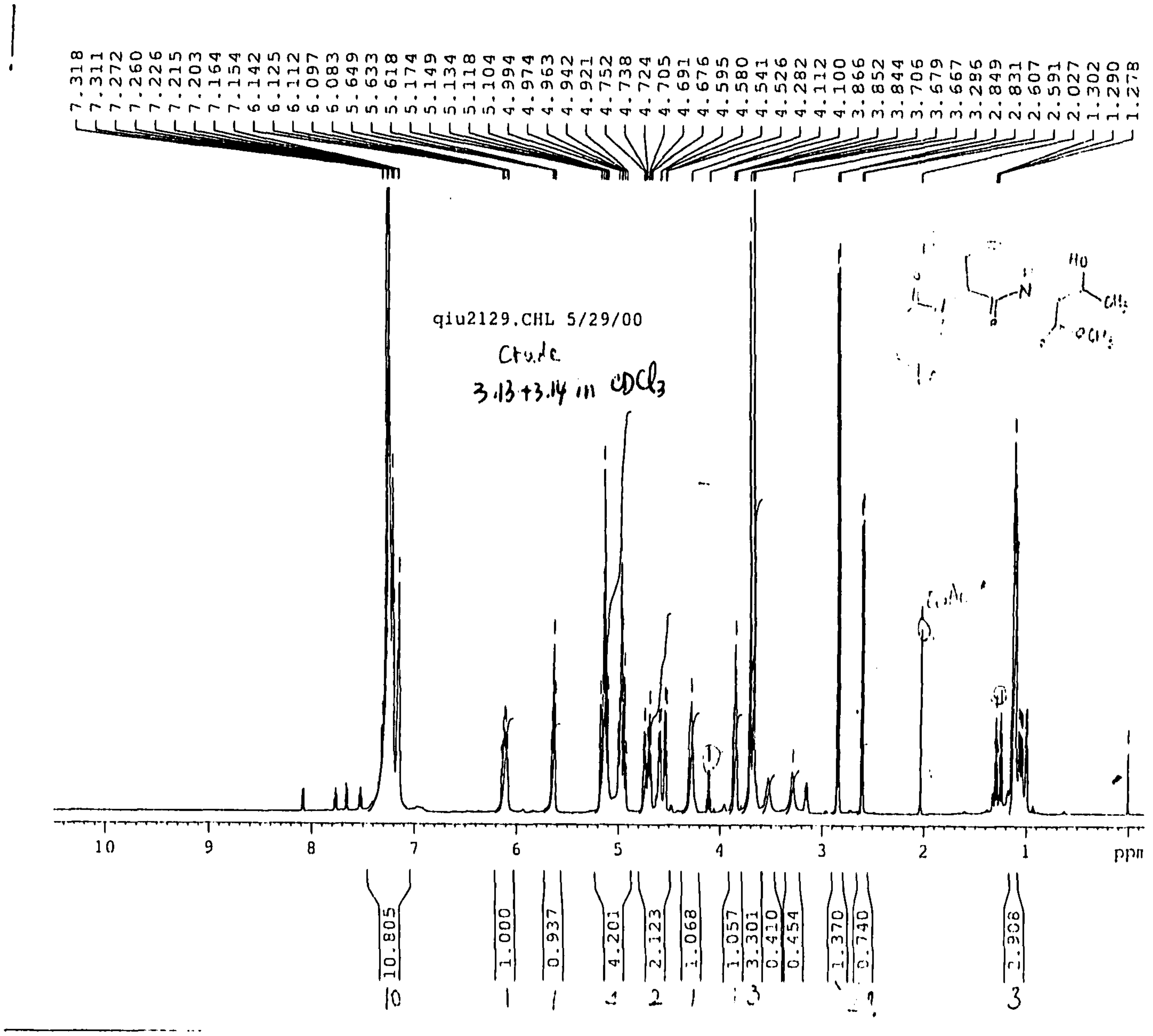
7.318 7.311 7.272 7.260 7.226 7.215 7.203 7.164 7.154 6.142 6.125 6.112 6.097 6.083 5.649 5.633 5.618 5.174 5.149 5.134 5.118 5.104 4.994 4.974 4.963 4.942 4.921 4.752 4.738 4.724 4.705 4.691 4.676 4.595 4.580 4.541 4.526 4.282 4.112 4.100 3.866 3.852 3.844 3.706 3.679 3.667 3.286 2.849 2.831 2.607 2.591 2.027 1.302 1.290 1.278
qiu2129.CHL 5/29/00
Crude
3.13+3.14 in CDCl3
10 9 8 7 6 5 4 3 2 1 ppm
10.805 1.000 0.937 4.201 2.123 1.068 1.057 3.301 0.410 0.454 1.370 0.740 2.908
10 1 1 2 1 3 3

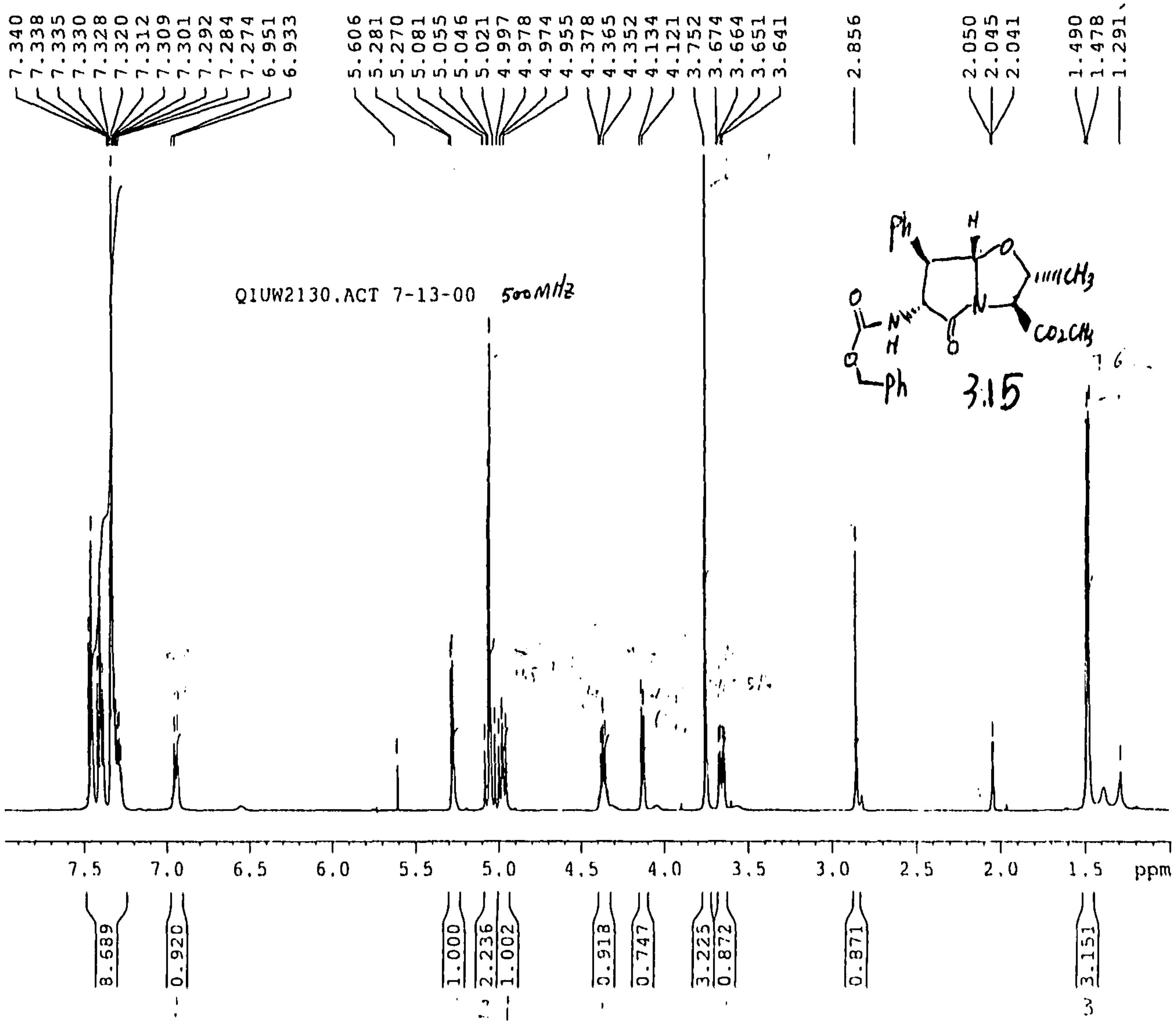
QIUW2130.ACT 7-13-00 500MHz
7.340
7.338
7.335
7.330
7.328
7.320
7.312
7.309
7.301
7.292
7.284
7.274
6.951
6.933
5.606
5.281
5.270
5.081
5.055
5.046
5.021
4.997
4.978
4.974
4.955
4.378
4.365
4.352
4.134
4.121
3.752
3.674
3.664
3.651
3.641
2.856
2.050
2.045
2.041
1.490
1.478
1.291
7.5 7.0 6.5 6.0 5.5 5.0 4.5 4.0 3.5 3.0 2.5 2.0 1.5 ppm
8.689
0.920
1.000
2.236
1.002
0.918
0.747
3.225
0.872
0.871
3.151
3
Ph
H
O
CH3
N
CO2CH3
NH
Ph
3.15

1D transient nOe of 3.15

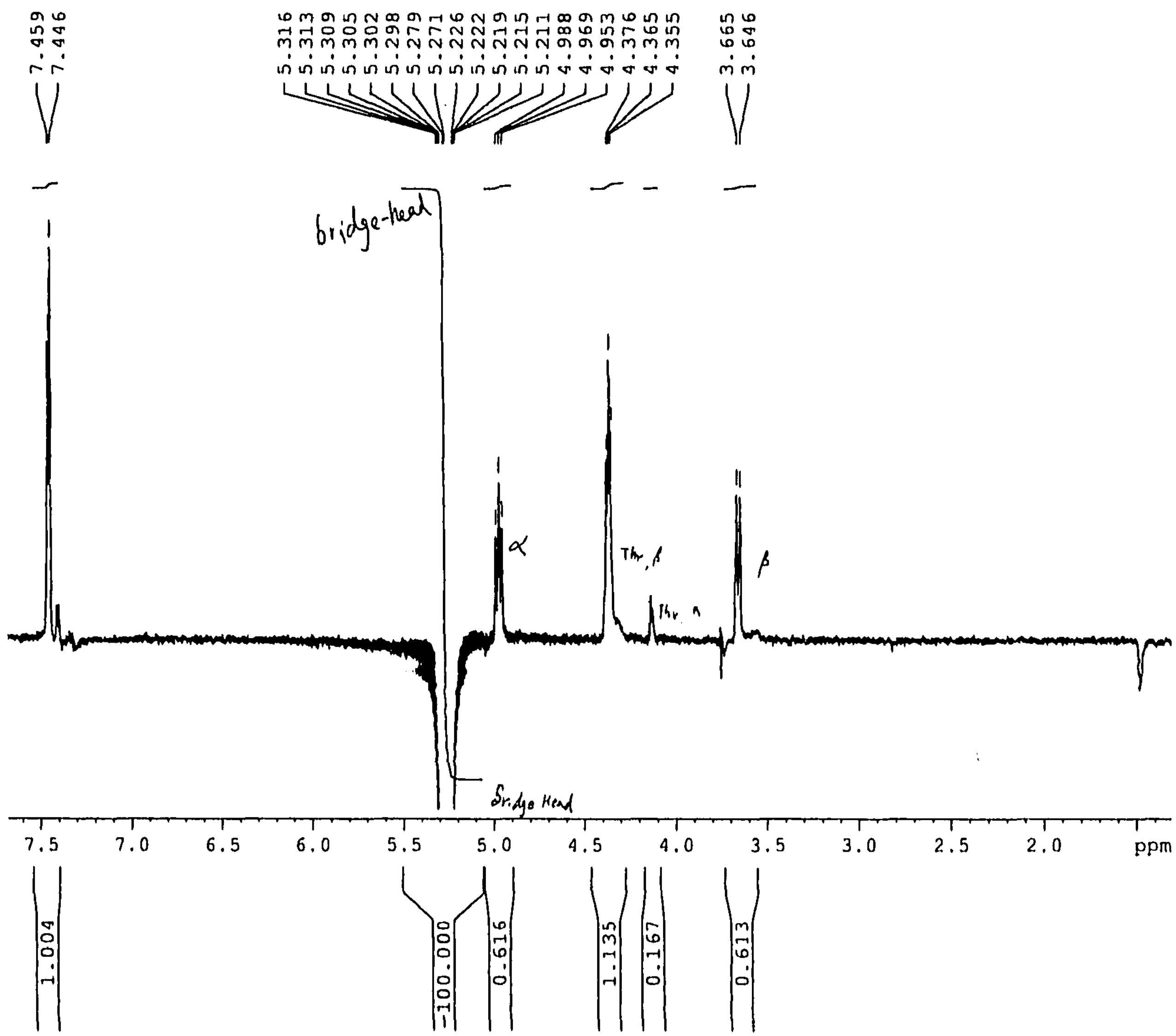

1D transient nOe of 3.15

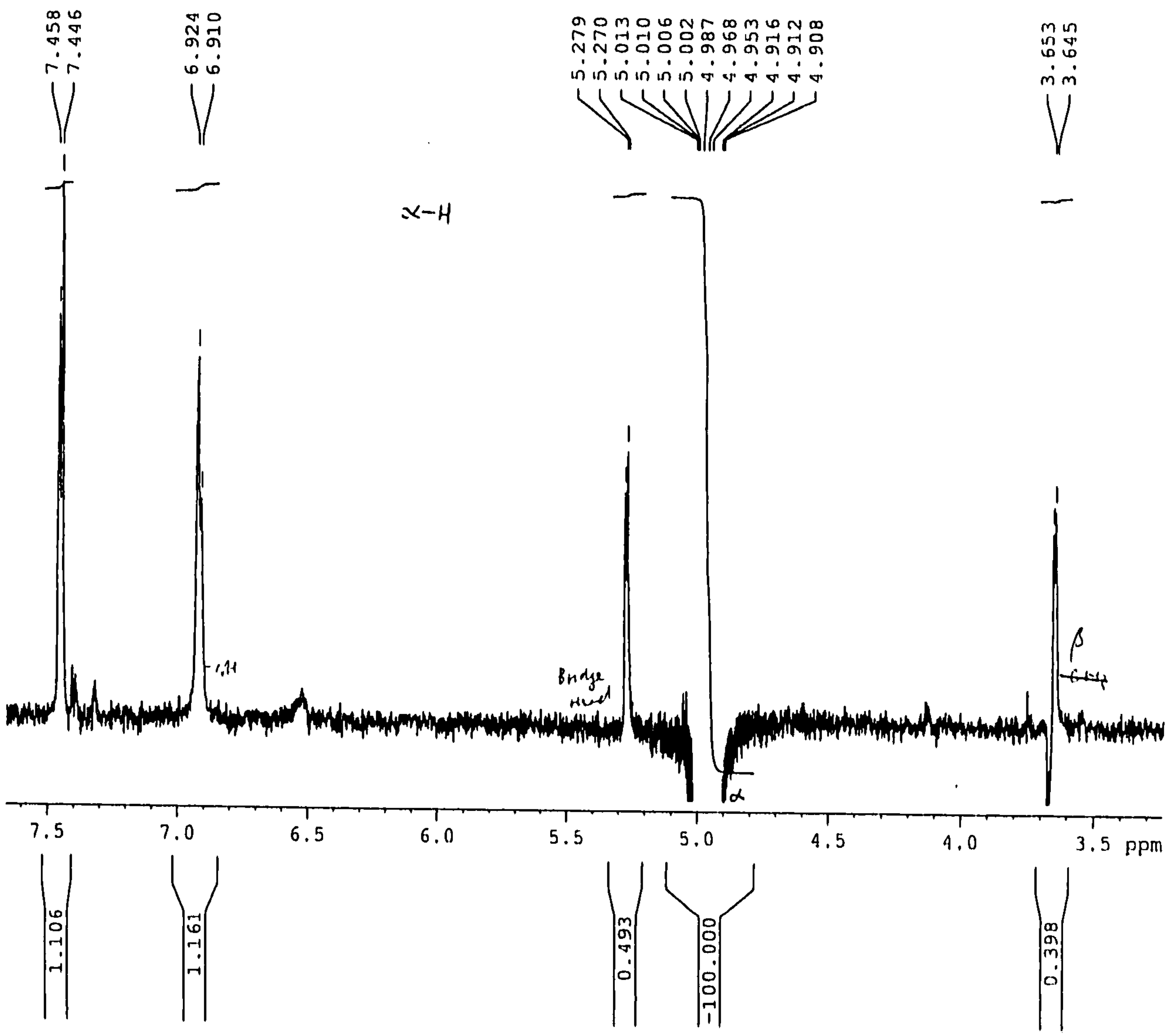

1D transient nOe of 3.15

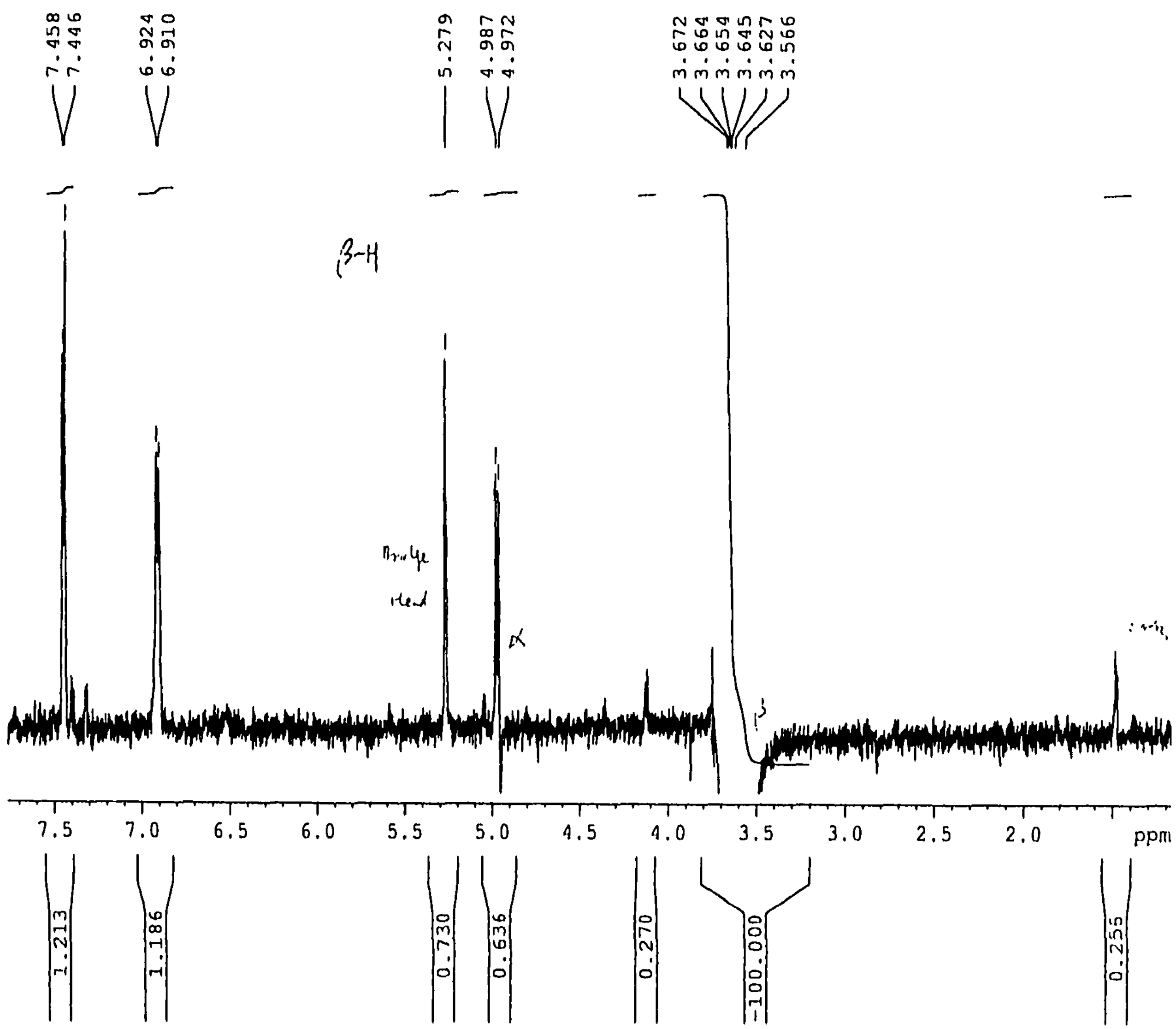

DQF-COSY of 3.15

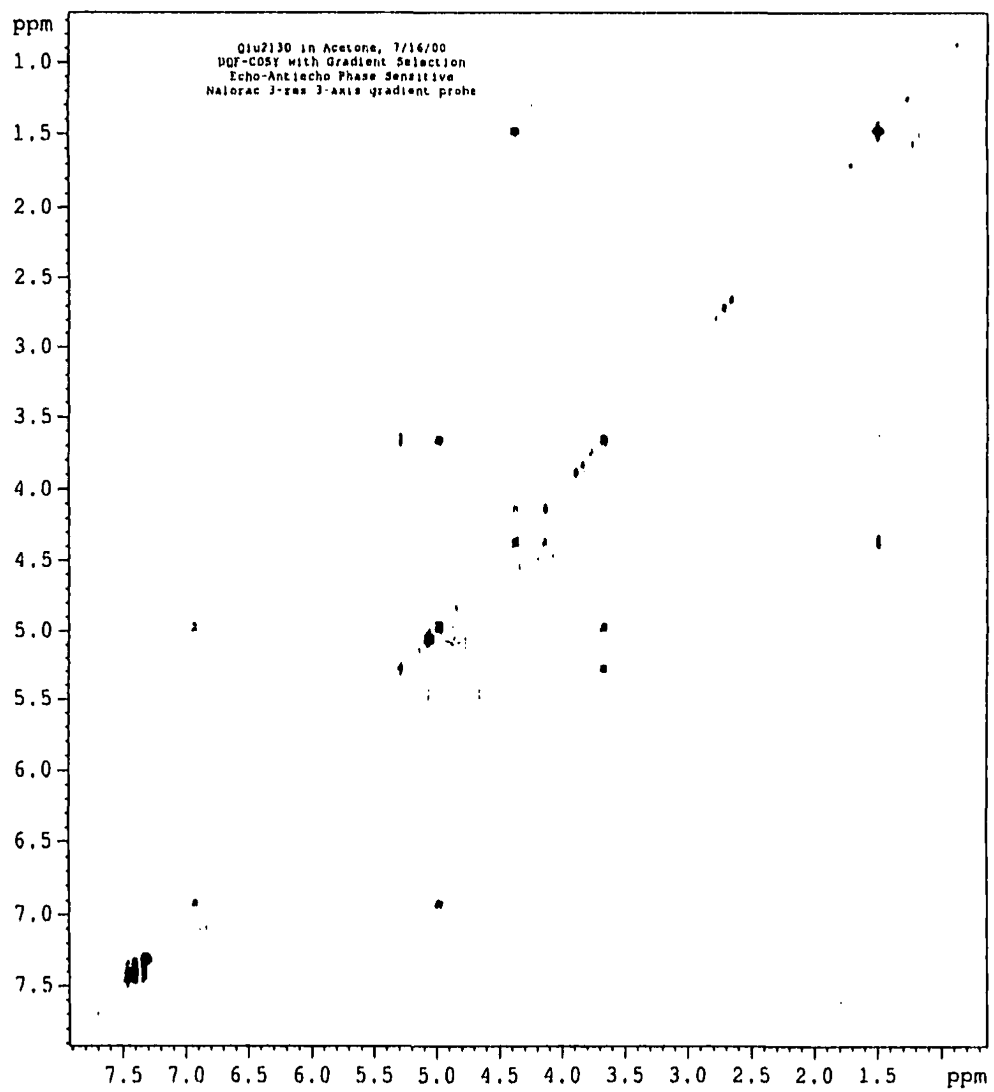

Current Data Parameters
NAME qiu2130.ACT
EXPNO 1
PROCNO 1

F2 - Acquisition Parameters
Date_ 20000716
Time 13.46
INSTRUM spect
PROBHD 5 mm IXI H-C
PULPROG cosydfetgp.2
TD 2048
SOLVENT CDCl3
NS 2
DS 16
SWH 4370.629 Hz
FIDRES 2.134096 Hz
AQ 0.2343412 sec
RG 20642.5
DW 114.400 usec
DE 6.00 usec
TE 298.0 K
d0 0.00000300 sec
D1 1.20000005 sec
d11 0.03000000 sec
D13 0.00000400 sec
D16 0.00020000 sec
DELTA 5000.00000000 sec
DELTA1 5000.00000000 sec
IN0 0.00022880 sec
l3 375
NUC1 1H
P1 9.30 usec
p2 18.60 usec
PL1 -3.00 dB
SFO1 600.1325830 MHz
GPNAM1 sine.250
GPNAM2 sine.250
GPNAM3 sine.250
GPX1 0.00 %
GPX2 0.00 %
GPX3 0.00 %
GPY1 0.00 %
GPY2 0.00 %
GPY3 0.00 %
GPZ1 10.00 %
GPZ2 10.00 %
GPZ3 50.00 %
P16 1000.00 usec

F1 - Acquisition parameters
ND0 1
TD 750
SFO1 600.1326 MHz
FIDRES 5.827506 Hz
SW 7.283 ppm

F2 - Processing parameters
SI 2048
SF 600.1300150 MHz
WDW SINE
SSB 1
LB 0.00 Hz
GB 0
PC 1.00

F1 - Processing parameters
SI 1024
MC2 echo antiecho
SF 600.1300162 MHz
WDW SINE
SSB 1
LB 0.00 Hz
GB 0

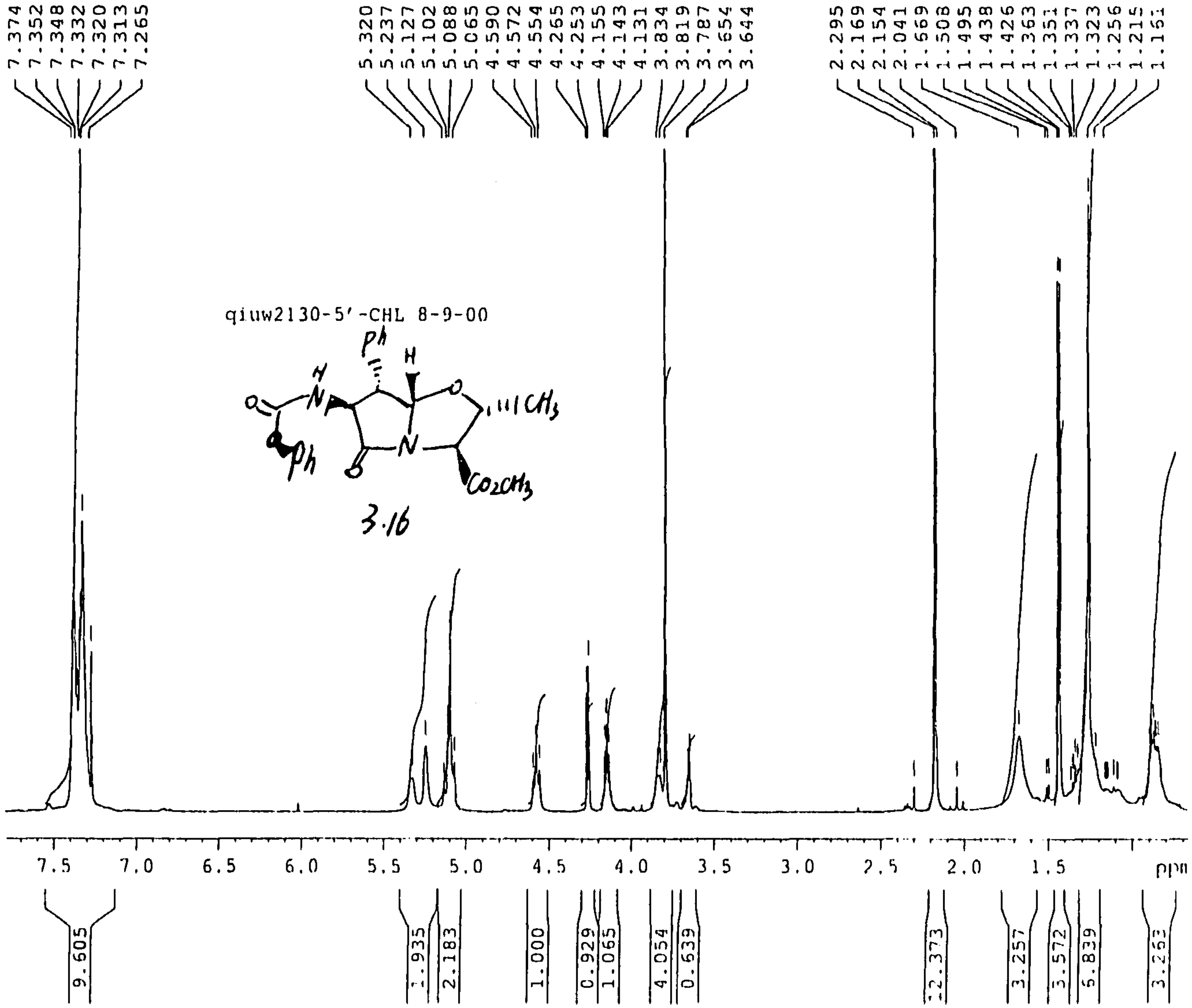
qiuw2130-5'-CHL 8-9-00
3.16
7.374
7.352
7.348
7.332
7.320
7.313
7.265
5.320
5.237
5.127
5.102
5.088
5.065
4.590
4.572
4.554
4.265
4.253
4.155
4.143
4.131
3.834
3.819
3.787
3.654
3.644
2.295
2.169
2.154
2.041
1.669
1.508
1.495
1.438
1.426
1.363
1.351
1.337
1.323
1.256
1.215
1.161
7.5
7.0
6.5
6.0
5.5
5.0
4.5
4.0
3.5
3.0
2.5
2.0
1.5
ppm
9.605
1.935
2.183
1.000
0.929
1.065
4.054
0.639
12.373
3.257
3.572
6.839
3.263

Current Data Parameters
NAME 2130-5.CHL
EXPNO 6
PROCNO 1

F2 - Acquisition Parameters
Date_ 20000812
Time 23.42
INSTRUM spect
PROBHD 5 mm Nalorac
PULPROG selnogp.3
TD 16384
SOLVENT CDCl3
NS 64
DS 4
SWH 6250.000 Hz
FIDRES 0.381470 Hz
AQ 1.3107700 sec
RG 64
DW 80.000 usec
DE 6.00 usec
TE 300.0 K
D1 2.00000000 sec
D8 0.34999999 sec
D16 0.00020000 sec
d20 50000000.00000000 sec
NUC1 1H
P1 9.50 usec
P2 19.00 usec
P12 35000.00 usec
PL0 120.00 dB
PL1 0.00 dB
SFO1 500.0328752 MHz
SP1 61.80 dB
SPNAM1 gauss.4k
SPOFF1 -795.55 Hz
GPNAM1 sine.100
GPNAM2 sine.100
GPNAM3 sine.100
GPNAM4 sine.100
GPX1 0.00 %
GPX2 0.00 %
GPX3 0.00 %
GPX4 0.00 %
GPY1 0.00 %
GPY2 0.00 %
GPY3 0.00 %
GPY4 0.00 %
GPZ1 11.00 %
GPZ2 17.00 %
GPZ3 40.00 %
GPZ4 -40.00 %
P16 1000.00 usec

F2 - Processing parameters
SI 16384
SF 500.0300000 MHz
WDW EM
SSB 0
LB 0.20 Hz
GB 0
PC 1.00

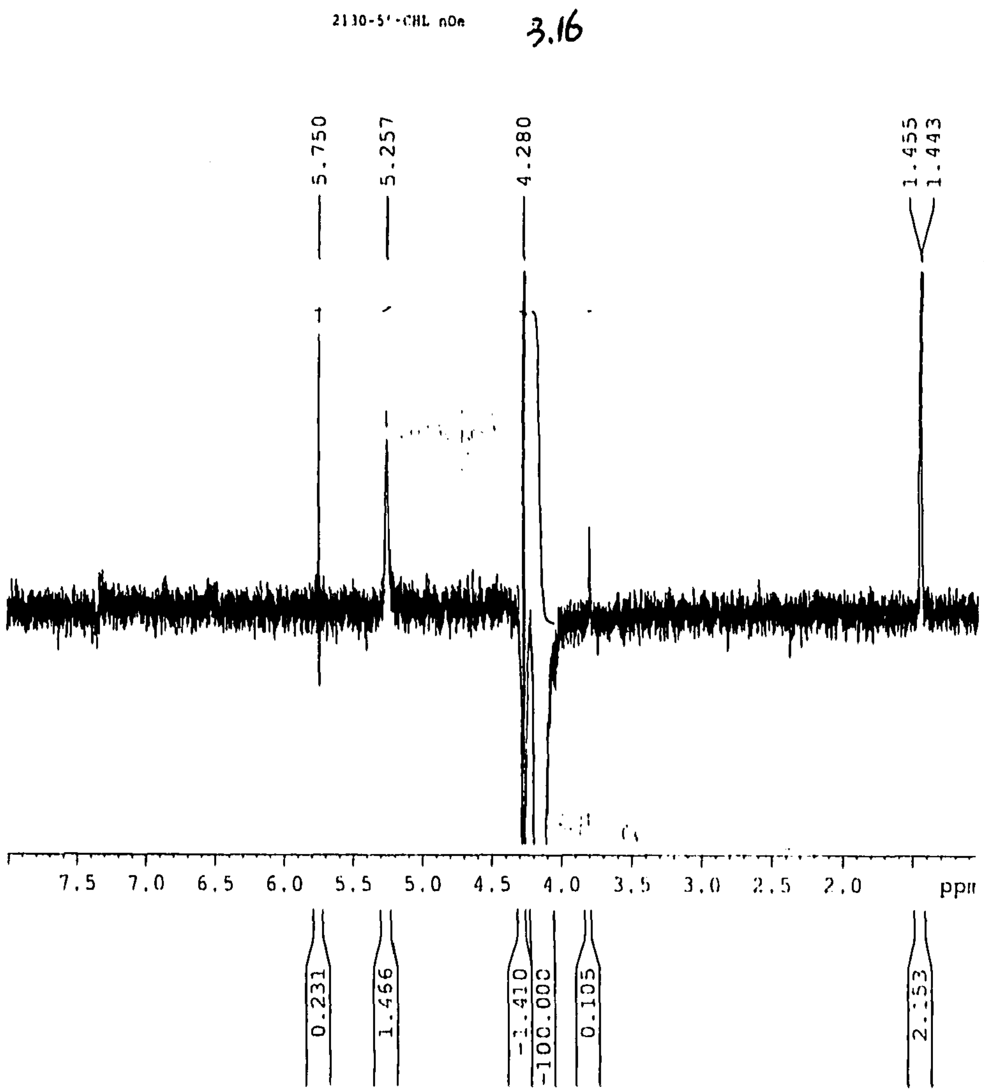

142

Current Data Parameters

NAME	2130-5.CHL	
EXPNO	7	
PROCNO	1	

F2 - Acquisition Parameters

Date_	20000812	
Time	23.46	
INSTRUM	spect	
PROBHD	5 mm Nalorac	
PULPROG	selnogp.3	
TD	16384	
SOLVENT	CDCl3	
NS	64	
DS	4	
SWH	6250.000	Hz
FIDRES	0.381470	Hz
AQ	1.3107700	sec
RG	64	
DW	80.000	usec
DE	6.00	usec
TE	300.0	K
D1	2.00000000	sec
D8	0.34999999	sec
D16	0.00020000	sec
d20	50000000.00000000	sec
NUC1	1H	
P1	9.50	usec
P2	19.00	usec
P12	35000.00	usec
PL0	120.00	dB
PL1	0.00	dB
SFO1	500.0328752	MHz
SP1	61.80	dB
SPNAM1	gauss.4k	
SPOFF1	-580.79	Hz
GPNAM1	sine.100	
GPNAM2	sine.100	
GPNAM3	sine.100	
GPNAM4	sine.100	
GPX1	0.00	%
GPX2	0.00	%
GPX3	0.00	%
GPX4	0.00	%
GPY1	0.00	%
GPY2	0.00	%
GPY3	0.00	%
GPY4	0.00	%
GPZ1	11.00	%
GPZ2	17.00	%
GPZ3	40.00	%
GPZ4	-40.00	%
P16	1000.00	usec

F2 - Processing parameters

SI	16384	
SF	500.0300000	MHz
WDW	EM	
SSB	0	
LB	0.20	Hz
GB	0	
PC	1.00	

2130-5'-CHL nOe 8-12-00 3.16

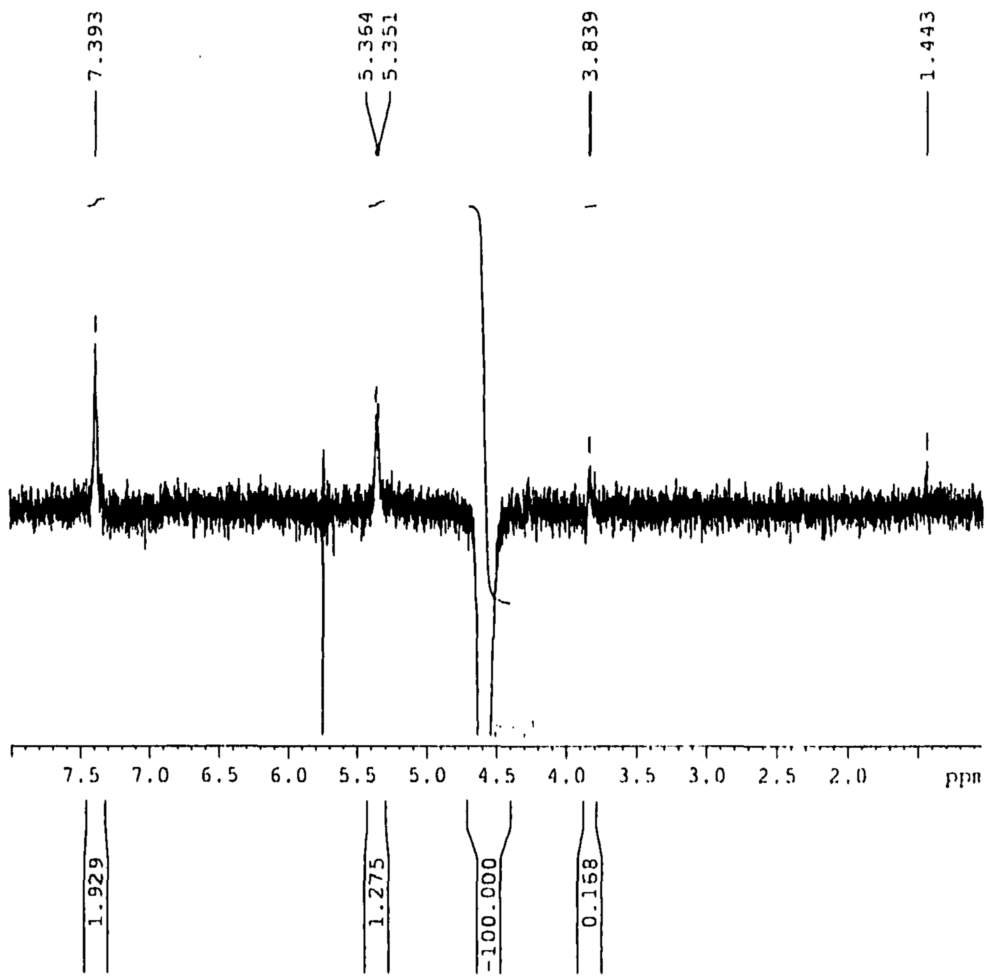

Current Data Parameters

NAME	2130-5.CHL
EXPNO	5
PROCNO	1

F2 - Acquisition Parameters

Date_	20000812	
Time	22.57	
INSTRUM	spect	
PROBHD	5 mm Nalorac	
PULPROG	selnogp.3	
TD	16384	
SOLVENT	CDCl3	
NS	64	
DS	4	
SWH	6250.000	Hz
FIDRES	0.381470	Hz
AQ	1.3107700	sec
RG	64	
DW	80.000	usec
DE	6.00	usec
TE	300.0	K
D1	2.00000000	sec
D8	0.34999999	sec
D16	0.00020000	sec
d20	50000000.00000000	se
NUC1	1H	
P1	9.50	usec
P2	19.00	usec
P12	35000.00	usec
PL0	120.00	dB
PL1	0.00	dB
SFO1	500.0328752	MHz
SP1	61.80	dB
SPNAM1	gauss.4k	
SPOFF1	-247.57	Hz
GPNAM1	sine.100	
GPNAM2	sine.100	
GPNAM3	sine.100	
GPNAM4	sine.100	
GPX1	0.00	%
GPX2	0.00	%
GPX3	0.00	%
GPX4	0.00	%
GPY1	0.00	%
GPY2	0.00	%
GPY3	0.00	%
GPY4	0.00	%
GPZ1	11.00	%
GPZ2	17.00	%
GPZ3	40.00	%
GPZ4	-40.00	%
P16	1000.00	usec

F2 - Processing parameters

SI	16384	
SF	500.0300000	MHz
WDW	EM	
SSB	0	
LB	0.20	Hz
GB	0	
PC	1.00	

QIUW2130-5'-CHL
Selective 1D Transient NOE
Nalorac 3-res 3-axis gradient probe

3.16

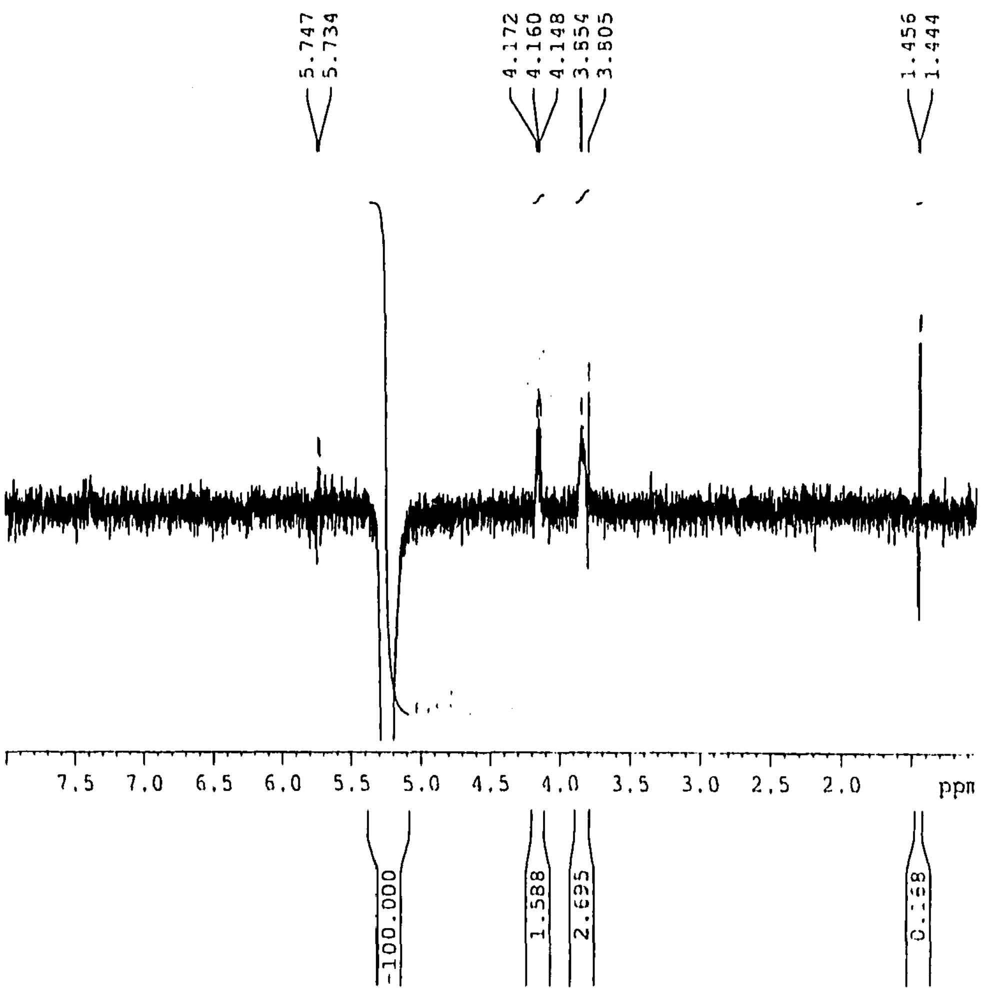

QIUN2130-5'.CHL 8-11-00
DQF-COSY with Gradient Selection
Echo-Antiecho Phase Sensitive
Nalorac 3-res 3-axis gradient probe

3.16

Current Data Parameters	
NAME	2130-5.CHL
EXPNO	2
PROCNO	1

F2 - Acquisition Parameters	
Date_	20000813
Time	15.23
INSTRUM	spect
PROBHD	5 mm Nalorac
PULPROG	cosydfetgp.2
TD	2048
SOLVENT	CDCl3
NS	2
DS	2
SWH	2730.178 Hz
FIDRES	1.362392 Hz
AQ	0.3670516 sec
RG	1625.5
DW	179.200 usec
DE	6.00 usec
TE	298.0 K
d0	0.00000300 sec
D1	1.00000000 sec
d11	0.03000000 sec
D13	0.00000400 sec
D16	0.00020000 sec
DELTA	5000.00000000 sec
DELTA1	5000.00000000 sec
IN0	0.00035940 sec
l3	375
NUC1	1H
P1	9.40 usec
p2	18.80 usec
PL1	0.00 dB
SFO1	500.0316001 MHz
GPNAM1	sine.100
GPNAM2	sine.100
GPNAM3	sine.100
GPX1	0.00 %
GPX2	0.00 %
GPX3	0.00 %
GPY1	0.00 %
GPY2	0.00 %
GPY3	0.00 %
GPZ1	30.00 %
GPZ2	10.00 %
GPZ3	50.00 %
P16	1000.00 usec

F1 - Acquisition parameters	
ND0	1
TD	512
SFO1	500.0316 MHz
FIDRES	5.449567 Hz
SW	5.580 ppm

F2 - Processing parameters	
SI	2048
SF	500.0300000 MHz
WDW	SINE
SSB	0
LB	0.00 Hz
GB	0
PC	1.00

F1 - Processing parameters	
SI	1024
MC2	echo-antiecho
SF	500.1300000 MHz
WDW	SINE
SSB	0
LB	0.00 Hz
GB	0

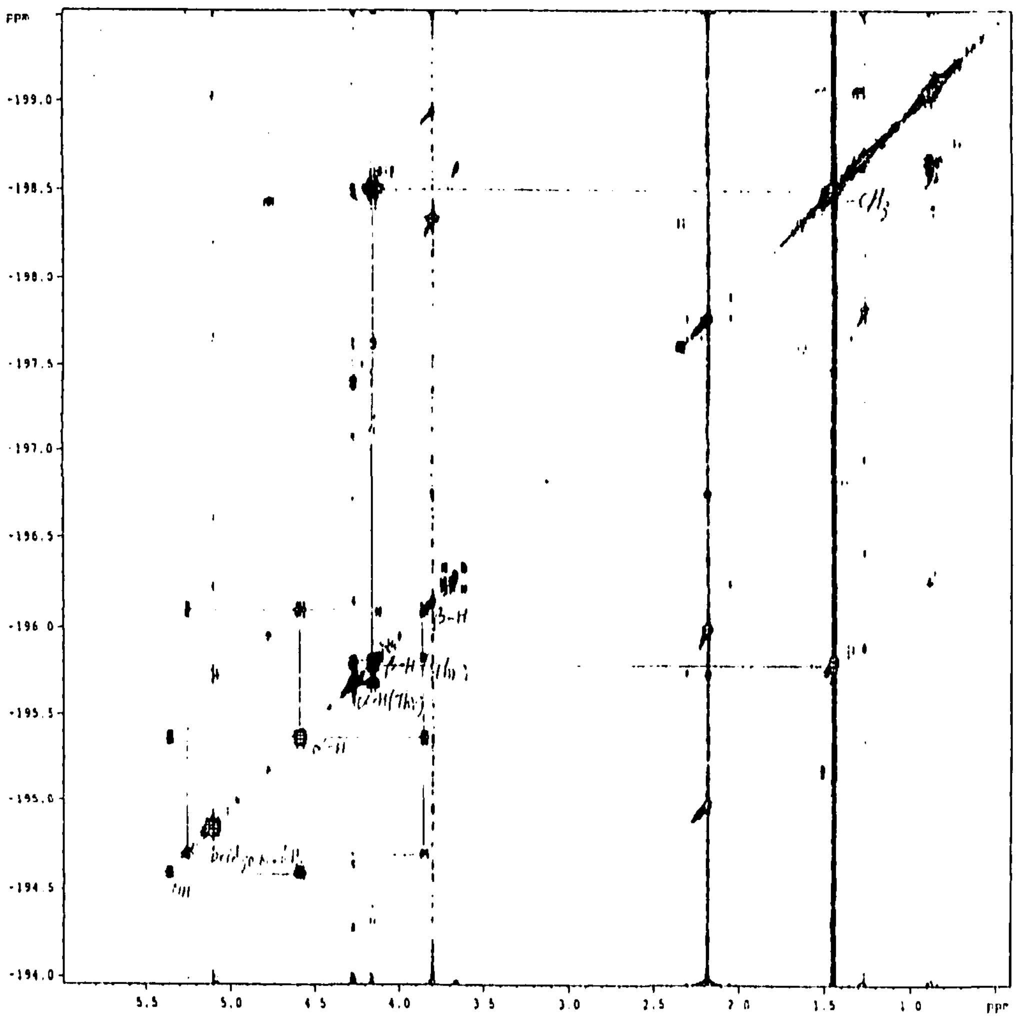

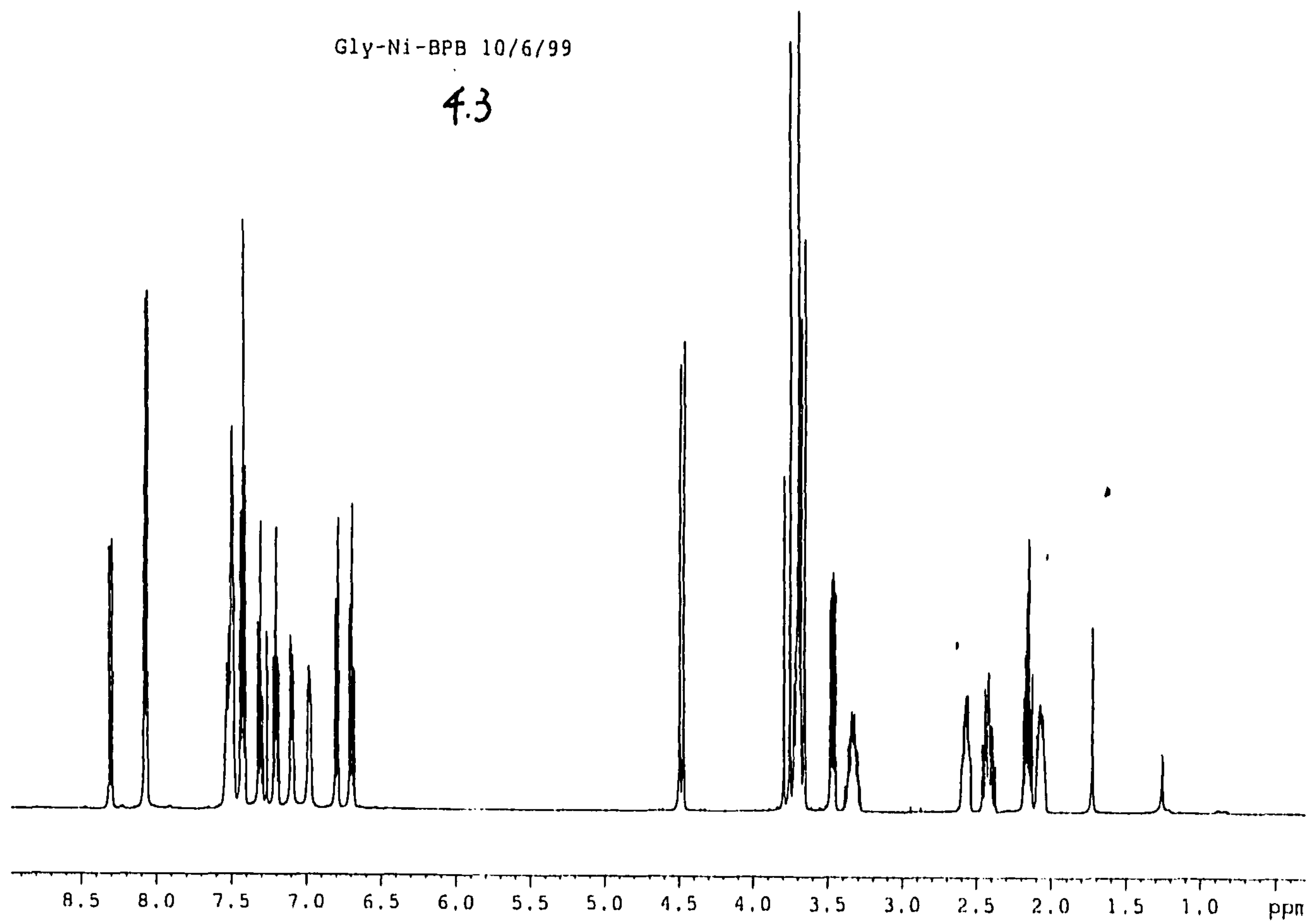
Gly-Ni-BPB 10/6/99
4.3
8.5 8.0 7.5 7.0 6.5 6.0 5.5 5.0 4.5 4.0 3.5 3.0 2.5 2.0 1.5 1.0 ppm

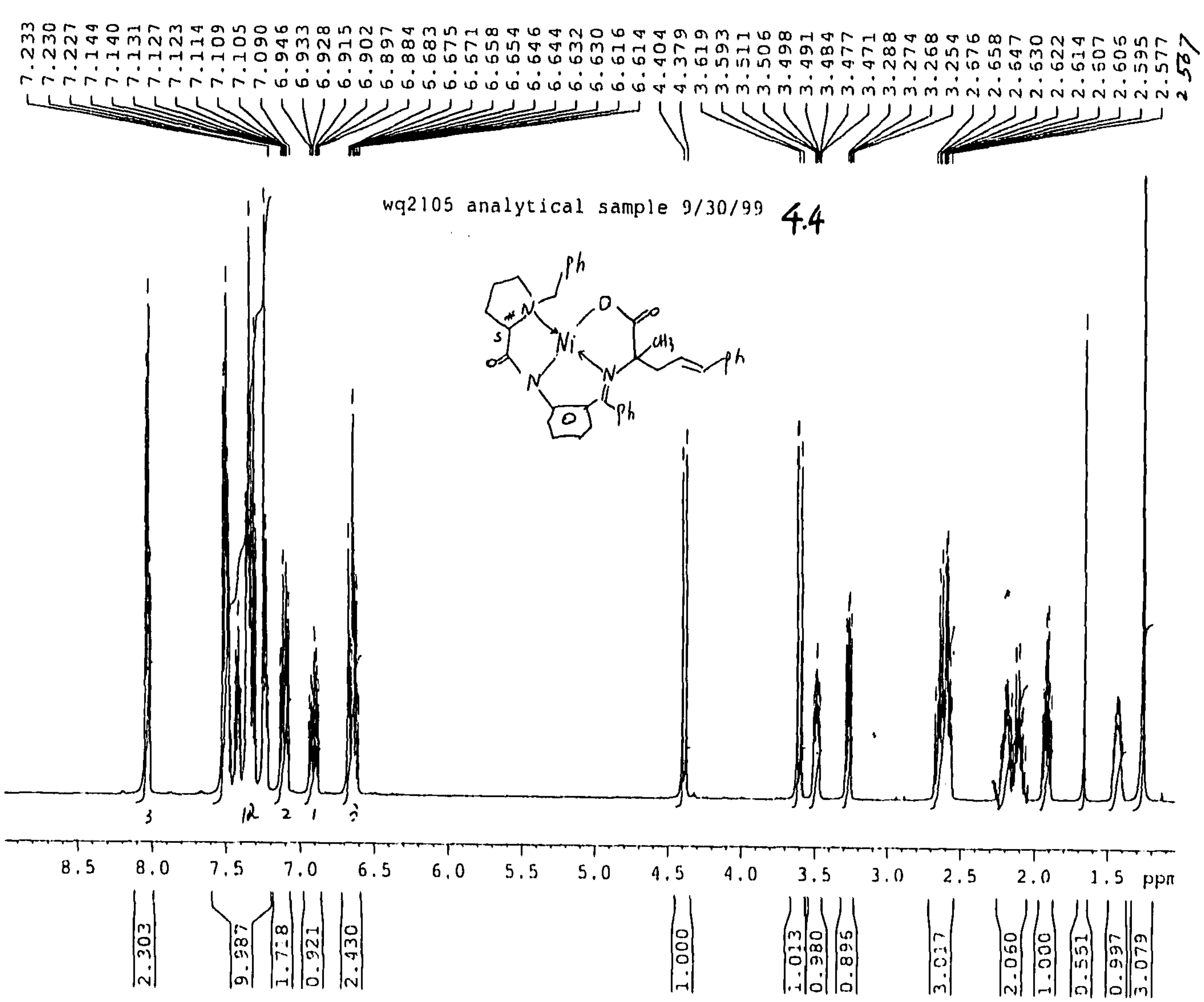
wq2105 analytical sample 9/30/99
4.4
7.233
7.230
7.227
7.144
7.140
7.131
7.127
7.123
7.114
7.109
7.105
7.090
6.946
6.933
6.928
6.915
6.902
6.897
6.884
6.683
6.675
6.671
6.658
6.654
6.646
6.644
6.632
6.630
6.616
6.614
4.404
4.379
3.619
3.593
3.511
3.506
3.498
3.491
3.484
3.477
3.471
3.288
3.274
3.268
3.254
2.676
2.658
2.647
2.630
2.622
2.614
2.607
2.606
2.595
2.577
2.587
8.5
8.0
7.5
7.0
6.5
6.0
5.5
5.0
4.5
4.0
3.5
3.0
2.5
2.0
1.5
ppm
2.303
9.987
1.718
0.921
2.430
1.000
1.013
0.980
0.896
3.017
2.060
1.000
0.551
0.997
3.079

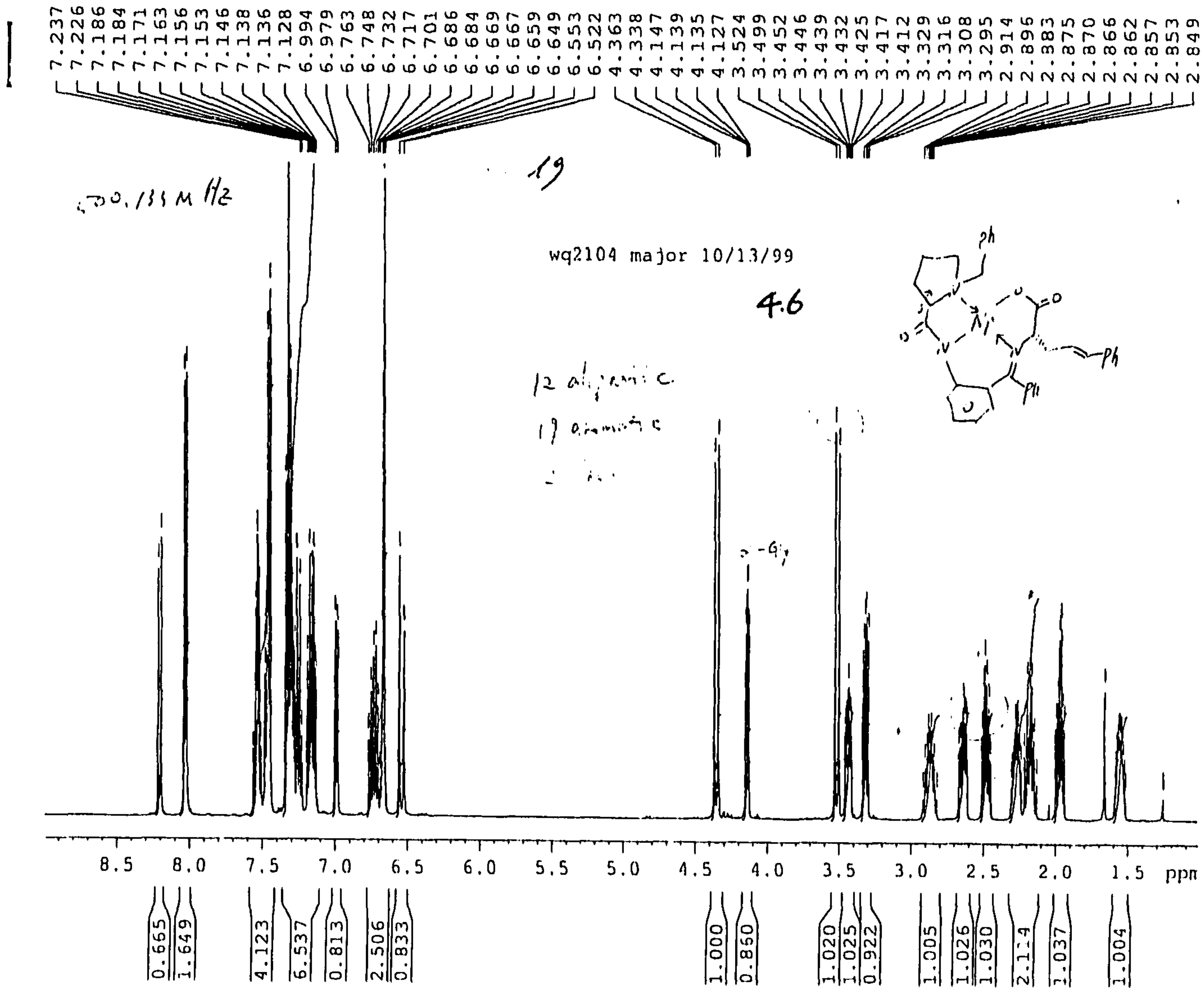
7.237
7.226
7.186
7.184
7.171
7.163
7.156
7.153
7.146
7.138
7.136
7.128
6.994
6.979
6.763
6.748
6.732
6.717
6.701
6.686
6.684
6.669
6.667
6.659
6.649
6.553
6.522
4.363
4.338
4.147
4.139
4.135
4.127
3.524
3.499
3.452
3.446
3.439
3.432
3.425
3.417
3.412
3.329
3.316
3.308
3.295
2.914
2.896
2.883
2.875
2.870
2.866
2.862
2.857
2.853
2.849
wq2104 major 10/13/99
4.6
Ph
Ph
8.5
8.0
7.5
7.0
6.5
6.0
5.5
5.0
4.5
4.0
3.5
3.0
2.5
2.0
1.5
ppm
0.665
1.649
4.123
6.537
0.813
2.506
0.833
1.000
0.850
1.020
1.025
0.922
1.005
1.026
1.030
2.114
1.037
1.004

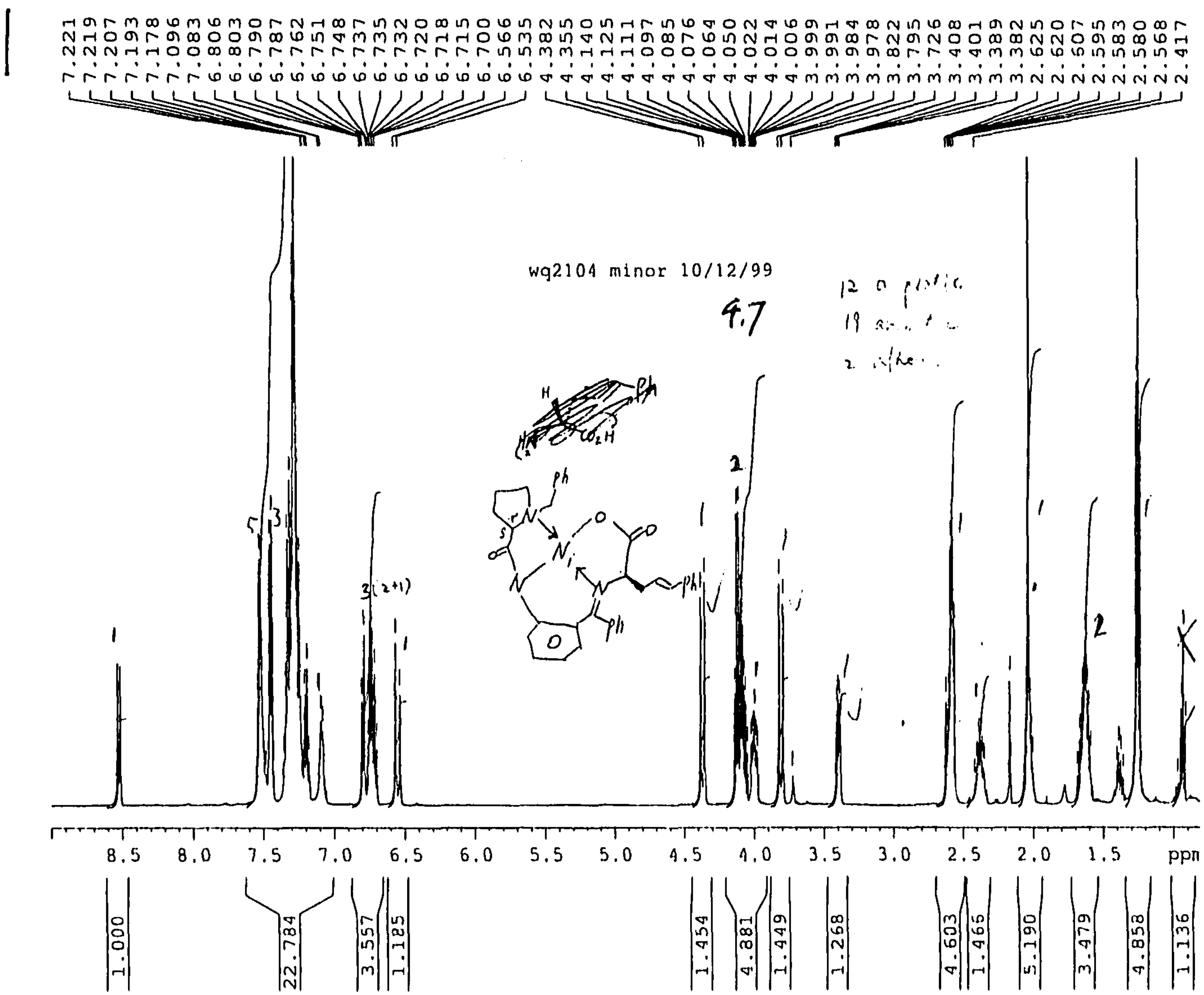
wq2104 minor 10/12/99
4.7
ppm

wq2088 1st spot after column 9/17/99

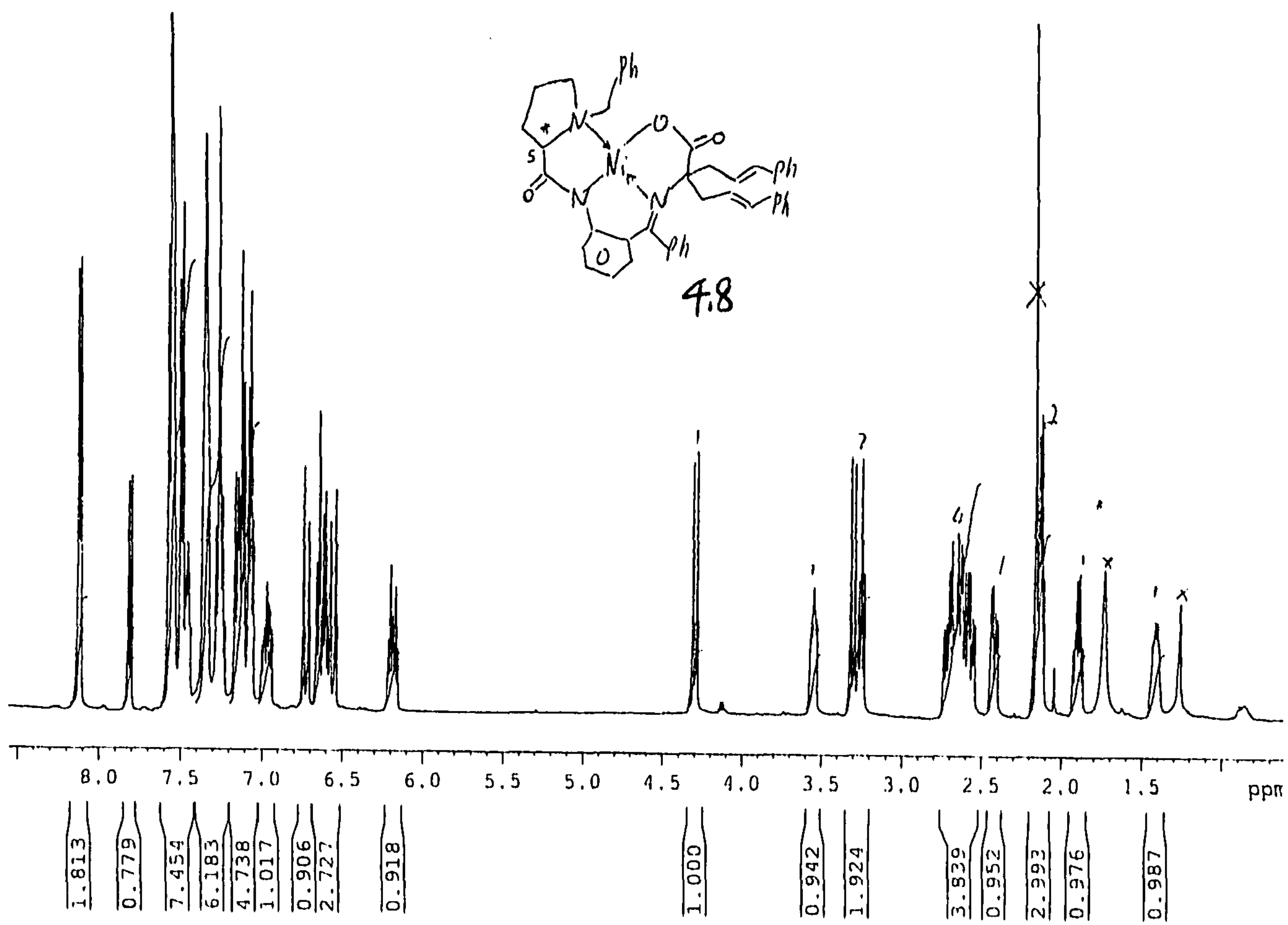

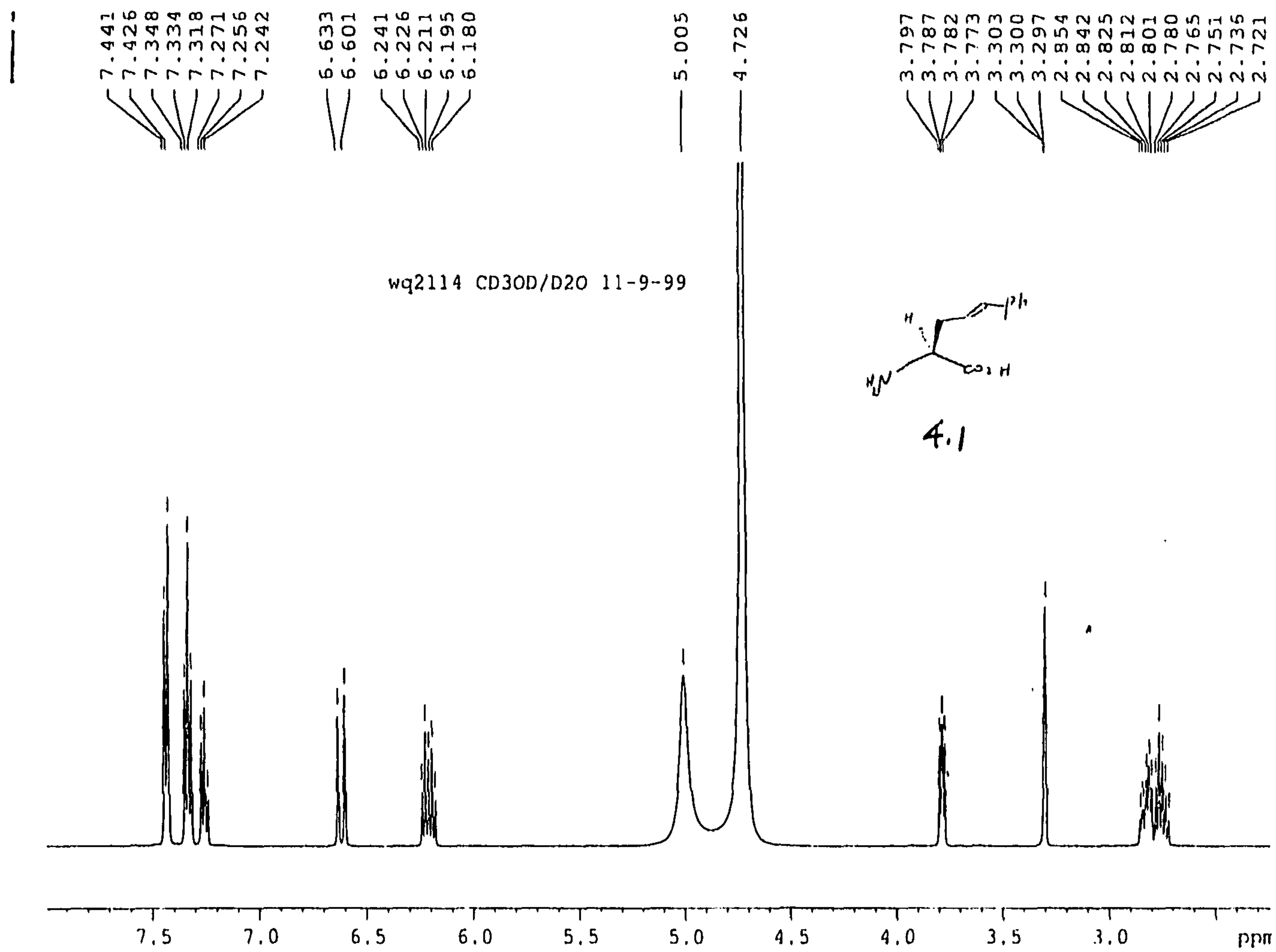

7.441
7.426
7.348
7.334
7.318
7.271
7.256
7.242
6.633
6.601
6.241
6.226
6.211
6.195
6.180
5.005
4.726
3.797
3.787
3.782
3.773
3.303
3.300
3.297
2.854
2.842
2.825
2.812
2.801
2.780
2.765
2.751
2.736
2.721
wq2114 CD3OD/D2O 11-9-99
4.1
7.5
7.0
6.5
6.0
5.5
5.0
4.5
4.0
3.5
3.0
ppm

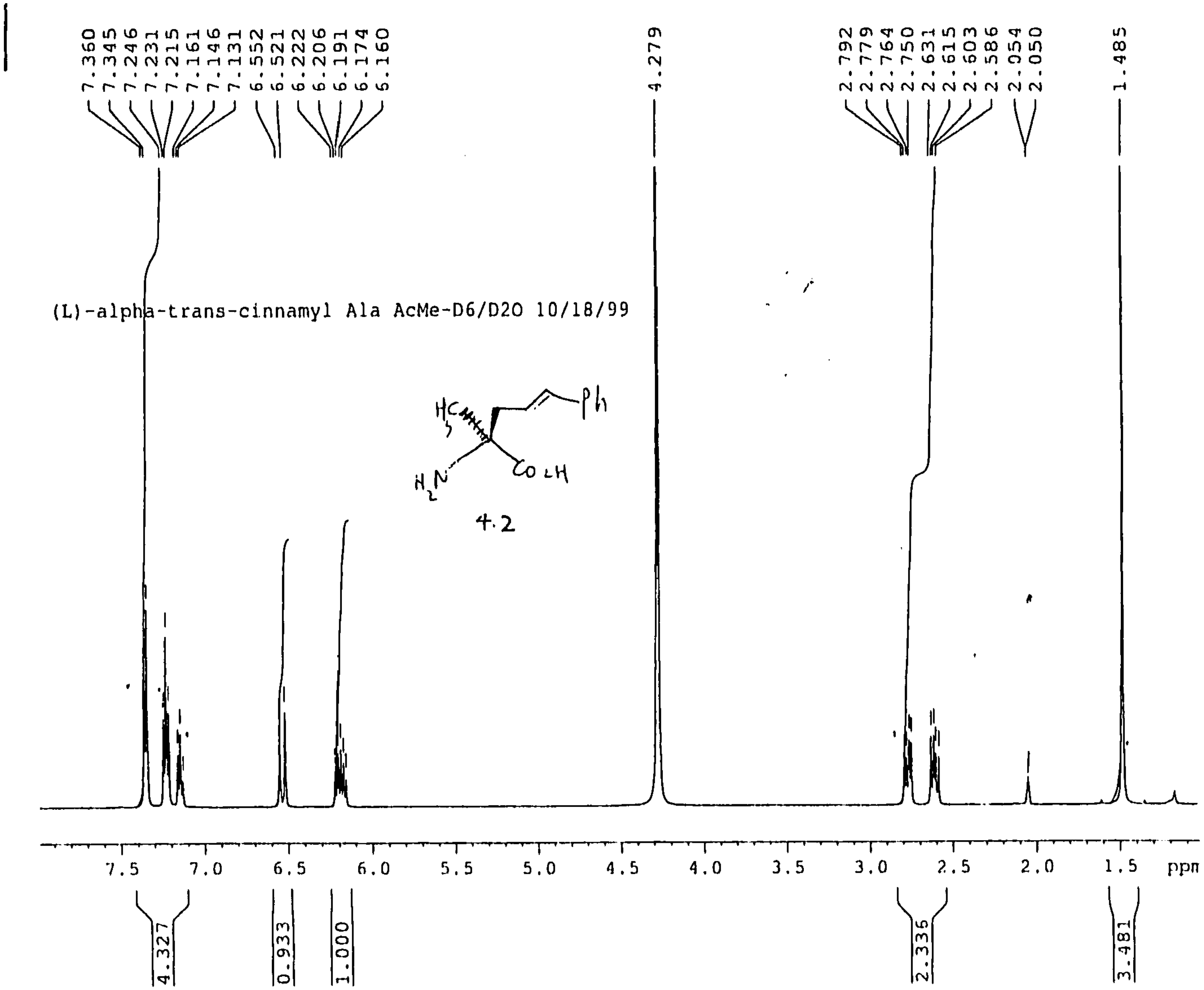
(L)-alpha-trans-cinnamyl Ala AcMe-D6/D2O 10/18/99
7.360
7.345
7.246
7.231
7.215
7.161
7.146
7.131
6.552
6.521
6.222
6.206
6.191
6.174
6.160
4.279
2.792
2.779
2.764
2.750
2.631
2.615
2.603
2.586
2.054
2.050
1.485
H3C
H2N
CO2H
Ph
4.2
7.5
7.0
6.5
6.0
5.5
5.0
4.5
4.0
3.5
3.0
2.5
2.0
1.5
ppm
4.327
0.933
1.000
2.336
3.481

REFERENCES

(1) Fruton, J. S. *Proc. Am. Philos. Soc.* **1985**, *129*, 313.

(2) Lehninger, A. L. *Nature* **1957**, *180*, 326.

(3) Hirschmann, R. *Angew. Chem. Int. Ed. Engl.* **1991**, *30*, 1278.

(4) Hruby, V. J.; Hadley, M. E. In *Design and Synthesis of Organic Molecules Based on Molecular Recognition*; VanBinst, G., Ed.; Springer-Verlog: Heidelberg, 1986; pp 269-289.

(5) Hruby, V. J.; Yamamura, H. I.; Porreca, F. *Ann. N. Y. Acad. Sci.* **1995**, *757*, 7.

(6) Schwyzer, R. *Ann. N. Y. Acad. Sci.* **1977**, *247*, 3.

(7) Hruby, V. J. *Drug Discovery Today* **1997**, *2*, 165.

(8) Hruby, V. J.; Slate, S. In *Advances in Amino Acid Mimetics and Peptidomimetics*; Abell, A., Ed.; JAI Press Inc.: Greenwich, 1999; Vol. 2, pp 191-220.

(9) Veber, D. F. In Smith, J. A., Ed.; Escom: Leiden, 1992; pp 3-14.

(10) Hruby, V. J. *Life Sci.* **1982**, *31*, 189.

(11) Kessler, H. *Angew. Chem. Int. Ed. Engl.* **1982**, *21*, 512.

(12) Hruby, V. J.; Al-Obeidi, F.; Kazmierzki, W. *Biochem. J.* **1990**, *268*, 249.

(13) Hruby, V. J. *Biopolymers* **1993**, *33*, 1073.

(14) Marshall, G. R. *Tetrahedron* **1993**, *49*, 3547.

(15) Giannis, A.; Kolter, T. *Angew. Chem. Int. Ed. Engl.* **1993**, *32*, 1244.

(16) Wiley, R. A.; Rich, D. H. *Med. Res. Rev.* **1993**, *13*, 327.

(17) Gante, J. *Angew. Chem. Int. Ed. Engl.* **1994**, *33*, 1699.

(18) Goodmann, M. In *Burger's Medicinal Chemistry and Drug Discovery.*; 5th ed.; Wolff, M. E., Ed.; John Wiley & Sons: New York, 1995; Vol. 1, pp 804-848.

(19) Hruby, V. J.; Li, G.; Haskell-Luevano, C.; Shenderovich, M. D. *Biopolymers* **1997**, *43*, 219.

(20) Rosenberg, S. H.; Boyd, S. A. In *Antihypertens. Drugs*; Zwieten, V., A., P., Greenlee, W. J., Eds.; Harwood: Amsterdam, 1997; pp 77-111.

(21) Nakanishi, H.; Kahn, M. In *Bioorg. Chem.: Pept. Proteins*; Hecht, S. M., Ed.; Oxford University Press: New York, N. Y., 1998; pp 395-419.

(22) Krebs, S.; Rognan, D. *Pharm. Acta Helv.* **1998**, *73*, 173.

(23) Horwell, D. C.; Prichard, M. C.; Raphy, J. *Adv. Amino Acid Mimetics Peptidomimetics* **1999**, *2*, 165-190.

(24) Freidinger, R. M. *Curr. Opin. Chem. Biol* **1999**, *3*, 395.

(25) Skotnicki, J. S.; Zask, A.; Nelson, F. C.; Albright, J. D.; Levin, J. I. *Ann. N. Y. Acad. Sci.* **1999**, *878*, 61.

(26) Thaisrivongs, S.; Strohbach, J. W. *Biopolymers* **1999**, *51*, 51.

(27) Liu, S.; Crider, A. M.; Tang, C.; Ho, B.; Ankersen, M.; Stidsen, C. E. *Curr. Pharm. Des.* **1999**, *5*, 255.

(28) Hruby, V. J. In Joosse, J., Buijs, R. M., Tilders, F. J. H., Eds.; Elsevier Science: Amsterdam, 1992; Vol. 92, pp 215-224.

(29) Ramachandran, G. N.; Sasisekharan, V. *Adv. Protein Chem.* **1968**, *23*, 283.

(30) Lewis, P. N.; Momany, F. A.; Scheraga, H. A. *Isr. J. Chem.* **1973**, *11*, 121.

(31) Lewis, P. N.; Momany, F. A.; Scheraga, H. A. *Biochem. Biophys. Acta* **1973**, *303*, 211.

(32) Kövér, K. E.; Jiao, D.; Fang, S.; Hruby, V. J. *Magn. Reson. Chem.* **1993**, *31*, 1072.

(33) Kövér, K. E.; Jiao, D.; Uhrin, D.; Forgo, P.; Hruby, V. J. *J. Magn. Reson. Series A* **1994**, *106*, 119.

(34) Valle, G.; Kazmierski, W. M.; Crisma, M.; Bonora, G. M.; Toniolo, C.; Hruby, V. J. *Int. J. Peptide Protein Res.* **1992**, *40*, 222.

(35) Spatola, A. F. In *Chemistry and Biochemistry of Amino Acids, Peptides and Proteins*; Weinstein, B., Ed.; Dekker: New York, 1983; Vol. 7, pp 267-357.

(36) Manavalan, P.; Momany, F. A. *Biopolymers* **1980**, *19*, 1943.

(37) Kawai, M.; Fukuta, N.; Ito, N.; Kagami, T.; Butsugan, Y.; Maruyama, M.; Kudo, Y. *Int. J. Peptide Protein Res.* **1990**, *35*, 452.

(38) Filatova, M. P.; Dri, N. A.; Komarova, N. A.; Orfkkchovich, O. M.; Reiss, V. M.; Liepinya, I. T.; Nikiforovich, G. V. *Bioorg. Khim.* **1986**, *12*, 59.

(39) Bovy, P. R.; Trapani, A. J.; McMahon, E. G.; Palomo, M. *J. Med. Chem.* **1989**, *32*, 520.

(40) Hruby, V. J.; Fang, S. N.; Knapp, R.; Kazmierski, W.; Lui, G. K.; Yamamura, H. I. In *Peptides: Chemistry, Structure and Biology*; Rivier, J. E., Marshall, G. R., Eds.; ESCOM: Lieden, 1990; pp 53-55.

(41) Boteju, L. W.; Nikiforovich, G. V.; Haskell-Luevano, C.; Fang, S.; Zalewska, D.; Stropova, D.; Yamamura, H. I.; Hruby, V. J. *J. Med. Chem.* **1996**, *39*, 4120.

(42) Boteju, L. W.; Zalewska, T.; Yamamura, H. I.; Hruby, V. J. *Bioorg. Med. Chem. Lett.* **1993**, *3*, 2011.

(43) Karle, I. L.; Balaram, P. *Biochemistry* **1990**, *29*, 6747.

(44) Toniolo, C. *Int. J. Peptide Protein Res.* **1990**, *35*, 287-300.

(45) Balaram, P.; Sudha, T. S. *Int. J. Peptide Protein Res.* **1983**, *21*, 381.

(46) Samanen, J.; Cash, T.; Narindray, D.; Brandeis, E.; Adams, J. W.; Weideman, H.; Yellin, T. *J. Med. Chem.* **1991**, *34*, 3036.

(47) London, R. E.; Stewart, J. M.; Cann, J. R. *Biochem. Pharmacol.* **1990**, *40*, 41.

(48) Chorev, M.; Goodman, M. *Acc. Chem. Res.* **1993**, *26*, 266.

(49) El Masdouri, L.; Aubry, A.; Sakarellos, C.; Gomex, E. J.; Cung, M. T.; Marraud, M. *Int. J. Peptide Protein Res.* **1988**, *31*, 420.

(50) Spatola, A.; Edwards, J. V. *Biopolymers* **1986**, *25*, 229.

(51) TenBrink, R. E. *J. Org. Chem.* **1987**, *52*, 418.

(52) Rodriguez, M.; Heitz, A.; Martinez, J. *Tetrahedron Lett.* **1990**, *31*, 7319.

(53) Rodriguez, M.; Amblard, M.; Galas, M. C.; Lignon, M. F.; Aumelas, A.; Martinez, J. *Int. J. Peptide Protein Res.* **1990**, *35*, 1184.

(54) Jones, W. C.; Nestor, J. J.; du Vigneaud, V. *J. Am. Chem. Soc.* **1973**, *95*, 5677.

(55) Cox, M. T.; Heaton, D. W.; Horbury, J. *J. Chem. Soc. Chem. Commun.* **1980**, 799.

(56) Lebl, M.; Sugg, E. E.; Van Binst, G.; Van der Elst, P.; Tourwe, D.; Slaninová, J.; Hruby, V. J. *Int. J. Peptide Protein Res.* **1987**, *30*, 318.

(57) Vara Prasad, J. V. N.; Rich, D. H. *Tetrahedron Lett.* **1990**, *31*, 1803.

(58) Beneditti, E.; Baroso, A.; Di Blasio, B.; Pavone, V.; Pedone, C.; Toniolo, C.; Bonora, G. M. *Biopolymers* **1983**, *22*, 305.

(59) Kazmierski, W. M.; Hruby, V. J. *Tetrahedron* **1988**, *44*, 697.

(60) Kazmierski, W. M.; Yamamura, I.; Hruby, V. J. *J. Am. Chem. Soc.* **1991**, *113*, 2275.

(61) Mosberg, H. I.; Hurst, R.; Hruby, V. J.; Gee, K.; Yamamura, H. I.; Galligan, J. J.; Burks, T. F. *Proc. Natl. Acad. Sci. U.S.A.* **1983**, *80*, 5871.

(62) Charpentier, B.; Pelaprat, D.; Durieux, C.; Dor, A.; Reibaud, M.; Blanchard, J. C.; Roques, B. P. *Proc. Natl. Acad. Sci. U.S.A.* **1988**, *85*, 1986.

(63) Charpentier, B.; Dor, P.; Roy, H.; England, H.; Pham, H.; Durieux, C.; Roques, B. P. *J. Med. Chem.* **1989**, *32*, 1184.

(64) Sawyer, T. K.; Hruby, V. J.; Darman, P. S.; Hadley, M. E. *Proc. Natl. Acad. Sci. U.S.A.* **1982**, *79*, 1751.

(65) Al-Obeidi, F.; Hadley, M. E.; Pettitt, B. M.; Hruby, V. J. *J. Am. Chem. Soc.* **1989**, *111*, 3413.

(66) Al-Obeidi, F.; de Lauro Castrucci, A.-M.; Hadley, M. E.; Hruby, V. J. *J. Med. Chem.* **1989**, *32*, 2555.

(67) Rizo, J.; Gierasch, L. M. *Ann. Rev. Biochem.* **1992**, *61*, 387.

(68) Schneider, J. P.; Kelly, J. W. *Chem. Rev.* **1995**, *95*, 2169.

(69) DeGrado, W. F. *Adv. Protein Chem.* **1988**, *39*, 51.

(70) Kemp, D. S.; Sun, E. T. *Tetrahedron Lett.* **1982**, *23*, 3759.

(71) Kemp, D. S.; Stites, W. E. *Tetrahedron Lett.* **1988**, *29*, 5057.

(72) Nagai, U.; Sato, K. *Tetrahedron Lett.* **1985**, *26*, 647.

(73) Hinds, M.; Richards, N. G. J.; Robinson, J. A. *J. Chem. Soc. Chem. Commun.* **1988**, 1447.

(74) Kleinhert, H. D.; Rosenberg, S. H.; Baker, W. R.; Stein, H. H.; Klinghofer, V.; Barlow, J.; Spina, K.; Polakowski, J.; Kovar, P.; Cohen, J.; Denissen, J. *Science* **1992**, *257*, 1940.

(75) McQuade, T. J.; Tomaselli, A. G.; Liu, L.; Karacostas, V.; Moss, B.; Sawyer, T. K.; Heinekson, R. L.; Tarpley, W. G. *Science* **1990**, *247*, 454.

(76) Rich, D. H.; Sun, C.-Q.; Vara Prasad, J. V. N.; Pathiasseril, A.; Toth, M. V.; Marshall, G. R.; Clare, M.; Mueller, R. A.; Houseman, K. *J. Med. Chem.* **1991**, *34*, 1224.

(77) Smith III, A. B.; Hirschmann, R.; Pasternak, A.; Akaishi, R.; Guzman, M. C.; Jones, D. R.; Keenan, T. P.; Sprengeler, P. A.; Darke, P. L.; Emini, E. A.; Holloway, M. K.; Schleif, W. A. *J. Med. Chem.* **1994**, *37*, 215.

(78) Smith III, A. B.; Hirschmann, R.; Pasternak, A.; Guzman, M. C.; Yokoyama, A.; Sprengeler, P. A.; Darke, P. L.; Emini, E. A.; Schleif, W. A. *J. Am. Chem. Soc.* **1995**, *117*, 11113.

(79) Qian, X.; Shenderovich, M. D.; K. E. Kövér; P. Davis; R. Horváth; Zalewska, T.; Yamamura, H. I.; Porreca, F.; Hruby, V. J. *J. Am. Chem. Soc.* **1996**, *118*, 7280.

(80) Qian, X.; Kövér, K. E.; Shenderovich, M. D.; Lou, B.-S.; Misicka, A.; Zalewska, T.; Horvath, R.; Davis, P.; Bilsky, E. J.; Porreca, F.; Yamamura, H. I.; Hruby, V. J. *J. Med. Chem.* **1994**, *37*, 1746.

(81) Nikiforovich, G. V.; Prakash, O. M.; Ghering, C. A.; Hruby, V. J. *Int. J. Pept. Prot. Res.* **1993**, *41*, 347.

(82) Tóth, G.; Russell, K. C.; Landis, G.; Kramer, T. H.; Fang, L.; Knapp, R.; Davis, P.; Burks, T. F.; Yamamura, H. I.; Hruby, V. J. *J. Med. Chem.* **1992**, *35*, 2384.

(83) Weber, S. J.; Greene, D. L.; Hruby, V. J.; Yamamura, H. I.; Porreca, F.; Davis, T. P. *J. Pharm. Exp. Therap.* **1992**, *263*, 1308.

(84) Wiliams, S. A.; Abbruscato, T. J.; Hruby, V. J.; Davis, T. P. *J. Neurochem.* **1996**, *66*, 1289.

(85) Greene, D. L.; Hau, V. S.; Abbruscato, T. J.; Bartosz, H., .; Misicka, A.; Lipkowski, A. W.; Hom, S.; Gillespie, T. J.; Hruby, V. J.; Davis, T. P. *J. Pharmacol. Exp. Therap.* **1996**, *277*, 1366.

(86) Hruby, V. J.; Kao, L.-F.; Pettitt, B. M.; Karplus, M. *J. Am. Chem. Soc.* **1998**, *110*, 3351.

(87) Matsunaga, T. O.; Collins, N.; Yamamura, S.; Ramaswami, V.; O'Brien, D. F.; Hruby, V. J. *Biochemistry* **1993**, *32*, 13180.

(88) Shenderovich, M. D.; Köver, K. E.; Nikiforovich, G. V.; Jiao, D.; Hruby, V. J. *Biopolymers* **1996**, *38*, 141.

(89) Pettitt, B. M.; Matsunaga, T. O.; Al-Obeidi, F.; Gehrig, C. A.; Hruby, V. J.; Karplus, M. *Biophysical J.* **1991**, *60*, 1540.

(90) Flippen-Anderson, J. L.; Hruby, V. J.; Collins, N.; George, C.; Cudney, B. *J. Am. Chem. Soc.* **1994**, *116*, 7523.

(91) Collins, N.; Flippen-Anderson, J. L.; Haaseth, R. C.; Deschamps, J. R.; George, C.; Kövér, K. E.; Hruby, V. J. *J. Am. Chem. Soc.* **1996**, *118*, 2143.

(92) Hruby, V. J.; Tóth, G.; Ghering , C. A.; Knapp, R. J.; Kao, L.-F.; Lui, G. K.; Yamamura, H. I.; Kramer, T. H.; Davis, P.; Burks, T. F. *J. Med. Chem.* **1991**, *34*, 1823.

(93) Qian, X.; K. C. Russell; L. W. Boteju; V. J. Hruby *Tetrahedron* **1995**, *51*, 1033.

(94) Jiao, D.; Russell, K. C.; Hruby, V. J. *Tetrahedron* **1993**, *49*, 3511.

(95) Evans, D. A.; Britton, T. C.; Ellman, J. A.; Dorow, R. L. *J. Am. Chem. Soc.* **1990**, *112*, 4011.

(96) Barner, B. A.; Meyers, A. I. *J. Am. Chem. Soc.* **1984**, *106*, 1865.

(97) Oppolzer, W.; Poli, G.; Kingma, A. J.; Starkemann, C.; Bernardinelli, G. *Helv. Chim. Acta* **1987**, *70*, 2201.

(98) Meyers, A. I.; Shipman, M. *J. Org. Chem.* **1991**, *56*, 7098.

(99) Fang, C.; Ogawa, T.; Suemune, H.; Sakai, K. *Tetrahedron Asymmetry* **1991**, *2*, 389.

(100) Touet, J.; Baudouin, S.; Bown, E. *Tetrahedron: Asymmetry* **1992**, *3*, 587.

(101) Dharanipragada, R.; VanHulle, K.; Bannister, A.; Bear, S.; Kennedy, L.; Hruby, V. J. *Tetrahedron* **1992**, *48*, 4733.

(102) Nicolas, E.; Rusell, K. C.; Hruby, V. J. *J. Org. Chem.* **1993**, *58*, 766.

(103) Nicolas, E.; Rusell, K. C.; Knollenberg, J.; Hruby, V. J. *J. Org. Chem.* **1993**, *58*, 7565.

(104) Li, G.; Rusell, K. C.; Hruby, V. J. *Tetrahedron Lett.* **1993**, 2565.

(105) Low, B.-S.; Li, G.; Lung, F.-D.; Hruby, V. J. *J. Org. Chem.* **1995**, *60*, 5509.

(106) Papa, A. J. *J. Org. Chem.* **1966**, *31*, 1426.

(107) Li, G.; Patel, D.; Hruby, V. J. *Tetrahedron Lett.* **1993**, *34*, 5393.

(108) Ripka, W. C.; De Lucca, G. V.; Bach II, A., C.; Pottorf, R. S.; Blaney, J. M. *Tetrahedron* **1993**, *49*, 3593.

(109) Kahn, M. E. *Tetrahedron* **1993**, *49*, Symposia 50, 3433-3677.

(110) Gillespie, P.; Cicariello, J.; Olson, G. L. *Biopolymers* **1997**, *43*, 191.

(111) Hanessian, S.; McNaughton-Smith, G.; Lombart, H. G.; Lubell, W. D. *Tetrahedron* **1997**, *53*, 12789.

(112) Fink, B. E.; Kym, P. R.; Katzenellenbogen, J. A. *J. Am. Chem. Soc.* **1998**, *120*, 4334.

(113) Hirschmann, R.; Hynes, J.; Cichy-Knight, M. A.; van Rijn, R. D.; Sprengeler, P. A.; Spoors, P. G.; Shakespeare, W. C.; Pietranico-Cole, S.; Barbosa, J.; Liu, J.; Yao, W.; Rohrer, S.; Smith, A. B. I. *J. Med. Chem.* **1998**, *41*, 1382-1391.

(114) Johannesson, P.; Lindeberg, G.; Tong, W.; Gogoll, A.; Karlen, A.; Hallberg, A. *J. Med. Chem.* **1999**, *42*, 601.

(115) Khalil, E. M.; Pradhan, A.; Ojala, W. H.; Gleason, W. B.; Mishra, R. K.; Johnson, R. L. *J. Med. Chem.* **1999**, *42*, 2977.

(116) Eguchi, M.; Lee, M. S.; Nakanishi, H.; Stasiak, M., Lovell, S.; Kahn, M. *J. Am. Chem. Soc.* **1999**, *121*, 12204.

(117) Gosselin, F.; Lubell, W. D. *J. Org. Chem.* **2000**, *65*, 2163-2171.

(118) De Weid, D.; Jolles, J. *J. Physiol. Rev.* **1982**, *62*, 976.

(119) De Weid, D.; Croiset, G. *Methods Achieve Exp. Pathol.* **1991**, *15*, 167.

(120) Walker, J. M.; Akil, H.; Watson, S. J. *Science* **1980**, *210*, 1247.

(121) Murphy, M. T.; Richards, D. B.; Lipton, J. M. *Science* **1983**, *221*, 192.

(122) Silman, R. E.; Chard, T.; Lowry, P. J.; Smith, I.; Young, I. M. *Nature* **1976**, *260*, 716.

(123) Smith, E. M.; Hughes, T. K.; Hashemi, F.; Stefano, G. B. *Proc. Natl. Acad. Sci. U.S.A.* **1992**, *89*, 782.

(124) Lerner, A. B.; McGuire, J. S. *Nature* **1961**, *189*, 176.

(125) Hadley, M. E.; Hruby, V. J.; Jiang, J.; Sharma, S. D.; Fink, J. L.; Haskell-Luevano, C.; Bentley, D. L.; Al-Obeidi, F. A.; Sawyer, T. K. *Pigment Cell Res.* **1996**, *9*, 213.

(126) Roselli-Rehfuss, L.; Mountjoy, K. G.; Robbins, L. S.; Mortrud, M. T.; Low, M. J.; Tatro, J. B.; Entwistle, M. L.; Simerly, R. B.; Cone, R. D. *Proc. Natl. Acad. Sci. U.S.A.* **1993**, *90*, 8856.

(127) Chhajlani, V.; Muceniece, R.; Wikberg, J. E. S. *Biochem. Biophys. Res. Commun.* **1993**, *195*, 866.

(128) Gantz, I.; Konda, Y.; Tashiro, T.; Shimoto, Y.; Miwa, H.; Munzert, G.; Watson, S. J.; DelValle, J.; Yamada, T. *J. Biol. Chem.* **1993**, *268*, 8246.

(129) Gantz, I.; Miwa, H.; Konda, Y.; Shimoto, Y.; Tashiro, T.; Watson, S. J.; DelValle, J.; Yamada, T. *J. Biol. Chem.* **1993**, *268*, 15174.

(130) Barret, P.; MacDonald, A.; Helliwell, R.; Davidson, G.; Morgan, P. *J. Mol. Endocrinol.* **1994**, *12*, 203.

(131) Desarnaud, F.; Labbé, O.; Eggerickx, D.; Vassart, G.; Parmentier, M. *Biochem. J.* **1994**, *299*, 367.

(132) Gantz, I.; Shimoto, Y.; Konda, Y.; Miwa, H.; Dickinson, C. J.; Yamada, T. *Biochem. Biophys. Res. Commun.* **1994**, *200*, 1214.

(133) Griffon, N.; Mignon, V.; Facchinetti, P.; Diaz, J.; Schwartz, J.-C.; Sokoloff, P. *Biochim. Biophys. Res. Commun.* **1994**, *200*, 1007.

(134) Labbé, O.; Desarnaud, F.; Eggerickx, D.; Vassart, G.; Parmentier, M. *Biochemistry* **1994**, *33*, 4543.

(135) Mountjoy, K. G.; Mortrud, M. T.; Low, M. J.; Simerly, R. B.; Cone, R. D. *Mol. Endocrinol.* **1994**, *8*, 1298.

(136) Fathi, Z.; Lawrence, G. I.; Parker, E. M. *Neurochem. Res.* **1995**, *20*, 107.

(137) Hruby, V. J.; Wilkes, B. C.; Cody, W. L.; Sawyer, T. K.; Hadley, M. E. *Pept. Protein Rev.* **1984**, *3*, 1.

(138) Vaudry, H.; Eberle, A. N. *Ann. N.Y. Acad. Sci.* **1993**, *680*, 687.

(139) Eberle, A. N. *The Melanotropins: Chemistry, Physiology, and Mechanism of Action*; Karger: Basel, Switzerland, 1988.

(140) Hruby, V. J.; Sharma, S. D.; Toth, K.; Jaw, J. Y.; Al-Obeidi, F.; Sawyer, T. K.; de Lauro Castrucci, A.-M.; Hadley, M. E. *Ann. N. Y. Acad. Sci.* **1993**, *680*, 51.

(141) Hruby, V. J.; Wilkes, B. C.; Hadley, M. E.; Al-Obeidi, F.; Sawyer, T. K.; Staples, D. J.; deVaux, A. E.; Dym, O.; Castrucci, A. M. L.; Hintz, M. E.; Reihm, J. P.; Rao, R. *J. Med. Chem.* **1987**, *30*, 2126.

(142) Sawyer, T. K.; Sanfilippo, P. J.; Hruby, V. J.; Engel, M. H.; Heward, C. B.; Burnett, J. B.; Hadley, M. E. *Proc. Natl. Acad. Sci. U.S.A.* **1980**, *77*, 5754.

(143) Bool, A. M.; Gray, G. H., II; Hadley, M. E.; Heward, C. B.; Hruby, V. J.; Sawyer, T. K.; Yang, Y. C. S. *J. Endocrinol.* **1981**, *88*, 57.

(144) Haskell-Luevano, C.; Sawyer, T. K.; Hendrata, S.; North, C.; Panahinia, L.; Stum, M.; Staples, D. J.; Castrucci, A. M. L.; Hadley, M. E.; Hruby, V. J. *Peptides* **1996**, *17*, 995.

(145) Hruby, V. J.; Cody, W. L.; de Lauro Castrucci, A. M.; Hadley, M. E. *Coll. Czech. Chem. Commun.* **1988**, *53*, 2549.

(146) Castrucci, A. M. L.; Hadley, M. E.; Sawyer, T. K.; Wilkes, B. C.; Al-Obeidi, F.; Staples, D. J.; deVaux, A. E.; Dym, O.; Hintz, M. F.; Reihm, J.; Rao, K. R.; Hruby, V. J. *Gen. Comp. Endocrinol.* **1989**, *73*, 157.

(147) Cody, W. L.; Stevenson, J. W. S.; Al-Obeidi, F.; Sugg, E. E.; Hruby, V. J. In Hadley, M. E., Ed.; CRC Press: Boca Raton, 1988; Vol. Vol. III, pp 93-109.

(148) Haskell-Luevano, C.; Shenderovich, M. D.; Sharma, S. D.; Nikiforovich, G. V.; Hadley, M. E.; Hruby, V. J. *J. Med. Chem.* **1995**, *38*, 1736.

(149) Haskell-Luevano, C.; Miwa, H.; Dickinson, C.; Hadley, M. E.; Hruby, V. J.; Yamada, T.; Gantz, I. *J. Med. Chem.* **1996**, *39*, 432.

(150) Hadley, M. E.; Abdel-Malek, Z.; Marwan, M. M.; Kreutzfeld, K. L.; Hruby, V. J. *Endocrinol. Res.* **1985**, *11*, 157.

(151) Haskell-Luevano, C.; Miwa, H.; Dickinson, C.; Hruby, V. J.; Yamada, T.; Gantz, I. *Biochem. Biophys. Res. Commun.* **1994**, *204*, 1337.

(152) Sawyer, T. K.; Castrucci, A. M. L.; Staples, D. J.; Affholter, J. A.; deVaux, A. E.; Hruby, V. J.; Hadley, M. E. *Ann. N.Y. Acad. Sci.* **1993**, *680*, 597.

(153) Al-Obeidi, F.; Hruby, V. J.; Hadley, M. E.; Sawyer, T. K.; Castrucci, A. M. L. *Int. J. Pept. Protein Res.* **1990**, *35*, 228.

(154) Hruby, V. J.; Sharma, S. D.; Lu, D.; Castrucci, A. M. L.; Al-Obeidi, F. A.; Cone, R.; Hadley, M. E. *J. Med. Chem.* **1995**, *38*, 3454.

(155) Al-Obeidi, F.; O'Connor, S. D.; Job, C.; Hruby, V. J.; Pettitt, B. M. *J. Peptide Res.* **1998**, *51*, 420-431.

(156) du Vigneaud, V.; Ressler, C.; Swan, J. M.; Roberts, C. W.; Katsoyannis, P. G.; Gordon, S. *J. Am. Chem. Soc.* **1953**, *75*, 4879.

(157) Hruby, V. J.; Smith, C. W. In *The Peptides: Analysis, synthesis, biology*; Smith, C. W., Ed.; Academic Press: Orlando, 1987; Vol. 8, pp 77-207.

(158) Williams, P. D.; Pettibone, D. J. *Curr. Pharm. Design* **1996**, *2*, 41.

(159) Hruby, V. J.; Lebl, M. In *CRC Handbook of Neurohypophyseal Hormone Analogues*; Jošt, K., Lebl, M., Brtnik, F., Eds.; CRS Press: Boca Raton, FL, 1987; Vol. 1, pp 105-155.

(160) Malon, P. In *CRC Handbook of Neurohypophyseal Hormone Analogues*; Jošt, K., Lebl, M., Brtnik, F., Eds.; CRS Press: Boca Raton, FL, 1987; Vol. 1, pp 211-228.

(161) Hempel, J. C. In *The Peptides: Analysis, Synthesis, Biology*; Smith, C. W., Ed.; Academic Press: Orlando, 1987; Vol. 8, pp 209-237.

(162) Urry, D. W.; Walter, R. *Proc. Natl. Acad. Sci. U.S.A.* **1971**, *68*, 956.

(163) Kotelchuck, D.; Scheraga, H. A.; Walter, R. *Proc. Natl. Acad. Sci. U.S.A.* **1972**, *69*, 3629.

(164) DeCoen, J. L.; Ralston, E. *Biopolymers* **1977**, *16*, 1929.

(165) Nikiforovich, G. V.; Leonova, V. I.; Galaktionov, S. G.; Chipens, G. I. *Int. J. Pept. Prot. Res.* **1979**, *13*, 363.

(166) Spasov, V. Z.; Popov, E. M. *Sov. J. Bioorg. Chem.* **1981**, *7*, 263.

(167) Hagler, A. T.; Dauber, P.; Osguthorpe, D. J.; Hempel, J. C. *Science* **1985**, *227*, 1309.

(168) Ward, D. J.; Chen, Y.; Platt, E.; Robson, B. *J. Theor. Biol.* **1991**, *148*, 193-227.

(169) Bhaskaran, R.; Chang, L.-C.; Yu, C. *Biopolymers* **1992**, *32*, 1599.

(170) Wood, S. P.; Tickle, I. J.; Treharne, A. M.; Pitts, J. E.; Mascarehas, Y.; Li, J. Y.; Husain, J.; Cooper, S.; Blundell, T. L.; Hruby, V. J.; Buku, A.; Fishman, A. J.; Wyssbrod, H. R. *Science* **1986**, *232*, 633.

(171) Liwo, A.; Tempczyk, A.; Oldziej, S.; Shenderovich, M. D.; Hruby, V. J.; Talluri, S.; Ciarkowski, J.; Grzonka, Z. *Biopolymers* **1996**, *38*, 157.

(172) Lebl, M. In *CRC Handbook of Neurohypophyseal Hormone Analogues*; Jošt, K., Lebl, M., Brtnik, F., Eds.: Boca Raton, FL, 1987; Vol. 2, pp 17-74.

(173) Tarnowska, M.; Liwo, A.; Shenderovich, M. D.; Liepina, I.; Golbraikh, A. A.; Grzonka, Z.; Tempczyk, A. *J. Comput. Aided Mol. Des.* **1993**, *7*, 699.

(174) Shenderovich, M. D.; Kasprzykowski, F.; Liwo, A.; Sekacis, I.; Saulitis, J.; Nikiforovich, G. V. *Int. J. Pept. Prot. Res.* **1991**, *38*, 528.

(175) Schmidt, J. M.; Ohlenschläger, O.; Rüterjans, H.; Grzonka, Z.; Kojro, E.; Pavo, I.; Fahrenholz, F. *Eur. J. Biochem.* **1991**, *201*, 355.

(176) Hill, P. S.; Smith, D. D.; Slaninova, J.; Hruby, V. J. *J. Am. Chem. Soc.* **1990**, *112*, 3110.

(177) Smith, D. D.; Slaninova, J.; Hruby, V. J. *J. Med. Chem.* **1992**, *35*, 1558.

(178) Shenderovich, M. D.; Balodis, J.; Mishlyakova, N.; Liwo, A.; Kasprzykowski, F.; Kasprzykowska, R.; Tarnowska, M.; Ciarkowski, J. In *22nd European Peptide Symposium*; Schneider, C. H., Eberle, A. N., Eds.; ESCOM, 1992; pp 535-536.

(179) Momany, F. A.; McGuire, R. F.; Burgess, A. W.; Scheraga, H. A. *J. Phys. Chem.* **1975**, *79*, 2361.

(180) Némethy, G.; Pottle, M. S.; Scheraga, H. A. *J. Phys. Chem.* **1983**, *87*, 1883.

(181) Shenderovich, M. D.; Kövér, K. E.; Wilke, S.; Collins, N.; Hruby, V. J. *J. Am. Chem. Soc.* **1997**, *119*, 5833.

(182) Hruby, V. J. *Trends in Pharmacol. Sci.* **1987**, *8*, 336.

(183) Hruby, V. J.; Han, G. In;; Cone, R. D., Ed.; Humana Press: Totowa, NJ, 2000; pp 239-261.

(184) Hruby, V. J.; Chow, M.-S.; Smith, D. D. *Ann. Rev. Pharmacol. Toxicol.* **1990**, *30*, 501.

(185) Kazmaier, U. *J. Org. Chem.* **1996**, *61*, 3694.

(186) Neises, B.; W., S. *Angew. Chem. Int. Ed. Engl.* **1978**, *17*, 522.

(187) Kazmaier, U. *SYNLETT* **1995**, 1138.

(188) Lin, J.; Liao, S.; Hruby, V. J. *Tetrahedron Lett.* **1998**, *39*, 3117.

(189) Li, G.; Haq, W.; Xiang, L.; Lou, B.-S.; Hughes, R.; De Leon, I. A.; Davis, P.; Gillespie, T. J.; Romanowski, M.; Zhu, X.; Misicka, A.; Lipkowski, A. W.; Porreca, F.; Davis, T. P.; Yamamura, H. I.; O'Brien, D. F.; Hruby, V. J. *Bioorg. Med. Chem. Lett.* **1998**, *8*, 555.

(190) Liao, S.; Shenderovich, M. D.; Lin, J.; Hruby, V. J. *Tetrahedron* **1997**, *53*, 16645.

(191) Haskell-Luevano, C.; Toth, K.; Boteju, L.; Job, C.; de Lauro Castrucci, A.-M.; Hadley, M. E.; Hruby, V. J. *J. Med. Chem.* **1997**, *40*, 2740.

(192) Yuan, W.; Hruby, V. J. *Tetrahedron Lett.* **1997**, *38*, 3853.

(193) Belokon', Y. N.; Kochetkov, K. A.; Churkina, T. D.; Ikonnikov, N. S.; Chesnokov, A. A.; Larionov, O. V.; Kagan, H. V. *Russ. Chem. Bull.* **1999**, *48*, 917.

(194) Chinchilla, R.; Galindo, N.; Najera, C. *Synthesis* **1999**, 704.

(195) Torrini, I.; Zecchini, G. P.; Paradisi, M. P.; Mastropietro, G.; Lucente, G.; Gavuzzo, E.; Mazza, F. *Tetrahedron* **1999**, *55*, 2077.

(196) Davis, F. A.; Liang, C.-H.; Liu, H. *J. Org. Chem.* **1997**, *62*, 3796.

(197) Shapiro, G.; Buechler, D.; Marzi, M.; Schmidt, K.; Gomez-Lor, B. *J. Org. Chem.* **1995**, *60*, 4978.

(198) Danho, W.; Tilley, J. W.; Shiuey, S. J.; Kulesha, I.; Swistok, J.; Makofske, R.; Michalewsky, J.; Wagner, R.; Triscari, J.; Nelson, D.; Chiruzzo, F. Y.; Weatherwood, S. *Int. J. Peptide Protein Res.* **1992**, *39*, 337.

(199) Evans, D. A.; Britton, T. C.; Ellman, J. A.; Dorow, R. I. *J. Am. Chem. Soc.* **1991**, *113*, 2275.

(200) Fitzi, R.; Seebach, D. *Tetrahedron* **1988**, *44*, 5277.

(201) Gibson, S. E.; Guillo, N.; Tozer, M. J. *Tetrahedron* **1999**, *55*, 585.

(202) Liao, S.; Lin, J.; Shenderovich, M. D.; Han, Y.; Hosohata, K.; Davis, P.; Qiu, W.; Porreca, F.; Yamamura, H. I.; Hruby, V. J. *Bioorg. Med. Chem. Lett.* **1997**, *7*, 3049.

(203) Kaptein, B.; Boesten, W. H. J.; Broxterman, Q. B.; Peters, P. J. H.; Schoemaker, H. E.; Kamphuis, J. *Tetrahedron: Asymmetry* **1993**, *4*, 1113.

(204) Baldwin, J. E.; North, M.; Flinn, A.; Moloney, M. *Tetrahedron* **1989**, *45*, 1465.

(205) Schöllkopf, U.; Hartwig, W.; Groth, U. *Angew. Chem. Int. Ed. Engl.* **1979**, *18*, 863.

(206) Schöllkopf, U.; Groth, U.; Deng, C. *Angew. Chem. Int. Ed. Engl.* **1981**, *20*, 798.

(207) Schöllkopf, U.; Hartwig, W.; Pospischil, K.-H.; Kehne, H. *Synthesis* **1981**, 966.

(208) Schöllkopf, U.; Groth, U.; Deng, C. *Synthesis* **1981**, 969.

(209) Alonso, F.; Davies, S. G.; Elend, A. S.; Haggitt, J. L. *J. Chem. Soc., Perkin Trans. I* **1998**, 257.

(210) Carloni, A.; Porzi, G.; Sandri, S. *Tetrahedron: Asymmetry* **1998**, *9*, 2987.

(211) Burk, M. J.; Allen, J. G.; Kiesman, W. F. *J. Am. Chem. Soc.* **1998**, *120*, 657.

(212) Kazmaier, U.; Schneider, C. H. *Synthesis* **1998**, 1321.

(213) Belokon', Y. N. *Janssen Chim. Acta* **1992**, *10*, 4.

(214) Belokon', Y. N. *Pure Appl. Chem.* **1992**, *64*, 1917.

(215) Kukhar', V. P.; Resnati, G.; Soloshonok, V. A. In *Fluorine-Containing Amino Acids. Synthesis and Properties*; Kukhar', V. P., Soloshonok, V. A., Eds.; Wiley: Chichester, 1994; Chapter 5.

(216) Soloshonok, V. A. In *ACS Books*; Ojima, I., McCarthy, J. R., Welch, J. T., Eds.; American Chemical Society: Washington, D. C., 1996; Chapter 2.

(217) Soloshonok, V. A. *Enantiocontrolled Synthesis of Fluoro-Organic Compounds: Stereochemical Challenges and Biomedicinal Targets*; Wiley: Chichester, 1999.

(218) Soloshonok, V. A.; Avilov, D. V.; Kukhar', V. P.; Tararov, V. I.; Savel'eva, T. F.; Churkina, T. D.; Ikonnikov, N. S.; Kochetkov, K. A.; Orlova, S. A.; Pysarevsky, A. P.; Struchkov, Y. T.; Raevsky, N. I.; Belokon', Y. N. *Tetrahedron: Asymmetry* **1995**, *6*, 1741.

(219) Soloshonok, V. A.; Avilov, D. V.; Kukhar, V. P. *Tetrahedron: Asymmetry* **1996**, *7*, 1547.

(220) Soloshonok, V. A.; Avilov, D. V.; Kukhar, V. P. *Tetrahedron* **1996**, *52*, 12433.

(221) De, B. B.; Thomas, N. R. *Tetrahedron: Asymmetry* **1997**, *8*, 2687.

(222) Soloshonok, V. A.; Cai, C.; Hruby, V. J. *Tetrahedron: Asymmetry* **1999**, *10*, 4265.

(223) Soloshonok, V. A.; Cai, C.; Hruby, V. J.; Meervelt, L. V. *Tetrahedron* **1999**, *55*, 12045.

(224) Soloshonok, V. A.; Cai, C.; Hruby, V. J.; Meervelt, L. V.; Mischenko, N. *Tetrahedron* **1999**, *55*, 12031.

(225) Soloshonok, V. A.; Cai, C.; Hruby, V. J. *Angew. Chem. Int. Ed. Engl.* in press.

(226) Belokon', Y. N.; Tararov, V. I.; Maleev, V. I.; Savel'eva, T. F.; Ryzhov, M. G. *Tetrahedron: Asymmetry* **1998**, *9*, 4249.

(227) Belokon', Y. N.; Bakhmutov, V. I.; Chernoglazova, N. I.; Kochetkov, K. A.; Vitt, S. V.; Garbalinskaya, N. S.; Belikov, V. M. *J. Chem. Soc. Perkin Trans. 1* **1988**, 305.

(228) Kukhar', V. P.; Belokon', Y. N.; Svistunova, N. Y.; Soloshonok, V. A.; Rozhenko, A. B.; Kuzmina, N. A. *Synthesis* **1993**, 117.

(229) Coulter, A. W.; Lombardini, J. B.; Talalay, P. *Mol. Pharm.* **1974**, *10*, 305.